UNIVERSITY OF BIRMINGHAM

Solvothermal Production of Dimethylfuran from Sugar Derivatives toward Future Transport Fuel

BY

BAYONLE AYOKUNLE KAYODE

A thesis submitted to
The University of Birmingham
for the degree of
DOCTOR OF PHILOSOPHY

School of Chemical Engineering
College of Engineering and Physical Science
University of Birmingham
June 2015

Abstract

In a time of steady decline in petroleum reserves, instability in oil prices, strong environmental legislation and concerns of global warming, researchers and petroleum industries are actively searching for cost-effective processes to convert renewable biomass resources into biofuels and other value-added chemicals. 2,5-dimethylfuran (2,5-DMF) has gathered interest as an energy-dense compound with similar fuel properties to gasoline. Of the main biomass-derived compounds is 5-hydroxymethylfurfural (5-HMF), a versatile platform chemical that can serve as an intermediate to different chemical products and biofuels. This thesis describes the catalytic hydrogenation of 5-hydroxymethylfurfural to 2,5-dimethylfuran (2,5-DMF), employing three different hydrogen donor systems (molecular H_2, azeotropic mixture of formic acid and triethylamine and 2-propanol) and seven catalysts.

Transmission electron microscope (TEM) analysis showed that the bio-Pd synthesised by *D. desulfuricans* were generally larger than both the monometallic bio-Ru and bimetallic bio-Pd/Ru synthesised by *B. benzeovorans.* While scanning electron microscope (SEM) analysis confirmed that that experiments carried out with all the catalyst in molecular hydrogen and 2-propanol showed less degradation compared to that in $HCOOH/Et_3N$ solvent mixture. This possibly suggests why majority of the catalysts employed in molecular hydrogen could be reused after the first run of experiment.

Hydrogenation of 5-HMF to 2,5-DMF was studied over both conventional Ru/C and Pd/C (ruthenium on carbon and palladium on carbon) and bacteria supported metal catalyst in molecular hydrogen using a batch Parr autoclave reactor. Under optimised conditions (260 ^oC, 50 bar of hydrogen, 700 rpm of stirring), 5 wt% Ru/C catalyst achieved 96.4% of 5-HMF conversion in 2 hours and produced 95.1% yield of 2,5-DMF; in contrast a bacterial supported

bimetallic catalyst 20 wt% Bio-Ru/Pd gave 95.3% conversion and 60.3% yield of 2,5-DMF at the same operating conditions.

Catalytic transfer hydrogenation (CTH) of 5-HMF to 2,5-DMF was investigated over the same set of catalysts in formic acid/triethylamine ($HCOOH/Et_3N$) mixture. Optimisation of reaction parameters showed that temperature, time, $HCOOH/Et_3N$ molar ratio, 5-HMF concentration as well as agitation speed played important roles in the selectivity to the targeted 2,5-DMF. It was possible to achieve 93.4% of 5-HMF conversion in 4 hours and produced 92.1% yield of 2,5-DMF at 210 ^oC, 5:2 molar ratio of $HCOOH/Et_3N$ and 300 rpm agitation speed. It is interesting to note that 96.9% of 5-HMF conversion and 56.7% yield of 2,5-DMF was achieved using the bimetallic 20 wt% Bio-Ru/Pd catalyst at similar reaction conditions. Among all the catalyst investigated, 5 wt% Ru/C catalyst exhibited superior catalytic activity with a product yield of 92.1%.

Transfer hydrogenation of 5-hydroxymethylfurfural to 2,5-dimethlyfuran in 2-propanol was studied over both conventional and biomass supported catalysts. The conventional 5 wt% Ru/C catalyst also showed the best catalytic activity among all the catalysts investigated in this section. The yield of 2,5-DMF was enhanced with increasing reaction temperature and/ or time. Optimum conditions were attained at 260 ^oC after 2 hours of reaction time, where 5-HMF conversion and 2,5-DMF yield reached 94.3% and 70.2% respectively. At similar operating conditions, 94.5% of 5-HMF conversion and 42.6% yield of 2,5-DMF was attained over bimetallic 5 wt% Bio-Ru/Pd catalyst.

Reaction kinetics of 5-HMF hydrogenation in molecular H_2 was evaluated, with the experimental data fitted a second order reaction with respect to 5-HMF as the key reactant with a rate constant of 8.1×10^{-3} mol/L.min and activation energy of 49.5 kJ/mol. Similarly, the

kinetic analyses of 5-HMF hydrogenation in 2-propanol showed that the experimental data also fitted second order reaction with respect to 5-HMF as the key reactant with an activation energy (E_a) of 229.2 kJ/mol. This implies that the doubling 5-HMF concentration will quadruple the reaction rate. In addition, the high activation energy required on 2-propanol suggests that 5-HMF hydrogenation in 2-propanol is a slow reaction hence, it requires a large amount of energy is required to initiate the reaction.

It is concluded that catalytic hydrogenation of 5-HMF in molecular H_2 offer superior advantages to catalytic transfer hydrogenation in HCOOH/Et_3N mixture and 2-propanol in terms of product yield and selectivity. However, transfer hydrogenation in hydrogen donor systems is also promising because it is safe and gives very high yield of 2,5-DMF compared to molecular hydrogen which is not economical nor entirely green due to the high pressure H_2 required.

Dedication

This thesis is dedicated to God almighty that have always been my pillar of support throughout my PhD programme.

Acknowledgement

I would like to express gratitude to God for successful completion of this programme. I appreciate the financial support from Petroleum Technology Development Fund (PTDF), Nigeria.

My deepest appreciation to: Dr. Bushra Al-Duri for her leadership supervision, practical advice, patience, parental advice, financial support and constant encouragement throughout the period of this project, Prof. Joseph Wood for his co-supervision and advice, Dr. Mohamed M. Farah, Dr. Chi Tsang, Dr. Helen Onyeaka, Dr. Akeem M. Lawal, Dr Abarasi Hart, Abel Alonso for their contributions. Thanks to Mr Jacob Omajali who manufactured the bio-catalyst used in this study.

My parents (Elder and Deaconess F.A. Kayode), they invested so much in me. Thanks for your prayers, financial and moral support. To my siblings: (Mayowa, Tobiloba and Okikiola), I appreciate you all. I appreciate my church: The Redeem Christian Church of God, Covenant Restoration Assembly, Birmingham for their prayers and support throughout my stay in the United Kingdom. I also appreciate my wife, Temitope Oluwakemi Kayode for her patience and understanding.

I want to seize this opportunity to appreciate the Catalysis and Reaction Engineering Research Group at School of Chemical Engineering, University of Birmingham for their support in the successful completion of this study. The chemical engineering workshop team for their technical contribution towards the maintenance of the experimental rig. I cannot forget to mention the administrative support and care from Ms Lynn Draper throughout my stay at the university.

Lastly, special thanks to my friends for their understanding and encouragement. It goes a long way to successfully complete this project.

Table of Contents

List of Figures

List of Tables

Chapter 1. Introduction

1.1 Background and Motivation

The primary source of energy used in the world today is fossil fuel, which is mostly consumed in the transportation sector (Escobar *et al*., 2009). However, as petroleum reserves are declining steadily in addition to instability in price, attention has been shifted to alternative fuel sources to supplement the rising demand. Additionally, strong environmental legislation and the concerning of global warming arising from the consumption of fossil fuels calls for sustainable, renewable and alternative energy sources with lesser emissions (Singh *et al*., 2010). Although fossil fuels are currently important as raw materials for energy supply, the consumption of non-renewable sources could result in long-term climate change. It is generally known that the combustion of fossil fuels leads to the emission of CO_2, thereby resulting in climate problems such as global warming. Figure 1.1 shows that the world CO_2 emission is enormously increasing in which CO_2 emission from coal shows the highest share of greenhouse gas emissions.

In future, biofuels, natural gas, synthetic gas (syngas) and hydrogen are likely to be considered as the four important sustainable fuel sources among many energy alternatives (Nigam and Singh, 2011). Among these four important sustainable fuel sources, biofuels have emerged as the most environment-friendly energy source due to the abundance of raw materials and lesser emission of greenhouse gases (GHGs).

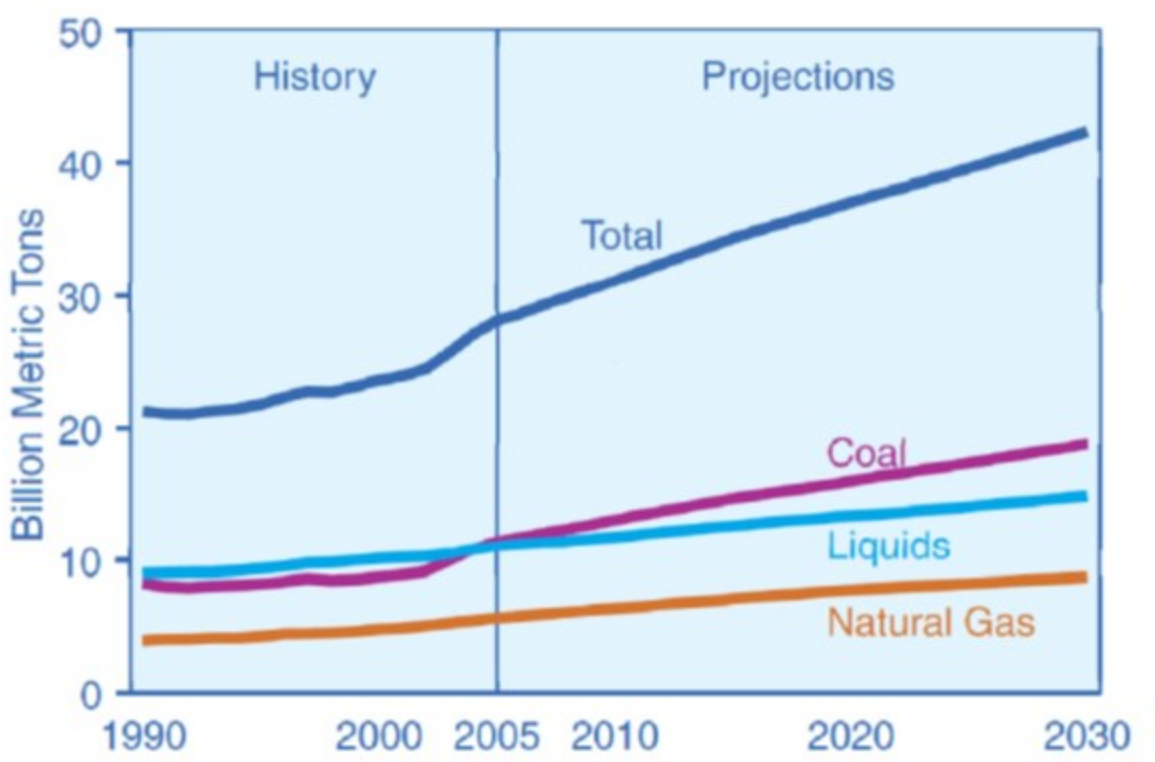

Figure 1.1 Global emission of carbon dioxide by fuel type (Adapted from Pupovac, 2013).

Moreover, due to increasing energy demand; instability in oil prices; and concern over emissions from fossil fuels, new technologies to replace the use of non-renewables are continuously sought after. With these problems in mind, the use of biomass for energy generation is increasing significantly. Hence, biofuels are regarded as a favourable choice of fuel consumption because they are biodegradable, renewable and generate lesser amount of greenhouse gases.

The total biomass in the world is 4 billion tons in the ocean and 1800 billion tons on land (Pupovac, 2013). This makes biomass the 4th largest source of energy in the world and it accounts for nearly 15% of the total energy supply (Nikolau et al., 2003). However, due to different compositions and origins, wide ranges of biomass are in existence, e.g. energy crops,

forestry, wastes and agricultural residues (Tumurlu et al., 2011; Pupovac, 2013). As a result of wide ranges of biomass, the use of one universal method for conversion purposes is extremely challenging. The oldest process to produce energy from biomass is via direct combustion (Pupovac, 2013). Recently, the latest technologies used for biomass conversion involve biochemical and thermochemical processes. Biochemical processes include fermentation, saccharification and anaerobic digestion while thermochemical processes involves liquid phase processing, pyrolysis, liquefaction and hydro treating. Figure 1.2 shows the main biofuel classification and conversion possibilities from different biomass sources.

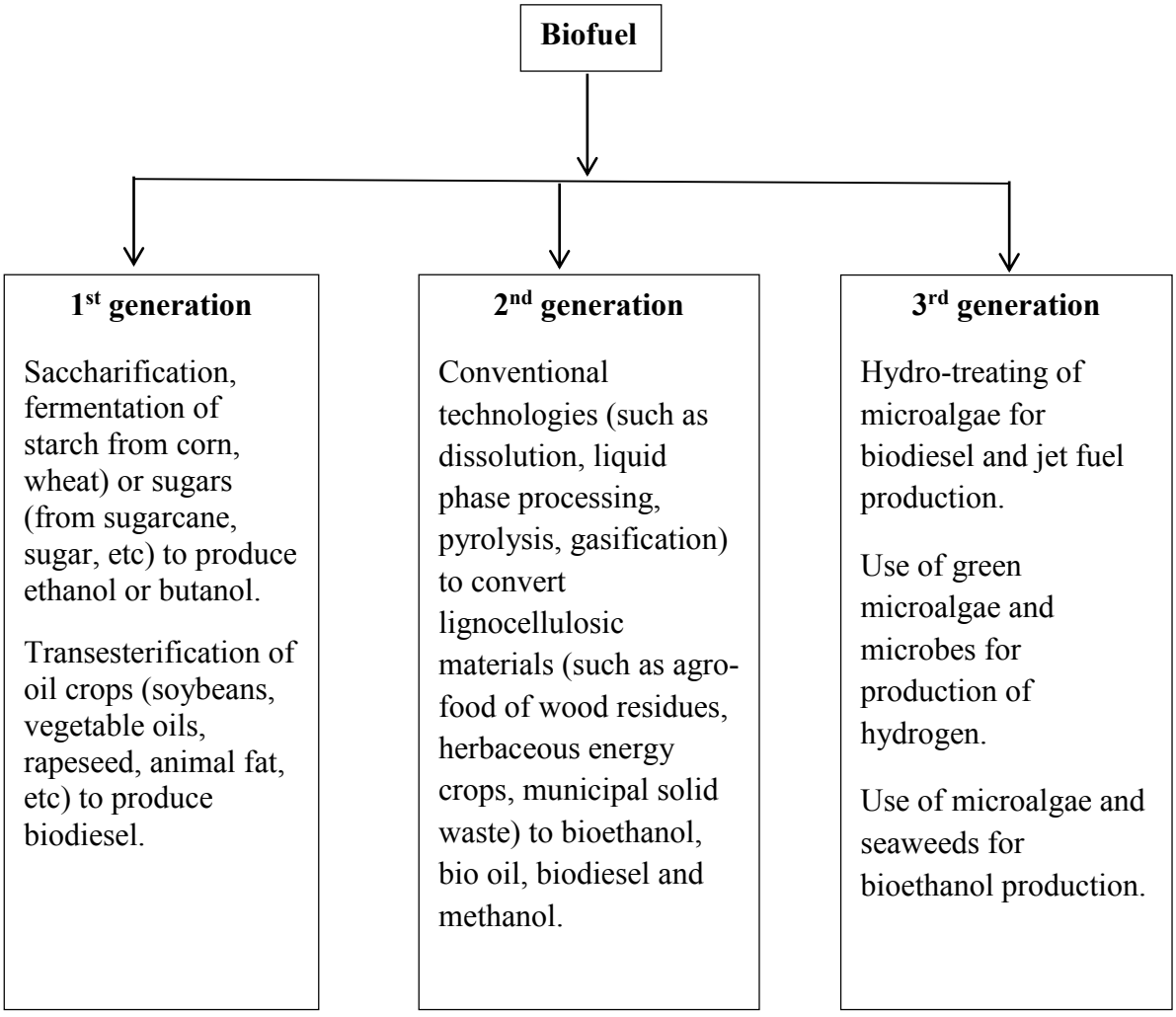

Figure 1.2 Main classifications of biofuels (modified from Dragone et al., 2010).

The production of biofuels worldwide increased from 4.4 to 50.1 billion litres between 1980 and 2005 (Armbruster and Coyle 2006-2007), with further increase more recently (Licht, 2008). Biofuels exist either as a solid, gas or liquid fuels. Fuels that can be produced from biomass includes 2,5-dimethylfuran, methanol, hydrogen, biodiesel, ethanol and methane. Today, a wide range of advanced and conventional technologies for biofuel conversion already exists. Based on processing technologies, the three main classifications of biofuels are: first generation, second generation, third generation biofuels as shown in Figure 1.2 (Sims et al., 2010; An et al., 2011).

First generation biofuels are liquid fuels made from food crops such as sugars, seeds, maize, sweet sorghum, starch and vegetable oils such as palm oil, Jatropha and soybean oil (Ravindranath et al., 2011). First generation biofuels are in existence and require a simple process to make the finished fuel product (Nigam and Singh, 2011). However, the cost of production is very high because of food-fuel competition. In other words, the cost of certain food stuffs and crops has increased due to rapid expansion of global biofuel production from sugar, starch and oilseed crops. As a result of these limitations, non-edible biomass is required for the production of biofuels. First generation biofuels are produced and used in a number of countries in significant quantities such as Brazil, United States of America (USA), Germany, France, Sweden, China, South Africa and India. Ethanol is the most well-known first generation biofuel made by sugar fermentation extracted from crop plants and starch foods (Larson, 2008). Other examples of first generation biofuels include biodiesel, bio alcohols, bio ethers and green diesel.

Second generation biofuels are liquid biofuels made from lignocellulosic biomass which are either non-edible whole plant biomass or non-edible residues of food crop production such as tall grasses, woody biomass, plantation residues (saw-dust, leaves, etc), agricultural residues (straw, bagasse shells, leaves and reproductive parts) (Ravindranath, et al., 2011). The feedstock for second generation biofuels can be harvested at a cheaper cost and are also available in abundance (Sims et al., 2008). The potential benefit in the production of second generation biofuels over first generation biofuels is that it limits the food versus fuel competition associated with first generation biofuels. Second generation biofuels are also known as advanced biofuels because of the advanced conversion technologies, many of which are still under development.

The raw materials involved in the production of second generation biofuels can be bred specifically for energy generation, enabling higher production per unit land area and a large amount of above-ground plant material can be converted and used for biofuel production (Nigam and Singh, 2011). Ethanol and butanol are examples of second generation biofuels produced via biochemical route while dimethyl ether (DME) and refined Fischer-Tropsch liquids (FTL) are examples of second generation biofuels produced via thermochemical routes (Larson, 2008; Nigam and Singh, 2011). USA and Brazil are known to be the largest producers of bioethanol in the world (Larson, 2008).

Third generation biofuels are liquid fuels produced from microscopic organisms. As a result of the unsolved issues from the production of first and second generation biofuels, such as advanced technologies, food competition, and high cost of production, third-generation

biofuels are the latest generation of biofuels researchers have focussed on. Third-generation biofuels are derived specifically from microbes and algae and are considered to be a source of alternative energy that is free from the major drawbacks found in first and second-generation biofuels (Nigam and Singh, 2011). However, the down side of third generation biofuels is that the algae used for production of fuels require large amounts of water, phosphorus and nitrogen to grow. This means that algae-based biofuel will cost more than fuel from other sources. For example, Exxon Mobil invested more than $600 million USD into algae research and development in 2013 and concluded that algae-based biofuels will not be feasible for at least 25 years (biofuel.org.uk). Microbial species such as fungi, yeast and microalgae have been used as potential sources for biodiesel production (Xiong et al., 2008). Other fuels that can be derived from microscopic organism includes; ethanol, butanol and jet fuel.

However, it is well known that gasification is one of the oldest methods of biomass processing and is converted into syngas at very high temperatures (999.85 ^{o}C) through partial combustion (Goswami, 1986; Pupovac, 2013). Liquid fuels such as gasoline and diesel can be synthesized by upgrading the Fisher-Tropsch synthesis syngas (Dry, 2002). Pyrolysis unlike gasification, takes place at relatively low temperatures (299.85 – 499.85 ^{o}C) and in the absence of oxygen (Lange, 2007). During pyrolysis, biomass is converted into bio-oil (Alonso et al., 2010) and is not suitable for immediate use in engines as a result of its high oxygenate content and acidity (Pupovac, 2013). Moreover, bio-oils can be converted into useful products through upgrading technologies such as steam reforming (Huber et al., 2006) and hydrogenation (Furimsky, 2000; Pupovac, 2013).

The use of biofuels to generate energy is expected to grow significantly in the next few years, thus, there are broad investigations currently focused on the development of new and effective technologies for biofuel production (James et al., 2010; Alonso et al., 2010). In the last two decades, biomass-derived carbohydrates have been used as a starting material for biofuel production. Many valuable platform chemicals such as levulinic acid (LA), furfural, 5-hydroxymethylfurfural (5-HMF), furfuryl alcohol (FA) have been synthesized from carbohydrates and can be further upgraded to useful chemical products and fuels.

It is well known that fossil fuels are of high importance in the transportation sector. With that in mind, 2,5-dimethylfuran (2,5-DMF) is considered as a useful fuel with similar energy density, toxicological and mechanical properties (see Section 2.6.1) to petroleum based gasoline fuel compared to other biofuels. 2,5-DMF is produced from fructose in a two-step reaction (Roman-Leshkov et al., 2006; Chheda et al., 2007). Firstly, fructose is converted to 5-HMF via a dehydration reaction and then undergoes catalytic hydrogenation/hydrogenolysis to 2,5-DMF.

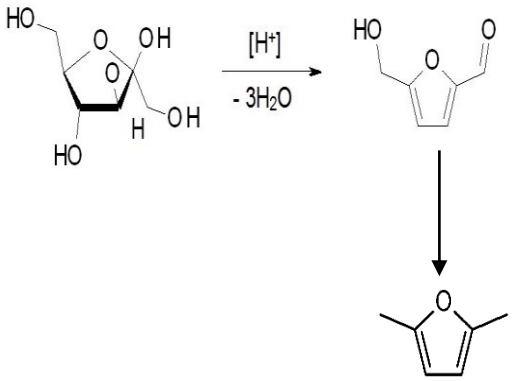

Figure 1.3: Fructose conversion to 2,5-Dimethylfuran

Hitherto, the major challenge in biomass conversion to liquid fuels and products is the development of novel catalytic strategies that will address the shortcomings of the three main biofuel classifications. With regard to aforementioned challenge and the similar properties between petroleum based fuel and 2,5-DMF, the motivation for this research is to asses and compare different hydrogen donor systems for the hydrogenation/hydrogenolysis of 5-Hydroxymethylfurfural into 2,5-Dimethylfuran (2,5-DMF). The objectives of this study and thesis organisation are detailed in Sections 1.2 and 1.3, respectively.

1.2 Aim and Objectives of the Study

The main aim of this work is to identify and compare the most effective hydrogen donor system for hydrogenation of 5-HMF to produce 2,5-DMF to achieve the highest yield and selectivity and how they respond to changes in reaction conditions. The main objectives investigated in the current study were:

1. To identify the most suitable hydrogen donor system and catalyst, for maximum conversion and yield.

2. To investigate the effectiveness and performance of commercial catalysts under different reaction parameters across all hydrogen donor systems, by evaluation of;
    a. Effect of reaction temperature and reaction time.
    b. Effect of initial reactant concentration and pressure.
    c. Effect of catalyst amount and agitation speed.

3. To investigate the use of bio-support as a novel metal support for the hydrogenation of 5-HMF to produce 2,5-DMF.

4. To understand the plausible reaction pathways for each solvent systems by qualitative analysis of reaction intermediates using gas-chromatography mass spectroscopy (GC-MS).

5. To evaluate some preliminary reaction kinetics in order to identify the reaction order and activation energy.

1.3 Thesis Organisation and Overview

The ten (10) Chapters presented in this thesis demonstrated the experimental technique of catalytic conversion of 5-HMF into 2,5-DMF. The study investigated both commercial and bio-catalysts and compared hydrogenation solvent system with hydrogenation in molecular hydrogen. The result was evaluated in terms of 5-HMF conversion and 2,5-DMF yield.

Chapter 1 gives an in-depth overview to the study and motivation. It also identified the importance of biofuels in the energy sector, provides an introduction of different biomass conversion technologies, and identified the major challenges from previous studies that require further study. Chapter 2 is a literature survey on the use of carbohydrates as renewable raw materials, properties, synthesis and applications of 5-HMF. This chapter includes properties and different catalytic systems for 2,5-DMF production from 5-HMF, heterogeneous catalysis, advances and future challenges. Chapter 3 describes the experimental materials, procedures,

equipment and analytical techniques used in this study. The result Chapters in this thesis are presented in form of a scientific paper; starting with an abstract and introduction which states the focus of the chapter and present information related to the work. Thereafter, the procedure; analytical section; results and discussion section and conclusion followed. Participations in conferences and other relevant work are presented in the appendix section.

Chapter 4 discusses few catalysts characterization used in this study Chapter 5 discusses the synthesis of 2,5-DMF from 5-HMF in molecular H_2 over both conventional and bio-supported metal catalysts. Chapter 6 discusses the synthesis of 2,5-DMF from 5-HMF through catalytic transfer hydrogenation in azeotropic mixture of formic acid and triethylamine over both set of metal catalysts support. Chapter 7 discusses the synthesis of 2,5-DMF from 5-HMF through catalytic transfer hydrogenation in 2-propanol over both conventional and biomass supported metal catalysts.

Chapter 8 focussed on the comparison between the 3 hydrogen donor systems employed while Chapter 9 describes some preliminary reaction kinetics for 5-HMF hydrogenation in molecular hydrogen and 2-propanol while. Chapter 10 presents conclusions drawn from the studies presented in this PhD thesis and highlight various aspects of this study that still need further investigations.

Chapter 2. **Literature Review**

2.1 Overview

This chapter opens with an introduction about the use of carbohydrates as renewable raw materials for production of chemicals in Section 2.2. Different chemical products can be generated from biomass degradation but 5-HMF is our specific focus in this study. 5-HMF is known to be a giant molecule which can be converted to different chemical products. Section 2.3 shows the versatility of 5-HMF and its applications. The general properties of 5-HMF are therefore discussed in Section 2.4. As a result of its versatility, 5-HMF has been synthesized using different solvent systems. Section 2.5 therefore review the commonest solvent system described in the literature.

Thereafter, 2,5-DMF as a biofuel candidate produced from 5-HMF is introduced in Section 2.6. The general properties (physical, chemical, toxicological and mechanical) of 2,5-DMF are also discussed in Section 2.6. Subsequently, the use of different catalytic and solvent system used for 2,5-DMF production from 5-HMF are reviewed in Section 2.7. In addition, the overall results, advantages and challenges of each system used are also presented in Section 2.7 while the use of heterogeneous catalysts for transformation reactants to useful chemical products is discussed in Section 2.8. Finally, Section 2.9 presents some conclusions and rationales for the current work.

2.2 Renewable Raw Materials for 5-HMF AND 2,5-DMF Production

The most abundant carbohydrate with six-carbons is known as hexoses and is used as feed stocks for production of furan derivatives (Corma *et al*., 2007). The catalytic transformation of six-carbon sugars into furanic products are of general interest due to their abundance, economic feasibility and also due to several reactions involved in producing different chemical products via dehydration, isomerisation, hydrogenation, hydrolysis and oxidation reactions.

Similarly, other carbohydrate materials such as lignocellulosic biomass, starch and inulin are also used as chemical feed stocks for the production of furanic products. Lignocellulose consists of cellulose, lignin and hemicellulose, and is the major building block of all plants. Figure 2.1 shows the chemical composition of plant biomass. Cellulose and hemicellulose displays the largest fraction in plant biomass resulting to ca. 65% of the total biomass composition (Palkovits, 2011) while lignin shows an estimated ca. of 20% (Fengel et al., 1984). Other extractives such as proteins, lipids, inorganics, oils, and other natural compounds denote a minor component with a share of ca. 5% (Kamm et al., 2006).

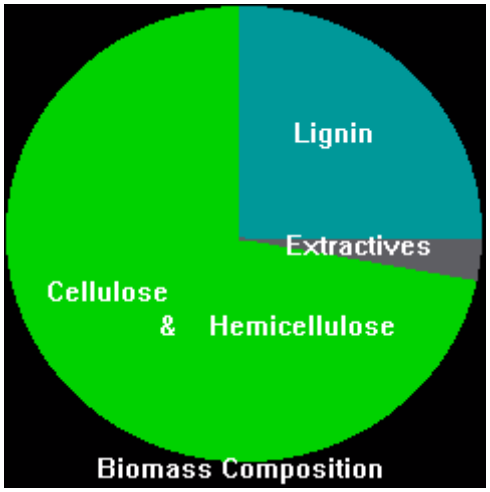

Figure 2.1: Chemical composition of plant biomass (INFORSE, 2015).

Cellulose is abundant in nature and is used as a raw material for production of furanics. It is a linear glucose polymer made up of several anhydroglucose units joined together by β-(1,4)-glycosidic bonds (Figure 2.2). The main problem associated with the use of cellulose is the depolymerisation process to form glucose which involves breaking down the crystalline structure of cellulose followed by hydrolytic cleavage. The next step involves the removal of oxygen molecules in such a way that the loss of energy value is minimized during the process (Schmidt and Dauenhauer, 2007).

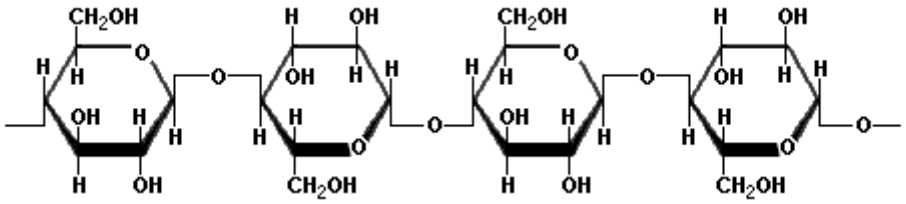

Figure 2.2: Cellulose structure

Unlike cellulose, hemicellulose polymer is an amorphous compound made up of five different monosaccharide units with short branches, usually 5 carbon sugars (mostly xylose and

arabinose) and 6 carbon sugars (mostly mannose, glucose and galactose). As a result of its amorphous structure, (in comparison with cellulose), hemicellulose can be hydrolysed easily to its sugar monomer as shown in Figure 2.4.

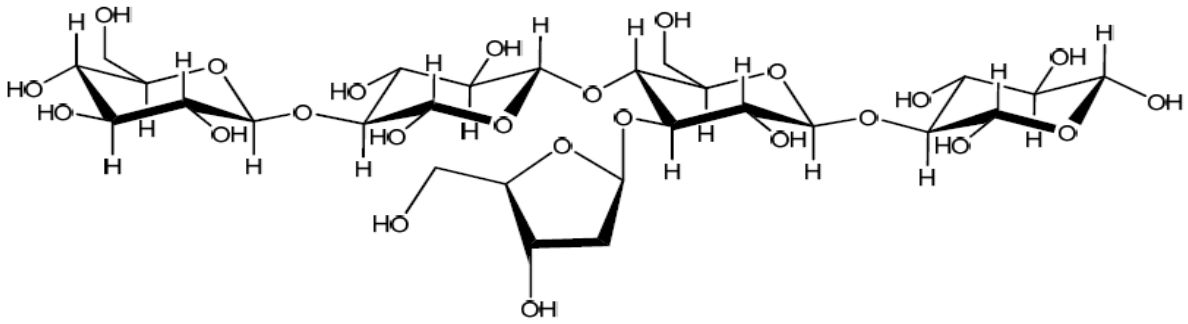

Figure 2.3: Hemicellulose structure

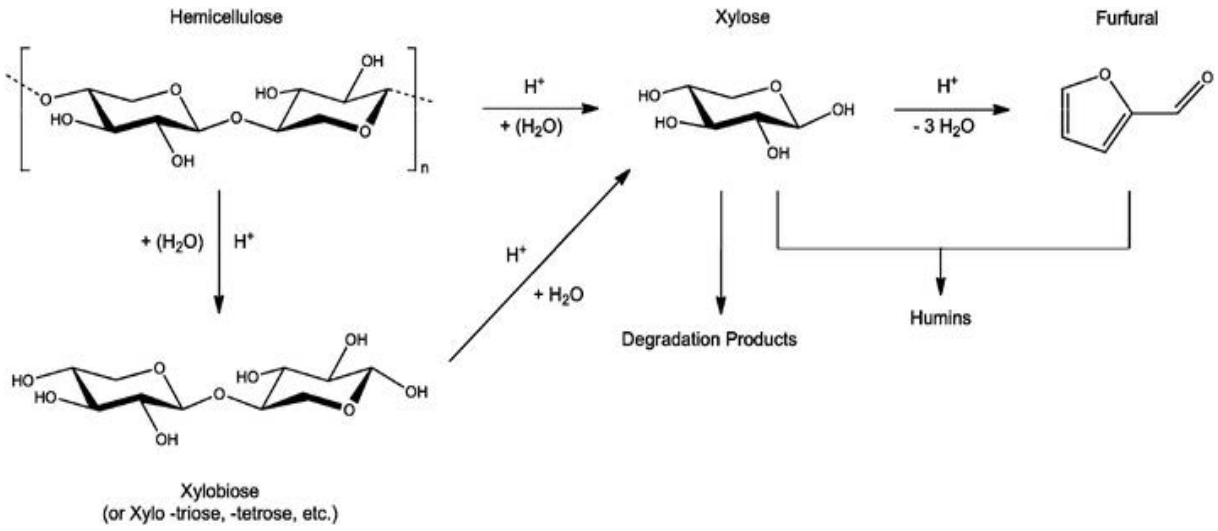

Figure 2.4: Hydrolysis of hemicullose to xylose (Enslow and Bell, 2012)

As shown in Figure 2.5, lignin is made up of a complex three-dimensional structure with a high molecular weight. It is made up of non-sugar type of macromolecules (Pupovac, 2013) and is known to be a highly cross-linked polymer made up of hydroxyphenylpropene units with sinapyl, coniferyl and p-coumaryl alcohol as the 3 dominant monomers (Peterson et al., 2008). It is very reactive due to the presence of phenols, biaryls, aryl ethers, etc. Moreover, lignin is considered as a powerful radical scavenger due to the phenol present in its structure (Dorrestijn et al., 2000; Pupovac, 2013).

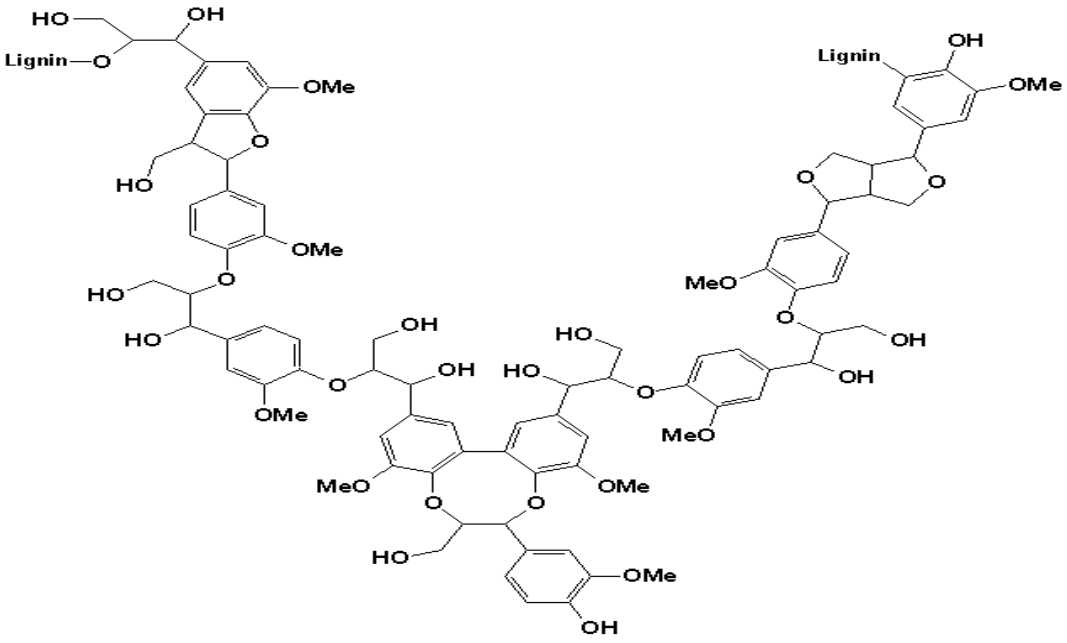

Figure 2.5: Lignin structure (Adapted from Pupovac, 2013)

Majority of the renewable carbohydrates produced annually are polysaccharides and are used in paper, coating and textile industries. However, carbohydrates with low molecular weight (monosaccharides and disaccharides) such as glucose, fructose and sucrose (Figure 2.6) can be obtained freely on a large scale based on polysaccharides. The bulk of articles reported

on 5-HMF production focused on fructose as the starting material. Only few articles have reported the use of glucose and cellulose as starting material for 5-HMF synthesis.

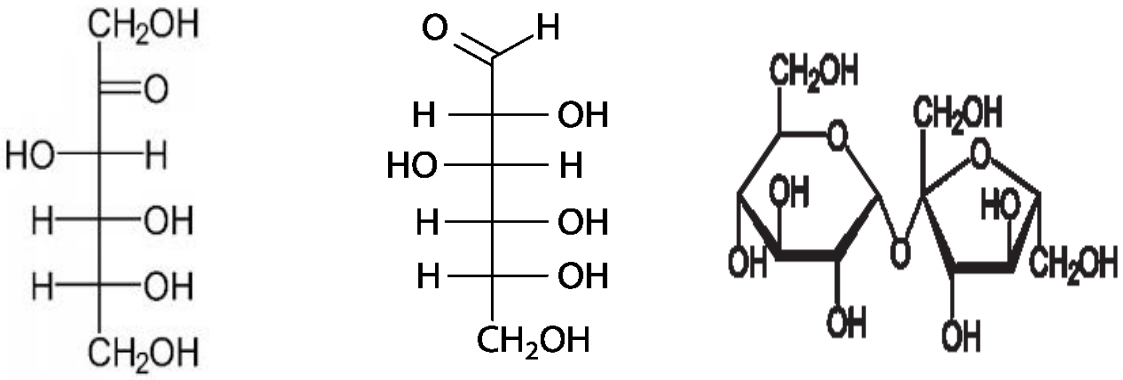

Figure 2.6: Structure of monosaccharides D-fructose and D-glucose, disaccharide sucrose.

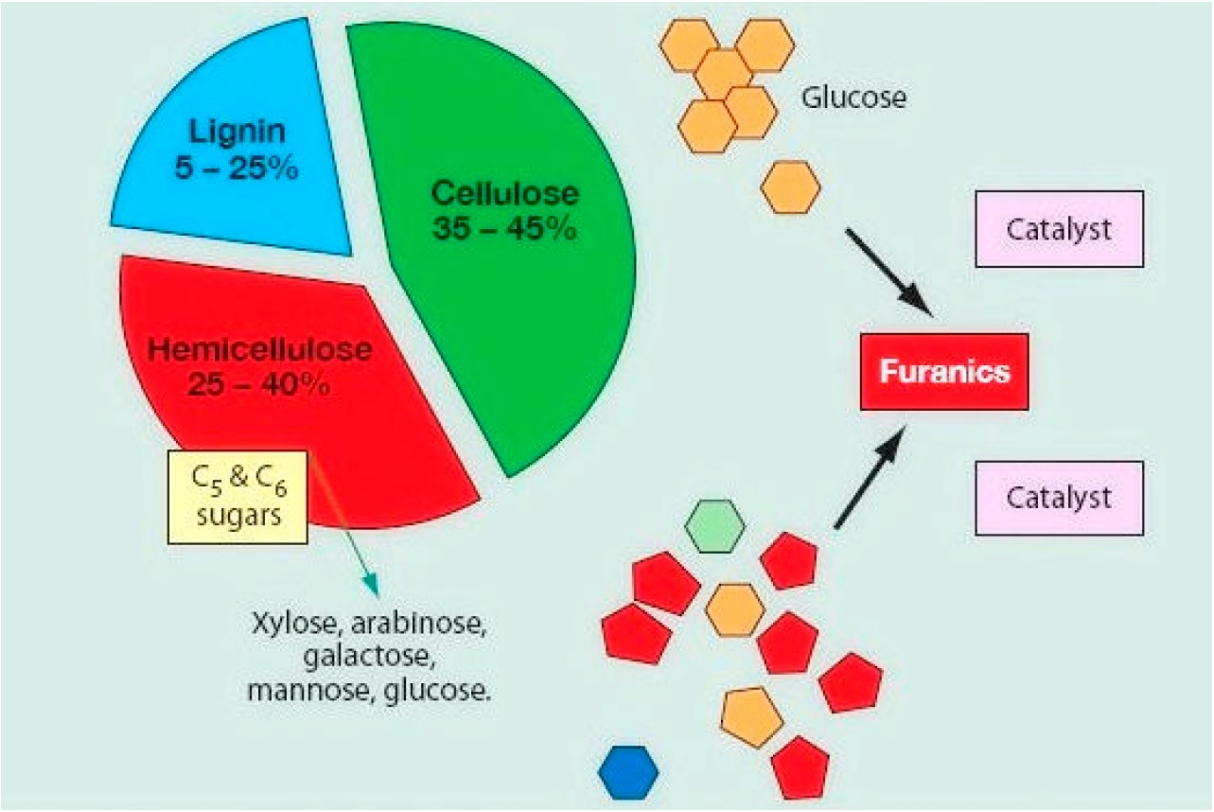

Figure 2.7: Conversion of Lignocellulosic feedstock to furan intermediates (Adapted from de Jong and Jan Gruter, 2009).

2.3 5-HMF as a Versatile Compound and Applications

5-hydroxymethyfurfural is versatile in nature and known to be a good starting material for the synthesis of polymers, pharmaceuticals, polyesters, amino alcohols, dialdehydes and some organic intermediates (Tong *et al*., 2010). Other products such as surface-active agents, biofuels (2,5-dimethylfuran and 2-methylfuran), solvents and resins are also derived from using 5-HMF as a starting material (Chheda *et al*., 2007). As shown in Figure 2.8, 5-hydroxymethylfurfural is a giant molecule involved in the transformation of carbonhydrates into various furanics products such as levulinic acid, formic acid, 2,5-dimethylfuran (2,5-DMF), 2,5-diformylfuran (2,5-DFF) and 2,5-furandicarboxylic acid (2,5-FDCA). Thus, all these furanics products are formed via rehydration, hydrogenolysis and oxidation reaction respectively.

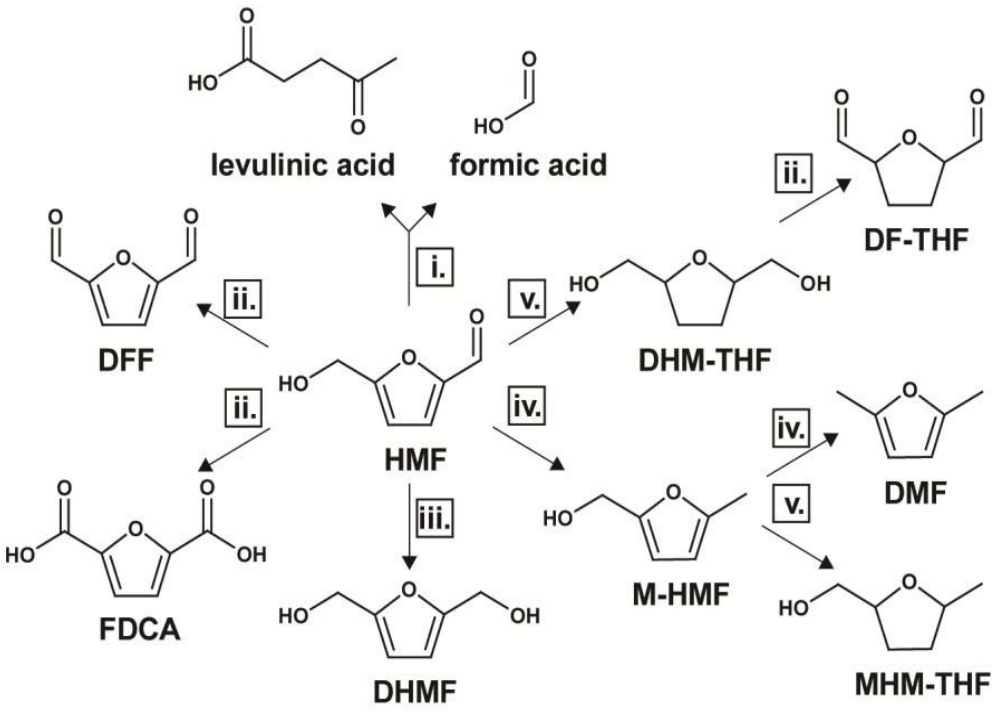

Figure 2.8: 5-HMF as a Platform Chemical (i) rehydration, (ii) oxidation, (iii) reduction, (iv) hydrogenolysis, and (v) hydrogenation (Richards, 2012).

5-HMF has also been used to produce monomers for polymers which are of high industrial potential. In addition to 2,5-FDCA, other furanic chemicals such as; 2,5-bishydroxymethylfuran, 2,5-diformylfuran (2,5-DFF), 5-Hydroxymethylfuroic acid and 2,5-diaminomethylfuran are of high industrial potential because they are monomers with six-carbon and have the ability to replace, for example, alkyldiols, adipic acid or hexamethylenediamine in the manufacture of polymers (Lewkowski, 2001; Ganidi, 2011; Lichtenthaler, 2008; Ganidi and Belgacem., 1997; Van Putten et al., 2013). Also, 2,5-diformylfuran is an attractive product from 5-HMF which can be further transformed into new chemical products. 2,5-DFF has been polymerised to polyvinyls and polypinacols; products which can be further used as a starting material for the production of ligands, antifungal agents and pharmaceuticals (Amarasekara, 2012; Van Putten et al., 2013; Amarasekara et al., 2008). In addition, 5-HMF has been used to produce fine chemicals, agrochemicals, flavors and fragrances. Fine chemicals such as levulinic acid can undergo further transformation to derivatives which have been proposed for fuel applications, for example ɣ-valerolactone (VL), ethyl levulinate and methyl-tetrahydrofuran (MTHF) (Geilen et al., 2010; Hayes et al., 2006; Van Putten et al., 2013).

In spite of the advantages of 5-HMF as a versatile compound and its applications, the industrial production has not been feasible so far due to technical barriers, optimization approaches and cost of raw materials required (Torres *et al*., 2012; Qu *et al*., 2012), hence 5-HMF is synthesized using different laboratory scale methods (Roman-Leshkov *et al*., 2006). Different methods of 5-HMF production from carbohydrate derived biomass require optimization approaches and process design so as to obtain maximum conversion yield with high selectivity. The main method used for 5-HMF production involves the removal of three

molecules of water from hexose sugars, a process known as dehydration of sugars catalysed by different types of acids (Roman-Leshkov *et al*., 2007; Qi *et al.*, 2010).

During the laboratory scale production of 5-HMF from monosaccharide sugars, different side-products such as a brown-black compound known as humins, formic and levulinic acid can occur therefore lowering the efficiency of the process significantly. The most interesting part of these side-products formation involves dependence on the amount or concentration of sugar in solution which means higher rates of side-products are formed as a result of higher sugar concentration used in the reaction.

To date, the vast majority of research on 5-HMF production summarised in this thesis focused on the reaction optimization factors such as solvent system used, reaction pressure, catalyst and reaction temperature but only few dealt with the issue of separating the 5-HMF product from the solvent system used. There has been little attention on 5-HMF purification and efficient recycling of catalysts and extraction solvents.

2.4 Properties of 5-Hydroxymethylfurfural (5-HMF)

This section focused on the physiochemical and toxicological properties of 5-HMF.

2.4.1 Physiochemical Properties of 5-HMF

5-HMF has an IUPAC name of 5-(hydroxymethyl)-2-furaldehyde and is a six-carbon compound with molecular formula $C_6H_6O_3$. 5-HMF has a structure made up of a furan ring and consists of both alcohol and aldehyde functional groups as shown in Figure 2.9. It is known to be a giant molecule with high industrial prospect but despite this, it has not been produced on an industrial scale. At room temperature, 5-HMF is a yellow solid with molar mass of 126.11g/mol and dissolves readily in water. It is known to be an intermediate between sugar chemistry and oil-based industrial chemistry (Gruter and Jong, 2009). It has been widely established in the literature that 5-HMF is an unstable molecule produced from acid-catalysed dehydration of carbohydrate materials (Boisen *et al*., 2009; Kazi *et al*., 2011; Yang *et al*., 2011; Lima *et al*., 2009). As a result of its poor fuel properties, 5-HMF has not been regarded as a fuel additive or as a fuel (Gruter and Jong, 2009).

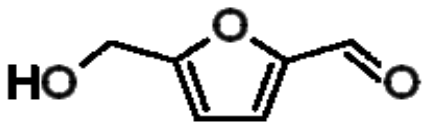

Figure 2.9: 5-Hydroxymethylfurfural (5-HMF) Structure

Table 2.1: Physical and Chemical Properties of 5-HMF (Jan van Putten et al., 2013)

CAS Registry	67-47-0
EC-No	200-654-9
Molecular formula	$C_6H_6O_3$
Molecular weight	126.11 g/mol
Chemical Abstract name	5-(hydroxymethyl)-2-furancarboxaldehyde
Description	Yellow powder[a]; odour of camomile flowers[b]
Synonyms	5-(hydroxymethyl)-2-furaldehyde, HMF, 5-(hydroxymethyl)-2-furancarbonal, hydroxymethyl furfuraldehyde
Melting point	31.5 °C[b], 28-34 °C[a]
Boiling point	114-116 °C at 1 hPa[a], 110 °C at 0.02 mmHg[b]
Density	1.24 at 25 °C
Refractive index	1.57 at 18 °C[b]
UV absorption maximum	283 nm
Smiles	C1=C(OC(=C1)C=O)CO
Flash point	79 °C, closed cup[a]
Solubility	Freely soluble in water, ethanol, methanol, ethyl acetate, acetone, dimethylformamide; soluble in benzene, ether, chloroform; less soluble in carbon tetrachloride; sparingly soluble in petroleum ether[b]

a- Sigma-Aldrich Catalogue; Sigma-Aldrich: St. Louis, MO, 2010.

b- The Merek Index; 11 ed.; Budavari, S., Ed.; Merek & Co., Inc.: Rahway, NJ, 1989, p767.

2.4.2 Toxicological properties of 5-HMF

5-HMF is known to be present in human diet as it is a product of thermal decomposition of carbohydrates (Jan van Putten et al., 2013). 5-HMF is an intermediate formed during caramelization (Kroh et al., 1994) and Maillard reactions (Kus et al., 2005; Martins et al., 2005).

Maillard reactions usually occur at room temperature while fructose caramelization reactions start at 110 ^{o}C and other hexoses start caramelizing at temperatures above 160 ^{o}C (Jan van Putten et al., 2013). However, 5-HMF was initially assumed to have some negative side-effects (Surh et al., 1994) but recent papers have shown that 5-HMF also possesses positive pharmacological activities such as blood circulation, antioxidant activity (Li et al., 2009; Fu et al., 2008), propelling and activity against sickle cell disease (Abdulmalik et al., 2005).

To date, it is yet to be determined whether normal human dietary consumption of 5-HMF causes a potential health risk, though 5-HMF is known to be cytotoxic at very high concentrations, thus resulting in irritation to the upper respiratory tract, eyes, mucus membranes and skin (Jan van Putten et al., 2013). In the year 2000, Janzowski and colleagues conducted a broad study to investigate the potential toxicity of 5-HMF by evaluating growth inhibition, mutagenicity and cytotoxicity (Janzowski et al., 2000). The authors went further to investigate cellular gluthathione depletion and DNA damage in mammalian cells while genotoxicity was studied in Salmonella typhimurium. It was concluded that 5-HMF is safe and does not pose a significant health risk (Janzowski et al., 2000; Jan van Putten et al., 2013). Moreover, the genotoxic effect of 5-HMF using Ames test was studied by Severin et al., (2010). The authors concluded that irrespective of the concentration used in the study, 5-HMF did not cause any genetic mutation in bacteria (Severin et al., 2010; Jan van Putten et al., 2013).

Furthermore, several other studies have been conducted to determine whether 5-HMF poses a significant health risk and most conclusions made so far indicated that the current safety margins are generally satisfactory (Abraham et al., 2011; Florian et al., 2012; Glatt et al., 2012).

2.5 Production of 5-Hydroxymethylfurfural (5-HMF)

5-HMF has been in existence since late 18th century and about 20% yield was first extracted from the reaction of sucrose and fructose catalysed by oxalic acid (Dull, 1895; Kiermayer, 1895). An extensive research was conducted on 5-HMF by Fenton and colleagues in 18th and 19th century (Fenton & Gostling, 1899; Fenton & Robinson, 1909). In 1909, the proper structure of 5-hydroxymethyfurfural was designated by (van Enenstein and Blanksma 1909).

To date, the acid catalysed dehydration of carbohydrate materials most especially fructose and glucose to an extent, has been carried out in ionic liquids and aqueous reaction media (Boisen *et al*., 2009). However, water is considered as the preferred choice of solvent during the acid-catalysed dehydration of carbonhydrates to 5-HMF due to greenness of the reaction process, abundance, usefulness in sustainable chemistry, non-hazardous properties and good solvent for dissolving 5-HMF product and hexose substrates (glucose and fructose). Conversely, using water as a choice of solvent resulted in a competitive rehydration reaction process which gives rise to formation of side-products such as formic acid, levulinic acid and a brown-black compound known as humins. Van Dam *et al*., (1986) reported that the brown-black compound are insoluble and soluble products of polymerisation formed due to the self and cross-polymerisation of fructose, 5-HMF and other side-products most especially in aqueous reaction media when compared to organic medium.

Hitherto, the solvents commonly used for 5-HMF production are aqueous media, ionic liquids, modified aqueous media and two-phase systems, non-aqueous organic solvents and supercritical/subcritical solvents.

2.5.1 Synthesis in Aqueous Media

From an environmental and economical point of view, water is known to be an interesting solvent that exists among many other solvents. Water is a clear choice of solvent due to its ability to dissolve very high concentrations of sugars unlike organic solvents (Jan van Putten et al., 2013). However, in agreement with the development of green processes, the use of homogenous catalysts is less efficient than heterogeneous catalysts. This is due to the fact that heterogeneous catalysts are in a distinct phase with respect to the reaction medium thereby making separation of catalysts easy and cheap compared to homogeneous catalysts. It has been reported that only few acidic solid catalysts can retain their acidity particularly in water and other protic solvents (Okuhara, 2002; Carniti et al., 2011). Tables 2.2 – 2.4 show an overview of selected published results on dehydration of fructose and glucose to 5-HMF under aqueous media.

Table 2.2: Dehydration of Fructose and Glucose to 5-HMF in Aqueous Systems without a Catalyst

Temp (°C)	Time (min)	Fructose conc (wt %)	Conversion (%)	Yield (%)	Selectivity (%)	Reference
200[a]	30	11	89	51	57	Li et al., 2009
140[a]	60	5	-	4	-	Seri et al., 2001
175[a]	90	4.5	72	56	78	Kuster & Temmink, 1977
200[a]	5	9	40	21	53	Watanbe et al., 2005
200[b]	10	9	31	7	23	Watanbe et al., 2005
220[b]	30	1	71	32	45	Jing & Lu, 2008
200[b]	5	9	21	3	15	Watanbe et al., 2005

[a]Fructose. [b]Glucose.

The dehydration of monosaccharides (glucose and fructose) to 5-HMF has been catalysed by several homogeneous catalysts such as H_3PO_4, H_2SO_4 and HCl (Roman-Leshkov *et al*., 2006). However, high conversion yield and selectivity are observed in aprotic high-boiling point solvents such as dimethylsulfoxide (DMSO) than reactions conducted via aqueous reaction media because DMSO also serves as a catalyst (Musau and Munavu, 1987). Despite high conversion, yield and selectivity, the disadvantages of using high-boiling point solvents such as DMSO includes; high viscosity, high cost of separation from the 5-HMF product and also lowering its efficiency making it unsuitable for large-scale production (Boisen et al., 2009).

Table 2.3: Dehydration of Fructose and Glucose in Aqueous Systems, Catalysed by Homogeneous Catalysts

Temp (°C)	Time (min)	Catalyst	Catalyst Loading	Conversion (%)	Yield (%)	Reference
200[a]	20	Acetic acid	100 wt %	92	58	Li et al., 2009
200[a]	10	Formic acid	100 wt %	96	58	Li et al., 2009
200[a]	5	H_2SO_4	1 mM	93	23	Watanbe et al., 2005
95[a]	16	HCl	400 mol %	46	26	Kuster & Van der Baan, 1977
95[a]	24	HCl	400 mol%	62	30	Kuster & Van der Baan,1977
120[b]	20	$AlCl_3$	50 mol %	-	40	De et al., 2011
200[b]	3	H_2SO_4	50 wt %	11	2	Qi et al., 2008
200[b]	5	H_2SO_4	1 mM	32	2	Watanbe et al., 2005

[a]Fructose. [b]Glucose.

The use of heterogeneous catalysts such as niobic acid, niobium phosphate (Carniti *et al*., 2006), zirconium and titanium phosphates (Moreau *et al*., 1996) have drawn more attention due to the cheap cost of separation and recycling factors. Carniti and his co-workers reported that niobic acid and niobium phosphate serves as acidic heterogeneous catalysts in 5-HMF production which resulted in 80% conversion yield of fructose and intermediate selectivity of 30% (Carniti *et al*., 2006).

Table 2.4: Dehydration of Fructose and Glucose in Aqueous Systems, Catalysed by Heterogeneous Catalysts

Temp (°C)	Time (min)	Catalyst	Catalyst Loading	Conversion (%)	Yield (%)	Reference
200[a]	5	TiO_2	100 wt %	98	22	Watanbe et al., 2005
200[a]	5	ZrO_2	50 wt %	65	31	Qi et al., 2008
200[a]	5	ZrO_2	100 wt %	90	15	Watanbe et al., 2005
240[a]	2	ZrP	50 wt %	81	49	Asghari & Yoshida, 2006
160[b]	3	HY-zeolite	50 wt %	83	8	Lourvanij & Rorrer, 1993
200[b]	3	ZrO_2	50 wt %	57	10	Qi et al., 2008
200[b]	5	A-TiO_2	100 wt %	814	20	Watanbe et al., 2005

[a]Fructose. [b]Glucose.

Recently, (Carniti et al., 2011) reported the absence of expected side-reactions in the dehydration of fructose to 5-HMF in water over niobic acid catalyst. Niobic acid is known to be a water-tolerant solid acid and it has been reported to be a very promising catalyst for fructose dehydration in water (Carnili et al., 1999). In this research work, it was reported that HMF is a final stable product and there was no formation of levulinic acid (LA) which could either be derived directly from fructose transformation or from a consecutive reaction of HMF (Carniti et al., 2011). In addition, LA does not undergo further reactions to give condensation products with any other chemical reaction species present in the mixture.

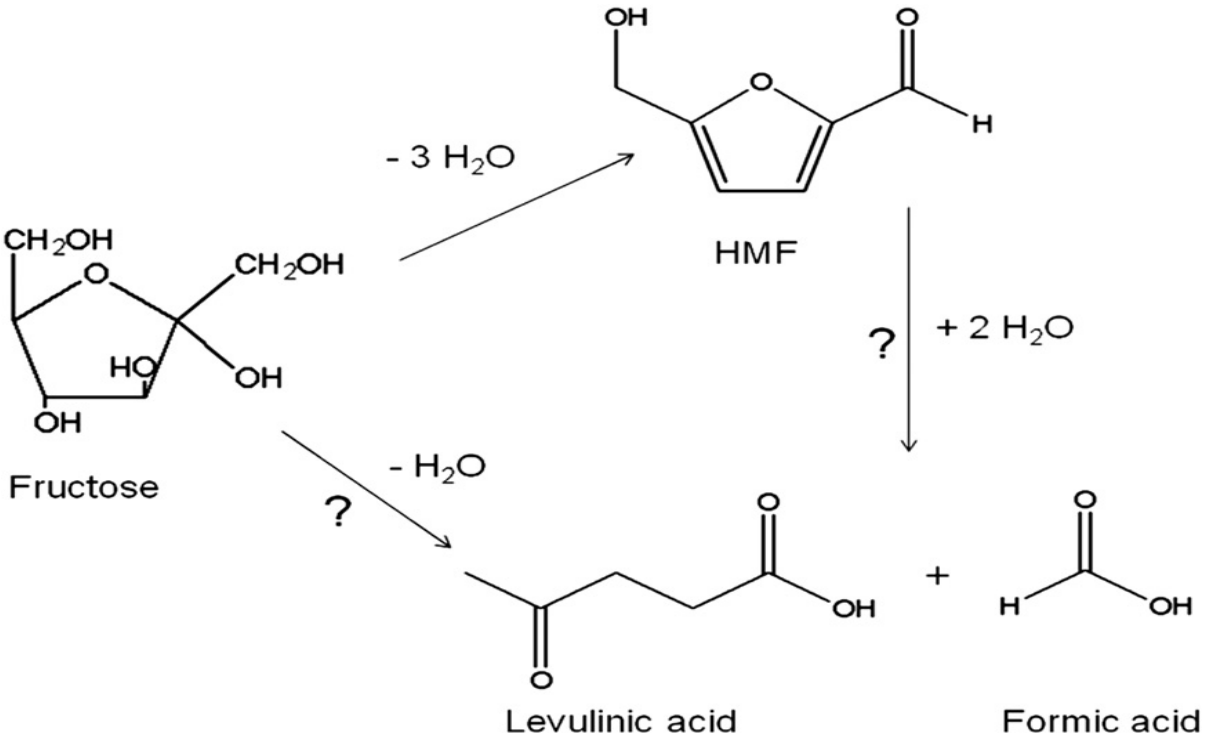

Figure 2.9: Possible reaction paths of the catalytic dehydration of fructose on NBO carried out in water. (Carniti et al., 2011).

Moreover, Moreau and his co-workers produced 5-HMF using water as the solvent system catalysed by zirconium and titanium phosphate/pyrophosphates. In their research work, it was shown that a selectivity of about 100% was achieved at reaction temperature of 100^{o}C and reaction time of 18 minutes. Also, it was reported that the selectivity of 5-HMF drops faster as a result of increase in reaction time which is due to the formation of polymeric side-products (Moreau *et al.*, 1996).

In conclusion, it can be observed that there is no clear trend in the results published with homogeneous and heterogeneous catalysts in aqueous systems. Under the same reaction conditions and catalysts, a huge difference in the reported yields of 5-HMF can be observed

thus, making it difficult to compare the use of homogeneous and heterogeneous catalysts in aqueous media (Jan van Putten et al., 2013).

2.5.2 Synthesis in Supercritical/Subcritical Solvents

A very good alternative to high-boiling organic solvents for hexose dehydration to 5-HMF is the use of low-boiling solvents in their supercritical or subcritical state (Boisen *et al*., 2009). In recent years, subcritical water has been a preferred choice to organic solvents in 5-HMF production industrially due to its unique acidic and basic properties. Simkovic and his co-workers dehydrated glucose using pure subcritical water as solvent system. It was reported that under same reaction temperature and pressure, the selectivity of 5-HMF formed was greater than when using sodium hydroxide or sulphuric acid as catalysts (Simkovic et al., 1987).

Asghari *et al*., (2006) reported 5-HMF production from fructose in subcritical water and compounds such as humins, aldehydes, furfural, soluble polymers, organic acids, ketones and monosaccharides (as shown in Figure 2.11) were produced at residence time up to 15 minutes and reaction temperature (473-593 K) without a catalyst. It was also reported that the amount of side-products (precisely lactic and formic acids) increased with temperature increase. Furthermore, until approximately 200 seconds reaction time, 5-HMF production was favoured and after this time, the 5-HMF was converted to organic acids (Asghari *et al*., 2006).

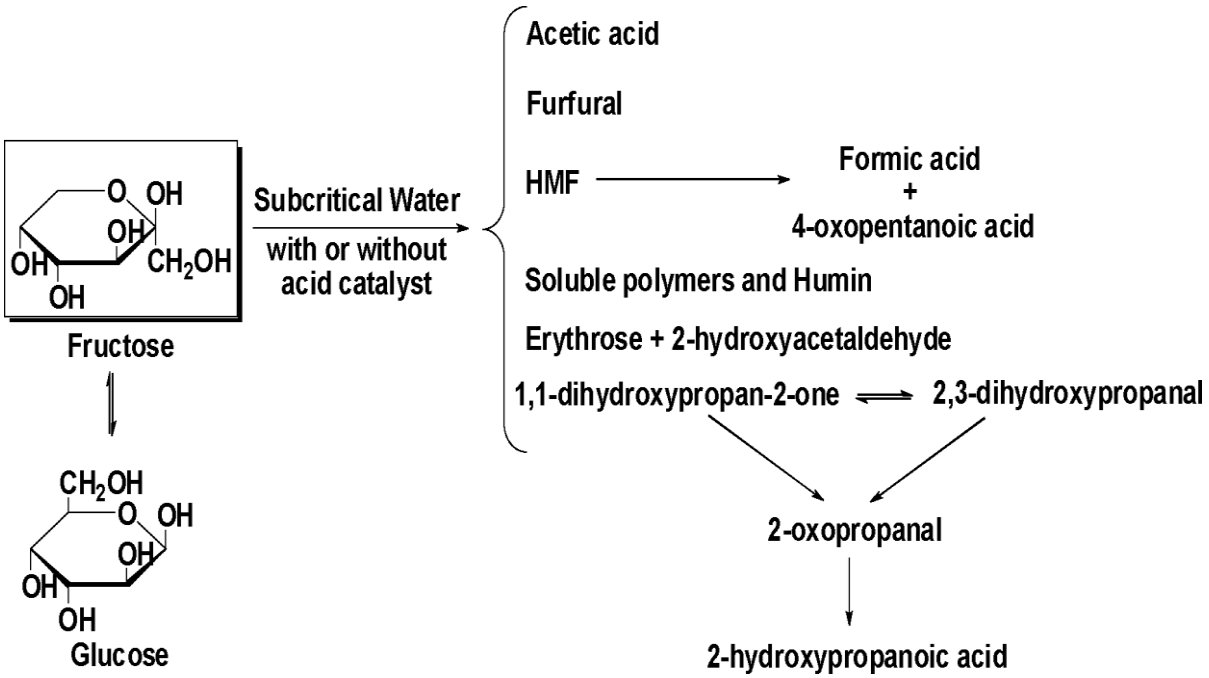

Figure 2.10: Production of 5-HMF from fructose in subcritical water (Asghari et al., 2006; Rosatella et al., 2011)

Furthermore, the use of different ZrO_2 and TiO_2 as catalysts in the conversion of glucose to 5-HMF in highly compressed water was investigated by Watanbe et al., (2005a). It was reported that the anatase-TiO_2 catalysed the dehydration of glucose to 5-HMF showing both the acidic and basic properties during the conversion process. During the conversion process, it was suspected that the basic properties of the catalyst play a huge role in catalysing glucose isomerisation to fructose while the acidic properties catalysed the dehydration process (Watanbe *et al*., 2005b). When TiO_2 was used as a catalyst in glucose conversion to 5-HMF, over 90% selectivity and 20% conversion yield were obtained unlike 50% conversion yield obtained in subcritical water using fructose as the starting material and catalysed by different zirconium phosphates (Watanbe *et al*., 2005a).

The kinetics of D-fructose and D-glucose dehydration as well as 5-HMF under similar conditions have been studied extensively by researchers in supercritical and subcritical water (Chuntanapum *et al*., 2008; Asghari and Yoshida, 2007) but nevertheless, the results obtained using supercritical and subcritical water for 5-HMF production have not been encouraging in terms of 5-HMF yields (Boisen *et al*., 2009). Bicker *et al*., (2003) also investigated the use of low-boiling solvents such as acetic acid, methanol and acetone for 5-HMF production. Fructose was successfully converted to 5-HMF at reaction temperature 180^{o}C and 20MPa reaction pressure using acetone/water mixture and a selectivity of 77% and 99% fructose conversion were obtained. The results obtained were encouraging and was explained based on the structural similarities between DMSO and acetone which ultimately promote fructofuranose (furanoid form of fructose) and hence favours 5-HMF formation (Bicker *et al*., 2003).

2.5.3 Synthesis in Non-Aqueous Organic Solvents

The production of 5-hydroxymethylfurfural from fructose dehydration in high-boiling organic solvents have been the best results obtained so far (Boisen *et al*., 2009). The rehydration of 5-HMF to formic acid and levulinic acid is prevented due to low water concentration. In anhydrous dimethylformamide (DMF), the fructose part of sucrose was reported to undergo dehydration reaction at 100^{o}C catalysed by iodine. Under similar reaction conditions, it was observed that glucose was unaffected (Bonner *et al*., 1960). However, many researchers have reported high 5-HMF yields in DMSO without the use of a catalyst at low temperatures. This raises confusion in the effectiveness of some catalytic reactions investigated in DMSO. Tables 2.5 – 2.7 show an overview of selected published results on dehydration of fructose and glucose to 5-HMF in non-aqueous organic solvents.

Table 2.5: Dehydration of Fructose in Non-Aqueous Organic Solvents without a Catalyst

Temp ^{o}C	Time (min)	Solvent	Conversion (%)	Yield (%)	Selectivity (%)	Reference
130	30	DMSO	0	0	0	Sidhpuria et al., 2011
130	240	DMSO	100	72	72	Yan et al., 2009
150	-	DMSO	-	92	-	Musau & Munavu, 1987

Furthermore, Nakamura and Morikawa (1980) used dimethylsulfoxide (DMSO) as a solvent system for fructose dehydration at 80^{o}C catalysed by a strong-acidic ion-exchange resin. After 8 hours of reaction time, a conversion yield of 90% was obtained and it was observed that the type of resin used strongly affected the rate of the reaction (Nakamura and Morikawa, 1980). Moreover, Szmant and Chundury, (1981) used boron trifluoride etherate to catalyse the conversion of fructose to 5-HMF in DMSO and obtained high 5-HMF yield of > 90%. The authors investigated fructose dehydration at different catalyst concentrations, temperatures and fructose concentrations. At reaction time of 30 -180 minutes, the authors obtained maximum 5-HMF yield varied between 55% and 99%.

Table 2.6: Dehydration of Fructose and Glucose in Non-Aqueous Organic Solvents, Catalysed by Homogeneous Catalysts

Temp ^{o}C	Time (min)	Solvent	Catalyst	Catalyst Loading	Conversion (%)	Yield (%)	Reference
120[a]	120	1,4-dioxane	$Sc(OTf)_3$	10 wt %	86.2	16	Wang et al., 2011
100[a]	240	DMA	$LaCl_3$	2.5 mol %	-	92	Seri et al., 2000
100[a]	240	DMF	$LaCl_3$	2.5 mol %	-	92	Seri et al., 2000
140[a]	5	DMSO	$AlCl_3$	50 mol %	-	69	De et al., 2011
120[a]	120	DMSO	$Ho(OTf)_3$	10 wt %	100	78	Wang et al., 2011
100[a]	60	Sulfolane	HBr	11 mol %	-	93	Caes & Raines, 2011
100[a]	300	Sulfolane	$LaCl_3$	2.5 mol %	-	52	Seri et al., 2000
100[b]	180	DMSO	$SnCl_4$	10 mol %	96	44	Hu et al., 2009
120[b]	120	DMSO	$LaCl_3$	5 mol %	-	9.8	Seri et al., 2000
100[b]	180	DMSO	CrCl3	7 mol %	79	28	Wei et al., 2011
140[b]	4.8	DMSO	$AlCl_3$	50 mol %	-	52	De et al., 2011
120[b]	180	DMF	H_3BO_3	80 mol %	64	7	Stahlberg et al., 2011
100[b]	75	DMF	$GeCl_4$	10 mol %	85	34	Zhang et al., 2011

[a]Fructose. [b]Glucose.

In addition, DMSO is known to be unstable at temperatures over 100 ºC, a factor which is very important in its catalytic activity (Jan van Putten et al., 2013). Therefore, the separation of desired product from high-boiling aprotic solvent is very difficult as a result of the miscibility between water and high-boiling aprotic solvents such as DMSO and dimethylformamide (DMF).

Table 2.7: Dehydration of Fructose and Glucose in Non-Aqueous Organic Solvents, Catalysed by Heterogeneous Catalysts

Temp ^{o}C	Time (min)	Solvent	Catalyst	Catalyst Loading	Conversion (%)	Yield (%)	Reference
120[a]	120	DMSO	Amberlyst 15 powder	6 wt %	100	100	Shimizu et al., 2009
140[a]	10	DMSO	TiO_2	50 wt %	-	54	Dutta et al., 2011
120[a]	120	DMSO	H-BEA zeolite	6 wt %	100	51	Shimizu et al., 2009
120[a]	120	DMSO	$FePW_{12}O_{40}$	6 wt %	100	49	Shimizu et al., 2009
80[b]	180	DMSO	Hydrotalcite/Amberlyst 15 (2:1 w/w)	300 wt %	41	25	Ohara et al., 2010
130[b]	360	DMSO	SO_4^{2-}/ZrO_2-Al_2O_3 (Zr/Al = 1:1 n/n)	20 wt %	100	48	Yan et al., 2009
130[b]	900	DMSO	SO_4^{2-}/ZrO_2-Al_2O_3 (Zr/Al = 1:1 n/n	20 wt %	100	48	Yan et al., 2009
100[b]	180	MeCN + 3 vol% water	Hydrotalcite/Amberlyst 15 (2:1 w/w)	300 wt %	91	28	Ohara et al., 2010

[a]Fructose. [b]Glucose.

2.5.4 Synthesis in Modified Aqueous Media and Two-Phase Systems

One important solvent system used in 5-HMF production is modified aqueous media and two-phase systems. In the last decade, phase modifiers have been very effective in the conversion of fructose to 5-HMF. Phase modifiers used in fructose conversion to 5-HMF are usually polar organic solvents miscible with water (Boisen et al., 2009). The polar organic solvents function to reduce the rate of rehydration reaction forming side-products and also to speed up the rate of the reaction to 5-HMF (Van Dam *et al*., 1986). Table 2.8 – 2.9 show a summary of selected published results on dehydration of fructose and glucose to 5-HMF in two-phase systems.

Table 2.8: Dehydration of Fructose and Glucose in Two-Phase Systems, Catalysed by Homogeneous Catalysts

Temp ^{o}C	Time (Min)	Reaction Solvent	Extraction Solvent	Catalyst	Conversion (%)	Yield (%)	Reference
130[a]	5	H_2O	MIBK	50 mol% $AlCl_3$	-	61	De et al., 2011
150[a]	45	H_2O	MIBK	85 mol% H_3BO_3	43	22	Hansen et al., 2011
180[a]	2.5-3	H_2O	MIBK	0.25 M HCl	75	55	Roman-Leshkov et al., 2006
170[a]	4	1:1 H_2O/DMSO (w/w)	7:3 MIBK/2-Bu-OH (w/w)	pH 1 HCl	95	85	Chheda et al., 2007
150[b]	300	H_2O (0.87 M NaCl	MIBK	85 mol% H_3BO_3	41	14	Hansen et al., 2011
130[b]	5	H_2O	MIBK	50 mol% $AlCl_3$	-	43	De et al., 2011

[a]Fructose. [b]Glucose.

Several researchers have employed aqueous phase modifiers such as dimethylsulfoxide (DMSO), methylisobutylketone (MIBK), acetone and polyethylene glycol (PEG) (Qi *et al*., 2009; Chheda *et al*., 2007). The aqueous phase system can be modified to a two-phase system by introducing a second immiscible phase. In this case, the dehydration reaction takes place in the aqueous phase and an organic phase extracts the 5-HMF from the aqueous phase, therefore reducing the formation of side-products (Boisen *et al*., 2009).

Gaset et al (1986) used DMSO/MIBK as a two-phase system for fructose dehydration to 5-HMF. The authors dissolved 20 wt% fructose in DMSO at 76 ^{o}C in flow (213 mL/h) with MIBK as counterflow solvent (1500 mL/h) and obtained 97% yield of 5-HMF. In addition to the use of biphasic solvents for fructose dehydration, Dumesic group carried out an extensive research on two-phase systems by continuously extracting the aqueous reaction medium with an organic solvent from which 5-HMF was continuously recuperated via solvent evaporation (Roman-Leshkov et al., 2006; Roman-Leshkov & Dumesic, 2009). Fructose dehydration in 0.25 M HCl yielded 26% 5-HMF and 50% conversion at 180 ^{o}C, 30 wt% aqueous fructose for 2.5-3 minutes without an organic solvent (Roman-Leshkov et al., 2006). With the addition of 2 wt equivalent of MIBK, fructose conversion and 5-HMF yield improved further to 75% and 55% respectively. Moreover, it was observed that modification of both aqueous and organic phases lead to a significant increase in fructose conversion and 5-HMF yield. At 170 ^{o}C, 10 wt % fructose in water: DMSO (1:1 w/w) and 4 minutes reaction time, 95% fructose conversion and 85% 5-HMF yield was obtained with HCl at pH 1 in combination with 2 equivalent of 2-butanol/MIBK (3:7 w/w) (Chheda et al., 2007).

Table 2.9: Dehydration of Fructose and Glucose in Two-Phase Systems, Catalysed by Heterogeneous Catalysts

Temp ^{o}C	Time (Min)	Reaction Solvent	Extraction Solvent	Catalyst	Conversion (%)	Yield (%)	Reference
120[a]	60	H_2O	MIBK	6.7 wt % $Ag_3PW_{12}O_{40}$	84	75	Fan et al., 2011
170[a]	120	H_2O	MIBK	67 wt % Al-TUD-1	76	20	Lima et al., 2010
115[a]	60	H_2O	MIBK	20 wt % $Cs_{2.5}H_{0.5}PW_{12}O_{40}$	78	74	Zhao et al., 2011
76[a]	-	DMSO	MIBK	Fixed bed IE resin (acidic)	-	97	Gaset et al., 1986
130[b]	240	H_2O	MIBK	13 wt % $Ag_3PW_{12}O_{40}$	90	76	Fan et al., 2011
180[b]	2	H_2O	MIBK	Fixed bed TiO_2	-	29	McNeff et al., 2010
180[b]	2	H_2O	MIBK	Fixed bed ZrO_2	-	21	McNeff et al., 2010

[a]Fructose. [b]Glucose.

In addition, Chheda & Dumesic, (2007) studied different water/NMP and water/DMSO mixtures with either DCM or MIBK as extraction solvent. Fructose dehydration was catalysed by the acidic ion-exchange resin DIAION PK216 with fructose concentration of 10 wt% at 90 and 120 ^{o}C. With MIBK as extraction solvent, a fructose conversion of 98% and 83% yield of 5-HMF was obtained at 90 ^{o}C in 4:6 (w/w) H_2O/NMP after 18 hours. As feed concentration decreases, an increase in selectivity, NMP or DMSO content and increase in extraction solvent

was observed (Roman-Leshkov et al., 2006; Chheda et al., 2007; Chheda & Dumesic, 2007, Jan van Putten et al., 2013).

2.5.5 Synthesis in Ionic Liquids

To date, molecular solvents are used in carrying out most chemical reaction processes but recently, a new class of green solvents known as "ionic liquids" has emerged. This new class of green solvent also termed designer solvents are entirely made up of ionic species (cation and anion) and are fluids at room temperature (Earle and Seddon, 2000). As a result of fascinating properties such as non-flammability, extremely low vapour pressure, adjustable solvent power, emitting no volatile organic compounds (VOCs), low melting points, high chemical and thermal stability, ionic liquids have generated fundamental interest to all scientists (Earle and Seddon, 2000).

Ionic liquids are known as powerful solvents for conversion of biomass-derived sugars and have adjustable solvent power because they can be designed to suit a particular set of reaction properties in mind hence, termed "designer solvents". Simple changes to the structure of the ions can change reaction properties such as viscosity, hydrophobicity, density and melting point (Earle and Seddon, 2000). Some of the advantages of ionic liquids as solvent in the production of 5-HMF from biomass-derived sugars include; reduction in water content thereby reducing decomposition of 5-HMF to formic and levulinic acid. It also reduces the formation of insoluble amorphous polymers known as humins. Table 2.10 – 2.12 show a

summary of selected published results on dehydration of fructose and glucose to 5-HMF in ionic liquids.

Table 2.10: Dehydration of Fructose to 5-HMF in Ionic Liquids in the Absence of Additional Catalyst

Temp ^{o}C	Time (min)	Solvent	Conversion (%)	Yield (%)	Reference
120	180	[EMIm]Cl	100	78	Stahlberg et al., 2011
80	60	[HMIm]Cl	97	70	Hu et al., 2008
80	60	[BMIm]HSO4	100	57	Hu et al., 2008
140	50	[BMIm]Cl	100	60	Cao et al., 2011
140	50	[HMIm]Cl	85	22	Cao et al., 2011

Chidambaram and Bell, (2010) reported a two-step approach for the catalytic conversion of glucose to 2,5-DMF in ionic liquids. Heteropoly acids such as 12-molybdophodphoric acid (12-MPA), 12-tungstophoric acid (12-TPA) were reported to be good and selective catalysts for the conversion of glucose to 5-HMF. In addition, acids such as H_2SO_4, HCl, H_3PO_4, CF_3COOH, HNO_3 and CH_3SO_3H were also used as catalysts in glucose dehydration in ionic liquids and the composition of the liquid acid determines the conversion of glucose to 5-HMF and by-products. In their research work, the ionic liquid used for glucose dehydration was 1-butyl-3-methylimidazolium chloride [BMImCl]. Comparing the solid acid catalysts to liquid acid catalysts under same reaction conditions, it was reported that the solid acid catalysts gave more conversion, yield, higher 5-HMF selectivity and less by-products (Chidambaram and Bell, 2010).

In addition to the use of ionic liquids in biomass conversion to 5-HMF, Cao et al., (2011) have investigated the conversion of hexose into 5-HMF in imidazolium ionic liquids with and without a catalyst. In this research work, both fructose and glucose were converted into 5-HMF in various imidazolium ionic liquids such as 1-butyl-3-methylimidazolium chloride (BMImCl), 1-butyl-2,3-dimethylimidazolium chloride (BdMImCl), 1-benzyl-3-methylimidazolium chloride (BeMImCl), 1-hexyl-3-methylimidazolium chloride (HMImCl), 1-butyl-3-methylimidazolium p-toluenesulfonate (BMImPS) and 1-octyl-3-methylimidazolium chloride (OMImCl) (Cao et al., 2011).

Table 2.11: Dehydration of Fructose and Glucose to 5-HMF in Ionic Liquids, Catalysed by Homogeneous Catalysts.

Temp ^{o}C	Time (min)	Solvent	Catalyst	Conversion (%)	Yield (%)	Reference
120[a]	180	[BMIm]Cl	7 mol % $AuCl_3$	98	48	Wei et al., 2011
80[a]	180	[EMIm]Cl	6 mol % $CrCl_2$	100	60	Zhang et al., 2011
100[a]	120	[BMIm]Cl	10 mol % $CrCl_3.6H_2O$	100	75	Cao et al., 2011
100[a]	120	[BenzylMIm]Cl	10 mol % $CrCl_3.6H_2O$	100	71	Cao et al., 2011
100[a]	50	[HMIm]Cl	25 mol % H_2SO_4	100	82	Cao et al., 2011
100[a]	50	[HMIm]Cl	10 mol % H_2SO_4	100	83	Cao et al., 2011
100[b]	60	[BMIm]Cl	3.6 wt % $CrCl_3$	-	17	Li et al., 2009
120[b]	180	[BMIm]Cl	1 mol % CF3SO3H	87	40	Chidambaram & Bell, 2010
120[b]	180	[BMIm]Cl	1 mol % CF3COOH	58	44	Chidambaram & Bell, 2010
100[b]	180	[EMIm]Cl	6 mol % $CrCl_2$	93	62	Zhang et al., 2011

[a]Fructose. [b]Glucose.

Their result shows that the reactivity of both fructose and glucose were affected by the type of anions and alkyl groups of imidazolium cations (Cao et al., 2011). In addition, BMImCl and BeMImCl gave higher 5-HMF yields compared to other four ionic liquids (HMImCl, OMImCl, BdMImCl and BMImPS) which could not achieve more than 25% of 5-HMF yield

without a catalyst. In the presence of a catalyst such as sufficient quantities of sulphuric acid or $CrCl_3$, about 60-80% of 5-HMF yield were achieved in BdMImCl, HMImCl and BMImPS (Cao et al., 2011).

Furthermore, Qi et al., (2012) reported the synergistic conversion of glucose into 5-hydroxymethylfurfural in ionic liquid-water mixtures using ZrO_2 as a catalyst. The results reported in this work shows that the formation of 5-HMF from glucose was promoted by the addition of water (10-50 wt%) into 1,3-dialkylimidazolium chloride ionic liquid compared with that in the pure ionic liquid or pure water (Qi et al., 2012). Also, the researchers reported that 5-HMF formation was promoted by 1,3-dialkylimidazolium ionic liquids having HSO_4^- or Cl^- anions and 53% 5-HMF yield was obtained at 200^{o}C reaction temperature, 10 min reaction time and 50:50 w/w% water – 1-hexyl-3-methylimidazolium chloride mixture catalysed by ZrO_2 (Qi et al., 2012).

Table 2.12: Dehydration of Fructose and Glucose to 5-HMF in Ionic Liquids, Catalysed by Heterogeneous Catalysts.

Temp ^{o}C	Time (min)	Solvent	Catalyst	Conversion (%)	Yield (%)	Reference
80[a]	10	[BMIm]Cl	100 wt % Amberlyst 15	99	83	Qi et al., 2009
80[a]	1920	[BMIm]BF4/DMSO (5:3 v/v)	200 wt % Amberlyst 15	-	87	Lansalot-Matras & Moreau, 2003
25[a]	360	[BMIm]Cl/MeOH (6.6:1 n/n)	100 wt % Amberlyst 15	93	82	Qi et al., 2009*
80[a]	1920	[BMIm]BF4/DMSO (5:3 v/v)	100 wt % Amberlyst 15	-	75	Lansalot-Matras & Moreau, 2003
80[a]	180	[BMIm]BF4	267 wt % Amberlyst 15	-	52	Lansalot-Matras & Moreau, 2003
120[b]	180	[BMIm]Cl	1 mol % $H_3PW_{12}O_{40}$	82	66	Chidambaram & Bell, 2010
120[b]	180	[BMIm]Cl	1 mol % $H_3PMo_{12}O_{40}$	71	63	Chidambaram & Bell, 2010

[a]Fructose. [b]Glucose.

2.6 2,5-Dimethylfuran as a Biofuel Candidate

The search for renewable biofuel alternatives has never ceased even though there are limited fuels derived from biomass which can compete with fossil fuels (Tian et al., 2011). Fossil fuels are widely used in the transportation sector but due to instability in price, environmental legislation and high emissions, 2,5-DMF has been of interest to the scientific research community. This is because 2,5-DMF has several advantages compared to ethanol as a gasoline-alternative biofuel. As shown in Table 2.13, the lower heating value of 2,5-DMF is much closer to gasoline and roughly 1/3 higher than ethanol. As a result of its lower heating value, it improves mileage for the same size of fuel tank (Tian et al., 2011). Secondly, the boiling point of 2,5-DMF is higher than that of ethanol thus, making it less volatile and also to be used practically as a transportation fuel. Thirdly, 2,5-DMF insoluble in water and easier to store unlike ethanol which is highly soluble. Fourthly, the heat of vaporisation of 2,5-DMF is closer to that of gasoline thus overcoming the cold starts problems seen with ethanol (Tian et al., 2011).

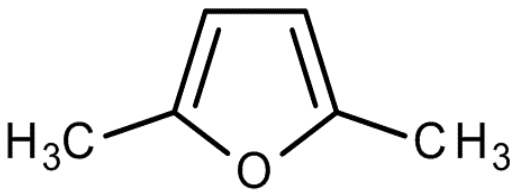

Figure 2.11: Structure of 2,5-Dimethylfuran (2,5-DMF)

2.6.1 Properties of 2,5-DMF

This section describes the physical, chemical, toxicological and mechanical properties of 2,5-DMF. Although, the physical properties of 2,5-DMF have been established for a long time; the reverse is the case for its chemical, toxicological and mechanical properties.

2.6.1.1 Physical Properties

2,5-Dimethylfuran is also known as 2,5-Dimethylfurane or 2,5-Dimethyloxole. 2,5-DMF is a furan derivative with molecular formula C_6H_8O and linear structural formula $(CH_3)_2C_4H_2O$. 2,5-DMF is a heterocyclic compound which is insoluble in water. It is a colourless liquid with spicy and smokey aroma and has a molecular mass of 96.13g/mol. The calorific value of 2,5-DMF is 30.4MJ/L and has a boiling point of (92-94^{o}C). Due to its boiling point, it is less volatile and less hygroscopic which makes it a liquid fuel. DMF has a density of 0.903g/ml at 25^{o}C and a refraction constant of 1.441 at 20^{o}C (Matkovskiy and Sedov, 2011).

Table 2.13: Main Properties of 2,5-DMF, Ethanol and Gasoline. (Tian et al., 2011)

Name (s)	2,5- Dimethylfuran Dimethylfurane 2,5-Dimethyloxole	Gasoline Petrol	Ethanol Ethyl Alcohol Ethyl hydroxide
CAS Number	625-86-5	8006-61-9 86290-81-5	64-17-5
Molecular Formula	C_6H_8O	$C_2 - C_{14}$	C_2H_6O
Molecular Mass	96.13g/mol	100-105g/mol	46.07g/mol
Water Solubility (25°C)	Insoluble	Insoluble	Highly Soluble
Relative Vapour Density	3.31	3-4	1.59
Structural formula	$(CH_3)_2C_4H_2O$	Variable	CH_3OCH_3
Safety	Flammable, Irritant	Highly Flammable, Irritant	Flammable, Irritant, CNS effect
Type of Substance	Heterocyclic	Aliphatic hydrocarbon mixture	Acyclic
Aroma	Spicy Smokey	Petroleum odour	Vinous
Lower Heating Value	33.7MJ/kg	42.9MJ/kg	26.9MJ/kg
Heat of Vaporization	332KJ/kg	373KJ/kg	840KJ/kg
RON	119	95	110
Molecule Schematic	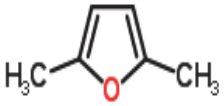	Variable	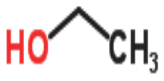

2.6.1.2 Chemical Properties

2,5-DMF is known to be an aromatic heterocyclic molecule which is made up of very strong C-H bonds. The C-H bonds are located between the methyl groups and ring carbon atoms and between hydrogen atoms and ring carbon atoms (Simmie and Würmel, 2013). The C-H bonds on the side-chain are considerably weaker (Simmie and Curran, 2009). 2,5-DMF is produced from 5-HMF via catalytic hydrogenation/hydrogenolysis reaction and has approximately 40% higher energy density compared to ethanol (Roman-Leshkov et al., 2007; Luque et al., 2008; Daniel et al., 2012).

In 1985, Grela and coworkers pioneered the stability of the furan ring present in 2,5-DMF structure (Grela et al., 1985; Simmie and Würmel, 2013). The authors investigated the very-low-pressure pyrolysis of 2,5-DMF, 2-methylfuran and furan and observed that the rate of decomposition is boosted by increase in methylation. Moreover, the thermal decomposition of 2,5-DMF behind reflective shock waves between 1070 to 1370 K was investigated by Lifshitz and colleagues (Lifshitz et al., 1998). The authors found over 20 intermediates; with 2-methylfuran and carbon monoxide to be the only oxygen-containing compounds present.

Furthermore, Matsumoto, (2011) studied the reaction kinetics of ozone with 2,5-DMF in a flow-tube reactor at room temperature. It was observed that 2,5-DMF is noticeably more reactive than either 2-methylfuran or furan. The authors also show that ozonolysis is more dangerous than the hydroxyl reactions in defining the atmospheric fate of 2,5-DMF because ozone are active all day while ·OH reactions are only effective during daylight (Matsumoto, 2011; Simmie and Würmel, 2013).

2.6.1.3 Toxicological Properties

The potential benefits of 2,5-DMF as a biofuel cannot be underestimated in the energy sector. In spite of this benefits, 2,5-DMF has recently generated concerns about its human health and downstream environmental impacts (Phuong et al., 2012; McKone et al., 2011; Luque et al., 2008). 2,5-DMF has been reported as an important metabolite present in the urine of humans exposed to hexane (Centres for Disease Control and Prevention, 2009; Phuong et al., 2012). Moreover, 2,5-DMF has also been identified as one of the important volatile organic compounds (VOCs) present in coffee vapour and cigarette (Alonso et al., 2010; Centres for Disease Control and Prevention, 2009; Perbellini et al., 2003). 2,5-DMF is known to be present in systemic blood, exhaled air and urine excreted by active and passive smokers of tobacco (Alonso et al., 2010). Although it is yet to be determined whether 2,5-DMF or any of its derivatives are associated with hexane neurotoxicity or smoking related diseases (Phuong et al., 2012).

Presently, there is little evidence to show that 2,5-DMF is biologically or environmentally toxic. Zeiger et al., (1992) showed that 2,5-DMF is not a mutagenic agent in the Ames bacterial tests and is probably not considered as a carcinogenic compound. However, it was recently discovered that 2,5-DMF caused chromosome aberrations in murine cell cultures, thus, considered to have a genotoxic action (Fromowitz et al., 2012). Furthermore, Phuong et al., (2012) investigated the ability of 2,5-DMF and combustion intermediates for potential persistence, bioaccumulation and aquatic toxicity (PBT) using PBT profiler. Their result shows that 2,5-DMF combustion intermediates had moderate or very high levels of aquatic toxicity while 2,5-DMF itself possess only moderate levels. They also observe that 9

out of 49 combustion intermediates are associated with 26 tumours and systematic diseases (Phuong et al., 2012; Simmie and Würmel, 2013).

In conclusion, the information reported on 2,5-DMF material safety data sheets (MSDS) shows that 2,5-DMF toxicity is similar to that of gasoline with regard to handling, safety, etc (Simmie and Würmel, 2013).

2.6.1.4 Mechanical Properties

Zhong et al., (2010) pioneered the combustion properties of 2,5-DMF, gasoline and ethanol in engines. The authors observed that the combustion properties of 2,5-DMF competes with that of gasoline and ethanol. They also showed that the regulated emissions (unburnt hydrocarbons, nitrogen oxides and carbon monoxide) generated in a single-cylinder gasoline direct-injection engine measure up with that of gasoline itself (Zhong et al., 2010). In addition to their investigations, they observed that there were no adverse effects on engine performance when pure 2,5-DMF was used as a fuel. Based on these observations, Zhong and coworkers concluded that no major alterations are required to an engine to change from gasoline to 2,5-DMF (Zhong et al., 2010).

To elaborate more on the combustion performance of 2,5-DMF in engines, Christensen et al., (2011) investigated a wide range of properties of blending gasoline with renewables. Such properties include; distillation, vapour pressure, density, vapour lock protection, viscosity, potential for extraction into water and octane rating (Christensen et al., 2011; Simmie and

Würmel, 2013). The authors observed that 2,5-DMF have a good potential and considered it as suitable candidate for blending with gasoline. Furthermore, Hu and coworkers showed that 2,5-DMF performed very well as an additive at the 4% level by volume and had a superior anti-friction and anti-ware properties than gasoline (Hu et al., 2012). Their result led Rothamer and Jennings to investigate 2,5-DMF/gasoline blends for engine knocking and observed that 2,5-DMF/gasoline blends displayed significant improvement over plain gasoline (Rothamer and Jennings, 2012).

Moreover, Daniel and colleagues conducted another study to investigate the ignition timing sensitivities of 2,5-DMF and gasoline in a direct-injection SI engine and showed that 2,5-DMF produced high exhaust-gas temperatures and had the potential to become an effective cold-start fuel (Daniel et al., 2012). In the same year, Daniel and coworkers investigated the concentrations of carbonyl compounds (ketones and aldehydes) and hydrocarbons in the exhaust of a single-cylinder direct-injection spark ignition engine (Daniel et al., 2012b). The authors observed that 2,5-DMF had the lowest overall carbonyl emissions compared to ethanol, methanol, gasoline and n-butanol.

With the limited reports on the combustion performance of 2,5-DMF in the literature, it has been established that 2,5-DMF is a suitable candidate in engines either as a blend with gasoline or on its own. It has also been demonstrated that there is no need for a major modification to an engine to change from gasoline to 2,5-DMF fuel.

2.7 Production of 2,5-Dimethylfuran

This section describes different methods or catalytic systems that have been used for 2,5-DMF production from biomass-derived sugars.

2.7.1 Synthesis in Biphasic Systems

The catalytic conversion from sugars to fuel can be more efficient and less expensive than biological methods (Schmidt and Dauenhauer, 2007). Roman-Leshkov and co-workers are known to be the first set of researchers to introduce the catalytic strategy of converting fructose to 2,5-Dimethylfuran via 5-Hydroxymethylfurfural (Roman-Leshkov et al., 2007). The catalytic strategy involves the selective removal of five oxygen atoms from fructose in two steps; firstly, three oxygen atoms were removed by acid-catalysed dehydration reaction in a biphasic reactor at 180^{o}C to produce 5-hydroxymethylfurfural (5-HMF). They used low boiling point solvents that are excellent fuel components themselves for the acid-catalysed dehydration of fructose in a biphasic reactor. This method shows that HMF can be produced in high yields and also eliminating the need for expensive separation steps to produce the final liquid fuel mixture (Roman-Leshkov et al., 2007).

In their research work, fructose and the acid catalyst are in the reactive aqueous phase in the biphasic reactor while the extracting phase is made up of a partially miscible organic solvent (such as butanol) which is used for continuous extraction of the 5-HMF product. Moreover, their work reported that the partitioning of the 5-HMF into the extracting phase

improved by adding a salt (NaCl) to the aqueous phase and this leads to increased 5-HMF yields in the absence of high boiling point solvents (Roman Leshkov et al., 2007).

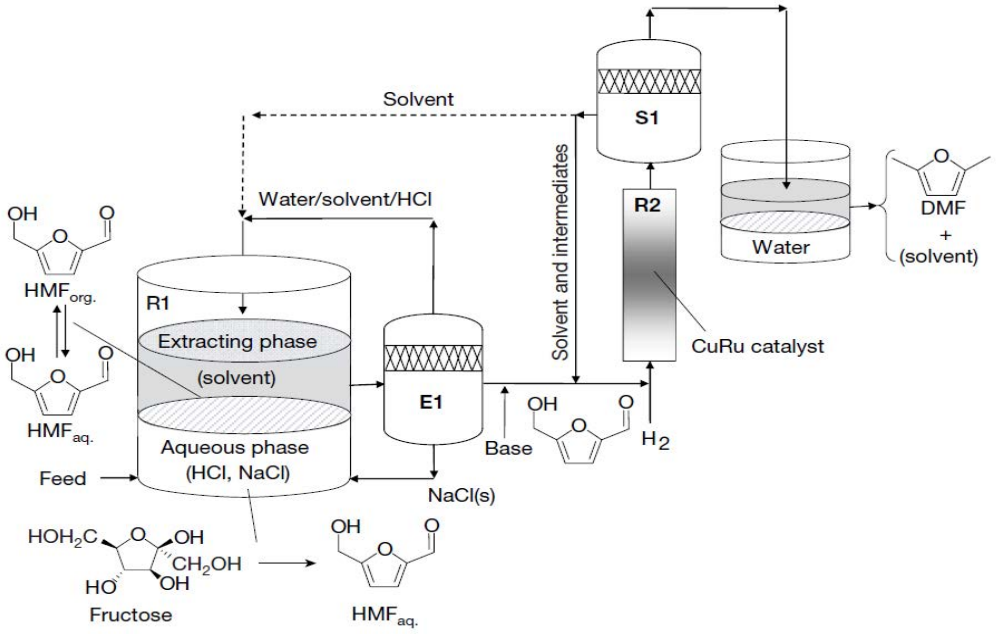

Figure 2.12: Schematic diagram of the process for conversion of fructose to 2,5-DMF.

Figure 2.12 shows fructose dehydration to produce 5-HMF using a biphasic reactor (R1); HCl and water are evaporated from the solvent which contains 5-HMF, resulting to NaCl precipitation (E1); 5-HMF hydrogenation to 2,5-DMF using CuRu catalyst (R2); 2,5-DMF separation from extracting solvent and unreacted intermediates (S1). **(Roman-Leshkov et al., 2007).**

Secondly, two oxygen atoms were removed by hydrogenolysis of 5-HMF to produce 2,5-DMF. The C-O bond in the 5-HMF undergoes hydrogenolysis over a copper-ruthenium (CuRu) catalyst. Roman-Leshkov et al (2007) developed a chloride–resistant carbon-supported copper-ruthenium (CuRu/C) catalyst to ease poisoning of the copper catalyst. In the presence of chloride ions, they observed that a carbon-supported ruthenium catalyst (Ru/C) was resistant to deactivation hence 5-HMF was converted to 2,5-dihydroxymethyltetrahydrofuran. Moreover, the mixture of copper and ruthenium creates a two-phase system in which the ruthenium phase

was coated with the copper phase due to the lower surface energy of copper to ruthenium and also because ruthenium and copper are immiscible (Roman-Leshkov et al., 2007).

A 2,5-DMF yield of 71%, 4% 2-methylfuran (MF) and 12% intermediates were produced from the liquid-phase hydrogenolysis of 5-HMF using a 3:1 (atomic ratio) Cu:Ru/C catalyst, 220^{o}C reaction temperature, 6.8 bar initial hydrogen pressure, stirring speed of 400 rpm and 10 hours reaction time. Also, a vapour-phase hydrogenolysis experiment was carried out using a flow reactor to wipe out the effects of chloride ions on CuRu/C. 2,5-DMF yield of 76-79% and ~5% intermediates were observed for 1.5 and 10 wt% 5-HMF feeds using a 3:2 Cu:Ru/C catalyst (Roman-Leshkov et al., 2007). Thus, Roman et al hypothesized that the CuRu/C catalyst may exhibit ruthenium-like chlorine resistance combined with copper-like hydrogenolysis behaviour.

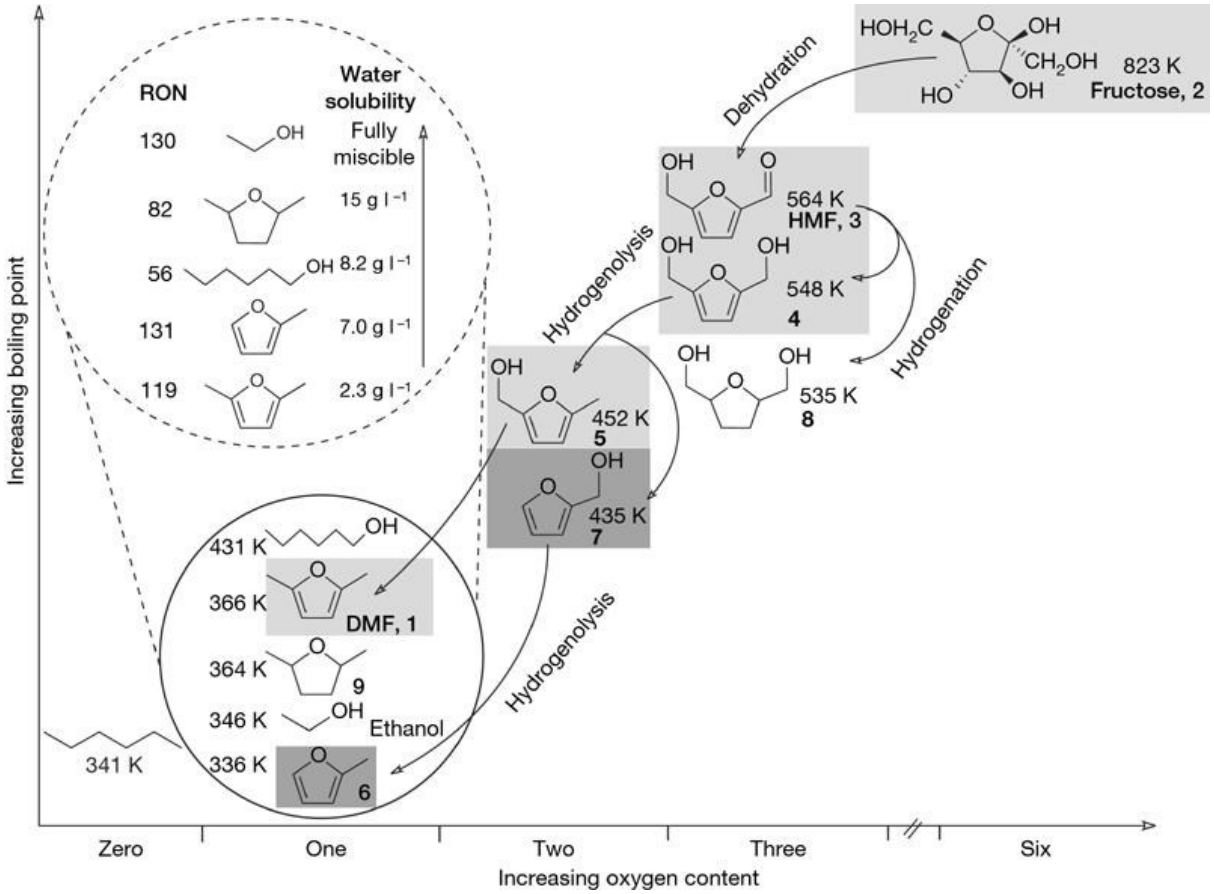

Figure 2.13: Normal boiling points of representative C6-hydrocarbons formed by removal of oxygen atoms from hexoses, compared to the normal boiling point of ethanol. (Roman-Leshkov et al., 2007).

2.7.2 Synthesis in N,N-Dimethylacetamide

Binder and Raines (2009) reported the transformation of lignocellulosic biomass into furans for fuels and chemicals. Their strategy involves synthesising 5-HMF from untreated lignocellulosic biomass, purified glucose, fructose and cellulose in a single step using N,N-dimethylacetamide (DMA) containing lithium chloride (Binder and Raines, 2009). The authors showed that the biomass components present in cellulose such as protein and lignin does not have a negative effect on the conversion of cellulose into 5-HMF. It was observed that the

method used for the production of 2,5-DMF from 5-HMF here is very similar to that reported by Dumesic and co-workers because the same reaction solvent, hydrogen source, reaction temperature and catalyst were used.

The process of 2,5-DMF synthesis from lignocellulosic biomass using this method involves two chemical reaction steps. The first step involves the production of 5-HMF from untreated corn stover using DMA-LiCl solvent system and the chloride ions present in the crude 5-HMF was removed by ion-exclusion chromatography. The removal of the chloride ions from the crude HMF is necessary so as to prevent the chloride from poisoning the copper hydrogenolysis catalyst (Binder and Raines, 2009). Secondly, the crude 5-HMF from corn stover was subjected to hydrogenolysis using 1-butanol and a carbon-supported copper-ruthenium catalyst. It is believed that the 5-HMF used contains trace amounts of chloride and a 49% molar yield of 2,5-DMF was obtained which is similar to that obtained by Dumesic's group. Furthermore, based on the cellulose content of the stover, the overall molar yield of 2,5-DMF obtained was 9% (Binder and Raines, 2009).

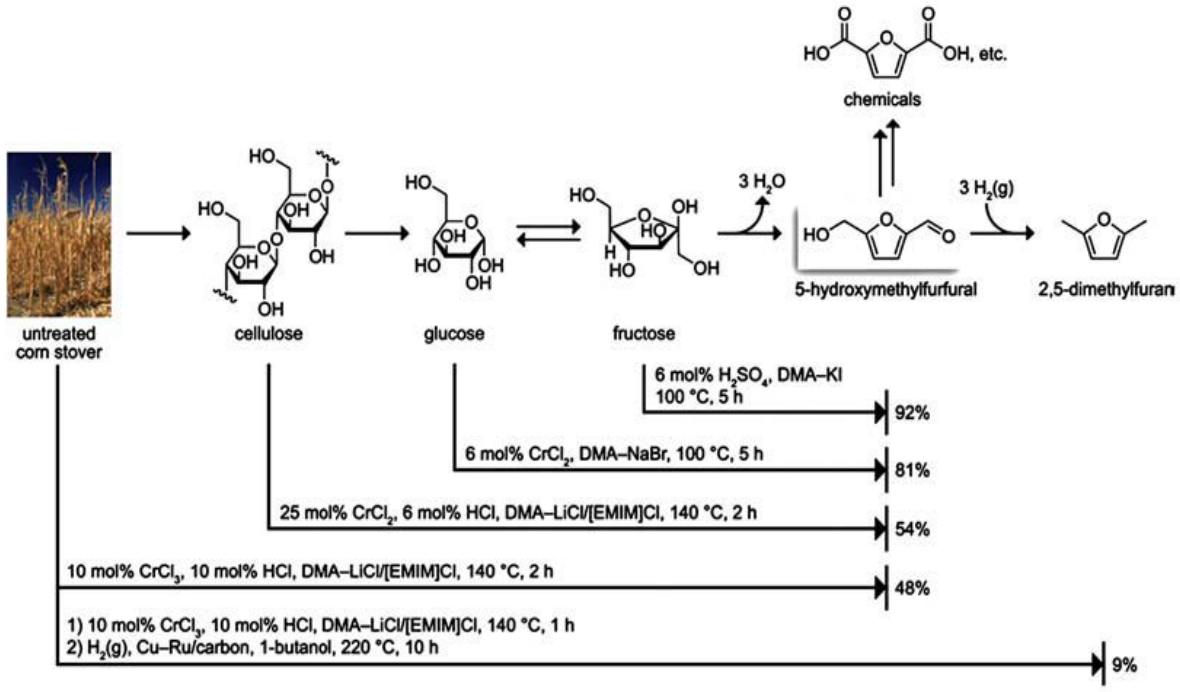

Figure 2.14: Schematic diagram of 2,5-DMF production in DMA (Binder and Raines, 2009).

2.7.3 Synthesis in Supercritical Methanol

Renewable feed stocks are required to obtain transportation fuels and chemicals since fossil fuels release significant amount of CO_2 after combustion. Hansen and co-workers reported a one-pot strategy to reduce 5-hydroxymethylfurfural via hydrogen transfer from supercritical methanol (Hansen et al., 2012). Hansen's research group is believed to be the first set of researchers to report the reduction of 5-HMF to 2,5-DMF in a supercritical solvent. 5-HMF was successfully converted to 2,5-dimethylfuran, dimethyltetrahydrofuran and 2-hexanol in good yields over a Cu-doped porous metal oxide in supercritical methanol. The hydrogen needed for this reduction was generated in situ from the supercritical methanol over the multifunctional Cu-PMO catalyst.

The Cu-doped porous metal oxide is a hydrotalcite catalyst precursor which has been successfully used in different chemical reactions, such as reduction reactions. Other suitable metal ions such as $Fe^{3+,}$ Ga^{3+}, Ni^{3+} etc can also be doped with porous metal oxide (Aramendia et al., 2003; Polato et al., 2008; Hansen et al., 2012). Before Hansen and coworkers reported the use of Cu-doped PMOs, some researchers have successfully proven the positive effect of Cu-doped PMOs in one step-one pot depolymerisation of organosolv lignin (Holladay et al., 2007) by extensive hydrogenation/deoxygenation in supercritical methanol (Sc-MeOH) (Hansen et al., 2012).

The results obtained by Hansen's group shows that a combined yield of 61% to DMF, DMTHF and 2-hexanol was achieved at 300^{o}C reaction temperature and 120 minutes reaction time (Hansen et al., 2012). Also, 48% yield of 2,5-DMF was obtained at 260^{o}C reaction temperature and 41% 2,5-DMF yield at 240^{o}C after 3 hours reaction time. Moreover, it was reported that there was no formation of higher boiling side products and undesired char from HMF under these reaction conditions (Hansen et al., 2012). The strategy reported here is very attractive but the selective transformation of 5-HMF to 2,5-DMF and DMTHF remains a huge challenge as it requires a C-O bond cleavage and also the amount of undesired side products should be reduced significantly.

2.7.4 Synthesis using Formic Acid as a Reagent

The use of formic acid as a hydrogen carrier and as a means of utilising carbon dioxide has recently generated a lot of interest in the area of green chemistry. Formic acid is one of the

by-products obtained from biomass degradation and is also produced industrially by hydrogenation of carbon dioxide, as well as the hydration of carbon monoxide (Reutemann and Kieczka, 2005). Thananatthanachon and Rauchfuss, (2010) are believed to be the first set of researchers to carry out the one pot synthesis of 2,5-DMF from fructose using formic acid as reagent. The strategy used here involves a single process whereby several steps could be conducted in one pot and the key to this strategy is the use of formic acid which serves as an acid catalyst, deoxygenation agent and a source of hydrogen (Thananatthanachon and Rauchfuss, 2010).

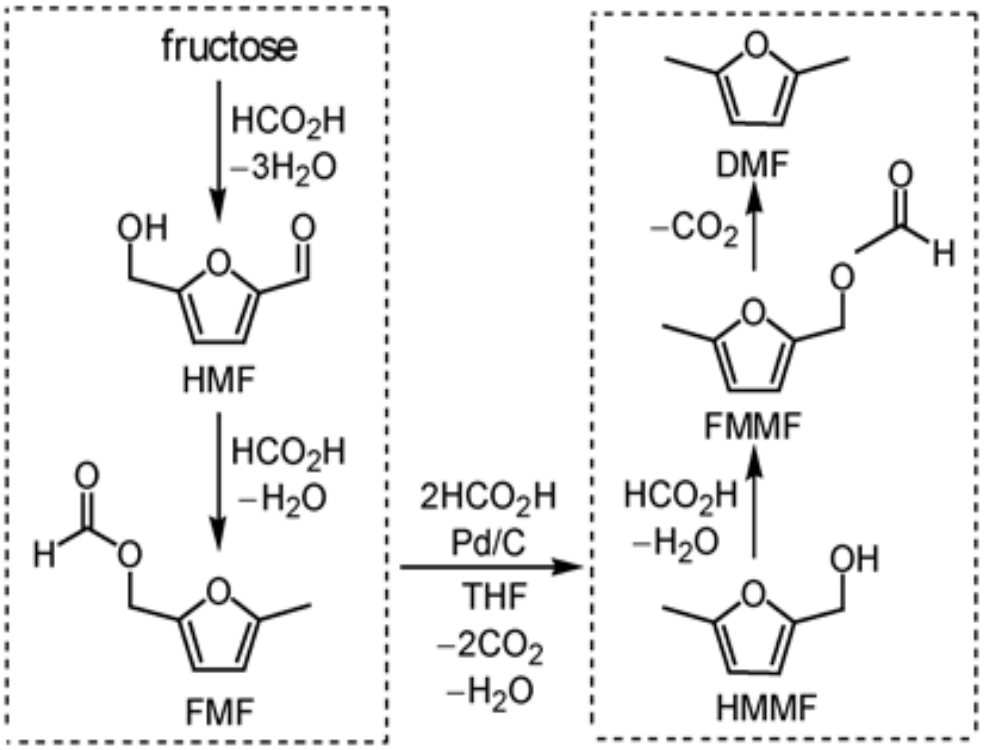

Figure 2.15: One-pot process to generate 2,5-DMF from fructose (Thananatthanachon and Rauchfuss, 2010).

In this one-pot process, the first reaction was to convert fructose to 5-HMF via acid catalysed dehydration at 150^{o}C reaction temperature and 2 hours reaction time. Secondly, the

5-HMF produced was subjected to hydrogenation/hydrogenolysis in refluxing tetrahydrofuran (THF) in the presence of 5wt% palladium on carbon (Pd/C) with sulphuric acid as additive at 70^{o}C reaction temperature and 15 hours reaction time (Thananatthanachon and Rauchfuss, 2010). The results obtained by these researchers shows a 95% yield of 2,5-DMF. The use of formic acid as a hydrogen source in their research work is otherwise referred to as catalytic transfer hydrogenation reaction instead of molecular hydrogen used by Roman-Leshkov and co-workers.

In addition, another set of researchers reported one-pot conversion of lignocellulosic and algal biomass into liquid fuels using a multicomponent catalytic system comprising $[DMA]^{+}[CH_3SO_3]^{-}$ (DMA = N,N-dimethylacetamide), ruthenium on carbon support catalyst (Ru/C) and formic acid as hydrogen source (De et al., 2012). The difference between their research work and that reported by (Thananatthanachon and Rauchfuss, 2010) is the 5 wt% Ru/C catalyst used instead of the 5wt% Pd/C used by the latter. De and co-workers revealed the effectiveness of the Ru/C catalyst for the first time for 2,5-DMF synthesis from readily abundant biomass sources (De at al., 2012).

The first step of the one-pot reaction involves synthesis of 5-HMF in-situ from fructose using formic acid (FA) as acid catalyst at 150^{o}C reaction temperature and 120 minutes reaction time and the $[DMA]^{+}[CH_3SO_3]^{-}$ (DMA = N,N-dimethylacetamide) catalyst for cellulose and untreated biomass (De et al., 2012). The second step involves the transformation of 5-HMF to 2,5-DMF by hydrogenation and hydrogenolysis reactions using formic acid and Ru/C catalyst. The results show that the Ru/C catalyst is quite effective and a maximum 2,5-DMF yield of

30% was obtained from fructose and 27% 2,5-DMF yield from agar. Similarly, using microwave irradiation as heating source, the maximum yield of 2,5-DMF obtained was 32%.

Furthermore, their result shows that α-cellulose, sugarcane bagasse and agar can be converted to 2,5-DMF using the BrØnsted-acidic ionic liquid catalyst the $[DMA]^+[CH_3SO_3]^-$,Ru/C catalyst, formic acid and sulphuric acid. The yield of 2,5-DMF obtained from α-cellulose is significantly lower than that obtained from fructose which could be due to the huge crystalline structure of α-cellulose, which is made up of a 3D network of hydrogen bonding interactions (Geboers et al., 2011; Van de Vyver et al., 2011). As a result, cellulose degradation into hexose units was carried out with a strong acidic ionic liquid catalyst $[DMA]^+[CH_3SO_3]^-$ (De et al., 2012).

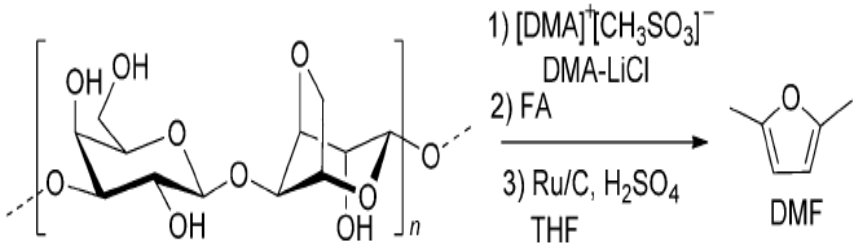

Figure 2.16: One pot conversion of microalgae-derived agar to 2,5-DMF (De et al., 2012).

2.7.5 Synthesis from a Sugar Mixture

The efficient production of furan derivatives from a sugar mixture by catalytic process was investigated by Zhang et al., (2012). Here, they present the results of an investigation targeted to identify catalysts for xylose and glucose dehydration to furfural and 5-HMF in a

diphasic reaction system. They further investigated the subsequent conversion of furfural and 5-HMF to 2-methylfuran (MF) and 2,5-DMF respectively.

With regards to xylose and glucose dehydration reaction, the authors prepared SO_4^{2-}/ZrO_2-TiO_2 solid catalysts by precipitation and impregnation method and investigated the effects of various reaction parameters and catalyst reuseability. A product yield of 54.3 mol % (furfural) and 30.9 mol % (5-HMF) was obtained under optimal experimental conditions (Zhang et al., 2012). Moreover, it was observed that the SO_4^{2-}/ZrO_2-TiO_2 catalyst could be recovered from the resulting product mixture and can be reused multiple times after calcination without any significant change on furfural and 5-HMF yield.

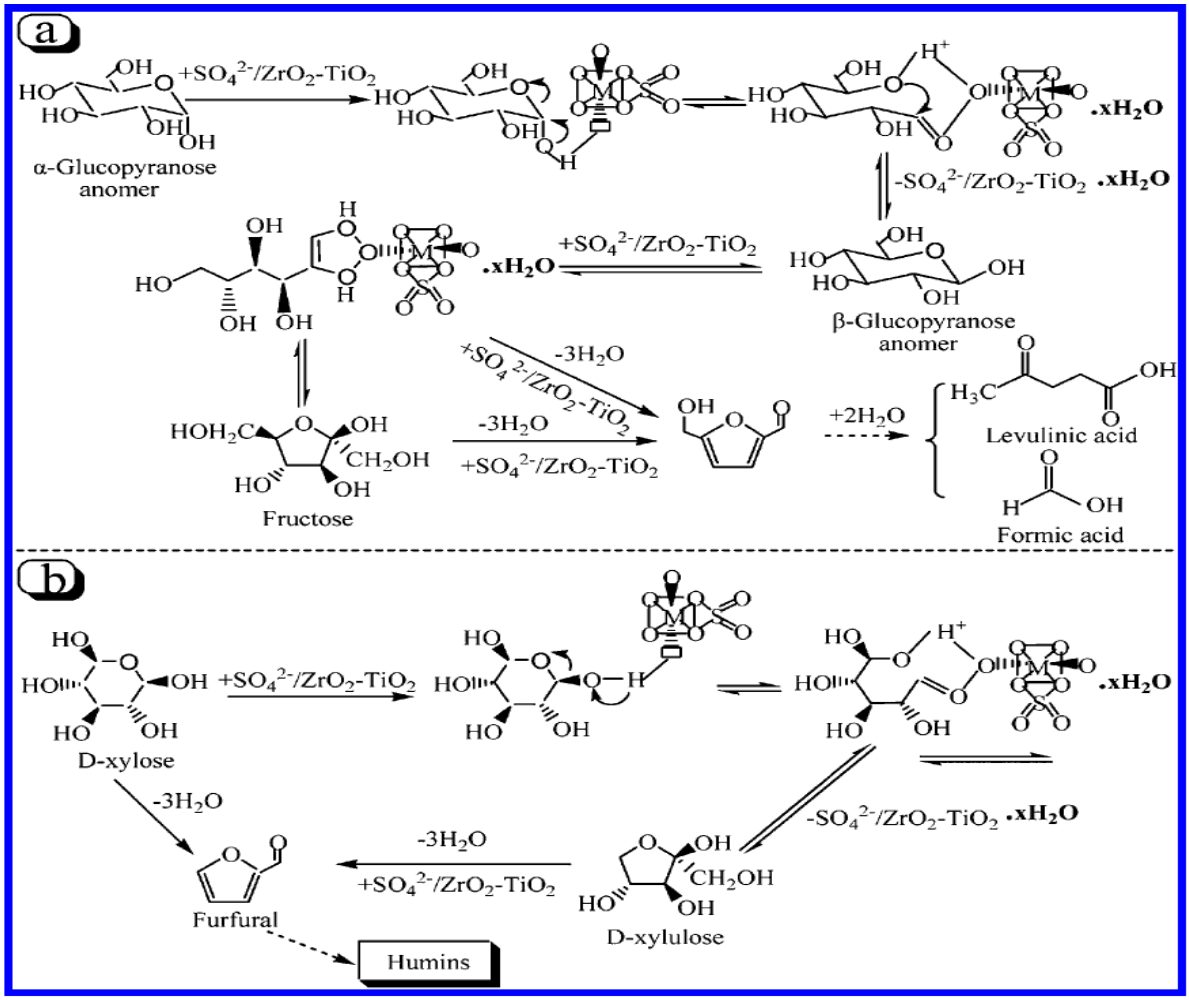

Figure 2.17: Proposed mechanism for the conversion of sugar mixtures to furfural by $SO4^{2-}/ZrO_2$-TiO_2 (Zhang et al., 2012).

Furthermore, the hydrogenation of furfural and 5-HMF was studied using either a neat mixture of furfural and 5-HMF or by xylose and glucose dehydration product obtained. The hydrogenation of furfural and 5-HMF was promoted in n-butanol as reaction system with carbon-supported ruthenium (Ru/C) as catalyst at different reaction temperature ranging between 180ºC – 260ºC. The highest yield obtained for 2-methylfuran and 2,5-DMF was 61.9 mol % and 60.3 mol % respectively using neat furfural and 5-HMF in pure n-butanol (Zhang et al., 2012).

However, when the furfural and 5-HMF produced from xylose and glucose dehydration was used for the hydrogenation reaction, the yield obtained for MF and 2,5-DMF was 17.5 and 32.7 mol % respectively. Their result indicated that the purification of the furfural and 5-HMF from the resulting product mixture is a key step for the further hydrogenation of furfural and 5-HMF to MF and 2,5-DMF respectively (Zhang et al., 2012).

2.7.6 Synthesis through Catalytic Transfer Hydrogenation in Alcohols

The use of molecular hydrogen for the hydrogenation reactions have been studied by several groups using various metal catalysts (Rao et al., 1999; Zheng et al., 2006; Roman-Leshkov et al., 2007; Sitthisa and Resasco, 2011). However, hydrogenation reaction which requires petroleum-derived H_2 is not entirely green nor economical due to the high-pressure H_2 required, therefore increasing the process costs. Recently, researchers are interested in an alternative route for the conversion of 5-HMF to 2,5-DMF through catalytic transfer hydrogenation reaction instead of molecular H_2.

Jae et al., (2013) reported the production of 2,5-DMF from 5-HMF through catalytic transfer hydrogenation with ruthenium supported on carbon. They investigated the catalytic transfer hydrogenation of 5-HMF using secondary alcohols (such as 2-propanol, butanol) and up to 80% 2,5-DMF selectivity was obtained. The use of alcohols as hydrogen sources is important because they can be produced efficiently from biomass; and they can also be regarded as reactants and solvents.

Several investigators have reported the catalytic transfer hydrogenation of other biomass-derived molecules using secondary alcohols (Kobayashi et al., 2011; Gandarias et al., 2011; Chia and Dumesic, 2011). For example, the catalytic hydrogenation of levulinic acid and its esters to y-valerolactone using 2-butanol over ZrO_2 was reported by Chia and Dumesic with a yield of 92% (Chia and Dumesic, 2011). Also, Kobayashi and co-workers reported the catalytic transfer hydrogenation of cellulose to sorbitol and mannitol (sugar alcohols) using 2-propanol over Ru/C with a yield of 45% (Kobayashi et al., 2011). In addition, Gandarias and co-workers used 2-propanol for the hydrogenation of glycerol to 1,2-propanediol over a Ni-Cu/Al_2O_3 with 65% selectivity (Gandarias et al., 2011).

The catalytic transfer hydrogenation reaction of 5-HMF to 2,5-DMF was carried out at reaction temperatures lower than 100^{o}C and 2,5-DMF selectivity increased with increase in reaction temperature (Jae et al., 2013). 2,5-bis(hydroxymethyl)furan (BHMF) was the main product obtained at low reaction temperature and as temperature increased to 190^{o}C at 300 min reaction time, BHMF was completely converted to 2,5-DMF with up to 81% selectivity. Some of the identifiable by-products observed at 130^{o}C and 160^{o}C reaction temperatures are hydrogenated furans such as 5-methylfurfural, 5-methylfurfuryl alcohol (MFA), 2-methylfuran (MF) and furfuryl alcohol (FA) (Jae et al., 2013).

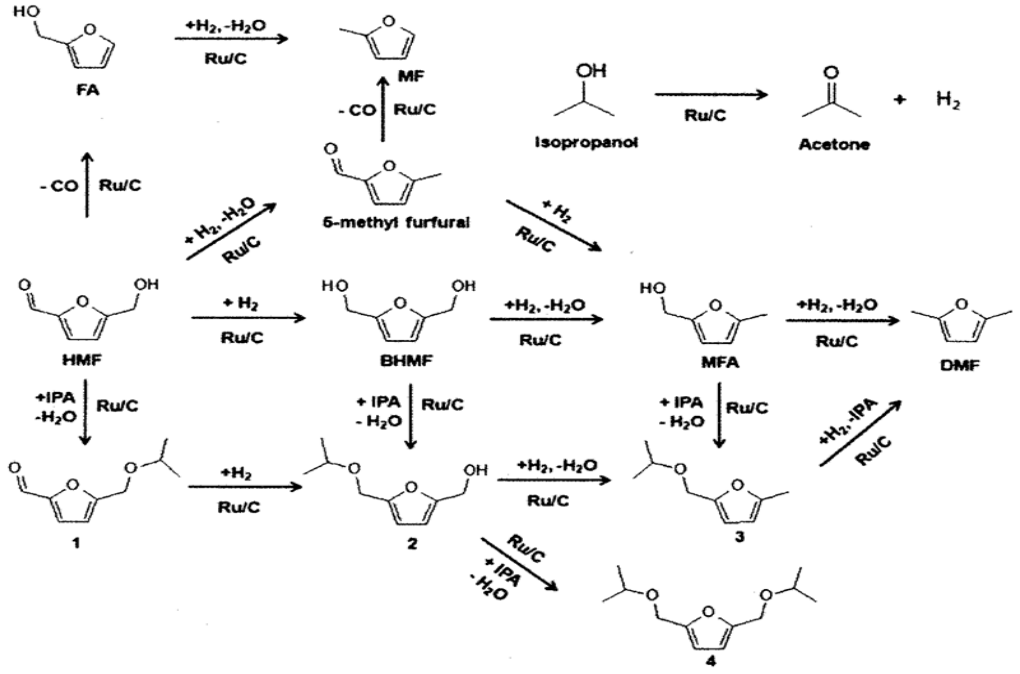

Figure 2.18: Reaction network of the hydrogenation of 5-HMF into 2,5-DMF using 2-propanol and Ru/C. (Jae et al., 2013).

2.7.7 Synthesis in Ionic Liquids

A two-step approach for the catalytic conversion of glucose to 2,5-dimethylfuran in ionic liquids was investigated by (Chidambaram and Bell, 2010). The authors identified catalysts for glucose dehydration to 5-hydroxymethylfurfural in ionic liquids and further conversion of 5-HMF to 2,5-DMF. The conversion of 5-HMF to 2,5-DMF was investigated using different metal catalysts (Ru, Pt, Pd, and Rh) supported on carbon and pure 1-ethyl-3-methylimidazolium chloride (EMImCl) as solvent. The 5-HMF conversion at 120^{o}C reaction temperature, 62 bar H_2 pressure, 600 rpm stirring speed and 60 minutes reaction time with acetonitrile as co-solvent gave a 2,5-DMF yield of 16% and 47% 5-HMF conversion using a

Pd/C catalyst. The authors attributed the lower yield of DMF to the lower reaction time, reaction temperature and low solubility of hydrogen in ionic liquids.

In the absence of acetonitrile as co-solvent, the conversion of 5-HMF after 60 minutes reaction time was 23% for Ru/C, 11% for Pt/C, 19% for Pd/C and 16% for Rh/C. Moreover, the highest 2,5-DMF selectivity obtained was 13% for Pd/C while Ru/C, Rh/C and Pt/C gave 0%, 6% and 2% 2,5-DMF selectivity respectively. Furthermore, apart from the desired product (2,5-DMF) obtained, five other known products (5-methylfurfural, 2,5-hexadione, 5-methylfurfuryl alcohol, 2,5-dihydroxymethlfuran and 5-methyltetrahydrofurfuryl alcohol) and little amounts of unknown products were also observed at this reaction conditions (Chidambaram and Bell, 2010).

In addition, the authors compared the hydrogenation of 5-HMF using three sources of 5-HMF and indicated that the 5-HMF source had a little effect on 5-HMF conversion or products distribution. Using the Pd/C catalyst, the neat 5-HMF resulted in 47% conversion and 32% 2,5-DMF selectivity while the extracted 5-HMF and 5-HMF in EMIMCl-CH_3CN resulted in 46% and 44% conversion with 2,5-DMF selectivity of 30% and 28% respectively. This means that glucose dehydration catalysed by 12-molybdophosphoric acid (12-MPA) will undergo hydrogenation reaction to form 2,5-DMF (Chidambaram and Bell, 2010).

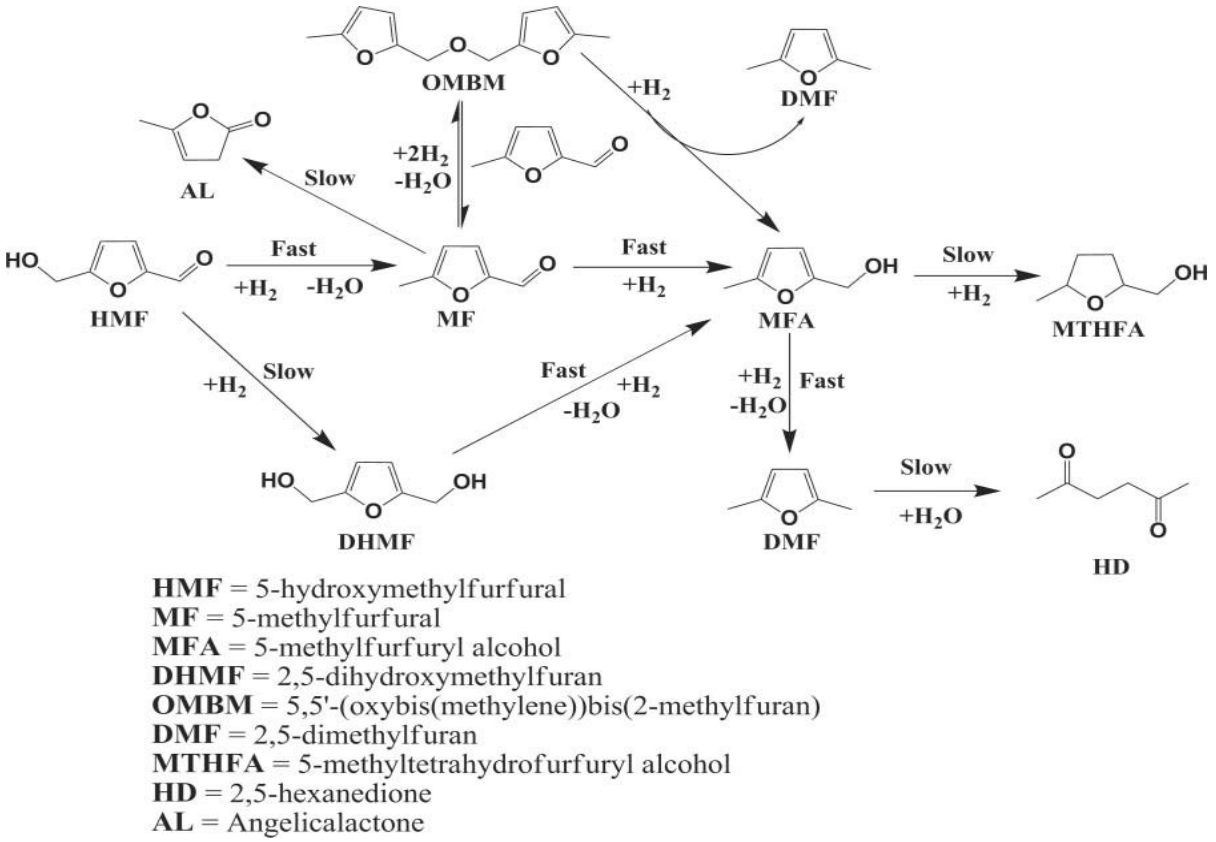

Figure 2.19: Reaction pathway for the hydrogenation of 5-HMF to 2,5-DMF in EMImCl and acetonitrile solvent using Pd/C as catalyst (Chidambaram and Bell, 2010).

2.7.8 Synthesis in Supercritical Carbon dioxide-Water System

The use of supercritical carbon dioxide as a solvent for chemical reactions provides a new medium in green chemistry. They possess several advantages such as low amount of by-products formed owing to side reactions, non-flammable, cost effective, non-toxic, low amount of VOC's in the atmosphere and perfect mixing of reagents in reactions involving gases. In addition, tuning the reaction temperature and pressure can enhance the selectivity and yield of the reaction (Chatterjee et al., 2014). Recently, the conversion of biogenic substrates in supercritical CO_2 was reported in the literature (Wu et al., 2010; Stevens et al., 2010; Bourne et al., 2007).

A tunable technique to 2,5-DMF synthesis from 5-HMF in supercritical carbon dioxide – water system was investigated by Chatterjee et al., (2014). Different metal catalysts (Pd, Ru, Pt, Rh) on various supports (mesoporous silica, activated carbon and alumina) was tested for 5-HMF hydrogenation. The optimum reaction condition reported in their study was 80^{o}C reaction temperature, 2 hours, 10 MPa CO_2 pressure, 1 MPa hydrogen pressure and catalyst was reused four times before a moderate decrease in activity. Among the catalysts investigated, Pd/C displayed the best catalytic activity with 5-HMF conversion of 100% and 2,5-DMF yield of 100%. So far in the literature, supercritical CO_2-water reaction medium gave the highest 2,5-DMF yield and also 5-HMF conversion.

The high yield of 2,5-DMF obtained with the Pd/C catalyst could be attributed to two factors. Firstly, as the reaction was conducted in water, the hydrophobic/hydrophilic nature of the support material might influence the catalytic behaviour. According to Chatterjee and co-workers, the TG/DTA of the Pd/C and other catalysts (Pd/MCM-41 and Pd/Al_2O_3) studied show that the hydrophobicity follows the order of C > MCM-41 > Al_2O_3, which could possibly be a reason for the highest activity of Pd/C and lowest activity of Pd/Al_2O_3, which has also been reported previously by Yamada and Goto, (2003) & Omota et al., (2005) (Chatterjee et al., 2014).

Secondly, the CO_2 pressure was observed to have a strong effect on the product distribution. The authors investigated 3 different CO_2 pressure regions (< 10 MPa, 10 MPa and > 10 MPa) hence, the reaction was conducted at 4, 10 and 16 MPa of CO_2 pressure in order to

gain insight into the phase behaviour during reaction and it was observed that using 10 MPa of CO_2 resulted in 100% yield of 2,5-DMF (Chatterjee et al., (2014). In addition, as the reaction was conducted in supercritical CO_2, the phase behaviour might be an important factor that contributed to the observed result. However, two phases (i) aqueous phase containing the dispersed catalyst and 5-HMF (bottom region) and (ii) CO_2-H_2 in gaseous state (upper region) were visible at 4 MPa CO_2 pressure. At 10 MPa, a different scenario was observed; where two immiscible liquid phases of (i) substrate-H_2O/catalyst (bottom region) and (ii) liquid phase (middle region) along with (iii) CO_2-H_2 in the gaseous state (Upper region) were observed. As a result of this observation at 10 MPa CO_2 pressure, the authors indicated and concluded that this scenario was favourable to 2,5-DMF formation, which is a hydrophobic product and can be separated continuously from water (Chatterjee et al., 2014; Roman-Leshkov et al., 2007). However, at 16 MPa, in comparison with the water/substrate-catalyst phase (bottom region), Chatterjee and co-workers observed that a large portion of the cell view was filled by CO_2-H_2 liquid phase (upper region) which ultimately favours further hydrogenation of 2,5-DMF to DMTHF.

Moreover, this reaction medium was also employed in furfural hydrogenation. Under the same reaction conditions, furfural was converted to 2-methyltetrahydrofuran (2-MTHF) within 2 hours. At 10 minutes reaction time, furfural was hydrogenated completely to 2-methylfuran. It was also observed that optimization of different reaction conditions, such as hydrogen pressure, CO_2 pressure changes the product profile (Chatterjee et al., 2014).

2.7.9 Synthesis from Electrocatalytic Hydrogenation of 5-HMF

Another novel medium reported for 2,5-DMF synthesis is the electrocatalytic hydrogenation of 5-HMF in the absence and presence of glucose (Kwon et al., 2013). This study investigated 5-HMF hydrogenation to 2,5-dihydroxymethylfuran (2,5-DHMF), 2,5-DMF and other products using different solid-monometallic electrodes. These solid-metal electrodes are used because they are very active for hydrogenation of glucose and this helps to understand the catalytic activity and selectivity by connecting the voltammetry and online product analysis (Kwon et al., 2013).

They studied three different groups of metal catalysts in their experiment: (1) metals that form 2,5-DHMF only (Ni, Fe, Zn, Ag, In and Cd), (2) metals that form 2,5-DHMF and other products depending on the potential applied (Pd, Bi, Al and Pb), and (3) metals that form other products only (Au, Co, Sb, Cu and Sn). In the absence of glucose, it was concluded that the presence of catalysts does not have a huge effect on 5-HMF hydrogenation because almost the same onset potentials (-0.5 ± 0.1 V) was displayed by all the catalysts. Thus, there is no clear relationship between the catalyst electronic structure and product distribution (Kwon et al., 2013). Although, all the catalysts tested showed different reaction pathways towards 2,5-DHMF and other products.

In the presence of glucose, a change in the distribution of 5-HMF reduction products was observed. For example, the onset potential of 2,5-DHMF shifted to -0.45 V on Fe, -0.51 V on Ag and -0.21 V on Ni in the presence of glucose while the onset potential of 2,5-DHMF

on Ni, Fe and Ag was -0.39 V in the absence of glucose. However, the delay observed on Fe and Ag onset potential was caused by the adsorbed glucose on the surface of the catalyst. This was not observed on Ni because glucose accelerated hydrogenation of 5-HMF (Kwon et al., 2013).

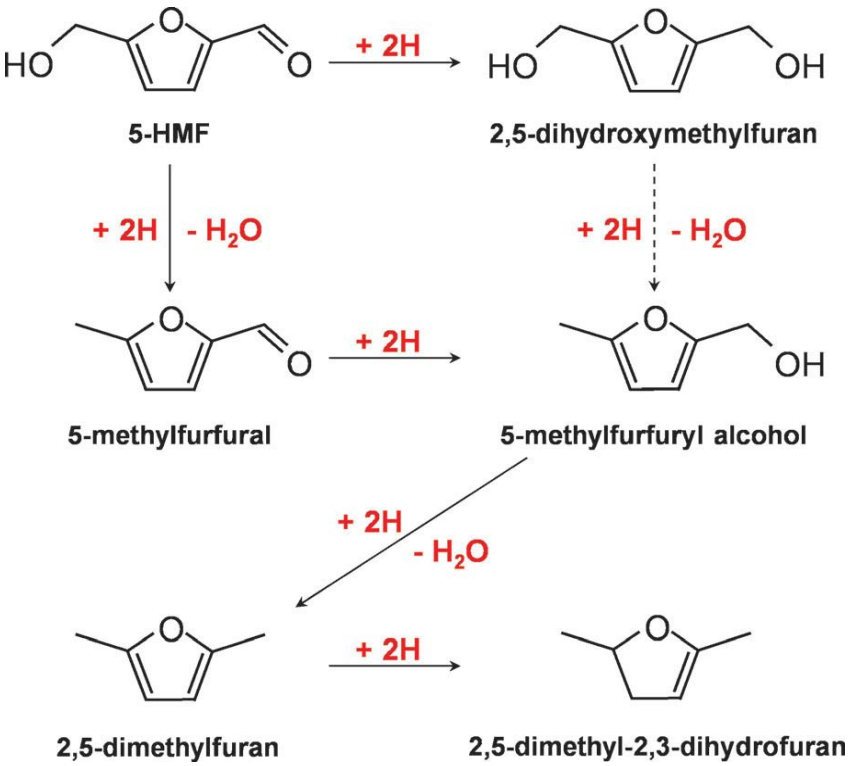

Figure 2.20: Electro catalytic hydrogenation of 5-HMF pathways (Kwon et al., 2013).

Furthermore, the direct electro catalytic hydrogenation of 5-HMF into 2,5-DMF was reported by Nilges and Schroder, (2013). Their study gives an insight on how to convert electric energy from renewables such as photovoltaics and wind into liquid fuels at room temperature and atmospheric pressure. From Figure 2.21, it can be observed that the reaction occurred as a series of uninterrupted 2-proton and 2-electron reduction steps. Materials with copper electrodes were reported to show the best activity compared with other electrodes such as

carbon, nickel, lead, iron, aluminium and platinum. It was also observed that the addition of solvents such as ethanol or acetonitrile improves the yield of 2,5-DMF and also supresses H_2 formation (Nilges and Schroder, 2013). Thus, the selectivities of 2,5-DMF, 5-MFA and 2,5-DHMF obtained were 35.6%, 11.1% and 33.8% respectively when 0.5 M sulphuric acid and copper electrodes in 1:1 mixture of ethanol and water was used. However, th e authors reported that, prolonging the reaction time will enable the 5-MFA and 2,5-DHMF intermediates to fully convert into 2,5-DMF.

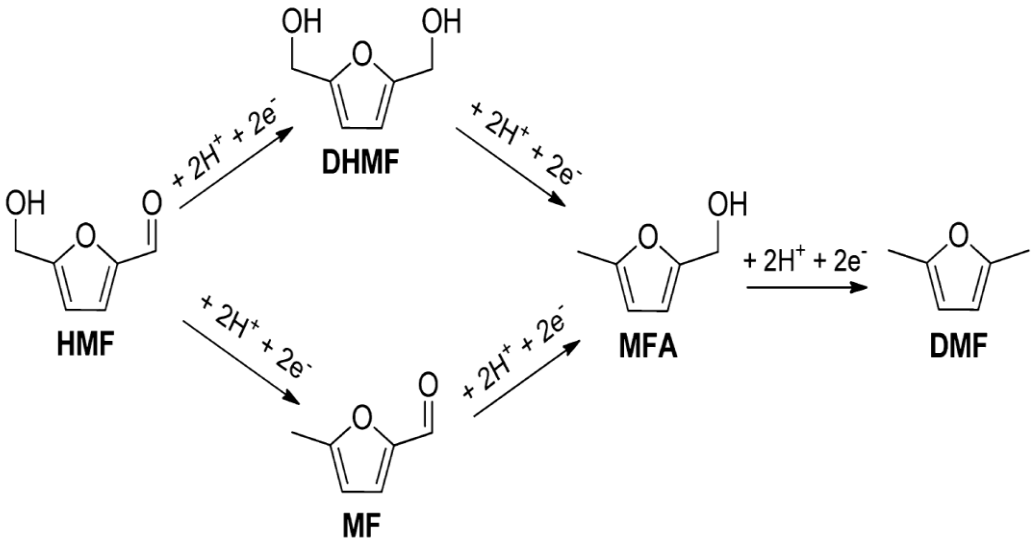

Figure 2.21: Direct electro catalytic hydrogenation of 5-HMF into 2,5-DMF (Nilges and Schroder, 2013).

2.7.10 Synthesis in a Continuous Flow Reactor

Many studies have reported the use of glass, batch and semi-batch reactors for catalytic hydrogenation of 5-HMF into 2,5-DMF. Recently, Luo et al., (2014) described the hydrogenation of 5-HMF over 10 wt% Pt/C in a continuous flow reactor using 1-propanol, ethanol and toluene as solvents. Their study investigated the importance of reactor configuration by carrying out the reaction in both batch and continuous flow reactors over the

same catalyst. It was observed that the reaction occurred in a sequential manner, with 5-HMF initially converted to furfuryl ethers and other hydrogenated intermediates. The furfuryl ethers were reported to react faster than 5-HMF towards 2,5-DMF synthesis (Luo et al., 2014).

A 70% yield of 2,5-DMF was achieved in the continuous flow reactor compared to the 10% yield obtained in the batch reactor. When the reaction was conducted in 1-propanol using a batch reactor at 180ºC, 33 bar H_2 and varying times of 0 to 8 hours, 5-HMF conversion was at 100% while 2,5-DMF yield obtained was 27.2%. However, when the reaction was carried out in a flow reactor under similar reaction conditions, a higher yield of 2,5-DMF was obtained. From Figure 2.22, it can be observed that the reaction occurred in a sequential manner. The 5-HMF in part A was partially hydrogenated to form reaction intermediates and ethers (part B). The intermediates and ethers formed in part B undergoes hydrogenation to form 2,5-DMF in part C. However, when the reaction time is prolonged, 2,5-DMF will undergo further hydrogenation to different products in part D (Luo et al., 2014).

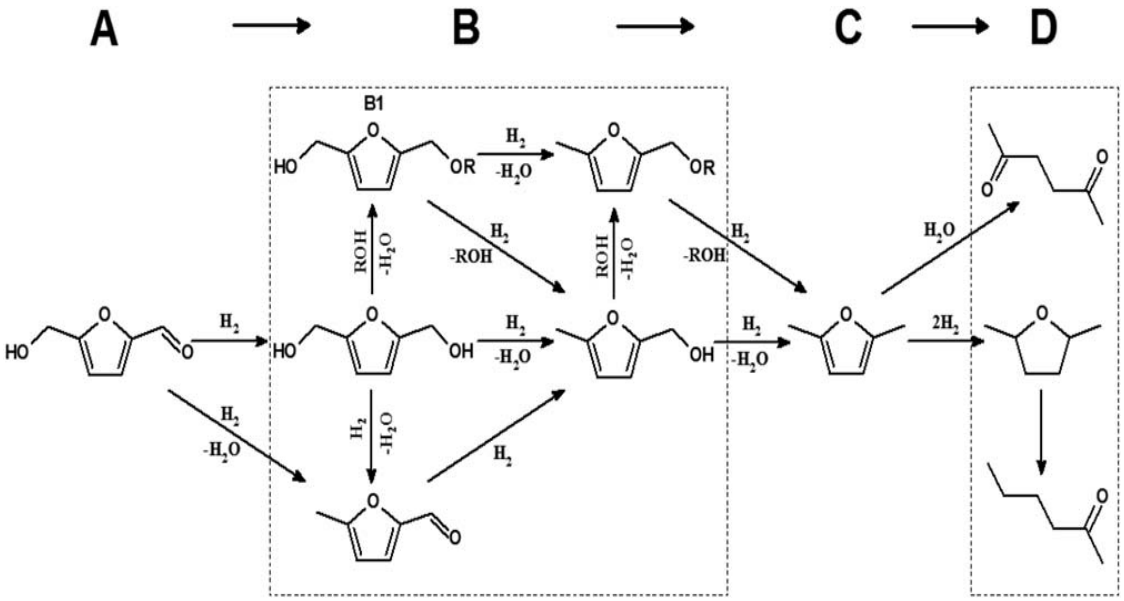

Figure 2.22: Reaction network for 5-HMF hydrogenation using alcohols as solvent (Luo et al., 2014).

Furthermore, the same sequential manner was observed when ethanol and toluene was used as a different solvent system. Under the same reaction conditions with increasing residence times, the reaction sequence above, A → B → C → D was equally observed when ethanol is used as a solvent. A higher 2,5-DMF selectivity of 71.9% was obtained in ethanol. This is slightly higher than the 63.7% obtained when 1-propanol was used (Luo et al., 2014). Their study concluded that the configuration of the reactor plays a huge role on the selectivities for 5-HMF conversion and 2,5-DMF yield. Therefore, higher selectivities and 2,5-DMF yields were obtained in the flow reactor than in the batch reactor because the side products are formed sequentially, rather than in parallel, demonstrating the importance of choosing the right type of reactor in catalyst screening.

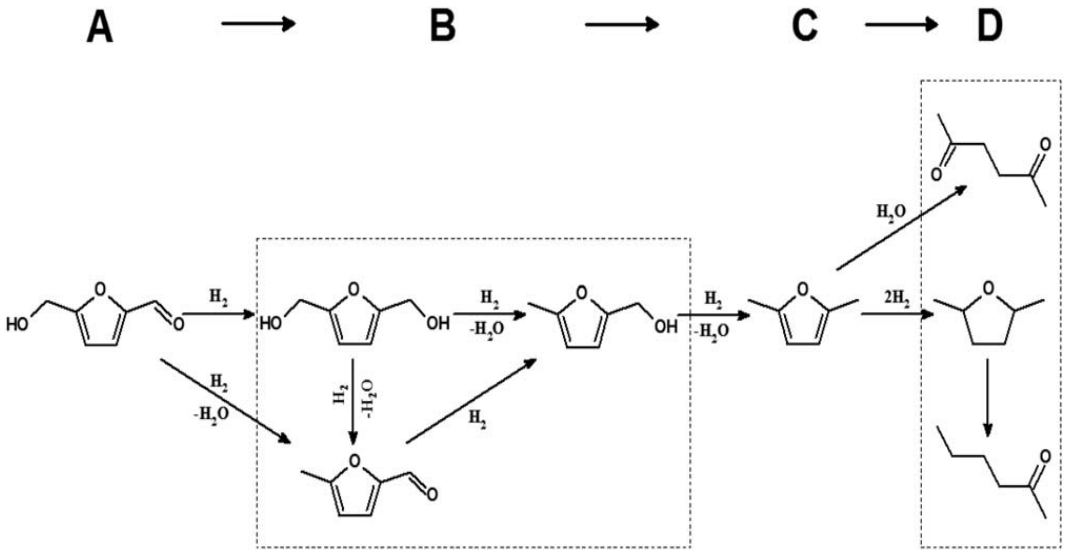

Figure 2.23: Reaction network of 5-HMF hydrogenation in toluene (Luo et al., 2014).

2.7.11 Synthesis over Bimetallic Catalysts

The properties of bimetallic catalysts are generally different from their monometallic counterparts due to the electronic and geometric effects between the metals present (Newton and Van Beek, 2010; Tao et al., 2012). It is therefore believed that an additional degree of freedom are provided by bimetallic catalysts which are used to change the electronic and geometric structures via changes in the size and composition, allowing the ability to tune their catalytic performance (Tao et al., 2012; Wang et al., 2014). The efficient production of liquid fuel 2,5-dimethylfuran from 5-hydroxymethylfurfural over Ru-Co_3O_4 catalyst was reported by Zu and co-workers (Zu et al., 2013). They investigated the performance of the catalyst, stability of the catalyst, reaction temperature, 5-HMF concentration, pressure and the Ru loading. The Ru-Co_3O_4catalyst was synthesized easily by co-precipitation method and under mild reaction condition, high activity and good reusability were obtained. Their results show that a 2,5-DMF yield of 93.4% was obtained at 130^oC reaction temperature, 7 bar hydrogen pressure and > 99%

5-HMF conversion. The Ru was reported to be responsible for the hydrogenation reaction while the Co_3O_4 is responsible for the absorption of the hydrogenation product and then beaks the C-O bond (hydrogenolysis of the hydroxyl group). Also, the Ru-Co_3O_4 catalyst was reused 5 times without loss of activity and possess excellent potential for biomass conversion into biofuels (Zu et al., 2013).

Furthermore, they also investigated one-pot synthesis of 2,5-DMF from fructose. The yield of 5-HMF obtained after the first reaction step (acid catalysed dehydration reaction) was 81%, then it was subjected to hydrogenolysis reaction using the Ru-Co_3O_4catalyst. The result shows that a 75.1% yield of 2,5-DMF could be reached indicating that the Ru-Co_3O_4catalyst is a good catalyst for the conversion of biomass into liquid fuels (Zu et al., 2013).

After their work, the use of bimetallic catalysts for hydrogenation of 5-HMF to 2,5-DMF received a lot of attention. The selective hydrogenation of 5-HMF to 2,5-DMF over carbon supported PdAu bimetallic catalyst under hydrogen pressure was investigated by Nishimura et al., (2014). The PdAu bimetallic catalysts has been used for different kinds of reaction such as; aerobic oxidation of alcohols (Enache et al., 2006; Balcha et al., 2011; Nishiruma et al., 2014), dehalogenation reaction (Yuan et al ., 2013) and direct production of hydrogen peroxide from H_2 and O_2 (Edwards et al., 2009a &b). In their research work, the PdAu bimetallic catalyst was prepared using a concurrent reduction method (Nishiruma et al., 2014). It was observed that the bimetallic PdAu catalyst displayed a higher catalytic activity than the monometallic Pd/C and Au/C under ambient conditions.

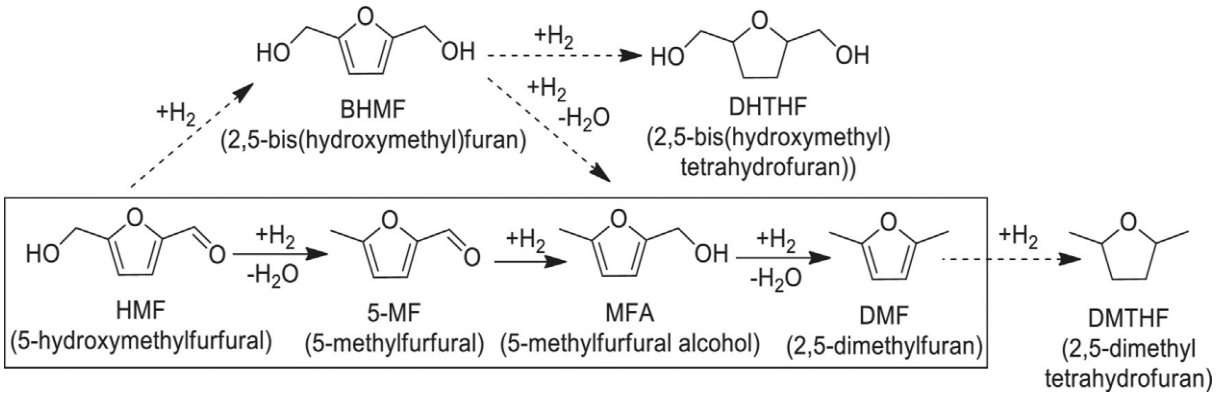

Figure 2.24: Reaction pathway for the hydrogenation of 5-HMF toward 2,5-DMF (Nishimura et al., 2014).

A very high >99% conversion of 5-HMF and >99.96% of 2,5-DMF yield was achieved with the $Pd_{50}Au_{50}$ catalyst in the presence of HCl as an acidic co-catalyst at 60°C temperature and 6 hours reaction time. (Nishimura et al., 2014). The effect of acidic support such as SiO_2, Amberlyst-15, β-zeolite and α-$Al_2O_3$was also investigated instead of the carbon support. The acidic support is reported to cause a 2,5-DMF ring opening. The hydrolytic cleavage of the C-O bond caused by the opening of the furan ring is supported with the use of BrØnsted acid sites of ion-exchange resins and aluminosilicates (Bui et al., 2013; Nishimura et al., 2014; Nikbin et al., 2013). According to the results obtained in their study, it was observed that, the change in acidity appeared to affect the catalytic acitivities (Nishimura et al., 2014). HCl and H_2SO_4 were tested as acidic co-catalyts in this work but HCl was reported to be the best. Lange and coworkers found out that the chloride ions in HCl plays a huge role for an effective and selective hydrogenation because the HCl co-catalyst boosted the hydrogenlysis step by the generation of an active chlorinated intermediate via nucleophilic substitution on the OH groups (Lange et al., 2012; Nishimura et al., 2014).

Nishimura's group further tested the direct production of 2,5-DMF from fructose and tagatose. In this case, the HCl serves as the acidic catalyst for the dehydration reaction to form 5-HMF from fructose. Under the same reaction conditions and over PdAu/C catalyst, 2,5-DMF yield of 10% and 40% were achieved from tagatose and fructose respectively. In addition, the bimetallic PdAu/C catalyst was applied for furfural hydrogenation reaction and 42% yield of 2-methylfuran (2-MF) was produced at 60°C. Their research group concluded that the PdAu/C catalyst displayed a good catalytic activity for direct hydrogenation of 5-HMF into 2,5-DMF in molecular hydrogen with the addition of HCl as acidic co-catalyst (Nishimura et al., 2014).

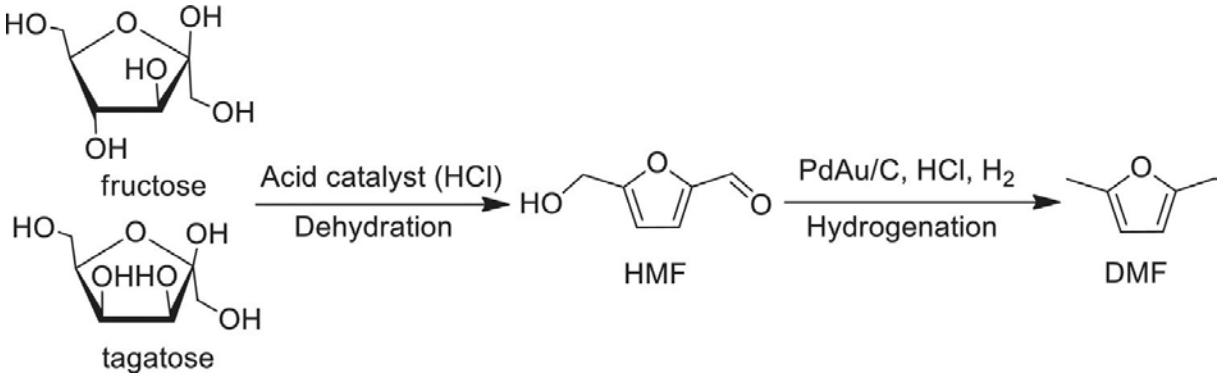

Figure 2.25: Direct synthesis of 2,5-DMF from ketoses (Nishimura et al., 2014).

Due to the excellent results obtained with the use of bimetallic catalysts, Huang's research group developed a new catalytic systems for the production of 2,5-DMF from biomass-derived molecules using nickel-tungsten carbide catalysts (Huang et al., 2014). In their study, different metal ratios of Ni-W catalysts were prepared using co-impregnation methods. The nickel-tungsten bimetallic catalyst was used because it serves as a multifunctional catalyst which possess good deoxygenation and hydrogenation ability. They investigated different reaction parameters and successfully obtained a 96% yield of 2,5-DMF at 180°C and 4 MPa.

Huang and coworkers suspected that the W_2C particles shows an outstanding deoxygenating ability in converting hydroxymethyl groups (-CH_2OH). In addition, the W_2C particles contains both metallic and acidic sites, thus catalyzing both hydrogenation and deoxygenation reactions (Wang et al., 2013;Huang et al., 2014). Due to this bifunctional properties, W_2C particles was expected to catalyze both reactions in another study but it displayed limited ability for hydrogenation reaction in converting –CHO to –CH_2OH (Ren et al., 2014). Thus, the authors speculated that the W_2C particles have a limited ability for the hydrogenation step. Instead, it plays a significant role in the deoxygenation step while the Ni particles are involved in the hydrogenation step. As a result of these roles, the synergistic effect between the Ni and W_2C particles with proper ratios showed the best catalytic perfomance in 5-HMF hydrogenolysis to 2,5-DMF (Huang et al., 2014).

Recently, the hydrogenolysis of 5-HMF to 2,5-DMF with the catalyst of hollow carbon nanosphere-supported platinum-cobalt (PtCo@HCS) was investigated by Wang et al., (2014). PtCo bimetallic catalyst have been reportedly used for selective hydrogenation of C=O bonds in the presence of C=C bonds, with very high (99%) selectivity obtained (Borgna et al., 2004; Tsang et al., 2008; Wu et al., 2012). After preparation of the catalyst, transmission electron images show that, the PtCo@HCS-500 nanoparticle has a diameter of 3.6 ± 0.7 nm located in the hollow cores (Wang et al., 2014). Results from their study also show that, a very high (100%) 5-HMF conversion was reached within 10 minutes while 98% yield of 2,5-DMF was obtained after 2 hours reaction and 180^{o}C reaction temperature.

The PtCo@HCS bimetallic catalyst was successfully used for the second cycle and 5-HMF conversion and 2,5-DMF yield remained at 100% and 98% respectively. Moreover, when Pt/GC and Pt/AC catalyst were used under the same reaction conditions, only 56% and 9% 2,5-DMF yield were obtained inspite of the high 5-HMF conversion (100 and 70% respectively). Conversly, when Pt/GC and Pt/AC were modified with cobalt to form PtCo/GC and PtCo/AC, 2,5-DMF yield increased to 98% for both catalyst while 5-HMF conversion increased to 100% (Wang et al., 2014). This shows that the alloy is important for the hydrogenation of 5-HMF into 2,5-DMF.

2.8 Heterogenuous Catalysis

Catalysis is a word coined by Baron Berzelius in 1835 to give a detailed account of substances that expedite chemical reactions without being used up in them (Davis & Davis, 2003). A catalyst can have a significant effect on reaction rate, but the equilibrium composition of reactants and products is still determined simply by thermodynamics (Davis & Davis, 2003). Heterogeneous catalysts differs from homogeneous catalysts by the different phases present during a chemical reaction. Heterogeneous catalysts are known to be solid and therefore have a different phase from the reactants and products, usually liquid while homogeneous catalysts are in the same phase as reactants and products. The preference for heterogeneous catalysts over homogeneous catalysts in continuous chemical processes is as a result of the relative ease of separation from the product mixture and tolerance for extreme operating reaction conditions.

The continuous use of metal nanoparticles (NPs) as highly desirable catalysts has generated significant attention and research since, compared with bulk metal, the remarkable surface-area-

to-volume ratio of metal nanoparticles confers a high reactivity (Zhu, 2014). In heterogeneous catalysis, chemical reactions are known to take place at the catalyst surface by adsorption of reactants from the fluid phase, surface reaction of adsorbed species, and desorption of products into the fluid phase (Davis & Davis, 2003). Beyond doubt, the use of a catalyst provide different sequence of elementary steps to achieve the desired chemical reaction from that in its absence. Therefore, the seven steps (as shown in Figure 2.26) involved in heterogeneously catalysed reactions are;

1. External diffusion of reactant (s) from the bulk fluid phase (fluid phase surrounding the catalyst particle) to the external surface of the catalyst (catalyst particle).
2. Internal diffusion of the reactant (s) from the external surface of the particle through the pores to the active sites on catalyst surface (interior surface).
3. Adsorption of the reactant (s) on the catalyst surface (active site).
4. Surface reaction
5. Desorption of the products from the catalyst surface.
6. Internal counter-diffusion of the desorbed products through the pores to the external surface.
7. External counter-diffusion of the products from the external surface to the bulk fluid phase.

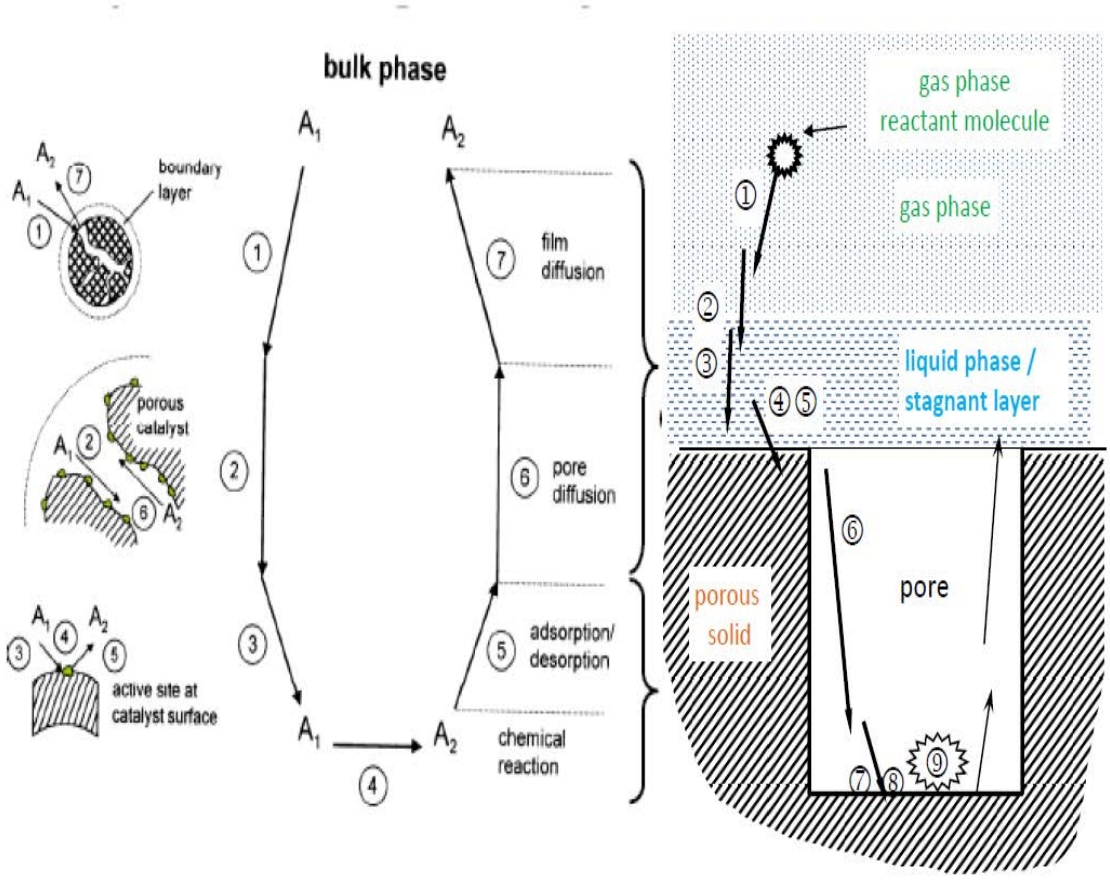

Figure 2.26: Individual steps of a simple heterogeneous catalysed reactions A1 – A2 carried out on a porous catalyst (Seelam, 2015).

The external diffusion steps (steps 1 and 7) occur in series with the chemical steps (steps 3 – 5). However, the external transfer occurs separately from the chemical reaction. The internal diffusion steps (steps 2 and 6) occur simultaneously with the chemical reaction. In addition, the adsorption, surface reaction and desorption are considered as sequential steps. However, when a chemical reaction takes place at the catalyst surface, the rate of mass transfer to intraparticle diffusion (reactive surface) is in a steady state and is the same to the reaction rate. Moreover, if steps 1,2,6 and 7 (mass transfer or diffusion steps) are very fast, there is little or no resistance for the mass transfer from the bulk to the catalyst surface and from the catalyst

surface to the active site in the pore (Klaewkla et al., 2011). At this point, the concentration around the sites of the catalyst is assumed to be equal to that of the bulk one. Under these conditions, the mass transferring steps does not have any effect on the rate of reaction (Klaewkla et al., 2011).

However, if the diffusion from the bulk to the surface of the catalyst is slow, (for example when the catalyst is in the solid phase while the reactants are in the gas phase), then the external mass transfer resistance is high and therefore an important factor to consider with respect to the overall reaction rate. After all, the particle size of the catalyst and flow conditions such as pressure, temperature and superficial velocity in the reactor affects the external mass transfer resistance (Klaewkla et al., 2011). Therefore, varying these reaction conditions can have a significant effect by limiting the external mass transfer resistance.

Furthermore, if there is no external mass transfer resistance and the internal diffusion effects are significant, then the concentration profile would vary across the catalyst pellet (Klaewkla et al., 2011).

2.9 Conclusion and Rationale For Current Studies

The following conclusions can be made from this chapter:

- 5-HMF as a giant molecule has the potential to serve as a building platform for different chemical products.

- Over 1500 papers has been published to access 5-HMF from carbohydrate materials, however more work (such as separation, purification) remains to be done.
- 2,5-DMF has very close properties to gasoline and therefore has a great promise to meet future fuel demands.
- 2,5-DMF is a suitable candidate to gasoline in engines and no major alterations are required in engines when 2,5-DMF is used.
- Hydrogenation of 5-HMF in molecular hydrogen appears to be to a promising method for producing 2,5-DMF due to very high yields reported in the literature. However, using petroleum-derived H_2 is not economical nor entirely green due to the high pressure H_2 required. Only few reports have investigated alternative hydrogen sources (transfer hydrogenation).
- Ru metal has been shown to be a good metal for hydrogenation/hydrogenolysis of 5-HMF into 2,5-DMF due to its outstanding catalytic activity.
- Bimetallic catalyts appears to be a promising catalyst for producing 2,5-DMF due to higher yields reported in the literature compared to their monometallic analogue.

Based on the literature review discussed above, it is clear that there are still challenges in producing 2,5-DMF without the use of molecular hydrogen. The work in this thesis compares three different sources of hydrogen for 5-HMF hydrogenation into 2,5-DMF in a batch reactor. Optimization of reaction parameters such as temperature, time, pressure, reactant concentration, agitation speed and catalyst amount were all investigated across the 3 hydrogen donor systems employed. The novelty of this research work lies with the use of azeotropic mixture of formic acid and triethylamine both as hydrogen donor and solvent system for hydrogenation of 5-HMF

to 2,5-DMF across all catalysts investigated. In addition, this research work pioneered the use of a bio-support for metal catalysts in all the hydrogen donor system studied for hydrogenation of 5-HMF to 2,5-DMF while also investigating the preliminary reaction kinetics on the existing work on the use of Ru/C and Pd/C catalysts for 5-HMF hydrogenation in molecular H_2 and 2-propanol. Therefore, the first part of the work will investigate the surface morphology of the commerical catalyst and bio-support metal catalysts used. In chapter 5, the use of molecular H_2 over both conventional (Ru/C and Pd/C) and bacterial supported metal catalysts was studied. In subsequent chapters, the mixture of formic acid/triethylamine and 2-propanol as hydrogen donor source over the same set of catalsysts will be investigated. In addition, comparison between the 3 hydrogen sources and preliminary reaction kinetics was explored and reported.

Chapter 3. **Experimental Set Up and Analytical Methods**

3.1 Overview

This chapter describes five experimental procedures or methods: i) the experimental plan, ii) the bio-catalyst preparation, iii) the experimental apparatus and standard operating procedure, iv) the analytical methodologies, and v) the catalyst characterisation techniques. Firstly, Section (3.2) gives a detailed list of commercial materials used in this study, including the specification and supplier information. This is followed by the experimental plan in Section (3.3), describing the method used in planning the experiments. Section (3.4) describes the bio-catalysts preparation. All the bio-catalysts used in this study were prepared by Mr Jacob Omajali from the School of Biosciences, University of Birmingham. The setup of the laboratory-scale semi-batch autoclave is then described in (3.5), along with detailed instructions of the operating procedure. The analytical methods (Gas Chromatography-Flame Ionisation Detector and Gas Chromatography-Mass Spectroscopy) used are then presented in Section 3.6. Finally, the catalyst characterisation techniques employed are detailed in Section 3.7 and error consideration in Section 3.8.

3.2 Materials and Methods

A detailed list of all the commercial chemicals and materials used in this study is presented in Table 3.1. All the chemicals were used as received from the supplier without

further purification, unless otherwise stated. A list of the instruments employed for various uses, such as product analysis and catalysts characterisation are provided in Table 3.2.

Table 3.1: Commercial chemicals and materials used in this study.

Material	Supplier	Specification
For chemical reaction		
Triethylamine	Sigma-Aldrich, UK	≥99% (hydrogenation reactants)
5-hydroxymethylfurfural	Sigma-Aldrich, UK	≥99% FG
2-propanol		≥99.5% ACS reagent
tetrahydrofuran		≥99.9% HPLC grade
hydrochloric acid		37% reagent grade
sulphuric acid		95-98% reagent grade
5-methylfurfural, 2,5-dimethylfuran, 2-hexanol,furfural, tetrahydrofurfuryl alcohol, diethyl ether, 2-methylfuran	Sigma-Aldrich, UK	99% (GC analytical standards)
α-angelica lactone, 2,5-hexadione,furfuryl alcohol		98% (GC analytical standards)
2,5-dimethyltetrahydrofuran	Sigma-Aldrich, UK	96% (GC analytical standards) mixture of cis and trans
2-methyltetrahydrofuran		≥99.0% (GC analytical standard) contains 250ppm BHT as stabilizer
formic acid	Acros Organics (Fisher Scientific)	99% (hydrogenation reactants)
acetone	Fisher Scientific	Analytical reagent grade
Commercial catalysts		
5 wt% Ru/C	Johnson Matthey	Powder, Paste Type 619
10 wt% Pd/C	Alfa Aesar	Powder, Type 487 dry
5 wt% Pd/C	Sigma-Aldrich, UK	Dry basis
Gas		
hydrogen	BOC, UK	>99.9% (gas reactant, GC)
nitrogen		>99.9% (inert gas)
helium		>99.9% (GC carrier gas)
compressed air		gas reactant, GC
Others		
Whatman filter paper	Sigma-Aldrich	8µm size
ZB-Semi-volatile column	Phenomenex, UK	30 m × 0.25 mm × 0.50µm

All the commercial catalysts used in this study were purchased from Johnson Matthey and Sigma-Aldrich.

Table 3.2: Instruments used in this study.

Instrument	Manufacture	Note
Emscope SC 500 sputter coater	Emscope	Gold coating
A&D analytical balance	A & D Instruments Ltd.	Series:HR-200
Parr autoclave	Parr Instrument Company	100 ml stainless steel
Philips XL-30 Environmental SEM-FEG	FEI Company	Oxford Inca 300 EDS system
JEOL 1200EX TEM	JEOL, Inc.	Lanthanum hexaboride (LaB6) filament
GC-Shimadzu 2010	Shimadzu	Flame Ionisation Detector (FID)
Agilent 7890A GC	Agilent	Flame Ionisation Detector (FID)
GC-MS	Waters GCT Premier Time of Flight-MS	Mass Spectroscopy

3.3 Experimental Plan

An experimental plan was conducted before starting the investigations. This was carried out because it allowed for a structured approach to the investigations. The two methods considered were one-factor-at-a-time (OFAT) and design of experiment (DOE). Engineers and scientists commonly favour DOE for reasons such as; less time for experiment, various reaction parameters can be investigated at once and obtain a large amount of data (Frey et al., 2003). OFAT is not commonly employed because it requires more experiments, time consumption, it can miss optimal settings of factors and it is be susceptible to bias due to time trends in experimental error. However, while the cautions listed above remain valid and should always be considered when using OFAT, some researchers have established a role for OFAT and proved that under certain conditions, they are more effective that DOE (Frey and Jugulum,

2006). The reliability of OFAT may seem paradoxical but there has been cases where OFAT approach offers some advantages.

For example, Frey and co-workers made a broader claim about the effectiveness of OFAT experimentation where they proposed an adaptive variant of OFAT experimentation in which changes that have a significant effect on the observed response of the system are retained and changes that do not have a positive response are reversed before proceeding with additional experimentation (Frey et al., 2003; Frey and Jugulum, 2006). The authors provided empirical support for the use of adaptive OFAT as an option to DOE and stated the criteria for determining the effectiveness of such approach. In their study, adaptive OFAT showed better results than DOE when either interactions are strong enough (which accounts for more than 25% of the sum squared factorial effects) or mild experimental error (which is enough to contribute variance of < 40% contributed by the sum squared factorial effects) (Frey et al., 2003; Frey and Jugulum, 2006).

In addition, Koita, (1994) supported the use of OFAT and showed that OFAT method was effective for identification of selected interactions after running DOE as part of an overall approach to sequential experimentation. Furthermore, McDaniel & Ankenman showed an empirical evidence that, for "small factor change problems" a strategy including OFAT and Box-Behnken designs worked better than a comparable method employing DOE when there is no error in the response (McDaniel and Ankenman, 2000). Moreover, it has been suggested that OFAT technique might be used in preference to balanced factorial plans when the researcher seeks an optimum within a system likely to contain interactions. The authors also suggested

that OFAT might offer some advantages since it focuses on observations in regions that are likely to contain the optimum (Frey and Jugulum, 2006; Friedman and Savage, 1947).

However, in this study, the OFAT experimental structure was chosen for two reasons; (i) It was compatible with the experimental apparatus available and (ii) specialist equipment such as multivariate analysing software and online analysers were required in order to use DOE. Therefore, due to unavailability of such equipment, DOE was not considered. The adaptive OFAT was used in this study instead of the commonly known OFAT methodology. Using the common OFAT methodology, one parameter would be changed at a time while other factors are kept constant. Using the adaptive OFAT requires the same approach but the only difference is that, the response generated by the system improved as the experiment progresses (Frey et al., 2003). In this study for example, it was observed that when a factor was changed and the response of the system was positive, then we retained that factor at that value for the next experiment. However, if a negative response was generated from the system, then the factor was changed back to its original value.

The parameters to be investigated were determined after establishing the experimental plan. They are:

- Reaction Temperature (100 – 300 ^{o}C)
- Initial 5-HMF concentration (0.05 – 1.4 Molar)
- Reaction Time (0 – 10 hours)
- Agitation Speed (0 – 1000 rpm)
- Catalyst Amount (0.05 – 0.5 grams)
- Molar Ratio of (FA/Et_3N) (1:1 – 4:1)

- Hydrogen Pressure (10 – 60 bar)
- Nitrogen Pressure (0 – 30 bar)

However, after identifying the optimal reaction conditions for the Ru/C catalysts across the H-donors investigated in this work, two different reactions across each H-donor system were conducted combining all the optimal reaction conditions obtained and used as control experiments. This was done to validate the individually obtained optimal reaction conditions when the OFAT technique was employed. This control experiment focused on 5-HMF conversion, selectivity and yield of 2,5-DMF obtained. However, further work is required to confirm whether the reactions are solely attributable to the metallic parts of the catalysts and not the supports.

Table 3.3: Control experiments in each H-donor system investigated

H-donor	**Molecular H_2**	**$HCOOH/Et_3N$**	**2-Propanol**
5-HMF conversion (%)	95.6 ± 0.8	92.7 ± 1.5	94.6 ± 0.5
Selectivity (%)	96.4 ± 1.6	94.8 ± 2.4	75.3 ± 1.7
2,5-DMF Yield (%)	93.4 ± 2.3	90.6 ± 1.8	72.7 ± 2.4

Errors are calculated as mean ± standard error of the mean from at least two experiments.

3.4 Bio-catalyst Preparation

The biomass-supported monometallic Pd, Ru and bimetallic RuPd nanoparticles (NPs) were synthesised based on hydrogen sacrifice strategy. The preparation method used in this work is described in the following section.

3.4.1 Bacteria and Growth Conditions

The following bacterial strains were used in this study: an aerobic *Bacillus benzeovorans* (NCIMB 12555) and an anaerobic *Desufovibrio desulfuricans* (NCIMB 8307). The aerobic *B. benzeovorans* was grown under an aerobic condition in a rotary shaker (180 rpm at 30^{o}C) in a nutrient medium with the following composition: 1.0g beef extract (Sigma-Aldrich), 2.0g yeast extract (Sigma-Aldrich), 5.0g peptone (Sigma-Aldrich) and 15.0g NaCl per litre of distilled water and adjusted to pH 7.3 (Omajali et al., 2015). The *D. desulfuricans* was grown in anaerobic medium (Postgate's C medium) (Postgate, 1979) and adjusted to pH 7.5. The bacteria were harvested (Beckman Coulter Avati J-25 Centrifuge, U.S.A) by centrifugation (9,094 x g, 15minutes at 4^{o}C) at mid-exponential phase, OD_{600} 0.7-1.0 and OD_{600} 0.5-.7 respectively. The cells were then washed three times in air with 20mM MOPS (morpholinepropanesulfonic acid)-NaOH buffer, pH 7.0 and then concentrated in a small amount of the same buffer. These were stored at 4^{o}C until needed for bio-NPs preparation. For ease of growth, the aerobic *B. benzeovorans* was chosen for the subsequent preparation of bimetallic bio-NPs and catalysis.

3.4.2 Preparation of Monometallic and Bimetallic Bio-nanoparticles (Bio-NPs)

The bio-NP catalyst preparation was done in two ways: The syntheses of monometallic and bimetallic biocatalysts were made differently. The monometallic bio-Pd nanoparticles (5% metal loadings) were initially made using *D. desulfuricans* NCIMB 8307 while both monometallic (20% bio-Ru) and bimetallic (5% and 20% bio-Pd/Ru) were prepared using *B. benzeovorans* NCIMB 12555. For all monometallic bio-NPs preparation, cell suspensions were transferred initially into 2 mM Pd (II) solution of Na_2PdCl_4 or 2 mM Ru (III) of $RuCl_3.H_2O$ solution (adjusted to pH 2 and left for biosorption for 30 minutes at 30^{o}C). For bio-Pd reduction,

H_2 was bubbled for 10 minutes and then saturated for an additional 15 minutes for reduction to reach completion. While for the preparation of the bio-Ru using a 2 mM solution of $RuCl_3.H_2O$, H_2 was bubbled for about 1hr and then saturated and then transferred to a shaker overnight at 180 rpm and 30^oC. For the synthesis of the bimetallic Pd/Ru, a 2mM Pd (II) and 1 mM Ru (III) was used in line with the method of Deplanche et al (2012) for Pd/Au synthesis. The reduced bio-NPs were then washed three times with distilled water and once with acetone (9,094 x g, 15minutes at 4^oC) and then dried. The dried samples were pulverized for catalytic reactions.

3.5 Apparatus and Procedure

Throughout the project, a 100 ml Parr autoclave reactor was used for all hydrogen transfer reactions. All experiments were conducted in the stainless steel autoclave reactor using a temperature range of 10 to 350^oC, and a maximum pressure 200 bar. The reactor was manufactured by Parr Instrument Company, Illinois, US. Figure 3.1 shows a schematic diagram of the stainless steel Parr autoclave reactor used in this study.

The autoclave is a 100 ml flat-bottomed and cylindrical vessel with inner dimensions of 11.68 cm (height) × 3.30 cm (diameter) fabricated from stainless steel. The reactor was equipped with an efficient gas entrainment impeller attached to a hollow stirring shaft to speed up the gas dispersion into a liquid system. The hollow four-bladed impeller with a diameter of 2.06 cm is designed specifically to allow the gas continuously recirculated from the space above the liquid into the liquid phase. It is well known with all impellers that a vacuum is created by the speed of the stirrer just at the tip of the impeller. Gas gain entrance through the openings

close to the top of the shaft and goes through the dispersion ports situated at the impeller tips. In the Parr autoclave, there are dispersion ports situated at the impeller tips, increasing the stirring speed generates higher vacuum and increased driving force for effective gas dispersion system.

The Parr autoclave also consists of a ceramic fibre heating jacket and a fixed thermocouple. The temperature and agitator speed control was achieved through an external controller supplied with the stainless steel autoclave. A full reactor specifications are available from Parr Instrument Company, Illinois, US.

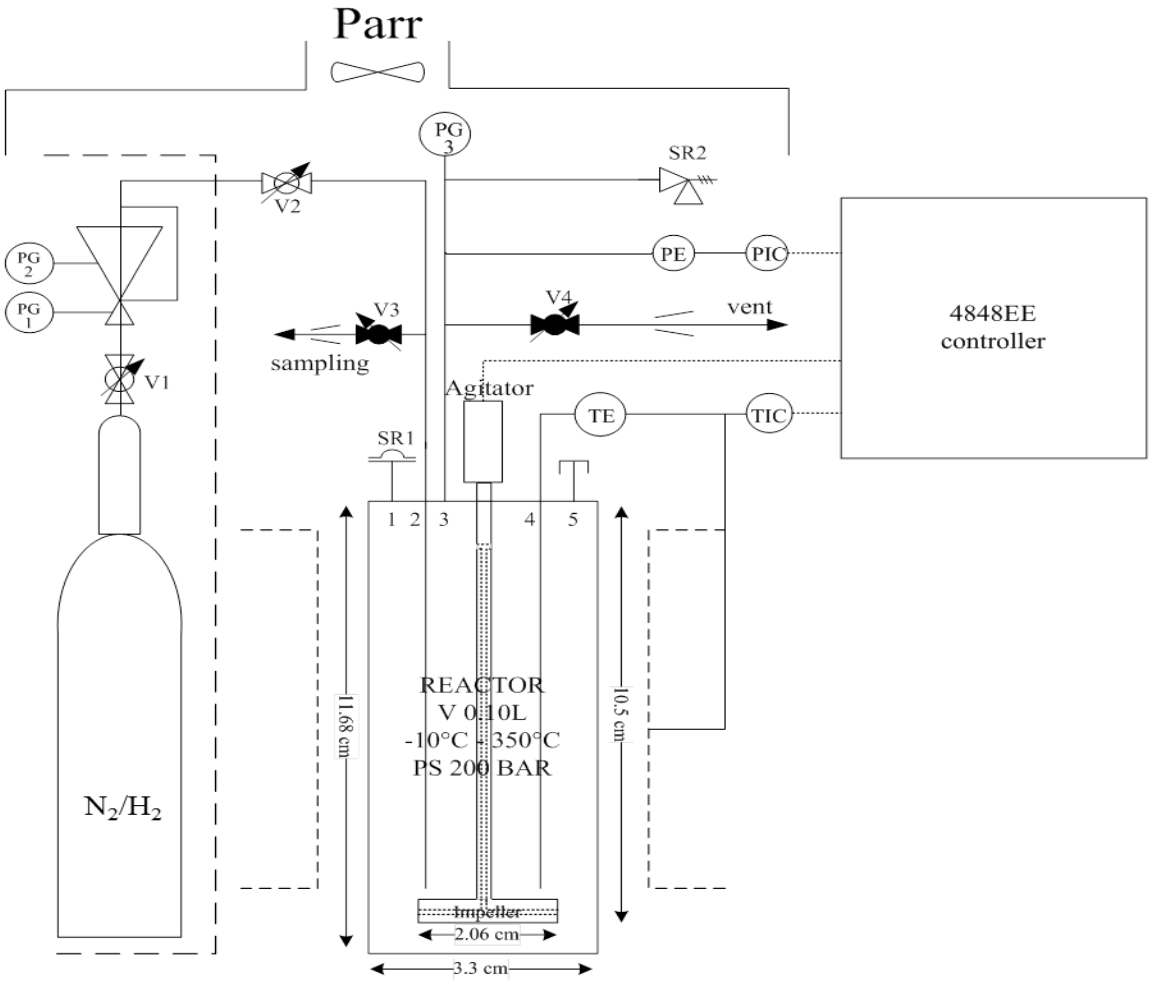

Figure 3.1: Schematic diagram of the original stainless steel Parr autoclave reactor.

3.6 Quantitative and Qualitative Analytical Methods

3.6.1 Gas Chromatography (Flame Ionisation Detector)

The compositions of the liquid sample mixtures were analysed using a Shimadzu 2010 gas chromatography equipped with a Flame Ionisation Detector (FID) (Figure 3.2). Helium is the carrier gas, while hydrogen and air are used to partially burn the organic constituents. As a

result, ionic sub-compounds that are detectable by FID are then produced and the signals obtained at different retention times are comparable to the quantity injected into the GC, with retention time consistent with individual components.

For effective chromatographic separation of components, selecting a proper capillary column is of high significance, and should be based on four important factors;

- Column I.D (depending on the sample size).
- Column Length.
- Stationary Phase (must be in accordance with sample polarity).
- Film Thickness (Depending on the sample volatility).

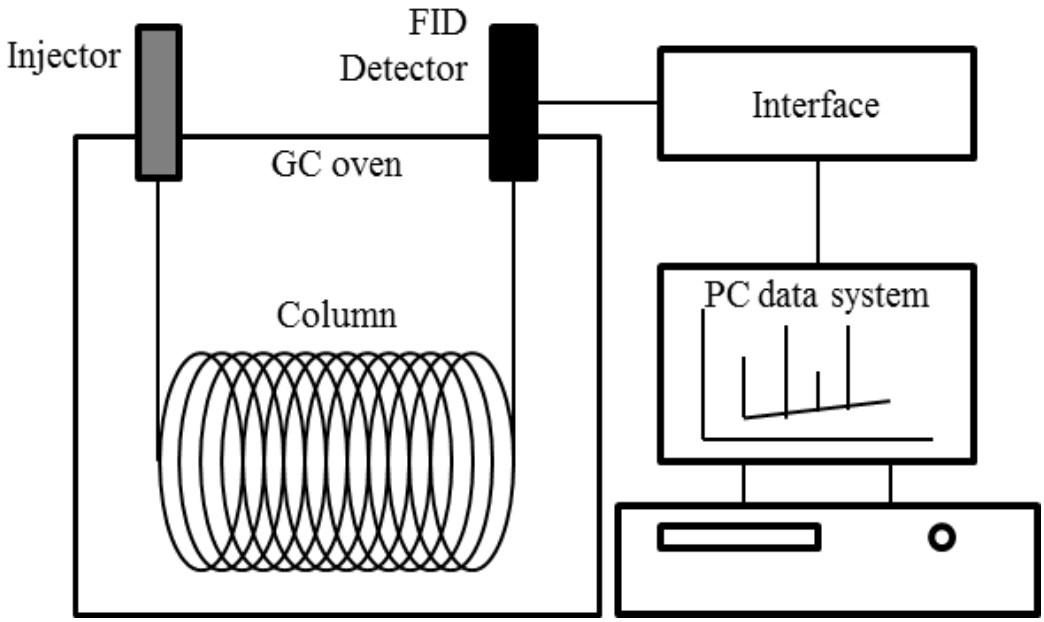

Figure 3.2: Simplified schematic of the gas chromatography-FID system (Zhu, 2014).

A suitable oven method is developed to keep the column at the right temperature condition, allowing the elution of different substrates to be separated easily from each other to obtain clear and sharp peaks within a reasonable time. Identification of compounds from experimental samples is done after the corresponding retention time of known chemical standards have been determined via injection into the GC system. A calibration plot between the peak area versus the analyte concentration can be established by injecting a standard of known concentrations in the GC which allows the quantifications of analyte concentrations in the experimental sample. This method is known as external calibration technique. This technique was used because it is the most commonly used method for routine analyses and a single calibration can serve a multitude of samples. This technique is particular popular in repetitive, routine analysis many similar samples and gains even greater weight when several calibration curves can be used to determine a number of components in each test sample.

In addition, the external calibration technique was used because of its stability. The chromatographic procedure was stable over a sufficient period of time, so as to avoid frequent calibration. Moreover, availability of suitable external standard (2,5-DMF) also encouraged the use of external calibration technique in this research work. Therefore in this study, 5-HMF, 2,5-DMF, and intermediates formed were analysed by GC (Shimadzu 2010) using a ZB-Semi Volatile Capillary Column (30 m × 0.25 mm × 0.50 μm). The injection volume was 1 μL, the injector temperature was 300^{o}C, the detector temperature was 300^{o}C, inlet pressure was 100 KPa, split ratio of 100:1, and the carrier gas was He with a flow rate of 1 mL/min. The initial column temperature of 50^{o}C was held for 5 min, and then, the temperature was ramped 16.6^{o}C/min until 133.3^{o}C was reached and held for 1.5 min; after that, the temperature was ramped until 300^{o}C was reached and held for 3.5 min.

3.6.2 Gas Chromatography (Mass Spectrometry)

The gas chromatography-mass spectrometry (GC-MS) uses the principles of both gas-liquid chromatography and mass-spectrometry to identify the components of liquid sample mixtures. In this study, an Agilent 7890A GC and Waters GCT Premier time-of-flight mass spectrometer (GC-TOFMS) (Micro mass, Manchester, UK) with a ZB-Semi Volatile-MS Capillary Column (30 m × 0.25 mm × 0.50 µm) was used. Waters Mass Lynx software (version 4.1) was used to operate the GC-TOFMS system. The source temperature was 200°C and electron energy was 70 eV.

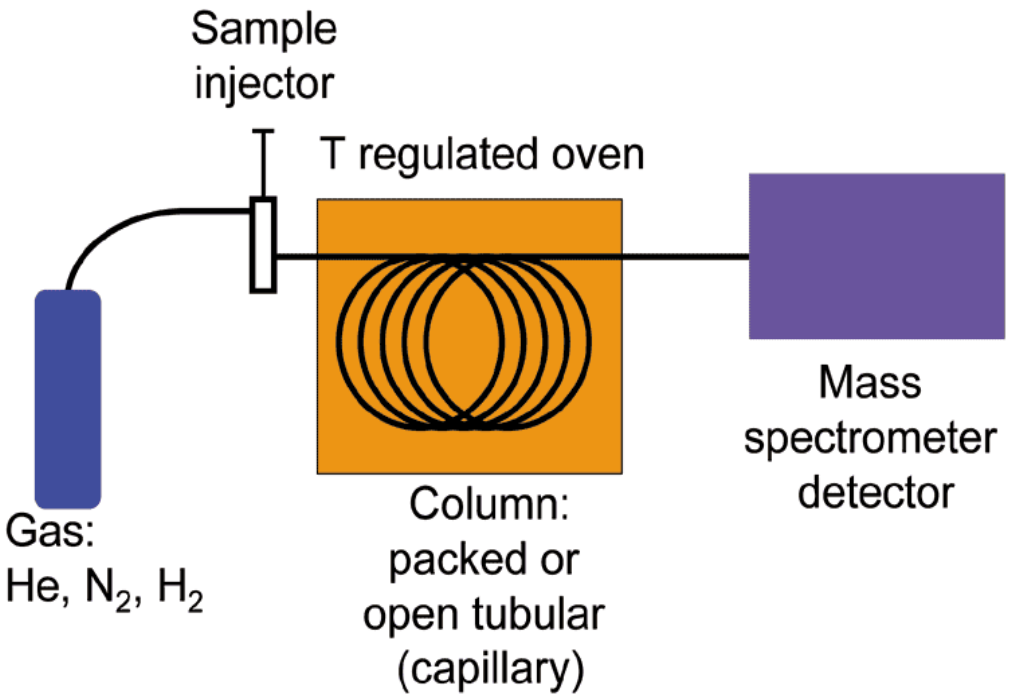

Figure 3.3: Simplified schematic of a gas chromatography-mass spectrometry system (Source: Wikipedia Images).

3.6.3 Calculation of 5-HMF Conversion, 2,5-DMF Yield and Selectivity

The results obtained from the experiments investigating the parameters were presented in terms of 5-HMF conversion, 2,5-DMF yield and 2,5-DMF selectivity. It is important to note that we used the moles of compounds to calculate conversion, yield and selectivity. It is also important to note that we assume the reactor to be a variable volume reactor because of the change in the volume of reactant contents after completion of the reaction. It should be noted here that 5-HMF conversion and DMF yield were based on external standard method and calculated using the equations in Table 3.3. The mass balance showing how much of the starting moles in the reaction has been identified as the products is not reported in this thesis due to inability to quantify the amount of reaction intermediates present in each system and utilization of equilibrium expressions to determine equilibrium compositions and extents of reactions.

Table 3.4: Calculation of 5-HMF Conversion, 2,5-DMF Yield and Selectivity.

$$\text{HMF Conversion (\%)} = \frac{(\text{Initial moles of HMF} - \text{Final moles of HMF})}{\text{Initial moles of HMF}} \times 100 \quad (3.1)$$

$$\text{DMF Yield (\%)} = \frac{\text{Moles of DMF in products}}{\text{Initial moles of HMF}} \times 100 \quad (3.2)$$

$$\text{Selectivity (\%)} = \frac{\text{Moles of DMF in products}}{(\text{Initial moles of HMF} - \text{Final moles of HMF})} \times 100 \quad (3.3)$$

3.7 Catalyst Characterisation Techniques

The activity of the catalyst and selectivity towards targeted products are determined by the catalyst morphology, active dispersion of metal particles and interaction with the support. This section outlines the catalyst characterisation techniques employed in this study.

3.7.1 Scanning Electron Microscope Analysis (SEM)

A scanning electron microscope (SEM) was used to study the texture and external morphology of the fresh 5 wt% Ru/C, 5 wt% Pd/C, 10 wt% Pd/C, 5 wt % Bio-Ru/Pd, 20 wt% Bio-Ru/Pd, 5 wt% Bio-Pd and 20 wt% Bio-Ru catalyst as well as the spent catalysts employed in this study. A Philips XL 30 Scanning Electron Microscope (XL 30 ESEM-FEG) fitted with a LaB5 emission source was used because it is capable of examining the natural state of the catalyst powder without preparing or modifying it. This technique was useful because it scans a sample with high-energy beam of secondary electrons in a raster scan pattern. The atoms that make up the sample then interact with the secondary electrons to produce images that show the information about the specimen's surface region.

In addition, the Philips XL-30 ESEM-FEG includes an Energy-Dispersive X-ray spectroscopy (EDX) which is a powerful technique used for chemical characterization of a sample or elemental composition analysis of the catalysts before and after reactions. This investigation largely depends on the interaction of an X-ray excitation source and the sample. Its characterization abilities rely on the fundamental principle that an element is made up of a unique atomic structure which allows X-rays similar to an elements atomic structure to be

distinguished from each other. The photomicrographs from the ESEM were collected over a selected region of the catalyst surface.

In this study, samples of dried catalyst powder were mounted on a microscope stub and coated with gold using Emscope SC 500, then examined using the Philips XL-30 Environmental SEM equipped with an Oxford Instruments Inca energy dispersive X-ray spectroscopy (EDX) system, operating at an accelerated voltage of 15 kV.

3.7.2 Transmission Electron Microscope (TEM)

Transmission electron microscope was used to capture images of materials as trivial as a sole column of atoms at a significantly high resolution (~20 nm). This technique operates in such a way that electron beams are transmitted through an ultrathin specimen which relates with the specimen as it goes through, resulting in the generation of a conforming image at a detector (Zhu, 2014). The sample to be used must have a low density to let electrons travel through it.

In this study, TEM samples of catalysts were prepared by selecting samples of the bio-NPs-deposited on bacterial cells; washed twice with distilled water and then fixed with 2.5% (w/v) glutaraldehyde fixative in 0.1M cocadylate buffer (pH 7.0) at 4^{o}C and stained with 1% osmium tetraoxide. The cells were then dehydrated in an ethanol series. This was followed by embedding cells in epoxy resins and then cut into sections of about 100-150 nm thick. Finally, the samples were viewed under a transmission electron microscope (JEOL 1200 EX) with an

accelerating voltage of 80 kV (Omajali et al., 2015). For easy image visualization using JEOL 1200 EX electron microscope, higher metal loadings (20%) of the bio-NPs were considered. The TEM images of the bionanoparticles were acquired using the Gatan Digital Micrograph and then processed using Image J software.

3.7.3 BET Analysis

The Brunauer – Emmett – Teller (BET) method according to ASTM C1274 by physical adsorption was used to measure the pore size and surface area of the catalysts. This was achieved by carrying out nitrogen adsorption and desorption on the catalysts pellets at a temperature of 77K with the help of a Micromeretics Analytical Instrument ASAP* 2010, which forms an adsorption isotherm. Before the analysis was carried out, the catalysts about 0.45 grams were degassed at high temperature to eliminate/get rid of contaminants. The integrated ASAP.2010V5.03 software enables automatic and easy analysis. The BET equation (1) presented below explains the relationship between adsorbed nitrogen at a given partial pressure and the adsorbed volume at monolayer coverage. The production of monolayer (i.e., a layer of gas adsorbed one molecule thick) of gas molecules on the catalyst surface is used to determine the exact surface area, while the principle of capillary condensation of the nitrogen gas allows the estimation of pore volume, pore size and size distribution. Nitrogen is commonly employed because it is inert, cost-effective, available in high purity and its molecular size is well established.

$$\frac{P}{V(P_o - P)} = \frac{1}{V_m C} + \frac{(C-1)P}{V_m C P_o} \qquad (3.4)$$

Where P_o is the saturation pressure at the experimental temperature, p is the partial pressure of N_2, V_m volume adsorbed at monolayer coverage, V volume adsorbed at P, and C a constant.

Therefore, the BET surface area (S_{BET}) is then calculated from the following equation:

$$S_{BET} = \frac{v_m n_a a_m}{m_v} \quad (3.5)$$

Where n_a is the Avogadro's number (6.022×10^{23} mol^{-1}), m_v is the gram-molecule volume (22.414 mL) and a_m is the cross-sectional area occupied by each adsorbate molecule at 77K (0.162 nm^2).

3.7.4 Error Consideration

All experiments in this study were repeated thrice to ensure data reproducibility. However, it is still highly possible that few errors were generated from the experimental data. For example, since we used a batch system in this study, it was not possible to take sample during the reaction without compromising the system. For this reason, the data used for reaction kinetic studies is believed to have some error because all the data points obtained were from different reaction batches. This could possibly explain why the coefficients of determinations for some of the graphs were very low. Moreover, the reaction heated up to the set point temperature at different rates; therefore the exact reaction time varied since the reaction begins as the system is heated up.

Chapter 4. **Catalyst Characterisation**

4.1 Abstract

This Chapter presents the catalyst characterisation techniques employed throughout in this study such as; Transmission Electron Microscopy (TEM), Scanning Electron Microscopy (SEM) and Brunauer – Emmett – Teller (BET) analysis. The TEM analysis was used to characterise the metal depositions on the bacteria strain used for the production of biocatalysts. In addition, the SEM analysis was conducted to reveal the surface morphology of all the catalysts. The elemental constituents of the catalysts were confirmed by Energy Dispersive X-ray Spectroscopy (EDX) while the catalyst surface area was determined by BET analysis.

4.1.1 Surface Characteristics of bio-Nanoparticles (bio-NPs) in Transmission Electron Microscopy (TEM)

Transmission Electron Microscopy (TEM) allows the visualisation of the cell-bound Pd and Ru metals in the bacterial cell sections. The bacteria serve as a support to the precious metals used during the catalytic synthesis. These bacteria are composed of various functional groups such as carboxyl groups, amine groups and phosphoryl groups on their surfaces which bind to cationic metal ions. These functional groups together with enzymes such as hydrogenases and other yet unknown reductases/other biomolecules reduce the metal ions in the presence or absence of exogenous electron donors, leading to the patterning and stabilization of the metal nanoparticles on the surface of the bacteria (Omajali et al., 2015). This metal NPs form an extended surface around the bacteria forming a catalyst (metal/bacterial support) ready to be used after grinding into powder in a range of catalytic reactions.

The TEM images shown in Figure 4.1 present some morphological characteristics of the bio-NPs on bacterial support. This gives an idea of some surface properties of the bio-NPs before use as a bio-support in catalytic reactions. The monometallic bio-Pd (0) produced by *D. desulfuricans* were mostly found on the periplasmic surface of the bacterial support as Pd-NPs and were generally larger. However, smaller Pd-NPs were seen within the intracellular matrix (Fig 4.1a) as supported by new findings (Omajali et al., 2015) using high resolution STEM-HAADF (Scanning-Transmission Electron Microscope) with a (High-Angle Annular Dark Field) detector which was quite unclear when JEOL 1200 EX electron microscope was used. The synthesis of monometallic bio-Ru by *B. benzeovorans* was mostly extracellular (Fig 4.1b) with no intracellular deposition of ruthenium nanoparticles (NPs) which was different when bimetallic bio-Pd/Ru was synthesized by *B. benzeovorans* (Fig 4.1c). There was both extracellular and intracellular deposition of bio-Pd/Ru using *B. benzeovorans* with occasional larger agglomerates within the intracellular compartment (Fig 4.1c). Overall, the bio-Pd (0) NPs synthesized by *D. desulfuricans* were larger than both the monometallic bio-Ru and bimetallic bio-Pd/Ru produced by *B. benzeovorans*. This may be due to different mechanisms in the synthesis of nanoparticles by the two bacteria. Generally, *D. desulfuricans* NCIMB 8307 has been known to possess hydrogenases which play a key role in the synthesis and reduction of palladium (Mikheenkho et al., 2008), and are mostly found within the periplasmic layer. This was also confirmed using hydrogenase deficient mutants (Mikheenkho et al., 2008; Deplanche et al 2010). The bio-NPs produced by this particular strain have equally been used in various catalytic reactions (Bennett et al., 2013; Creamer et al., 2007; Deplanche et al., 2014). However, while *B. sphaericus* has been used to synthesize catalytically active Pd-NPs (Creamer et al., 2007) of which the formation of the Pd-NPs was mainly attributed to its highly phosphorylated S-layer protein (Fahmy et al., 2006; Pollmann et al. 2005), *B. benzeovorans* was used for the

first time to synthesize catalytically active Pd-NPs. The mechanism by which this happens is yet to be elucidated. The preference for using *B. benzeovorans* was mainly due to the ability to produce the cells in large quantities especially as *Bacillus* spp. are major by-products of pharmaceutical industries. The use of *D. desulfuricans* would be limited due to the challenge of scale up and also their by-product during production is H_2S, which is a strong catalyst poison. The differences in the surface properties of the bio-NPs (monometallic *vs* bimetallic) produced using the two bacteria (Gram negative and Gram positive) may be key to differences in catalytic properties. Strain-dependent properties have been shown to play a major role in the effect of Pd-NPs in Heck-Coupling reactions (Deplanche et al., 2014).

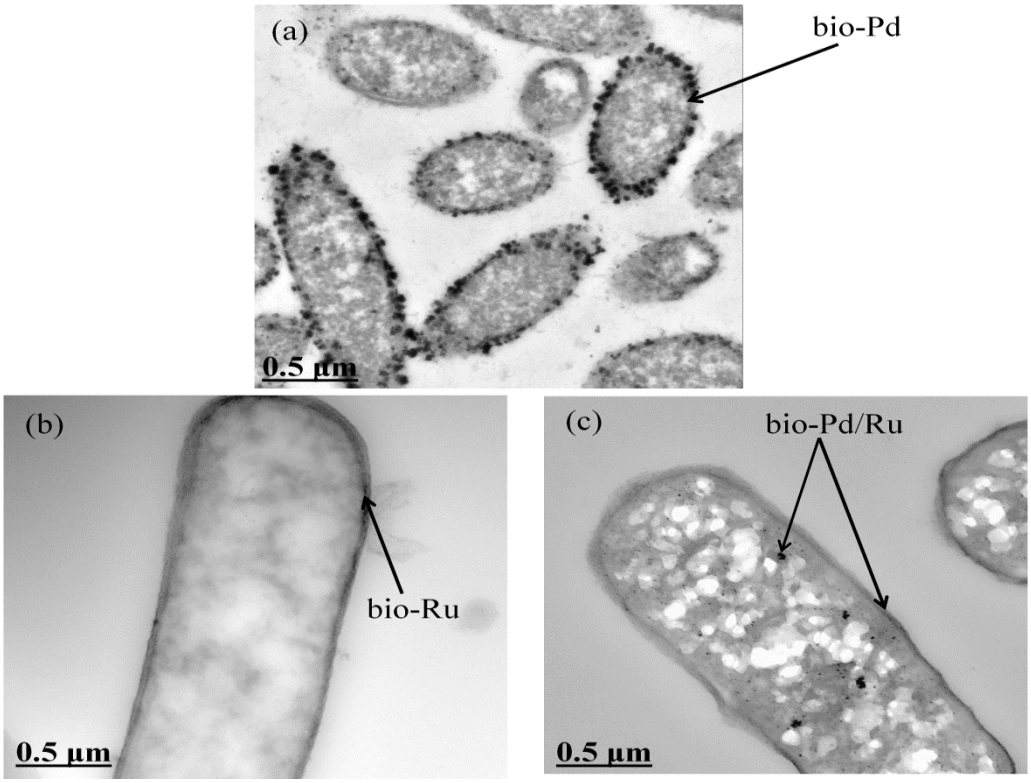

Figure 4.1: Shows TEM images of bio-NPs.

(a) 20% bio-Pd produced by D. desulfuricans NCIMB 8307 while (b) and (c) 20% bio-Ru and 20% bio-Pd/Ru produced by B. benzeovorans respectively. Pd: palladium, Ru: ruthenium.

4.1.2 Scanning Electron Microscopy (SEM) and EDX

This section focused on the examination of the morphological characteristics of all the catalysts used in this study under the electron microscope.

4.1.2.1 Surface Morphology and Elemental Confirmation (SEM/EDX)

The commercial catalysts are black powder which consists of the metal (Ru or Pd) on the activated carbon support. However, the metal bio-supported catalysts are black powder in which the metal particles are supported on the bacterial biomass. This provides a similar role

to conventional supports such as alumina, silica and carbon. Typical SEM images of the dry 5 wt% Ru/C powder is presented in Figure 4.2 a-e.

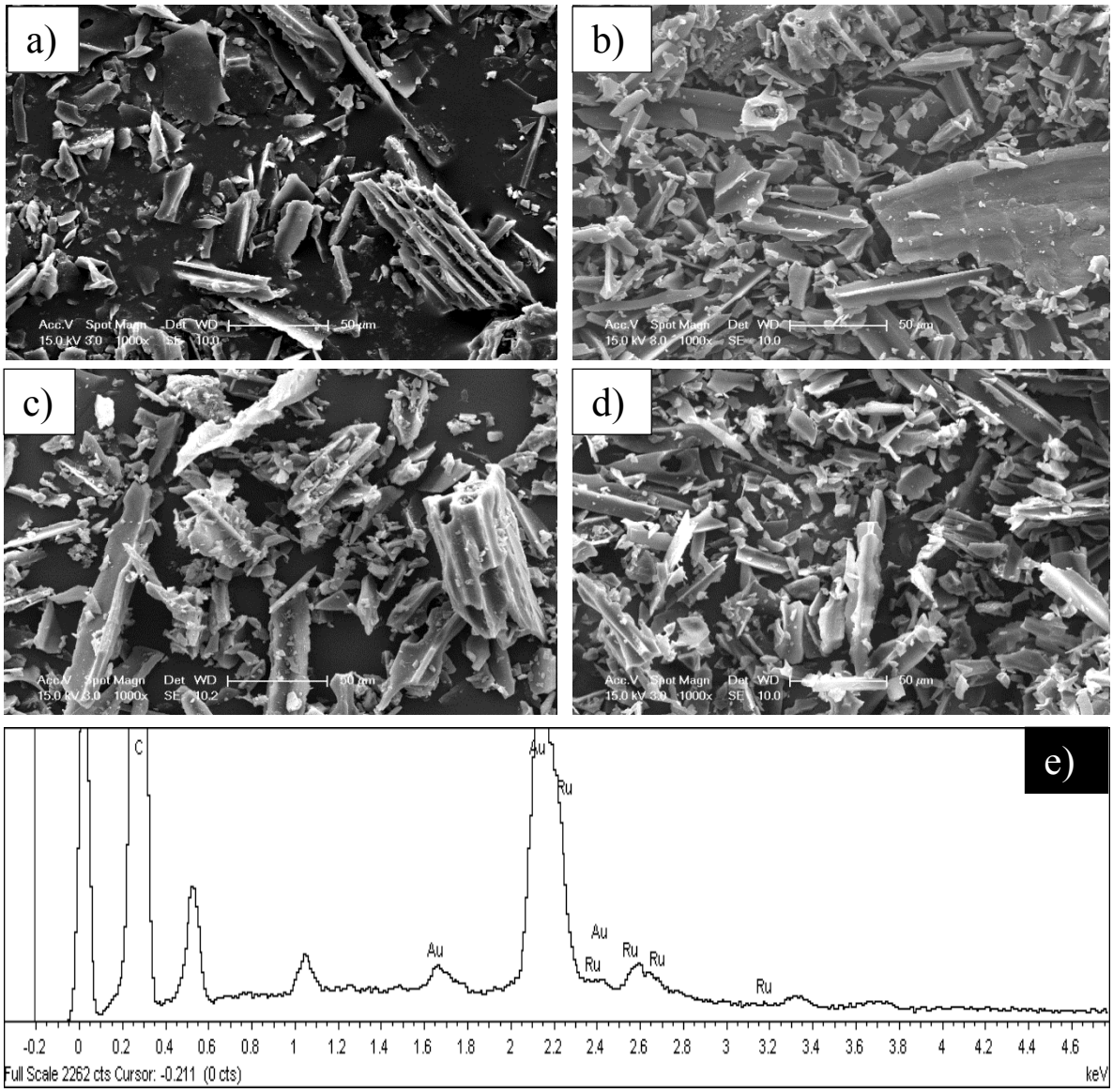

Figure 4.2: SEM images of Ru/C catalyst.

a) SEM image of fresh 5 wt% Ru/C catalyst powder; b) SEM image of spent 5 wt% Ru/C in molecular H_2; c) SEM image of spent 5 wt% Ru/C in HCOOH/Et_3N mixture; d) SEM image of spent 5 wt% Ru/C in 2-propanol; e) Corresponding EDX spectrum of fresh 5 wt% Ru/C catalyst.

The photomicrographs of the fresh and spent 5 wt% Ru/C catalyst are given in Figure 4.2 a-e. It can be seen from Figure 4.2a that the fresh Ru/C catalyst shows fine particle size with

wide carbon tubes of size range 15 – 50 μm. This means that the fresh Ru/C catalyst has a wide particle size distribution. However, after the fresh Ru/C catalyst was used in catalytic hydrogenation of 5-HMF to 2,5-DMF in molecular H_2, it can be seen from Figure 4.2b that the carbon tubes have broken down to smaller particles of size range 10 – 30 μm due to degradation in spite of the un-noticeable difference in the morphologies. This implies that the 5 wt% Ru/C catalyst could possibly be reused for another cycle but further analysis are required to confirm this. In addition, when the Ru/C catalyst was used in the catalytic transfer hydrogenation of 5-HMF to 2,5-DMF in HCCOH/Et_3N mixture, it can be observed from Figure 4.2c that the carbon tubes have broken down into smaller particles of size range 6 – 30 μm when compared to the fresh Ru/C and the spent Ru/C in molecular H_2. This is as expected due to the presence of formic acid used during the reaction. This is in agreement with Gladiali and Alberico, (2006) who reported that some catalyst may either lose their catalytic activity completely or undergo decomposition early in a reaction involving HCCOH/Et_3N mixture. The extent of degradation of the catalyst makes it challenging to recover/recycle after reaction. Moreover, when the Ru/C catalyst was employed in 2-propanol, it can be seen in Figure 4.2d that the catalyst undergoes degradation but to a lesser extent compared to that observed in HCCOH/Et_3N mixture. Consequently, there is not much difference in the morphology, thus the catalyst can be reused for another cycle. However, further analysis are required to confirm this. Finally, the

corresponding EDX spectrum in Figure 4.2e confirms the presence of ruthenium, carbon and gold peak in the spectra.

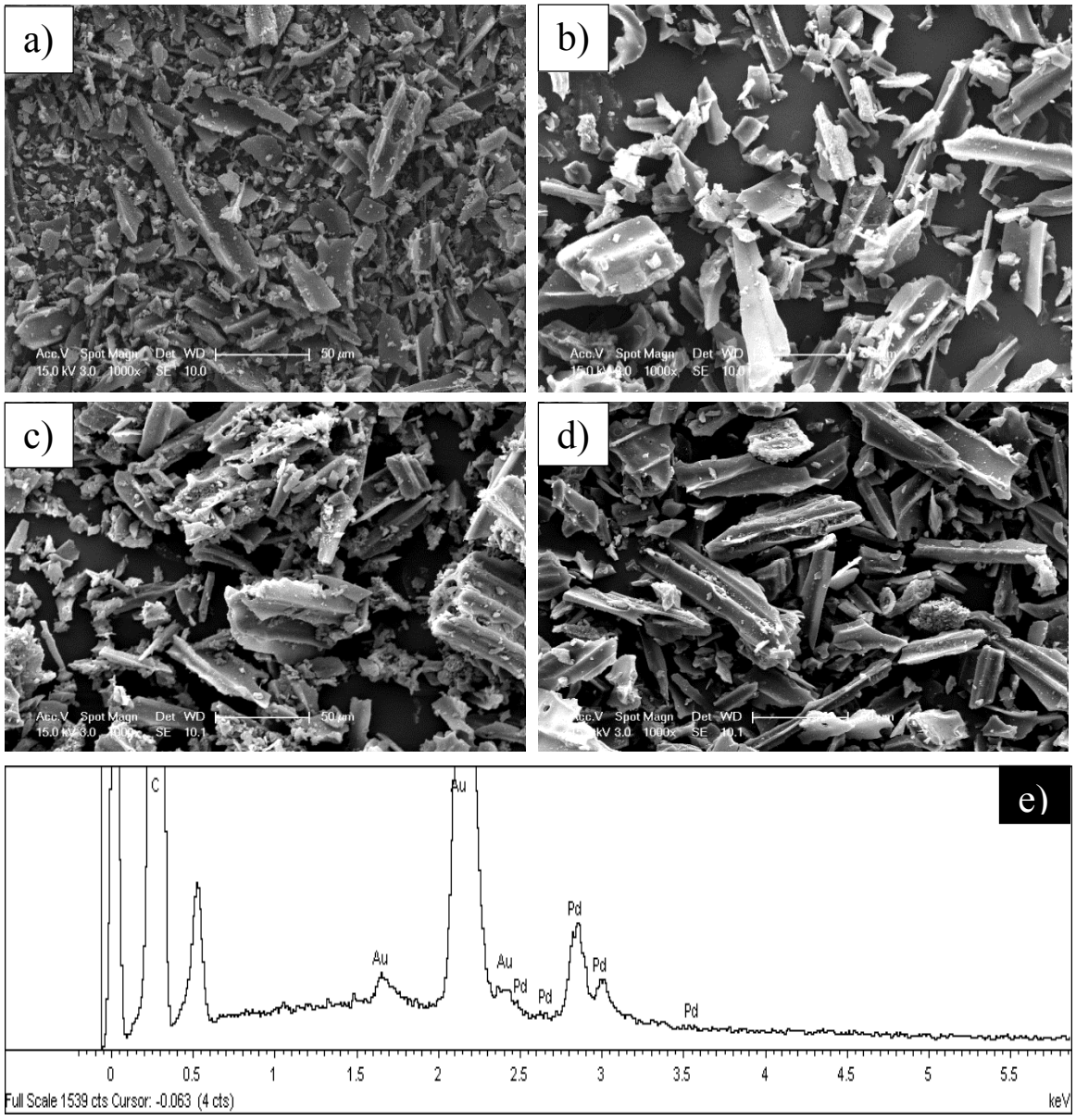

Figure 4.3: SEM images of 5 wt% Pd/C catalyst.

a) SEM image of fresh 5 wt% Pd/C catalyst powder; b) SEM image of spent 5 wt% Pd/C in molecular H_2; c) SEM image of spent 5 wt% Pd/C in HCOOH/Et_3N mixture; d) SEM image of spent 5 wt% Pd/C in 2-propanol; e) Corresponding EDX spectrum of fresh 5 wt% Pd/C catalyst.

The photomicrographs of the fresh and spent 5 wt% Pd/C catalyst are shown in Figure 4.3a-e. It can be observed from Figure 4.3a that the fresh 5 wt% Pd/C does not form

agglomerate. However, the structure shows carbon micro tubes of size range 10 – 50 μm. The singleness characteristic of the Pd/C will help performance and dispersion of the catalyst during the reaction. When the catalyst was used in molecular H_2, it can be seen in Figure 4.3b that there is not much difference in morphology despite the occurrence of degradation. This may be attributed to the agitation speed, high temperature or solvent system effect employed during the reaction. Furthermore, when the catalyst was used in HCOOH/Et_3N mixture, it can be seen in Figure 4.3c that the carbon micro tubes have been deactivated due to deposits on the catalyst, caused by the acidic solvent system used. Also, as shown in Figure 4.3d, it can be observed that degradation occurs when the catalyst was used in 2-propanol. Based on the observed morphology in Figure 4.3b & d, the catalyst could be reused, since there is not much difference in the catalyst morphology after reaction. Further analysis are required to confirm the reusability of the catalyst. The EDX spectra presented in Figure 4.3b & d re-affirms that the catalyst can be reused. In addition, Figure 4.3e shows the corresponding EDX spectrum confirming the presence of palladium, carbon and gold peak in the spectra.

The photomicrographs of the fresh and spent 10 wt% Pd/C are shown in Figure 4.4a-e. It can be seen from Figure 4.4a that the fresh 10 wt% Pd/C has polydispersed carbon micro tubes with fine particles. It can be seen from Figure 4.4b & d that there is not much change in morphology when the catalyst was used in molecular H_2 and 2-propanol, hence a possibility that the catalyst could be reused for another reaction cycle. In contrast, it can be observed from Figure 4.4c that there was a break down in the carbon micro tubes either due to the higher metal content or strong effect of the HCOOH/Et_3N mixture. In addition, Figure 4.4e shows the corresponding EDX spectrum confirming the presence of palladium, carbon and gold peak in

the spectra. The EDX spectra of fresh and spent 10 wt% Pd/C catalyst are presented in Figure B.0.3 (see Appendix B).

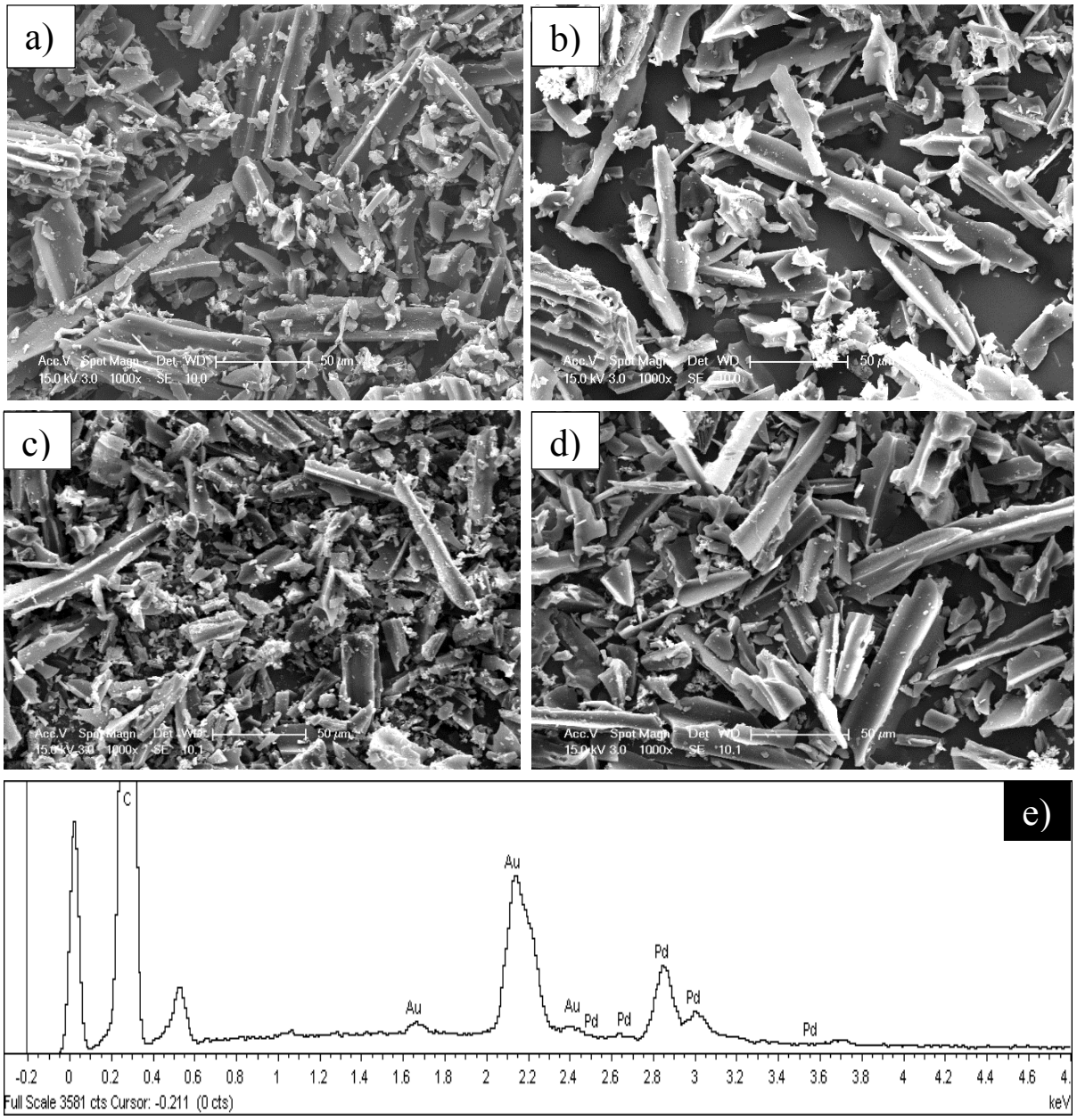

Figure 4.4: SEM images of 10 wt% Pd/C catalyst.

a) SEM image of fresh 10 wt% Pd/C catalyst powder; b) SEM image of spent 10 wt% Pd/C in molecular H_2; c) SEM image of spent 10 wt% Pd/C in HCOOH/Et_3N mixture; d) SEM image

of spent 10 wt% Pd/C in 2-propanol; e) Corresponding EDX spectrum of fresh 10 wt% Pd/C catalyst.

Figure 4.5a- d shows the photomicrographs of the fresh and spent 5 wt% bio-Pd. It can be seen from Figure 4.5a that the particles are of different size ranges. The particles are polydispersed due to different sizes ranging between 10 – 80 µm.

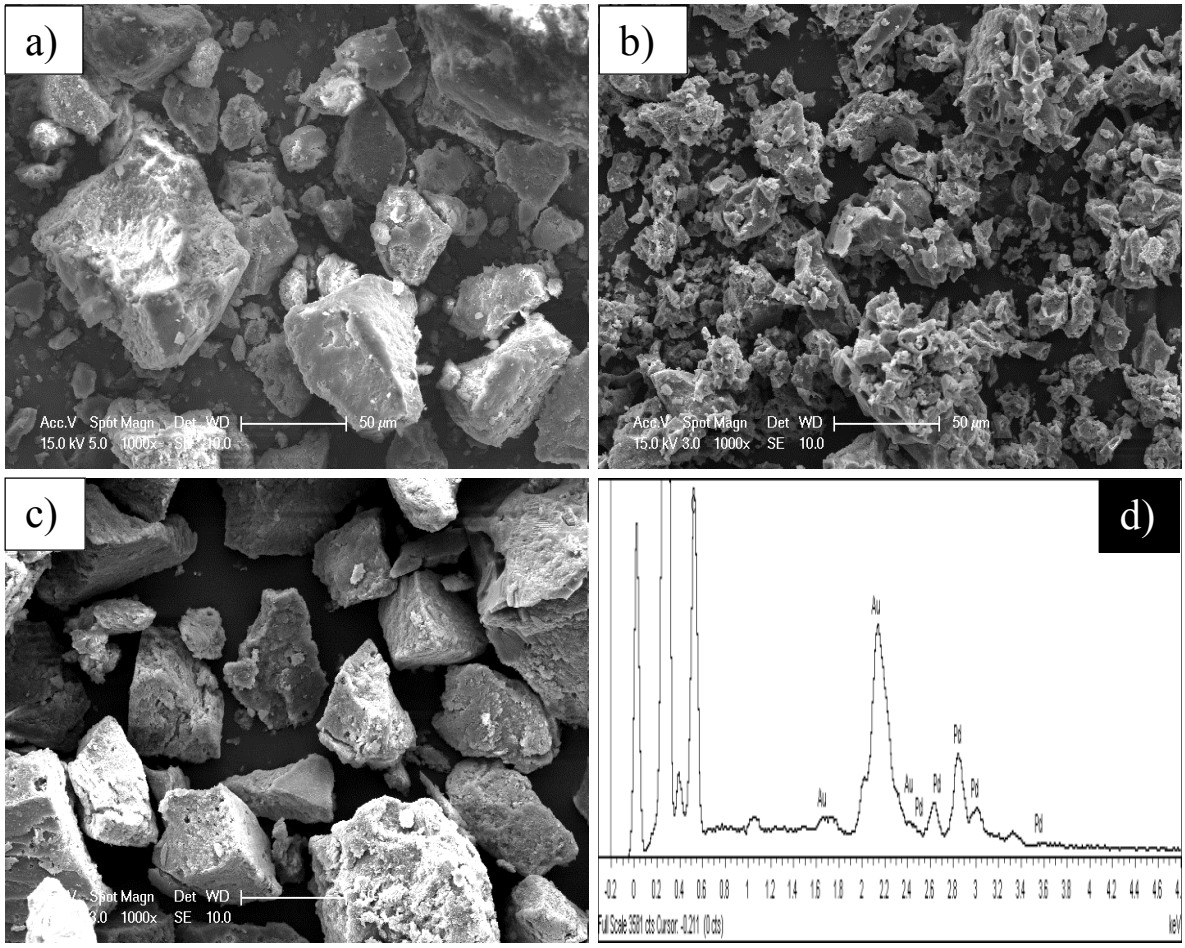

Figure 4.5: SEM images of 5wt% bio-Pd.
a) SEM image of fresh 5 wt% bio-Pd catalyst powder; b) SEM image of spent 5 wt% bio-Pd in molecular H_2; c) SEM image of spent 5 wt% bio-Pd in 2-propanol; d) Corresponding EDX spectrum of fresh 5 wt% bio-Pd.

When the 5 wt% bio-Pd catalyst was used in molecular H_2, a spongy structure can be noticed in Figure 4.5b. This is because the Pd metal is loosed during the hydrogenation reaction. In 2-

propanol, it can be observed that there is not much difference in morphology even though the particles break down. This possibly suggests the catalyst could be reused for another reaction cycle. However, due to the strong effect of HCOOH/Et_3N mixture on the bio-Pd, it was a challenge to recover the catalyst after the reaction. The EDX spectrum in Figure 4.5d confirmed the presence of palladium, carbon and gold peak in the spectra.

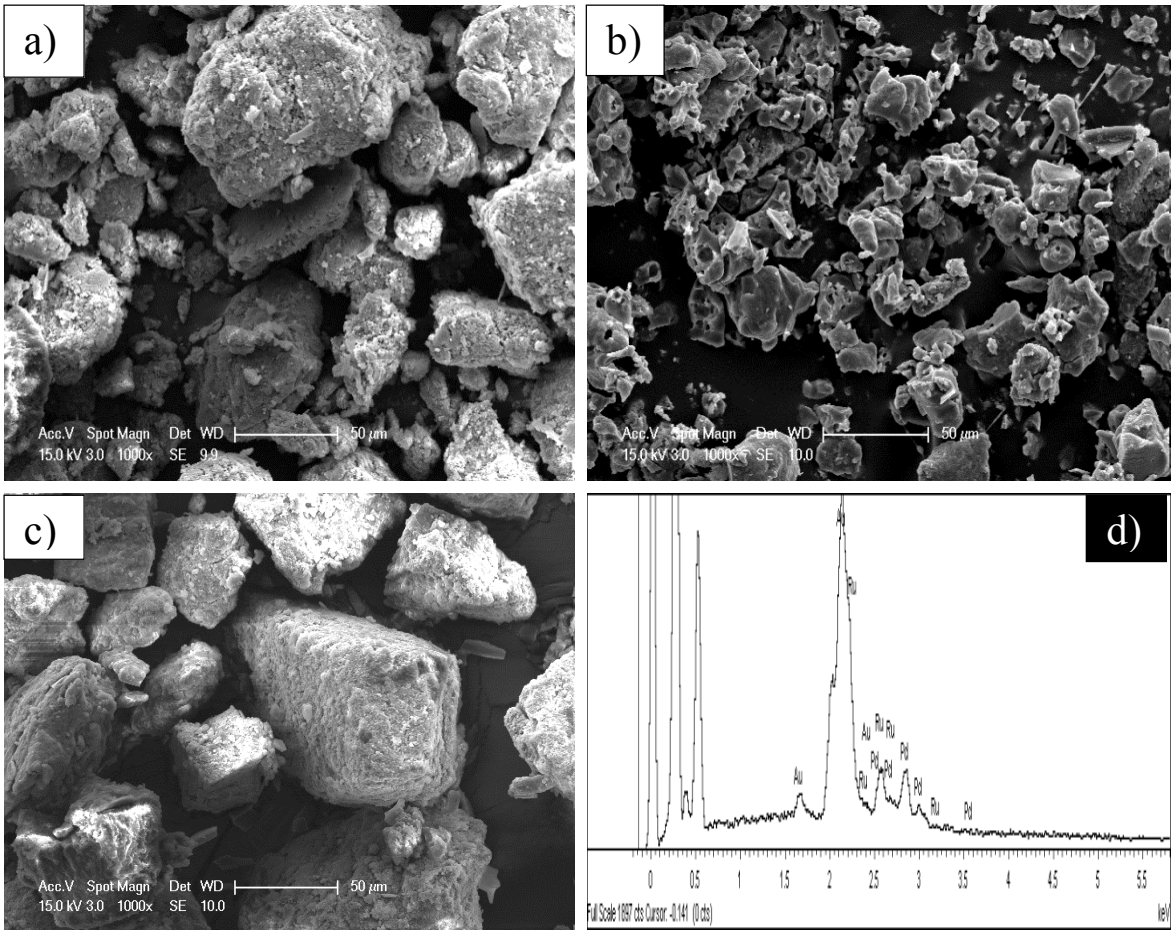

Figure 4.6: SEM images of 5wt% bio-Ru/Pd.

a) SEM image of fresh 5 wt% bio-RuPd catalyst powder; b) SEM image of spent 5 wt% bio-RuPd in molecular H_2; c) SEM image of spent 5 wt% bio-RuPd in 2-propanol; d) Corresponding EDX spectrum of fresh 5 wt% bio-RuPd.

The photomicrographs of the fresh and spent 5 wt% bio-RuPd are shown in Figure 4.6a-d. It can be seen from Figure 4.6a that there was no agglomerate formed in the fresh bio-RuPd with particle size range between 12 and 50 μm. After the used of the bio-RuPd in molecular H_2 as shown in Figure 4.6b, it can be seen that the particles are broken down with some agglomeration due to either the high temperature used during the reaction or the agitation speed. Moreover, upon the use of 2-propanol, the spent catalyst morphology was not altered when compared to the fresh counterpart (see Figure 4.6c), hence a possibility that it can be reused. It must be stated here that it was also a challenge to recover the bio-RuPd catalyst after reaction in HCOOH/Et_3N solvent mixture. Figure 4.6d shows the presence of ruthenium, palladium and gold peaks in the EDX spectra.

In addition, Figure 4.7a-d shows the photomicrographs of the fresh and spent 20 wt% bio-RuPd. The higher the metal content, the higher the tendency to form agglomeration even though the particle sizes were smaller as it can be seen from the fresh catalyst in Figure 4.7a. However, after reaction in molecular H_2, it forms agglomerates as shown in Figure 4.7b. In 2-propanol, it can be seen from Figure 4.7c that bigger agglomerates were more than 50 μm,

because of the liquid-bridge of the solvent makes the particles connect together. Figure 4.7d confirmed ruthenium, palladium and gold peaks in the EDX spectra.

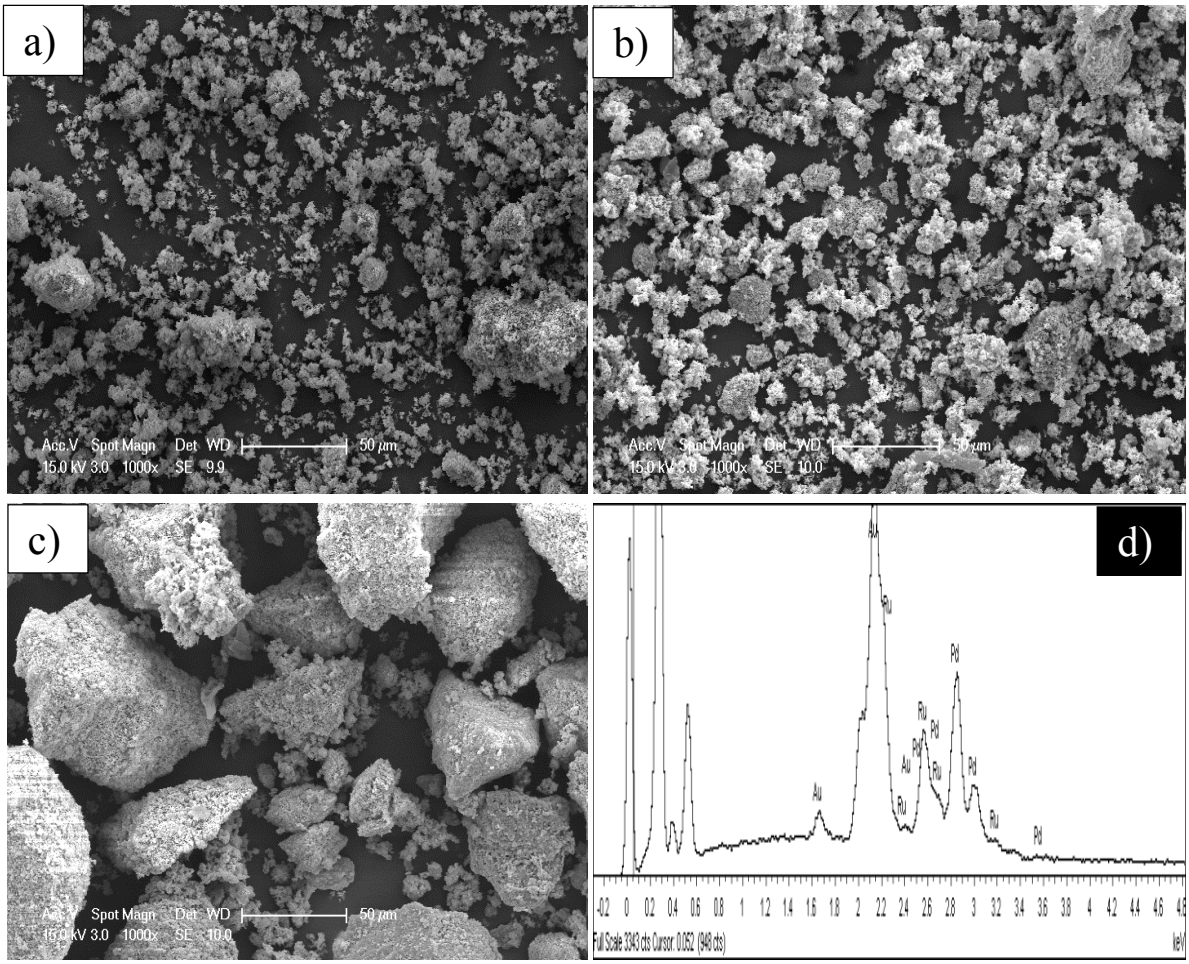

Figure 4.7: SEM images of 20 wt% bio-Ru/Pd.

a) SEM image of fresh 20 wt% bio-RuPd catalyst powder; b) SEM image of spent 20 wt% bio-RuPd in molecular H_2; c) SEM image of spent 20 wt% bio-RuPd in 2-propanol; d) Corresponding EDX spectrum of fresh 20 wt% bio-RuPd.

The photomicrographs of the fresh and spent 20 wt% bio-Ru are shown in Figure 4.8a-d. It can be noticed from Figure 4.8a that the particle size in the fresh catalyst was bigger (15 – 60 μm) because of the high metal content. However, after it was used in molecular H_2 as shown in Figure 4.8b, a spongy structure with holes were observed. This could be attributed to the fact

that ruthenium metal were mostly found on the extracellular surface of the bacteria support as shown in the TEM images in Figure 4.1b. In this case, the metal was involved in the hydrogenation reaction hence why the biomass loses the metal. In contrast, after it was used in 2-propanol, it can be seen from Figure 4.8c that there was no agglomeration and no obvious changes in the catalyst morphology. This suggests that the catalyst can be reused for another reaction cycle but further analysis are required to confirm this. Figure 4.8d shows the presence of ruthenium, and gold peaks in the EDX spectra.

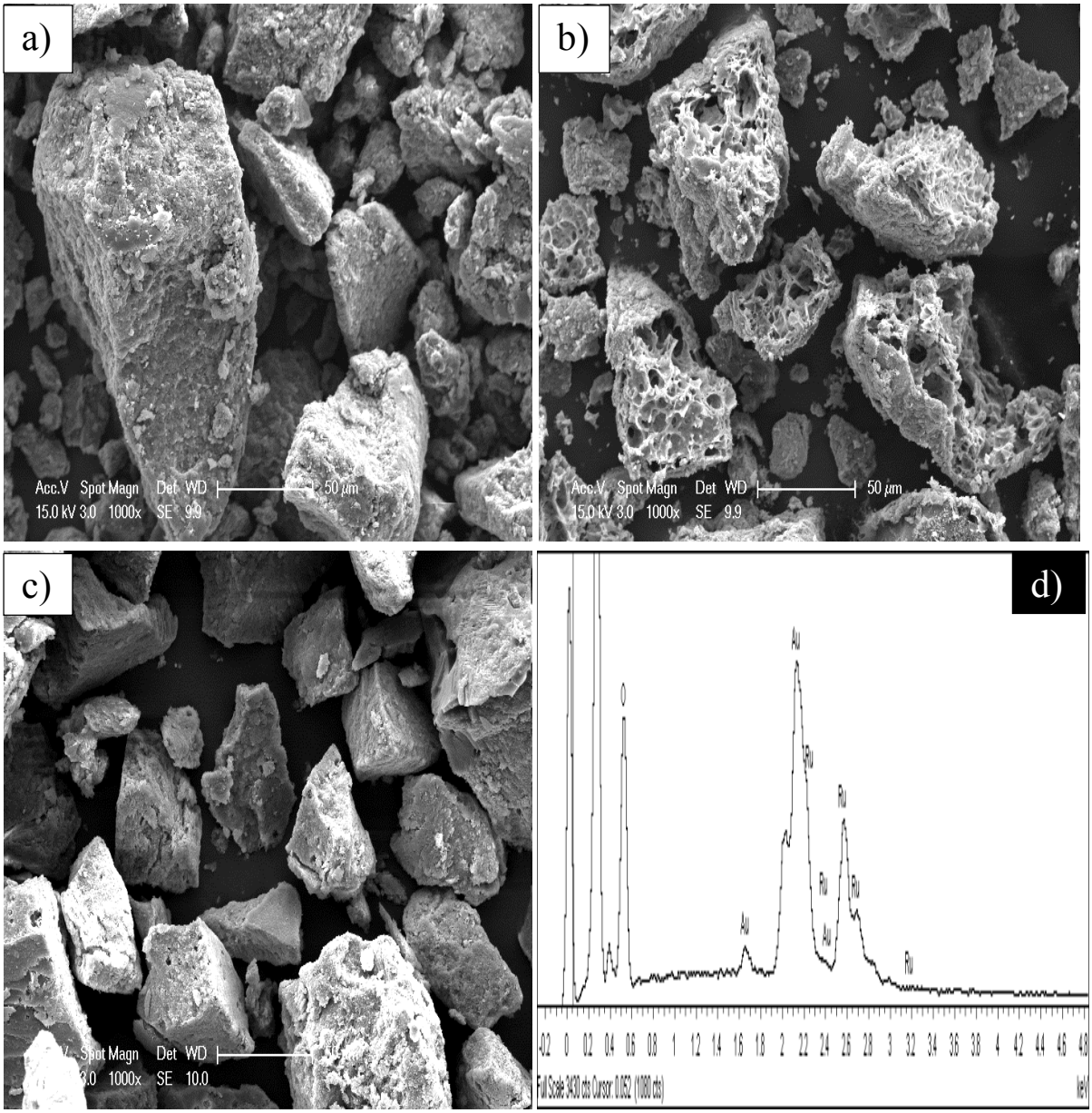

Figure 4.8: SEM images of 20 wt% bio-Ru.

a) SEM image of fresh 20 wt% bio-Ru catalyst powder; b) SEM image of spent 20 wt% bio-Ru in molecular H_2; c) SEM image of spent 20 wt% bio-Ru in 2-propanol; d) Corresponding EDX spectrum of fresh 20 wt% bio-Ru.

4.1.3 Brunauer – Emmett – Teller (BET) analysis

4.1.3.1 Nitrogen Adsorption-Desorption Isotherm of Catalysts

The nitrogen adsorption-desorption isotherm for 5 and 10 wt% Pd/C and 5 wt% Ru/C catalysts is presented in Figure 4.9a and that of 5 wt% bio-Pd in Figure 4.9b. It is clear from Figure 4.9a that the adsorption-desorption isotherm for the commercial catalysts are Type IV (Sing et al., 1985). This means that they are mesoporous materials with pore size ranging from 2 to 50 nm. It can also be seen that the increase in relative pressure increased uptake of nitrogen as pore become filled. However, comparing the 5 and 10 wt% Pd/C, it can be seen from Figure 4.9a that the addition of more metal reduces the surface area as well as the pore volume.

As seen in Figure 4.9b, the adsorption-desorption isotherm for the bio-Pd catalyst is Type II. The isotherm obtained is a characteristic of non-porous material. This means that the Type II isotherm shows unrestricted monolayer-multilayer adsorption (Sing et al., 1985).

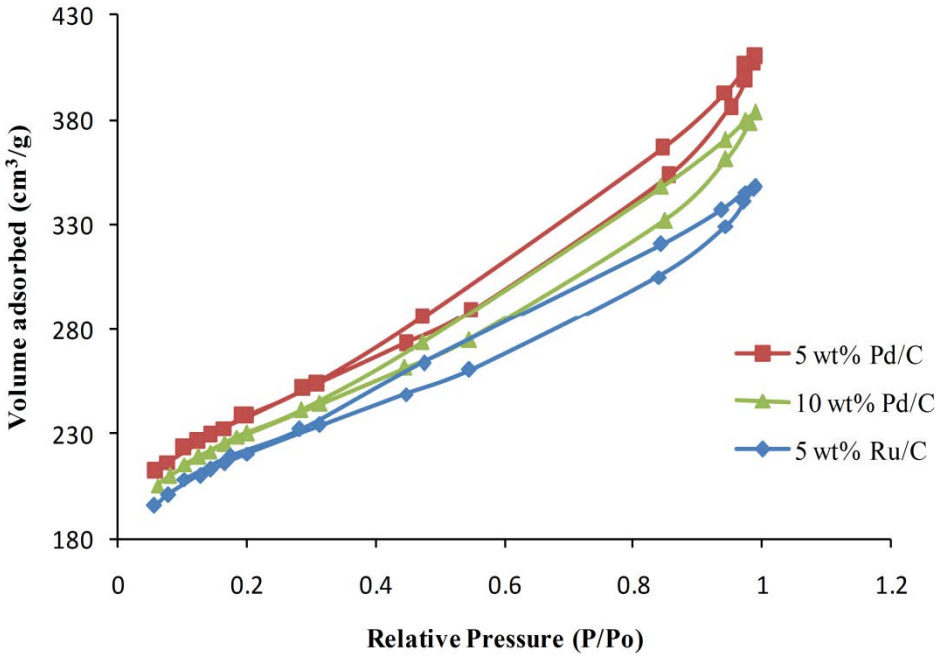

(a)

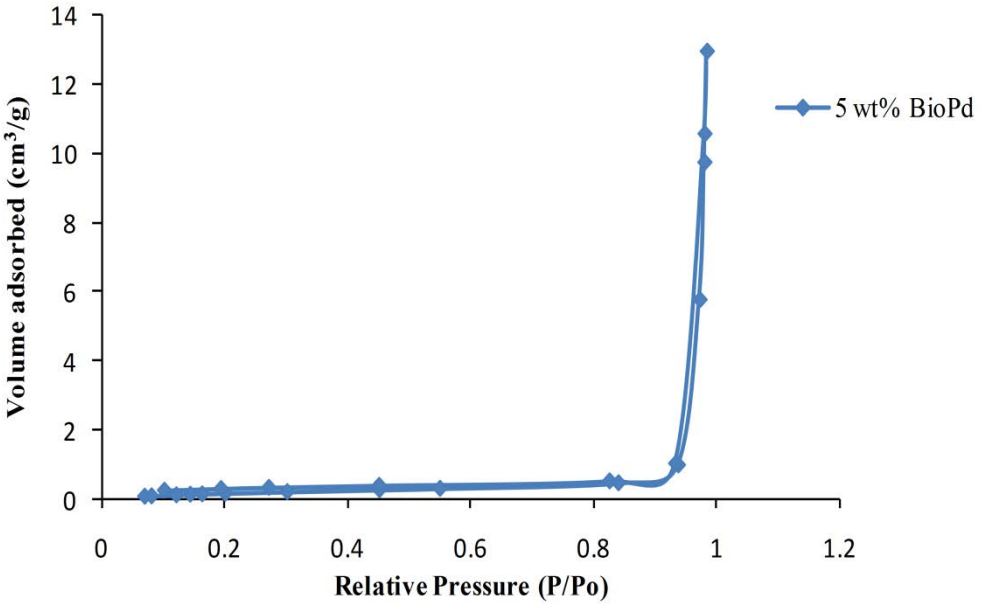

Figure 4.9: Nitrogen adsorption-desorption isotherm

(b)

(a) 5 wt% Pd/C, 10 wt% Pd/C and 5 wt% Ru/C, (b) 5 wt% Bio-Pd

4.1.3.2 Calculation of BET Surface Area

In Figure 4.10, the BET plot of the nitrogen sorption data of fresh 5 wt% Pd/C catalyst using BET equation presented in equation 3.4

$$\frac{P}{V(P_o - P)} = \frac{1}{V_m C} + \frac{(C-1)P}{V_m C P_o} \qquad (3.4)$$

where; P is the partial pressure of N_2, C is dimensionless constant related to the enthalpy of adsorption of the adsorbate gas on the powder sample, P_o is the saturation pressure at the experimental temperature, V_m volume adsorbed at monolayer coverage, and V volume adsorbed at P.

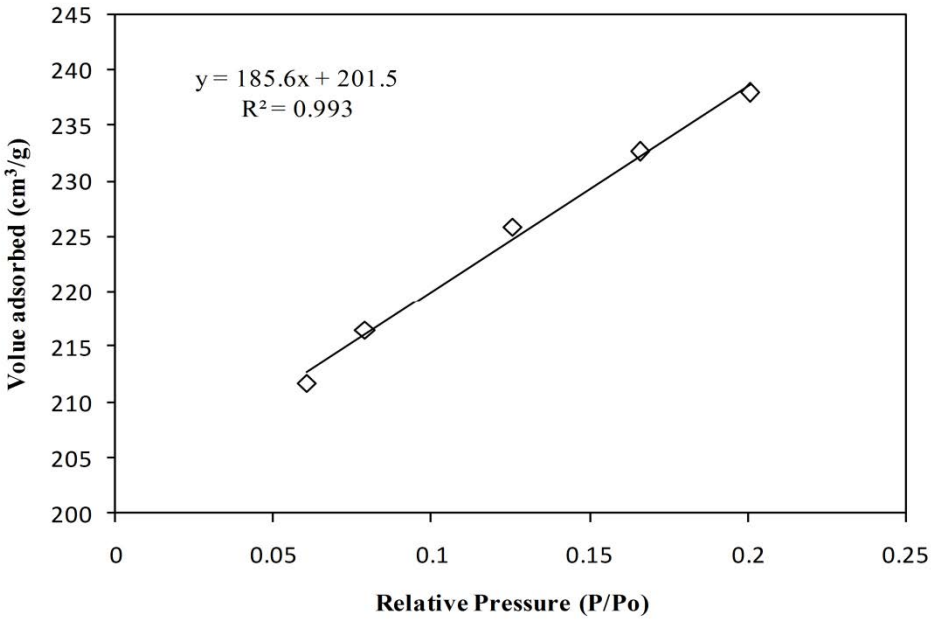

Figure 4.10: BET plot of fresh 5 wt% Pd/C catalyst.

From Figure 4.10;

$1 / V_m C = 201.5$

(C-1) / V_m C = 185.6

It follows that C = 1.9211 and V_m = 0.0026 cm^3/g. The BET surface area is however calculated using equation (3.5):

$$S_{BET} = \frac{v_m n_a a_m}{m_v} \quad (3.5)$$

Where; V_m is 0.0026 $cm^3.g^{-1}$, n_a is the Avogadro's number (6.022 x 10^{23} mol^{-1}), a_m is the cross-sectional area occupied by each adsorbate molecule at 77 K (0.162 nm^2) and m_v is the gram-molecule volume (22.414 mL). Therefore, S_{BET} for fresh 5 wt% Pd/C catalyst is 818.7 m^2/g. The surface area of other catalysts used in this study is calculated using the same approach and are listed in Table 4.1.

Table 4.1: Surface Area and Total Pore Volume of catalysts.

Catalyst	Surface Area (m^2/g)	Total Pore Volume (cm^3/g)
5 wt % Pd/C	818.7 ± 11.96	0.38
10 wt% Pd/C	789.2 ± 12.18	0.42
5 wt% Ru/C	759.1 ±11.99	0.33
5 wt% Bio-Pd	0.9 ± 0.0367	0.02

The BET surface area of 20 wt% Bio-Ru, 5 and 20 wt% Bio-Ru/Pd were not calculated due to insufficient amount of catalyst produced. It is important to note that a high surface area and moderate pore volume catalysts are known to be very active for hydrogenation reactions because of the efficient dispersion of active metals in the pores. On the other hand, catalysts with a small surface area and a large pore volume are known to be less active because of a lower

concentration of active sites. Therefore, the activated carbon support allows active component to have a larger exposed surface area (as shown in Table 4.1) in order to activate species at a very high temperature.

4.2 Conclusions

This chapter describes the catalyst characterisation techniques employed in this study. TEM analysis was carried out to investigate the surface characteristics of the biocatalyst used in this study. It was observed that the monometallic bio-Pd produced by *D. desulfuricans* were mostly found on the periplasmic surface of the bacterial support with smaller Pd nanoparticles seen within the intracellular matrix while the monometallic bio-Ru produced by *B. benzeovorans* were mostly extracellular with no intracellular deposition of ruthenium particles. Conversely, the bimetallic bio-Pd/Ru synthesised by *B. benzeovorans* were deposited in both extracellular and intracellular compartment with occasional larger agglomerates found within the intracellular region. Overall, it was observed that the bio-Pd synthesised by *D. desulfuricans* were larger than both the monometallic bio-Ru and bimetallic bio-Pd/Ru synthesised by *B. benzeovorans*.

The SEM analysis was conducted to investigate the surface morphology of all the catalyst employed in this study before and after reaction. Generally, it was observed that experiments carried out with all the catalyst in molecular hydrogen showed less degradation compared to that in $HCOOH/Et_3N$ and 2-propanol solvent mixture. This possibly suggests why

majority of the catalysts employed in molecular hydrogen could be reused after the first run of experiment.

Chapter 5. **Synthesis of 2,5-DMF in Molecular Hydrogen.**

5.1 Abstract

The catalytic hydrogenation of 5-hydroxymethylfurfural (5-HMF) with molecular hydrogen was studied over both palladium and ruthenium catalysts in tetrahydrofuran using a batch reactor. The ruthenium supported on carbon (Ru/C) catalyst showed the best catalytic activity among all the catalyst tested. A very high yield (95.1%) of 2,5-dimethylfuran (2,5-DMF) and 96.4% 5-HMF conversion was achieved after optimization of reaction parameters. Optimum reaction conditions are attained at 260^{o}C; 2 hours of reaction time; 50 bar H_2 pressure; and 700 rpm agitation speed. The plausible reaction mechanism has been explored through capture of reaction intermediates by gas chromatography-mass spectroscopy technique. To the Author's knowledge, this is the first time a bio-support has been used in the catalytic hydrogenation of 5-HMF into 2,5-DMF with molecular H_2. A very high yield of 2,5-DMF (60.3%) and 95.3% 5-HMF conversion was attained. This possibly implies that the 40% left over constitute reaction intermediates and by-products.

5.2 Introduction

Hydrogenation can simply be defined as a chemical reaction between an element or compound and molecular hydrogen. Gaseous hydrogen can be dissociated into atoms and is considered endothermic to a degree of 104 kcal mol^{-1} which is partly responsible for its low reactivity (James, 1973; Pupovac, 2013). Atomic hydrogen is considered endothermic because

it is stable only for a fraction of a second before it immediately reverts back to its molecular form, thereby liberating a large amount of energy. Thus, molecular hydrogen can be activated through different substances involving homogenous and heterogeneous catalysts with the latter being of countless significance to the chemical industry. Different metals such as copper, nickel, cobalt, ruthenium, palladium, platinum and iridium are known to show good catalytic activity in heterogeneously catalysed hydrogenation reactions. These metals can also combine with other elements so as to modify the catalyst activity or other catalytic properties. Catalytic hydrogenation reactions involve the addition of hydrogen to unsaturated bonds such as C≡C, C=C, C≡N, C=O, as well as hydrogenolysis which involves cleavage and reduction of C-O, C-C and other bonds. The currently used catalysts for different hydrogenation purposes are shown in Table 5.1.

Table 5.1: Catalysts for different hydrogenation reactions (Navalikhina et al., 1998).

Reaction	**Catalyst**
Hydrogenation of nitriles	Supported Pd, Ni and Pt
Hydrogenation of aromatic hydrocarbons	Supported Pd, Ni, Co-Mo, Rh and Raney Ni
Hydrogenation of CO and CO_2	Supported Cu, Ni, Pt, Rh, Co-Fe, Mo and W carbides
Hydrogenation of alkenes	Supported Cu, Ni, Ru, Pd, Rh and Pt
Hydrogenation of alkynes	Supported Pd, Ni, Co-Pd, Ni-Pd and Cu-Pd
Hydrogenation of carbonyl compounds	Skeletal and supported Ni and Co, Rh, Pd, Ru and Cu-Cr-O
Hydro refining of moto fuels	Ni-Mo, Ni, Co-Mo on Al_2O_3

With the exception of Raney-type catalysts, unsupported catalysts are rarely used for industrial processes. The presence of a support allows the active component to have a larger exposed surface area. This is of high significance particularly where a very high temperature is needed to activate the active species. Supports such as activated carbon, Al_2O_3, zeolites, TiO_2 and SiO_2 are commonly employed. Supported metal catalysts are known to be more resistant to poisons when compared to unsupported catalysts which are usually more sensitive towards impurities (Maxted et al., 1950). In addition, hydrogenation reactions catalysed by heterogeneous catalysts take place on the catalyst surface allowing the metal particles onto a carrier. This ultimately results to a higher surface to bulk ratio of the material which then leads to availability of higher active sites per gram of the metal (Pupovac, 2013).

Among the most valued synthetic transformations known, heterogeneously catalysed hydrogenation reactions are of high importance to the chemical industry. They are widely utilised in synthesis of fine chemicals, fats and oils for making nonedible and edible products, intermediates employed in pharmaceutical industry and monomers for the generation of different polymers.

Recently, the development of new catalytic technologies for biomass conversion into liquid fuels has generated much attention especially for use in the transportation sector. The initial conversion of biomass via pyrolysis, gasification, hydrolysis and liquefaction can progress without the use of hydrogen. However, the introduction of hydrogen becomes very important in the second stage of biofuel production where liquid fuels are produced through transformation of upgradeable platforms (Pupovac, 2013). Renewable hydrogen can be

produced from biomass using two catalytic methods. The commonest method occurs via gasification process, which can be joined with water-gas shift reaction to generate production of hydrogen from CO and H_2O as illustrated in equation 5.1. The second method involves aqueous phase reforming of oxygenates, as shown in equations 5.2 and 5.3.

$$CO + H_2O \rightarrow CO_2 + H_2 \qquad (5.1)$$

$$C_3H_8O_3 + 3H_2O \rightarrow 3\ CO_2 + 7\ H_2 \qquad (5.2)$$

$$C_6H_{14}O_6 + 6\ H_2O \rightarrow 6\ CO_2 + 13\ H_2 \qquad (5.3)$$

The well-known and widely accepted mechanism of catalytic hydrogenation in heterogeneous systems is that reported by Horiuti and Polanyi, (1934). This mechanism shows that hydrogen activation is formed from a dissociative chemisorption, prominent to σ-bonded hydrogen as shown in Figure 5.1, (1). Firstly, at the active surface metal sites, the C=C undergoes chemisorption through its π-system with important rehybridization of the sp^2 carbon atom orbitals to sp^3. Thus, this give rise to two σ-like catalyst-carbon bonds (Bond, 1962; Pupovac, 2013) See Figure 5.1, (2). However, the electron transfer from the C-C π-orbitals into vacant d-orbitals improved by back-bonding as a result of the electron transfer from the engaged metal d-orbitals into antibonding π-orbitals of the double bond (Chatt and Duncanson, 1953). This possibly explains the relationship between the C=C and the metal active sites. According to Horiuti and Polanyi, the activation of unsaturated compound (acceptor) and hydrogen is a reversible procedure which follows the addition of activated hydrogen step wisely.

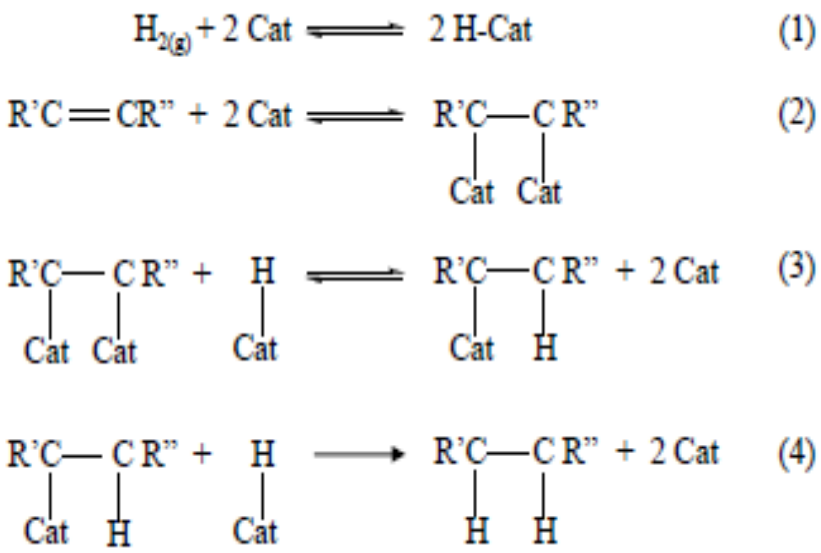

Figure 5.1: Horiuti-Polanyi mechanism of hydrogenation (Horiuti and Polanyi, 1934). (Adapted from Pupovac, 2013).

The catalytic hydrogenation of biomass-derived platform chemicals using molecular hydrogen has been widely reported in the literature. Roman-Leshkov and co-workers pioneered the conversion of 5-HMF using molecular hydrogen in 1-butanol over Cu-Ru/C catalyst (Roman-Leshkov et al., 2007) (See Section 2.7.1).

5.3 Representative Procedure

The catalytic transfer hydrogenation reactions were carried out in a 100 mL stainless steel Parr reactor autoclave with external temperature and stirring controllers. For a typical reaction, the reactor was charged with 0.08 M 5-HMF, 0.1 g Ru/C catalyst and 25 ml of tetrahydrofuran (THF), sealed, purged of air with 5 bar H_2 and charged with 50 bar H_2. The reactor was heated to 260^{o}C reaction temperature and stirred at agitation speed 500 rpm for 2 hours. After completion of the reaction, the reactor was quenched to room temperature in ice-

water bath; and the reaction mixture was filtered with 8µm Whatman quantitative filter paper. The liquid products were analysed using GC-FID (Shimadzu GC 2010).

5.4 Results and Discussion

This section describes the results obtained using molecular H_2 for the catalytic hydrogenation of 5-HMF to 2,5-DMF.

5.4.1 Catalytic Hydrogenation of 2,5-DMF Over Metal Catalyst using Molecular Hydrogen

In this study, the catalytic hydrogenation of 5-HMF to produce 2,5-DMF using molecular H_2 was investigated using 5 wt% Ru/C catalyst. 5-HMF is known to be a reactive compound because of the presence of the aldehyde group, hydroxyl group and the furan ring. In order to obtain the desired product, it is important to make sure that the furan ring structure remains intact during the reaction. Furthermore, the aldehyde and hydroxyl groups are prioritised to engage the hydrogenation reaction to produce 2,5-DMF.

5.4.2 Catalyst Screening

Three different metal catalysts 5wt% Pd, 10wt% Pd and 5wt% Ru on activated carbon (C) support were screened and the results obtained are shown in Table 5.2. For conditions of this study, no reaction was observed in the absence of a suitable metal catalyst. It is important to state here that the results obtained for 5 and 10 wt% Pd/C catalysts were based on identical reaction conditions to the 5wt% Ru/C catalyst. However, it must be noted that the use of these conditions to investigate the performance of the Pd/C catalysts does not entirely proof the effectiveness and performance of the Pd/C catalysts. Therefore, in order to investigate the

performance of the Pd/C catalysts for 5-HMF hydrogenation, optimization of reaction conditions is crucial. As Table 5.2 shows, both Pd/C catalysts gave high 5-HMF conversions (> 96%), yet 2,5-DMF yield and selectivity were low (<20%). Instead, the main product was observed to be 2,5-dimethyltetrahydrofuran (2,5-DMTHF). This implies that Pd/C catalysts promotes further conversion of 5-HMF to 2,5-DMTHF (See Section 5.6). Due to the unavailability of lower loading of the Pd catalyst (such as 1% or 2% Pd/C), it was not possible to investigate the catalytic behaviour at these loadings.

Table 5.2: Catalyst screening using molecular hydrogen

Entry	Catalyst	Conversion (%)	Yield (%)	Selectivity (%)
1	5 wt% Ru/C	96.4	95.1 ± 0.5	98.7
2	5 wt% Pd/C	96.5	19.9 ± 0.7	20.7
3	10 wt% Pd/C	96.5	18 ± 1.2	19.4

Reaction conditions: catalyst amount = 0.05 g; THF = 25 ml; temperature = 260°C; time =2 hours; H_2 pressure = 50 bar; 5-HMF concentration = 0.05 M; speed = 700 rpm. Note: 5-HMF concentration is relative to THF amount. Errors were calculated as mean ± standard error of the mean from at least three experiments.

5.4.3 Effect of Different Reaction Parameters on the Catalytic Hydrogenation of 5-HMF to 2,5-DMF.

In this section, the catalytic hydrogenation was investigated as function of different reaction variables namely; reaction temperature; time; 5-HMF concentration; catalyst amount; hydrogen pressure and agitation speed. Results are presented in terms of the reactant (5-HMF) conversion, and the product (2,5-DMF) yield and selectivity.

5.4.3.1 Effect of Reaction Temperature

Collision theory explains that running a reaction at a higher temperature would deliver more energy into the system, and thus more of the colliding particles will have the required activation energy resulting in more successful collisions by breaking the pre-existing bonds between reactants and generating in new bonds. The effect of temperature was investigated between 180ºC and 300ºC at 20ºC intervals. Figure 5.2 shows that 5-HMF conversion increased rapidly as temperature increased between 180 and 240 ºC, increasing from 46.7% at 180 ºC to 95.3% at 240 ºC followed by a slower increase to 97.9% at 300 ºC. With regard to 2,5-DMF yield, similar trend to 5-HMF conversion was observed as the yield increased rapidly then levelled off. A similar trend between reaction temperature and 2,5-DMF yield was reported by Hu et al., (2014).

Contrary to the results obtained in this study, Wang et al (2014) recently reported an optimum temperature of 180ºC for the hydrogenolysis of 5-HMF to 2,5-DMF catalysed by platinum-cobalt bimetallic nanoparticles in hollow carbon nanospheres. In their reaction, molecular hydrogen was employed as H-donor and 5-HMF conversion reached 100% at 10 minutes reaction time while 2,5-DMF yield obtained was 98% at 2 hours reaction time. Similar to the result reported by Wang et al (2014), Haung et al., (2014) reported 2,5-DMF production from biomass-derived molecules using nickel-tungsten carbide as catalyst and molecular H_2 as hydrogen source. In their experiment, an optimum reaction temperature of 180ºC was obtained with 100% 5-HMF conversion and 90% 2,5-DMF yield. The difference in optimum reaction temperature between these studies and that reported in this chapter can be ascribed to the bimetallic catalyst used by Wang et al., (2014) and Hang et al., (2014) whereas, a monometallic Ru/C was employed in this study.

As there was no significant increase in product yield and 5-HMF conversion after 260^{o}C, an optimum temperature of 260^{o}C was used throughout the optimization process. Therefore, a higher temperature suggests a higher average kinetic energy of reactants and more collisions per unit volume. Also, a higher reaction temperature affects the sorption processes on the catalyst surface, consequently having an effect on the reaction rate. In addition, changes in temperature affect not just the reaction rate but it is also believed to have an effect on the external and internal mass transfer. In order for hydrogen to take part in this reaction, it must diffuse through the gas phase followed by dissolving in the 5-HMF and then diffuse to the catalyst surface. The optimum reaction temperature obtained in this study is similar to that reported in chapter six where 2-propanol was used as hydrogen donor for the catalytic transfer of 5-HMF to 2,5-DMF.

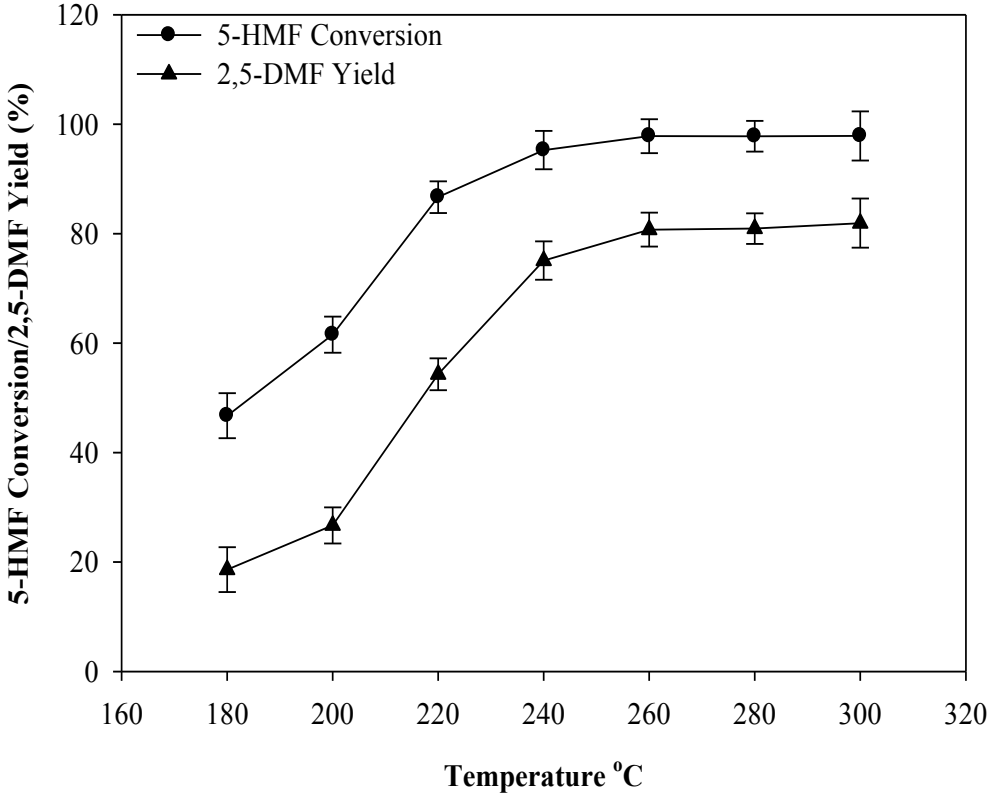

Figure 5.2: Effect of reaction temperature on 5-HMF conversion and 2,5-DMF yield.

Reaction conditions: catalyst amount = 0.1 g; THF = 25 ml; time = 2 hours; H_2 pressure = 50 bar; 5-HMF concentration = 0.08 M; speed = 700 rpm. Note: 5-HMF concentration is relative to THF amount. Where error bars are shown, these are calculated as mean ± standard error of the mean from at least three experiments.

5.4.3.2 Effect of Reaction Time

The effect of reaction time was investigated and the results are shown in Figure 5.3. It clearly shows that prolonging the reaction time beyond 2 hours does not have a significant effect on 2,5-DMF yield and 5-HMF conversion. When the reactor temperature reached set point (at t=0), 5-HMF conversion rapidly reached a value of 88.5% and 53.2% 2,5-DMF yield was obtained. An explainable reason for this could be the ready availability of hydrogen in the reaction system. At 2 hour reaction time, 5-HMF conversion and 2,5-DMF yield increased to

97.8% and 80.7% respectively. Furthermore, 2,5-DMF yield continued to increase to values of 83.3% and 84% at 4 and 6 hours respectively . However, 5-HMF conversion remained constant at 98% for both 4 and 6 hours reaction time. At 8 hours reaction time, it was clearly observed that 2,5-DMF yield decline slightly to a value of 79.3% while 5-HMF conversion remained at 98%. The decrease in 2,5-DMF yield after 8 hours could be ascribed to further hydrogenation of 2,5-DMF to 2,5-DMTHF. Moreover, the reaction rate can possibly decrease with time-on-stream due to deactivation of the Ru/C catalyst. When this is observed, it is suspected that the cause of the catalyst deactivation is related to the product or by-products formed in the reaction system which plug onto the catalyst pores, consequently, limiting the mass transfer process from the external pore mouth to the internal surface of the catalyst.

As there was no significant increase in 2,5-DMF yield after 2 hours, the optimum time was set to 2 hours in this study. This result is consistent with that reported in the literature where an optimum time of 2 hours was obtained for the catalytic hydrogenation of 5-HMF to 2,5-DMF using molecular hydrogen (Wang et al., 2014; Hu et al., 2014; Haung et al., 2014; Zhang et al.,2012).

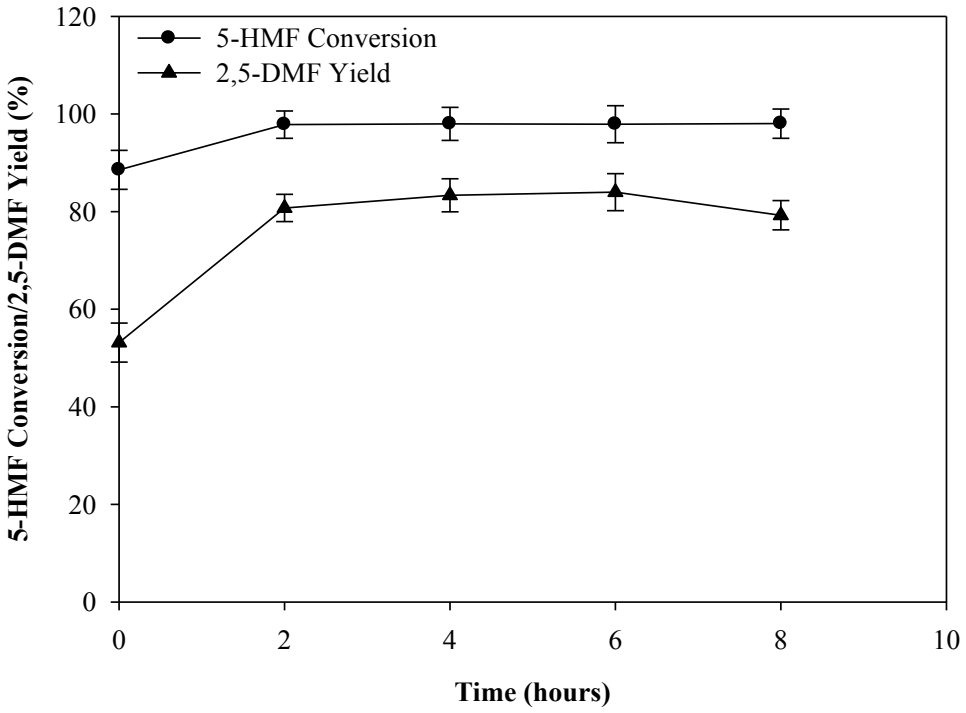

Figure 5.3: Effect of reaction time on 5-HMF conversion and 2,5-DMF yield.

Reaction conditions: catalyst amount = 0.1 g; THF = 25 ml; temperature = 260°C; H_2 pressure = 50 bar; 5-HMF concentration = 0.08 M; speed = 700 rpm. Note: 5-HMF concentration is relative to THF amount. Where error bars are shown, these are calculated as mean ± standard error of the mean from at least three experiments.

5.4.3.3 Effect of Hydrogen Pressure

Molecular H_2 was employed in this study for the catalytic hydrogenation of 5-HMF to 2,5-DMF. As shown in Figure 5.4, it can be observed that the importance of hydrogen pressure cannot be ignored. At 10 bar H_2 pressure, 5-HMF conversion obtained was 89.9% while 2,5-DMF yield was 23%. As hydrogen pressure was increased to 20 and 30 bar, 5-HMF conversion increased to 97.7% and 97.9% respectively while a significant increase in 2,5-DMF yield was reached at 62% and 69.5% respectively. Moreover, as the pressure was further increased to 40, 50 and 60 bar, 5-HMF conversion remained constant at 97.9% while 2,5-DMF yield obtained was 73.9%, 80.7% and 76.5% respectively. The increase in 5-HMF conversion and 2,5-DMF

yield after the injection of 20 bar H_2 might be attributed to high solubility of H_2 in the solvent which aided the catalytic hydrogenation of 5-HMF to 2,5-DMF (Hu et al., 2014). Also, H_2 is a reactant and having it at higher pressure (concentration) enhances the reaction towards products. Additionally, as the reactant (5-HMF) is in the liquid phase comprising of binary diffusion, the hydrogen pressure (gaseous reactant) is also believed to influence the reaction rate which shows the high conversion of 5-HMF obtained in molecular H_2. For the reactions under identical pressure and temperature, hydrogen mass transfer rate in the gas-liquid interface is determined by k_La. The volumetric liquid-side mass transfer coefficient k_La of hydrogen can be affected by different parameters such as agitation speed, reactor dimensions (for example type of impeller and diameter) and liquid/solid type (Zhu, 2014).

At 60 bar H_2 pressure, it was observed that 2,5-DMF yield decreased to 76.5%. This implies that there was excess hydrogen in the system which could promote further hydrogenation of the furan ring structure. Therefore, the optimum hydrogen pressure used in this work was 50 bar because it gave the highest yield of 2,5-DMF even though it might increase production cost and cause high risk due to high pressure in the system. This result in agreement with that reported by Haung et al., (2014) where 40 bar H_2 was reported as the optimum hydrogen pressure.

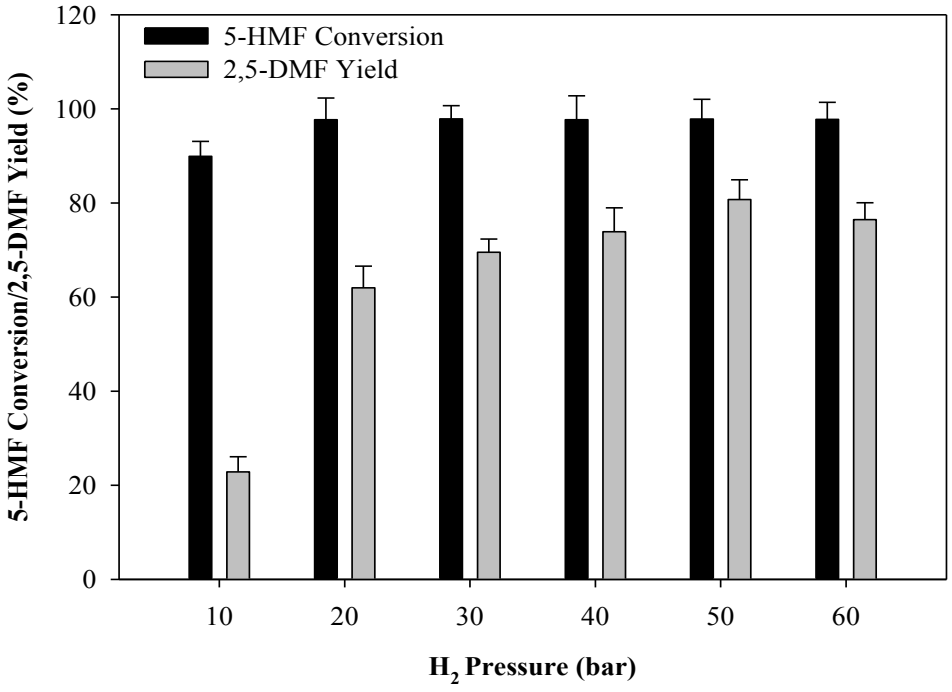

Figure 5.4: Effect of H_2 pressure on 5-HMF conversion and 2,5-DMF yield.

Reaction conditions: catalyst amount = 0.1 g; THF = 25 ml; temperature =260°C; time = 2 hours; 5-HMF concentration = 0.08 M; speed = 700 rpm. Note: 5-HMF concentration is relative to THF amount. Where error bars are shown, these are calculated as mean ± standard error of the mean from at least three experiments.

5.4.3.4 Effect of 5-HMF Concentration

The effect of initial 5-HMF concentration was investigated at optimum reaction temperature, time and hydrogen pressure obtained. As presented in Figure 5.5, it can be observed that the initial 5-HMF concentration plays an important role in the conversion of 5-HMF into 2,5-DMF. When the concentration of 5-HMF was 0.05 M, high 5-HMF conversion of 96.4% and 86.7% yield of 2,5-DMF was obtained. Furthermore, it can be seen that as the concentration of 5-HMF was increased to 0.08, 0.11, 0.14 and 0.18 M, 5-HMF conversion increased slightly to a value of 97.8%, 98.4%, 98.7% and 98.9% respectively. Conversely, a

decrease in 2,5-DMF yield was observed as the concentration of 5-HMF increased. The value obtained for 2,5-DMF yield were 80.7%, 78.5%, 74.3% and 67.8% respectively.

Despite a very high 5-HMF conversion, the decrease in 2,5-DMF yield could be attributed to the fact that hydrogenation of 5-HMF to 2,5-DMF was incomplete resulting in the formation of side products. It is believed that the hydrogenation was incomplete as a result of either; insufficient H_2 or less amount of catalyst in the reaction medium. There is also a possibility that 5-HMF competes with the product for catalyst active sites, thus slowing down the reaction. It is noteworthy to state that 5-HMF concentration is relative to THF while catalyst amount is relative to 5-HMF concentration. Therefore, 0.05 M was selected as the optimum 5-HMF concentration and was used throughout the optimization process.

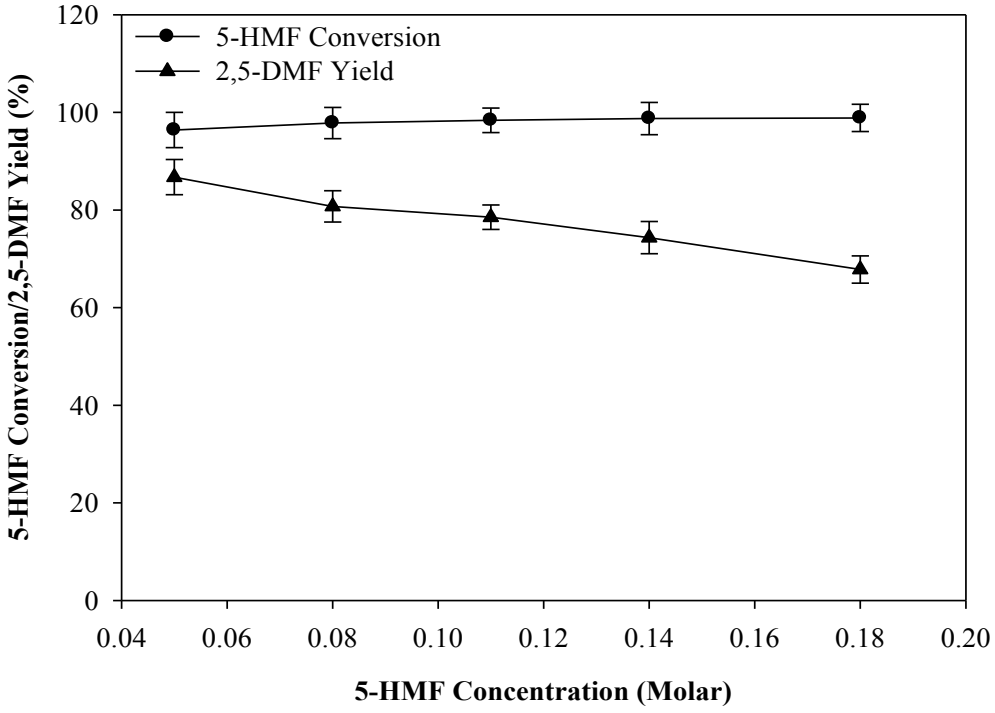

Figure 5.5: Effect of 5-HMF concentration on 5-HMF conversion and 2,5-DMF yield in molecular H2.

Reaction conditions: catalyst amount = 0.1 g; THF = 25 ml; temperature = 260°C; time =2 hours; H_2 pressure = 50 bar; speed = 700 rpm. Note: 5-HMF concentration is relative to THF

amount. Where error bars are shown, these are calculated as mean ± standard error of the mean from at least three experiments.

5.4.3.5 Effect of Catalyst Amount

The effect of catalyst amount was studied by keeping the optimum reaction temperature, time, hydrogen pressure and 5-HMF concentration constant. Figure 5.6 shows the variation of 2,5-DMF yield and 5-HMF conversion as a function of catalyst amount. As illustrated in Figure 5.6, when 0.1 g of catalyst was used, 96.4% 5-HMF conversion and 86.7% yield of 2,5-DMF was achieved. The high yield of 2,5-DMF obtained at 0.1 g of catalysts could be attributed to the large surface area of the Ru/C catalyst as displayed in Table 4.1. The large surface area of the Ru/C catalyst provides more collision sites due to the efficient dispersion of the Ru metal in the pores hence why a high yield of 2,5-DMF was obtained. However, decreasing the amount of catalyst to 0.05 g resulted in a higher yield of 2,5-DMF (93.7%) while 5-HMF conversion remained constant at 96.4%. Generally, upon increasing the catalyst amount above 0.1 g, a higher 5-HMF conversion was observed while 2,5-DMF yield decreased significantly. The observed decrease in 2,5-DMF yield could be related to the fact that an increase in the amount of catalyst resulted in speeding up 2,5-DMF formation and also promote 5-HMF hydrogenation. This result suggests that excess amount of catalyst promotes the formation of side products instead of 2,5-DMF. Hence, the catalyst amount is relative to 5-HMF concentration. Therefore, 0.05 g of Ru/C catalyst was employed throughout the optimization of reaction conditions.

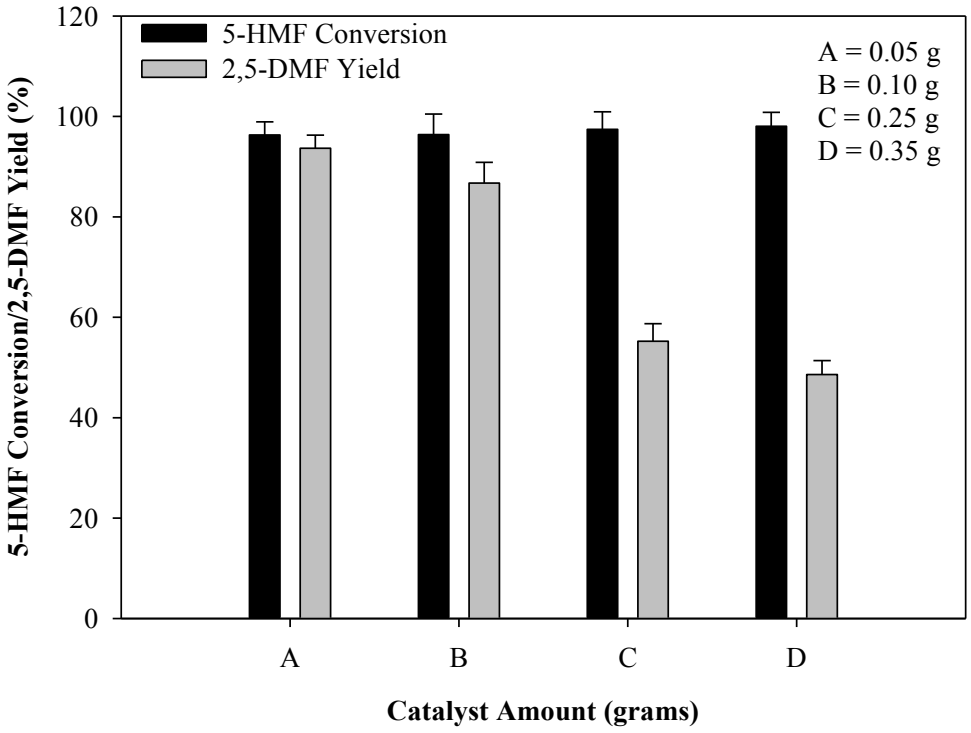

Figure 5.6: Effect of catalyst amount on 5-HMF conversion and 2,5-DMF yield.

Reaction conditions: H_2 pressure = 50 bar; THF = 25 ml; temperature =260°C; time = 2 hours; 5-HMF concentration = 0.05 M; speed = 700 rpm. Note: 5-HMF concentration is relative to THF amount. Where error bars are shown, these are calculated as mean ± standard error of the mean from at least three experiments.

5.4.3.6 Effect of Agitation Speed

The effect of agitation speed was monitored using the optimum reaction conditions determined previously by varying the mixing speed from 100-1000 rpm, and the results are presented in Figure 5.7. It can be observed that 5-HMF conversion remained constant at 96% throughout the speed investigated. This implies that the agitation speed does not have a significant effect on the conversion of 5-HMF. However, the agitation speed has a significant effect on 2,5-DMF yield. At 100rpm, 87.5% yield was obtained. A further increase in the speed from 100 rpm to 300, 500, 700 rpm resulted in a significant increase in 2,5-DMF yield

to 88.9%, 93.7% and 95.1%. The significant increase in 2,5-DMF yield is due to an increase in the external mass transfer between the catalyst and reaction medium. Impressed by this result, the agitation speed was further increased to 1000 rpm. A slight decrease in 2,5-DMF yield (91.7%) was obtained at this speed. These results show that the interfacial mass transfer resistance between the liquid phase and the Ru/C catalyst surface was negligible when the agitation speed was above 700 rpm; hence the agitation speed was set to 700 rpm in this experiment.

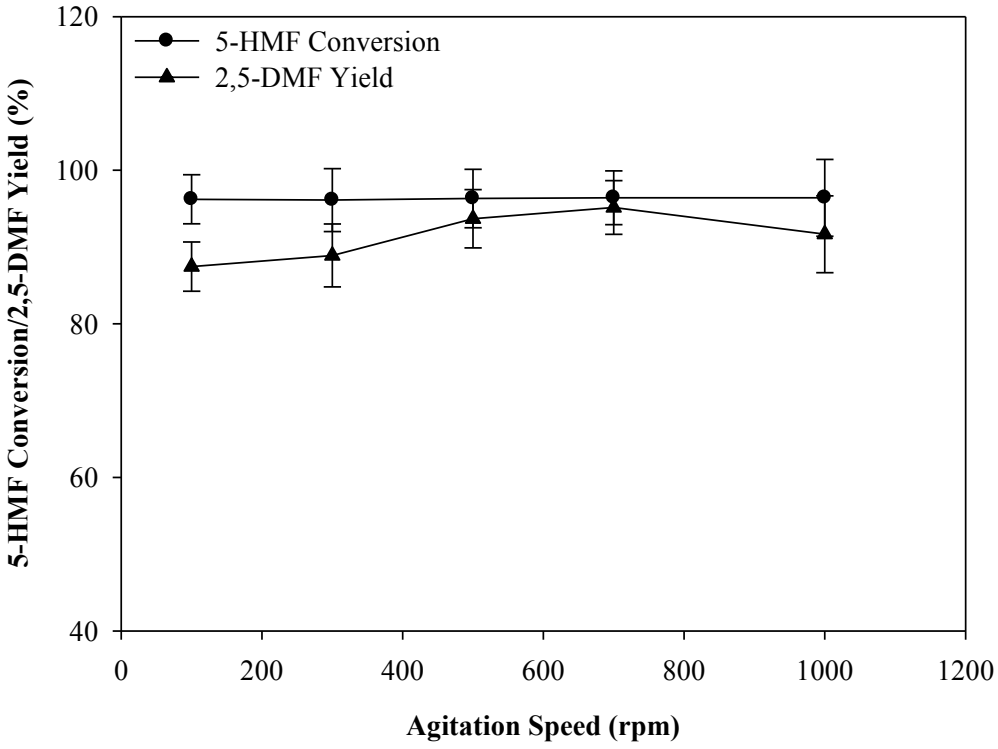

Figure 5.7: Effect of agitation speed on 5-HMF conversion and 2,5-DMF yield.

Reaction conditions: catalyst amount = 0.05 g; THF = 25 ml; temperature = 260°C; time =2 hours; H_2 pressure = 50 bar; 5-HMF concentration = 0.05 M. Note: 5-HMF concentration is relative to THF amount. Where error bars are shown, these are calculated as mean ± standard error of the mean from at least three experiments.

4.4.3.7 Catalyst Recycling

One of the advantages of using solid catalysts in chemical reactions is that it can easily be separated from the reaction mixture. More importantly, solid catalysts are widely used in the industry not only because of easy separation but also regeneration and recyclability play a vital role. Experiments to investigate the reusability of the Ru/C catalyst were not conducted in this study due to the amount of catalyst used for the hydrogenation reaction. As stated in Section 5.4.3.5, the optimum catalyst amount employed was 0.05g. This amount could not be fully recovered via filtration after the first run because the catalyst was scanty on the filter paper. This is caused possibly due to the fact that the particle size of the catalyst is smaller than that of the filter paper used during the filtration process. Hence, it was a challenge to recover the catalyst amount used after the first run of experiment. This therefore implies that the right recovery technique was not employed in this study. The use of centrifugation techniques could have been a better recovery process to obtain the catalyst after the first run of experiment.

However, the amount recovered was used for SEM analysis to reveal the surface morphology of the catalyst after reaction. It was observed from the SEM results (See Section 4.1.2.1 and Figure 4.2a & b) that there was no huge difference in morphology between the fresh Ru/C catalyst and the Ru/C catalyst after the first run. This possibly suggests that the Ru/C catalyst could be reused for another cycle. Further analysis are required to confirm this.

5.5 The Use of Bio-support for Catalytic Hydrogenation of 5-HMF to produce 2,5-DMF

This Section presents the results obtained for the catalytic hydrogenation of 5-HMF in molecular H_2 using four different bio-supported metal catalysts namely; 5 wt% Bio-Pd, 5 wt% Bio-Ru/Pd, 20 wt% Bio-Ru and 20 wt% Bio-Ru/Pd (See preparation method in Section 3.4). This study aim to investigate the effect of bimetallic catalyst on the bio-support; thus the 5 and 20 wt% Bio-Ru/Pd were prepared. For the purpose of comparison, all the catalytic hydrogenation experiments with the bio-catalysts were conducted at identical conditions to the 5 wt% Ru/C. However, it must be noted that the reaction conditions used does not entirely show the performance of the bio-supported metal catalysts in this research work. As a result, it is vitally important to investigate all reaction parameters so as to obtain the optimum conditions for each bio-catalyst studied. The optimization of the reaction parameters for the bio-supported metal catalysts was not done in this research work due to insufficient amount of catalysts produced by the supplier.

Bimetallic catalysts, as the name sounds, are made up of two separate metal elements. They have potential advantages over the monometallic catalysts because they can possibly lead to a huge improvement in catalytic properties since bi-metallization increases the catalytic properties of the original single-metal and also generates a new property (Ramsurn and Gupta, 2013). More properties of bimetallic catalysts are further discussed in Section 6.5.

Table 5.3: Comparison of bio-catalyst and commercial catalyst in molecular H_2

	5 wt% BioPd	5 wt% Pd/C	5 wt% BioRuPd	20 wt% BioRuPd	20 wt% BioRu	5 wt% Ru/C	10 wt% Pd/C
2,5-DMF Yield (%)	49.5±3.0	19.9±0.7	55.5±2.1	60.3±3.1	47.9±1.2	95.1±0.5	18±1.2
5-HMF Conversion (%)	88.9	96.5	94.7	95.3	95.1	96.4	96.5
Selectivity (%)	55.6	20.7	58.5	63.3	50.4	98.7	19.4

Reaction conditions: catalyst amount = 0.05 g; THF = 25 ml; temperature = 260°C; time =2 hours; H_2 pressure = 50 bar; 5-HMF concentration = 0.05 M; speed = 700 rpm. Note: 5-HMF concentration is relative to THF amount. Where errors are shown, these are calculated as mean ± standard error of the mean from at least three experiments.

Table 5.3 illustrates how 2,5-DMF yield, 5-HMF conversion and selectivity varied as a function of different bio-supported metal catalysts tested in this study. It can be seen that a high 5-HMF conversion between 88.9 – 96.5% was achieved across all the catalysts investigated. Considering the yield of 2,5-DMF and 5-HMF conversion obtained using the bio-support metal catalysts, it was clearly observed that the bimetallic 5 wt% Bio-Ru/Pd and 20 wt% Bio-Ru/Pd catalysts show higher catalytic activity compared to their monometallic counterpart 5 wt% Bio-Pd and 20 wt% Bio-Ru respectively. Due to unavailability of the 5 wt% Bio-Ru, it was not possible to compare the catalytic activity of the bimetallic 5 wt% Bio-Ru/Pd against the monometallic 5 wt% Bio-Ru. Though, it is clear from Table 5.3 that the bimetallic 20 wt% Bio-Ru/Pd shows higher catalytic activity (60.3% > 47.9%) than the monometallic 20 wt% Bio-Ru in terms of 2,5-DMF yield.

In addition, comparing the bimetallic bio-support catalysts at different metal loadings (5 and 20 wt% Bio-Ru/Pd), it can be observed that the 20 wt% Bio-Ru/Pd shows higher catalytic

activity than the 5 wt% Bio-Ru/Pd. 60.3% 2,5-DMF yield was obtained with the 20 wt% Bio-Ru/Pd while 55.5% was achieved with the 5 wt% loading even though there is no significant difference in 5-HMF conversion (94.7% and 95.3%) at both catalyst loading. However, in spite of the higher metal loading (20 wt %), one would have expected a significant increase in 2,5-DMF yield compared to the 5 wt% loading. It was observed from the GC-MS spectrum that 2,5-DMTHF is the major product in the 20 wt% metal loading. This suggests that the 20 wt% loading undergoes further hydrogenation. The further hydrogenation observed could be ascribed to the higher metal loading of the catalyst or excess hydrogen in the reaction medium. As 55.5% yield of 2,5-DMF was achieved with the 5 wt% Bio-Ru/Pd, one can conclude that the 5 wt% loading showed a higher catalytic activity per unit mass of catalyst than the 20 wt% loading. The result in this study is in agreement with the literature where a lower metal loading have been reported for the hydrogenation of 5-HMF into 2,5-DMF (Haung et al., 2014; Nishimura et al., 2014).

Finally, Table 5.3 also presents the comparison between both commercial and bio-sourced support investigated in this study. It is clear that the commercial 5 wt% Ru/C catalyst displayed higher catalytic activity amongst all the catalysts investigated. A very high 2,5-DMF yield of 95.1% was obtained after optimization of reaction conditions. In addition, the use of the optimal conditions for the Ru/C commercial catalyst in comparing the performance of all other catalysts is not entirely justified. This is because there is a high possibility that a higher yield of 2,5-DMF could be achieved with all other catalysts tested in this study if optimization of reaction conditions are carried out. However, due to time constraint and inadequate bio-supported metal catalysts produced, it was difficult to investigate the optimised reaction conditions for each catalysts studied. Therefore, based on the comparison conducted in this

study, one can conclude that the trend in the catalytic activity of the catalyst tested are 5 wt% Ru/C > 5 wt% Bio-Ru/Pd > 20 wt% Bio-Ru/Pd > 5 wt% Bio-Pd > 20 wt% Bio-Ru > 5 wt% Pd/C > 10 wt% Pd/C.

5.6 Plausible Reaction Pathway in Molecular H_2

Studying the reaction mechanism over a selective Ru/C catalyst will give a better understanding on the reactions going on during the catalytic conversion of 5-HMF to 2,5-DMF in molecular H_2. This was done by identifying reaction intermediates via gas-chromatography mass spectroscopy (GC-MS). It is known that the furan ring, hydroxyl group, aldehyde group and the removal of electron on the aldehyde group make the C2-aldehyde and C5-hydroxyl group in 5-HMF structure very unstable (Hu et al., 2014). Thus, they can undergo hydrogenation freely in the presence of hydrogen and a metal catalyst as illustrated in Horiuti-Polanyi mechanism of hydrogenation in Figure 5.1.

Some of the reaction intermediates detected were 5-methylfurfuryl alcohol (5-MFA), 2,5-hexadione, 5-methylfurfural and traces of 2,5-dimethyltetrahydrofuran. (2,5-DMTHF). Based on this intermediates, 5-HMF properties and previous literature (Hu et al., 2014; Zu et al., 2014; Roman-Leshkov et al., 2007; Luo et al., 2014; Haung et al., 2014), the possible reaction pathway for the catalytic hydrogenation of 5-HMF into 2,5-DMF in molecular H_2 was proposed in Figure 5.8. It can be seen from Figure 5.8 that 5-methylfurfural and 5-methylfurfuryl alcohol are two important intermediates formed from 5-HMF via partial

hydrogenation. This is evident in the reaction pathway described by Luo et al., (2014) and Hu et al., (2014).

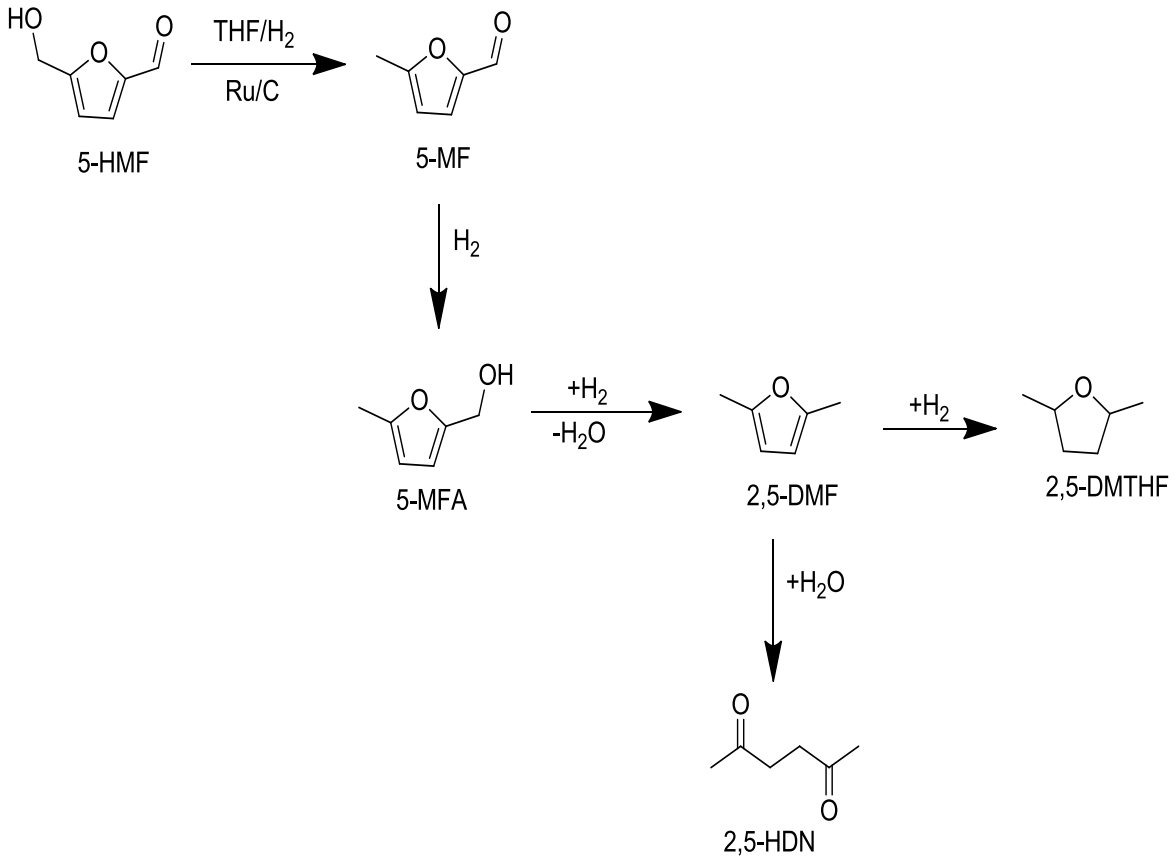

Figure 5.8: Plausible reaction pathway for the hydrogenation of 5-HMF toward 2,5-DMF in molecular H_2.

5.7 Conclusions

This chapter investigated the use of palladium and ruthenium catalyst supported on bacteria and activated carbon for hydrogenation of 5-HMF to 2,5-DMF in molecular hydrogen. A high yield of 2,5-DMF (95.1%), selectivity (98.7%) and 5-HMF conversion (96.4%) were obtained after investigation of reaction conditions using the Ru/C catalyst. The Ru/C catalyst

plays a significant role in the conversion of 5-HMF towards targeted product. The product distribution depended on various reaction parameters such as temperature, H_2 pressure, time, 5-HMF concentration, mixing speed and catalyst amount. Also, different reaction conditions offers the possibility to obtain various reaction intermediates such as 5-methylfurfural, 5-methylfurfuryl alcohol, 2,5-hexadione, hexan-2-ol and 2,5-DMTHF. With regards to the bio-supported metal catalysts, the bimetallic 5 wt% Bio-RuPd showed the highest catalytic activity compared to other bio-supported metal catalysts employed. Finally, comparing the commercial catalyst support (activated carbon) with the bio-supported metal catalysts at the same reaction conditions, the commercial Ru/C catalyst exhibited superior catalytic activity. This superior activity could be attributed to the large surface area and total pore volume of the activated carbon support which helps to activate species at high temperatures. Further work is therefore required to investigate the optimization of reaction conditions for each catalyst studied.

Chapter 6. **Synthesis of 2,5-DMF in Formic Acid-Triethylamine ($HCOOH/Et_3N$) Mixture.**

6.1 Abstract

This chapter describes the synthesis of 2,5-dimethylfuran from 5-hydroxymethylfurfural in formic acid-triethylamine mixture. The $HCOOH/Et_3N$ mixture serves as both solvent mixture and hydrogen donor compound in the reaction medium. The scope of this work is to investigate the catalytic asymmetric hydrogen transfer reaction of 5-hydroxymethylfurfural (5-HMF) to produce 2,5-dimethylfuran (2,5-DMF) in the presence of formic acid-triethylamine ($HCOOH/Et_3N$) over Ru/C catalyst as reductant system. Optimization of the reaction parameters showed that temperature, time, $HCOOH/Et_3N$ molar ratio, Ru/C dosage, HMF concentration as well as agitation speed played important roles in the selectivity to the targeted 2,5-DMF. The reaction mixture was analysed by GC-FID, which provides both qualitative and quantitative information about the reaction products. It was possible to achieve a very high yield (92.1%) of 2,5-DMF within the reaction time of 4 hours at 210°C. A significant effect of formic acid-triethylamine molar ratio was observed on the product distribution, where 5:2 molar ratio of $HCOOH/Et_3N$ gave the best yield of 2,5-DMF. It is interesting to note that a very high 5-HMF conversion was achieved particularly as temperature increased. Moreover, we investigated the effect of different metal catalyst such as 5 wt% and 10 wt% Pd/C; 5 wt% Ru/C; 5 wt% and 20 wt% Bio-Ru/Pd and 20 wt% Bio-Ru. Of all the catalysts screened during the transfer hydrogenation reactions in $HCOOH/Et_3N$ mixture, 5 wt% Ru/C catalyst gave the highest yield of 2,5-DMF. However, the intrinsic properties of the Ru/C catalyst determine the reaction pathway towards 2,5-DMF or other products.

6.2 Introduction

One of the most difficult challenges faced by humans in the nearest future is the generation of sufficient and favourable supply of energy. Hydrogen is known as an important energy carrier and the main obstacle in using it for energy applications is effective storage and handling. At atmospheric conditions, hydrogen has a low volumetric (52 g/L) and very high gravimetric energy density 43 (g/kg) (Loges et al., 2010). Therefore in order to balance both energy densities, pure hydrogen is stored either in compressed gaseous or liquid state (Eberle et al., 2009). Not long ago, liquid chemicals such as formic acid, methanol, and isopropanol have emerged as materials for hydrogen storage due to their inherent energy efficiency and effective handling abilities (Makowski et al., 2009).

The liberation of hydrogen from formic acid is a decomposition reaction which also produces carbon dioxide that may be recycled. The decomposition reaction occurs through two different reaction pathways which at standard conditions are thermodynamically favourable (see Figure 6.1). From Figure 6.1, it is clear that the dehydration/decarbonylation pathway is of little importance due to the carbon monoxide generated, which is considered as a catalyst poison. Therefore, the decarboxylation/dehydrogenation pathway is usually considered for hydrogen generation from formic acid.

In this study, the approach used is based on hydrogen generation from formic acid/triethylamine solvent. Such mixture is usually used as hydrogen donor compounds in asymmetric transfer hydrogenation (ATH) reactions (Matharu et al., 2006; Noyori and

Hashiguchi, 1997; Fukuzumi et al., 2008). During transfer hydrogenation reactions, several researchers have been able to generate significant amounts of hydrogen in HCOOH/Et_3N solvent especially with rhodium and ruthenium catalysts (Himeda et al., 2011; Fellay et al., 2008; Abura et al., 2003).

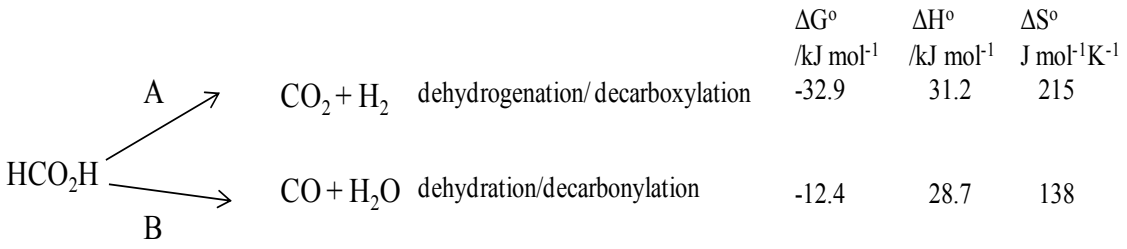

Figure 6.1: Formic acid decomposition pathways and their thermodynamic properties (Loges et al., 2010)

The majority of ATH metal catalysed reactions are either conducted in the azeotropic mixture of HCOOH/Et_3N, with molar ratio of 2.5:1 or isopropanol (IPA) (Haack et al., 1997; Uematsu et al., 1996; Cossy et al., 2001). The azeotropic mixture of HCOOH/Et_3N acts as both hydrogen donor and solvent. It is considered to be a better hydrogen donor solvent than isopropanol due to the stability and easy removal of the resulting carbon dioxide, thus making it an irreversible reaction (Xiaowei et al., 2012). Furthermore, one of the main disadvantages of using IPA in ATH reactions is the easy reversibility of the reduction reaction. It is noteworthy to state here that the main disadvantage of using HCOOH/Et_3N in ATH reactions is that some catalysts may either lose their catalytic activity completely or undergo decomposition early in the reaction (Gladiali and Alberico, 2006). Another drawback is that a long period of induction may exist, thereby giving rise to a longer reaction time to obtain good conversion (Xiaowei et al., 2012).

In this chapter therefore, the representative procedure for the transfer hydrogenation of 5-HMF to 2,5-DMF is presented in Section 6.3. The catalyst screening, optimization of reaction conditions are presented in Section 6.4, effect of bio-catalysts in Section 6.5, reaction mechanism in Section 6.6 and conclusion of the chapter in Section 6.7.

6.3 Representative Procedure

This section describes the procedure used during the reaction.

6.3.1 Preparation of 5:2 molar ratio of formic acid/triethylamine mixtures

As shown in Figure 5.2, a 50 mL three-necked, round-bottom flask equipped with a reflux condenser, magnetic stirrer, thermometer and a dropping funnel is charged with 14.9 mL, 2.01 mol of triethylamine. The triethylamine is cooled down to 4^{o}C in an ice bath and formic acid 10.1 mL, 5.0 mol is added slowly. Addition of formic acid to triethylamine is carefully controlled because the reaction is exothermic, generates CO_2 and may proceed violently.

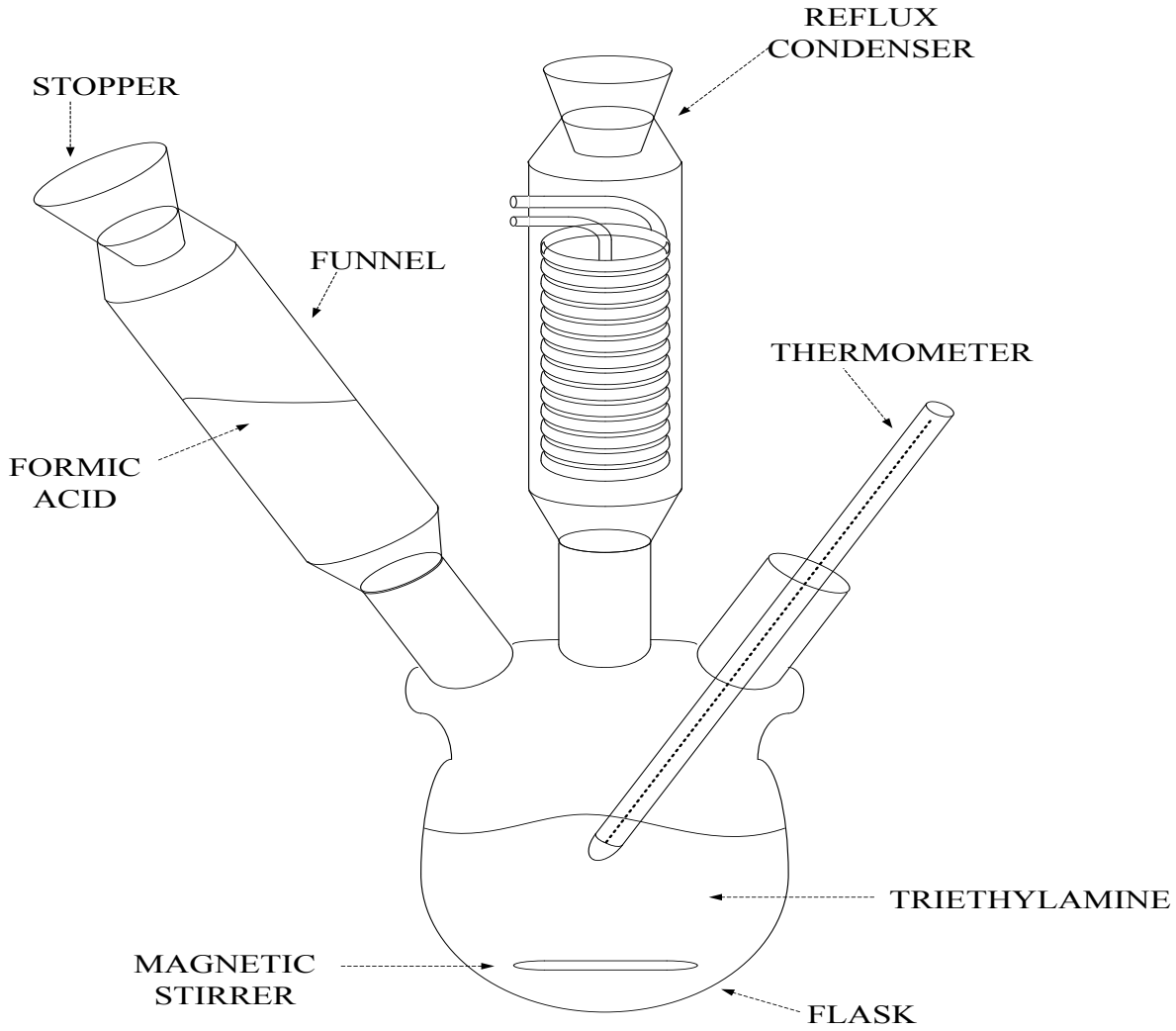

Figure 6.2: Schematic diagram for preparing 5:2 molar ratio HCOOH/Et3N mixtures.

6.3.2 Procedure For The Asymmetric Catalytic Transfer Hydrogenation of 5-HMF to 2,5-DMF in HCOOH/Et_3N Mixture

The catalytic transfer hydrogenation reactions were carried out in a 100 mL stainless steel Parr reactor with an external temperature and stirring controllers. For a typical reaction, the reactor was charged with 0.3 M 5-HMF, 0.1 g Ru/C catalyst and 25 mL of HCOOH/Et_3N,

sealed and purged three times with N_2 at 10 bar pressure, heated to 210°C, and stirred at a speed of 300 rpm for 4 hours. After completion of the reaction, the reactor was quenched to room temperature in an ice-water bath; and the reaction mixture was filtered with 8µm Whatman quantitative filter paper.

6.4 Results and Discussion

This section presents the results obtained in this chapter.

6.4.1 Catalytic Transfer Hydrogenation of 5-HMF to 2,5-DMF in HCOOH/Et_3N Mixture Over Metal Catalyst

It is well known that the presence of a furan ring, an aldehyde group and a hydroxyl group in 5-HMF makes it very reactive. The main issue in the hydrogenation reaction is to avoid further hydrogenation of the furan ring structure and also to make sure the hydroxyl and aldehyde group are prioritised during the reaction. The importance of using a catalyst for the hydrogenation of 5-HMF to 2,5-DMF in HCOOH/Et_3N mixture was investigated. When the reaction was carried out without catalyst, no 2,5-DMF was formed even though a significant amount of CO_2 and H_2 was produced during the reaction. The main products obtained without using a metal catalyst were small amount of unreacted 5-HMF, triethylamine, formic acid and 2,5-dihydroxymethylfuran. In this situation, 5-HMF was converted to 2,5-dihydroxymethylfuran. This could be attributed to the high amount of hydrogen generated from the HCOOH/Et_3N mixture. It must be stated here that the use of an appropriate metal catalyst is very important for the hydrogenation of 5-HMF to 2,5-DMF.

6.4.2 Catalyst Screening

Three different catalysts 5wt% Pd, 10wt% Pd and 5wt% Ru on activated carbon (C) support were screened for the hydrogenation of 5-HMF and the results obtained are shown in Table 6.1. The results displayed for 5wt% Pd and 10wt% Pd were based on identical reaction conditions to the 5wt% Ru/C catalyst. However, these reaction conditions does not justify the entire performance of the Pd/C catalysts in hydrogenation of 5-HMF. In order to determine the effectiveness and performance of the Pd/C catalysts, it is vital to carry out an optimization of all reaction conditions. Despite obtaining a high conversion of 5-HMF (97.49% and 97.34%) using both 5 and 10 wt% Pd/C respectively, the main product obtained was 2,5-dimethyltetrahydrofuran (2,5-DMTHF). Only a small yield (less than 30%) of 2,5-DMF was obtained using the Pd/C catalyst. As shown in Figure 6.3, it suggests that the 5-HMF undergoes further catalytic transfer hydrogenation to 2,5-DMTHF over the Pd/C catalyst. However, there is a possibility that using a lower loading of Pd catalyst such as 1% or 2% Pd/C could favour the hydrogenation of 5-HMF towards 2,5-DMF instead of the deeper hydrogenation product (2,5-DMTHF).

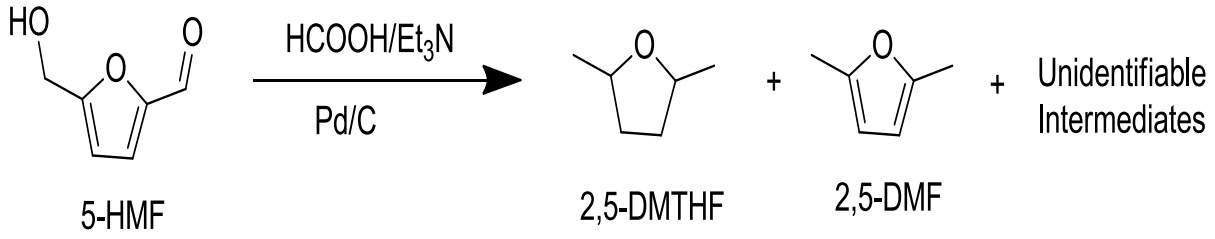

Figure 6.3: Plausible reaction pathway for the catalytic transfer hydrogenation of 5-HMF in HCOOH/Et3N over Pd/C catalyst.

Table 6.1: Catalyst screening in HCOOH/Et3N mixture

Entry	Catalyst	Conversion (%)	Yield (%)	Selectivity (%)
1	5 wt% Ru/C	93.4	92.1±0.4	98.6
2	5 wt% Pd/C	97.5	26.5±2.0	27.2
3	10 wt% Pd/C	97.3	24.4±1.6	25.0

Reaction conditions: catalyst amount = 100 mg; HCOOH/Et_3N = 25 ml; molar ratio = (5:2); temperature = 210°C; time = 4 hours; 5-HMF concentration = 0.3 M. Note: 5-HMF concentration is relative to HCOOH/Et_3N amount. Where errors are shown, these are calculated as mean ± standard error of the mean from at least three experiments.

6.4.3 Hydrogenation of 5-HMF to 2,5-DMF Under Various Reaction Conditions

The catalytic activity of the Ru/C catalyst for the hydrogenation of 5-HMF to 2,5-DMF in HCOOH/Et_3N mixture strongly depends on various reaction conditions such as; time, temperature, HCOOH/Et_3N molar ratio, catalyst dosage, agitation speed and 5-HMF concentration. In order to obtain the maximum yield of 2,5-DMF, these reaction parameters were investigated.

6.4.3.1 Effect of Reaction Temperature

The effect of temperature was studied between 100°C and 240°C at 20°C intervals. Figure 6.4 shows that 5-HMF conversion rapidly increased from 60.9% at 100°C to around 97% at 120°C then remained in the same range. As for the 2,5-DMF yield, it increased gradually from only 4.4% at 100°C to a maximum of 91% at 210°C after which, it declined to 59.1% at 240°C. It was observed that every 20°C rise in reaction temperature produced a corresponding 9 – 17% increase in the yield of 2,5-DMF up to 210°C. Thereafter, a decrease in 2,5-DMF yield with temperature rise was observed. A similar trend between reaction temperature and 2,5-DMF yield was observed by Hu and co-workers (Hu et al., 2014). The result obtained is also

consistent with previous result on the conversion of 5-HMF to 2,5-DMF reported by Roman-Leshkov et al (2007). They found an optimum temperature of 220^{o}C for the gas-phase conversion of bis (hydroxymethyl)-furan (BHMF) into 2,5-DMF.

Interestingly, Thananatthanachon and Rauchfuss, (2010) achieved a 2,5-DMF yield of 95% from one pot conversion of fructose using formic acid as hydrogen source and deoxygenating agent at 15 hours reaction time and Pd/C catalyst. Due to the one-pot reaction process, the total temperature used to achieve 95% 2,5-DMF yield was 220^{o}C. Surprisingly, a 2,5-DMF yield of 30% was obtained from one pot synthesis of 2,5-DMF in formic acid and Ru/C catalyst as reported by De et al., (2012). The total temperature used for the one pot synthesis was 225^{o}C at 17 hours reaction time and a lower yield was obtained.

In this study, the observed decrease in yield after 210^{o}C can be attributed to the increase in the rate of reaction, caused by the formation of 2,5-DMF and side-products formed. It was suspected that the turnover frequency (TOF) at 210^{o}C is higher than that at 100^{o}C hence the reaction rate at 210^{o}C was boosted. From the results obtained, a temperature of 210^{o}C would give best 5-HMF conversion of 97.3% and 2,5-DMF yield of 90.6%, and therefore was used throughout the optimization process. Thus, this result shows that 5-HMF has a high hydrogenation activity, and the yield of 2,5-DMF obtained from 5-HMF can reach a maximum under mild reaction temperature.

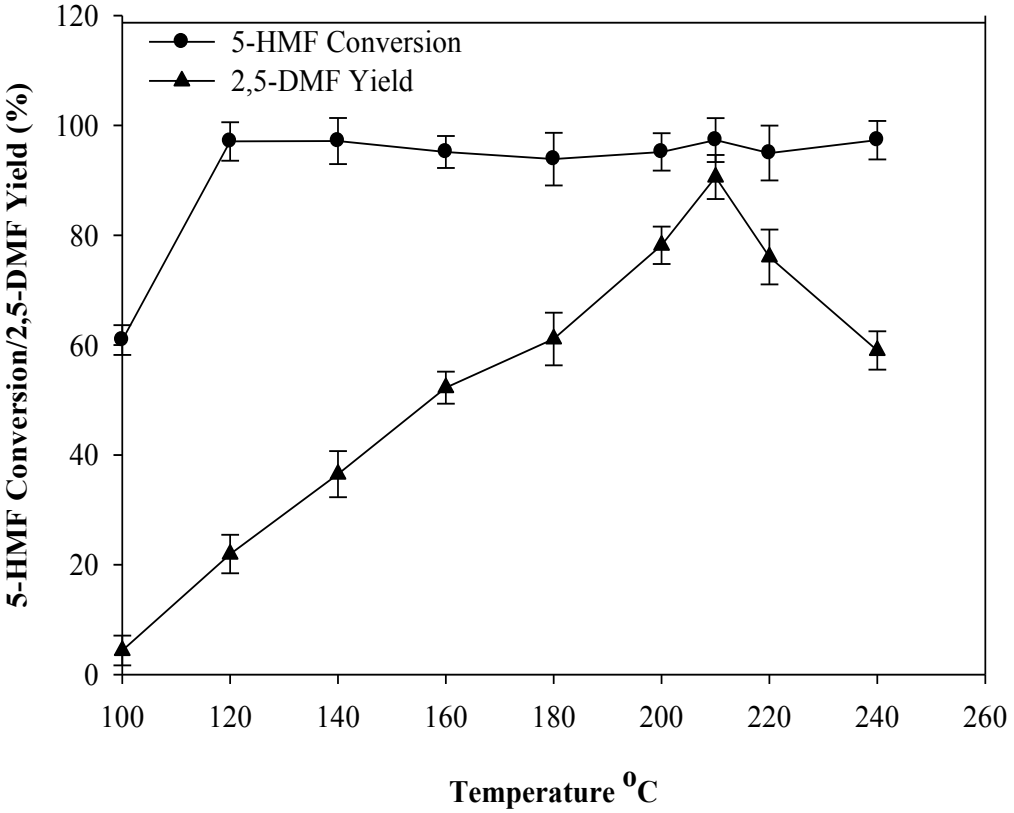

Figure 6.4: Effect of temperature on 5-HMF conversion and 2,5-DMF yield.

Reaction conditions: 5-HMF = 0.8 M; 5 wt % Ru/C = 0.1g; HCOOH/Et_3N = 25 ml; agitation speed = 300 rpm; time = 6 hours; molar ratio = (5:2). Note: 5-HMF concentration is relative to HCOOH/Et_3N amount. Where error bars are shown, these are calculated as mean ± standard error of the mean from at least three experiments.

6.4.3.2 Effect of Reaction Time

In order to have a full understanding of the reaction pathway, it is very important to identify the intermediate product/products formed during the hydrogenation reaction. Figure 6.5 shows conversion and yield of 5-HMF and 2,5-DMF respectively as function of time. Expectedly, 2,5-DMF yield increased with reaction time. At 1 hour, 2,5-DMF yield of 49.4% and 5-HMF conversion of 95.3% were obtained. This could be explained based on the ready availability of hydrogen generated from the HCOOH/Et_3N mixture. However, when the

reaction time was prolonged to 2 hours, a 2,5-DMF yield of 70.4% and 97.6% 5-HMF conversion were obtained. 2,5-DMF yield continued to increase further to values of 88.3%, 90.6%, 92%, 93% at reaction times 4, 6, 8 and 10 hours respectively. 5-HMF conversion remained high at 97.4% ± 0.2. As there was only a maximum of 5% increase in 2,5-DMF yield after 4 hours reaction time, we selected 4 hours as the suitable reaction time for most investigations.

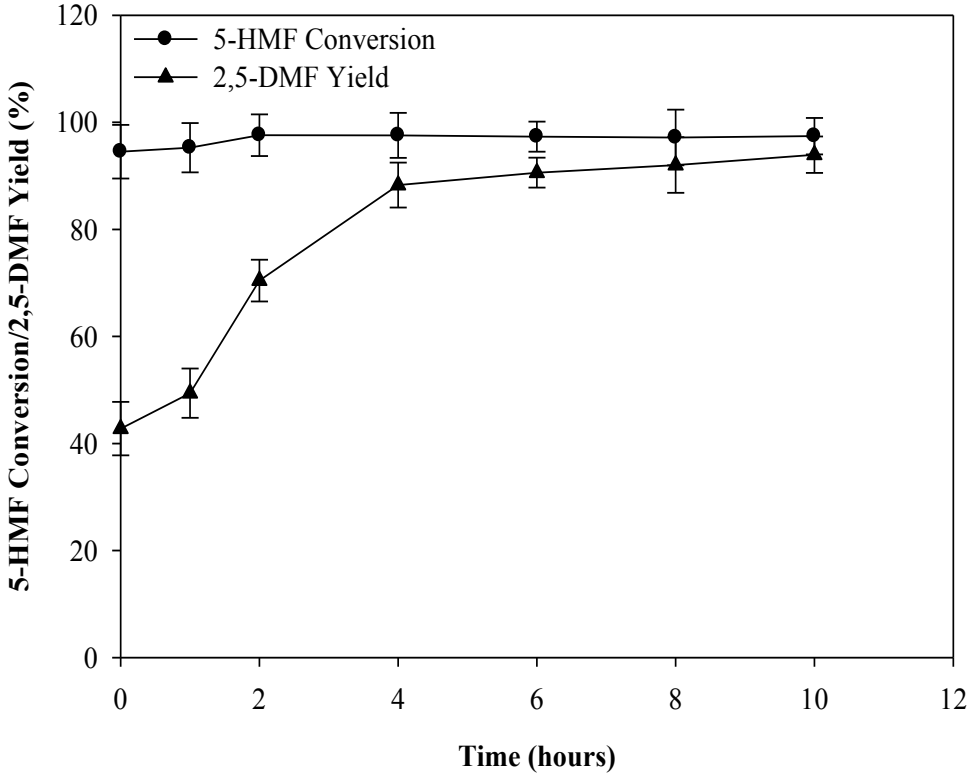

Figure 6.5: Effect of reaction time on 5-HMF conversion and 2,5-DMF yield.

Reaction conditions: 5-HMF = 0.8 M; 5 wt % Ru/C = 0.1g; HCOOH/Et_3N = 25 ml; agitation speed = 300 rpm; temperature = 210°C; molar ratio = (5:2). Note: 5-HMF concentration is relative to HCOOH/Et_3N amount. Where error bars are shown, these are calculated as mean ± standard error of the mean from at least three experiments.

6.4.3.3 Effect of 5-HMF Concentration

As shown in Figure 6.6, the 5-HMF concentration plays a significant role in the hydrogenation of 5-HMF to 2,5-DMF in HCOOH/Et_3N mixture. When the concentration of 5-HMF was 0.3 M, 93.4% 5-HMF was converted and a 2,5-DMF yield of 92.1% was obtained. It can be observed that as the concentration of 5-HMF was increased to 0.8, 1 and 1.4 M, the yield of 2,5-DMF decreases to 88.3%, 74.3% and 70.9% respectively. Although the 5-HMF conversion increased with 5-HMF concentration increase, its hydrogenation to 2,5-DMF in HCOOH/Et_3N mixture was incomplete; thus resulting in the formation of side-products such as 5-methylfurfural (5-MF), furfural, 2,5-dihydroxymethylfuran (DHMF), 5-methylfurfuryl alcohol (MFA) (as shown in Figure 6.10). This could be due to either insufficient amount of hydrogen generated from the HCOOH/Et_3N mixture since the concentration of 5-HMF was increased above 0.3 M or the catalyst amount used during the reaction.

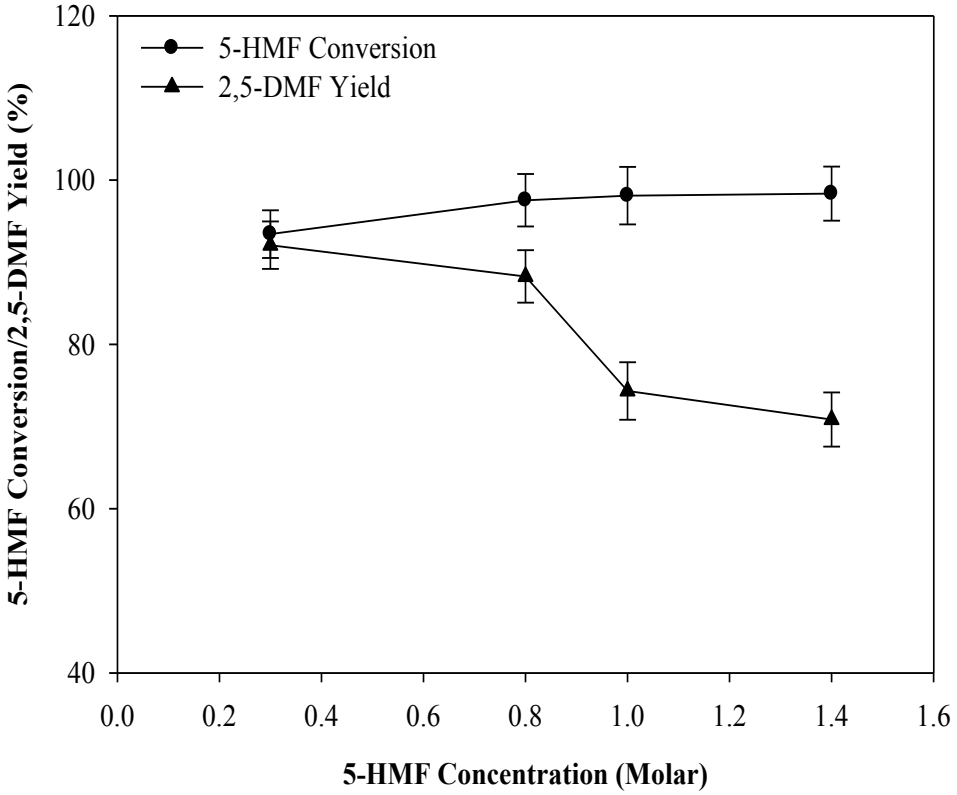

Figure 6.6: Effect of 5-HMF concentration on 5-HMF conversion and 2,5-DMF yield.

Reaction conditions: 5 wt % Ru/C = 0.1g; HCOOH/Et_3N = 25 ml; molar ratio = (5:2); temperature = 210°C; time = 4 hours. Note: 5-HMF concentration is relative to HCOOH/Et_3N amount. Where error bars are shown, these are calculated as mean ± standard error of the mean from at least three experiments.

6.4.3.4 Effect of HCOOH/Et_3N Molar Ratio

The use of formic acid in green chemistry has attracted great attention due to its hydrogen carrier capabilities and also as by-product from biomass degradation processes (Heeres et al., 2009). HCOOH/Et_3N mixture has been used for different transfer hydrogenation reactions (Kawasaki et al., 2005; Matharu et al., 2006). The role of triethylamine in the hydrogenation of 5-HMF in HCOOH/Et_3N mixture cannot be underestimated. The triethylamine-formic acid azeotrope favours the irreversible generation of H_2 from formic acid

by pushing the thermodynamics of H_2. It also plays the role of the base providing the right pH for the catalytic reaction to take place (Zhou et al., 2012; Wu et al., 2010). The HCOOH/Et_3N mixture is acidic and as the formic acid is used up during the reaction, the Et_3N may act to buffer the pH changes (Blaser and Schmidt, 2007). As shown in Figure 6.7, the molar ratio of HCOOH/Et_3N plays a huge role in the hydrogenation of 5-HMF to 2,5-DMF. When 1:1 molar ratio was used, a 2,5-DMF yield of 74.2% and 5-HMF conversion of 93.6% was obtained. Encouraged by this result, we extended our studies to 2:1, 3:1, 4:1 and 5:2 molar ratios HCOOHFA/Et_3N and a 2,5-DMF yield of 83.7%, 86.5%, 60%, 92.1% and 5-HMF conversion of 93.3%, 94.1%, 96.5%, and 93.4% were obtained respectively. It was clearly observed that the 5:2 molar ratio of HCOOH/Et_3N gave the highest yield of 2,5-DMF. This is in agreement with the result obtained by Mastharu *et al*., 2006; Kawasaki *et al*., 2005; Zhou *et al*., 2012. Thus, the 5:2 molar ratio of HCOOH/Et_3N was selected for the hydrogenation of 5-HMF to 2,5-DMF in this study. This is because the 5:2 molar ratio of HCOOH/Et_3N is the azeotrope of the two liquids. At ambient temperature, HCOOH/Et_3N is a single phase while other ratios tested were biphasic solutions. Naturally, a one-phase system provides much better heat and mass transfer quality than biphasic systems. Furthermore, the 5:2 molar ratio of HCOOH/Et_3N is frequently found to give the optimum rate of reaction and is also soluble in most organic solvents (Blaser and Schmidt, 2007).

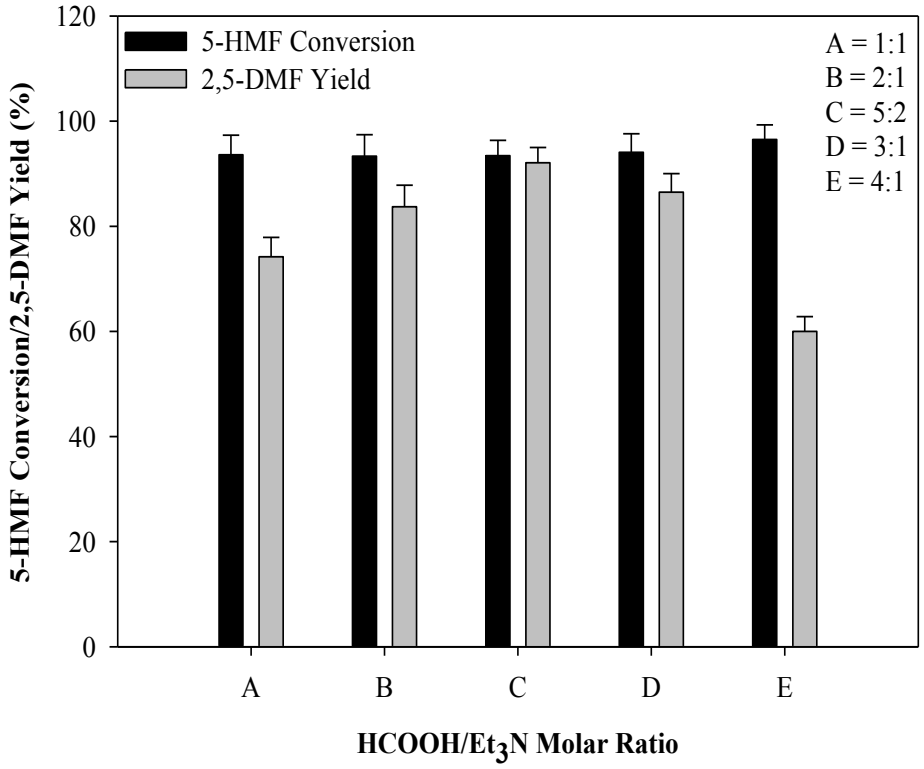

Figure 6.7: Effect of HCOOH/Et3N molar ratio on 5-HMF conversion and 2,5-DMF yield.

Reaction conditions: 5-HMF =0.3 M; 5 wt % Ru/C = 0.1g; HCOOH/Et_3N = 25 ml; agitation speed = 300 rpm; temperature = 210°C; time = 4 hours. Note: 5-HMF concentration is relative to HCOOH/Et_3N amount. Where error bars are shown, these are calculated as mean ± standard error of the mean from at least three experiments.

6.4.3.5 Effect of Ru/C Dosage

As shown in Figure 6.8, the amount of catalyst used in the hydrogenation of 5-HMF to 2,5-DMF is relative to 5-HMF concentration. When the amount of Ru/C catalyst was 0.05g, a 2,5-DMF yield of 68.7% was obtained even though 5-HMF conversion remained at 94.4%. However, when the Ru/C catalyst was increased to 0.1g, a significant increase (92.1%) in 2,5-DMF yield was observed. It should be stated here that the increase in Ru/C catalyst expedites 2,5-DMF formation and also foster the hydrogenation of 5-HMF. When the amount of Ru/C was further increased to 0.3g and 0.5g, 5-HMF conversion slightly increased while the yield of 2,5-DMF slightly declined to 87.9% and 86% respectively. The high 5-HMF conversion and

2,5-DMF yield at higher catalyst dosage can be attributed to the higher number of active sites present on the catalyst surface. The availability of higher number of active sites is due to the large surface area of the Ru/C catalyst as stated in Table 4.1. It should be stated here that 2,5-DMF yield is a function of 5-HMF concentration per unit mass of catalyst. Therefore, as mass of catalyst increases above 0.1g, 5-HMF/2,5-DMF ratio decreases and so does the yield. These results suggested that excess Ru/C does not particularly enhance the formation of 2,5-DMF.

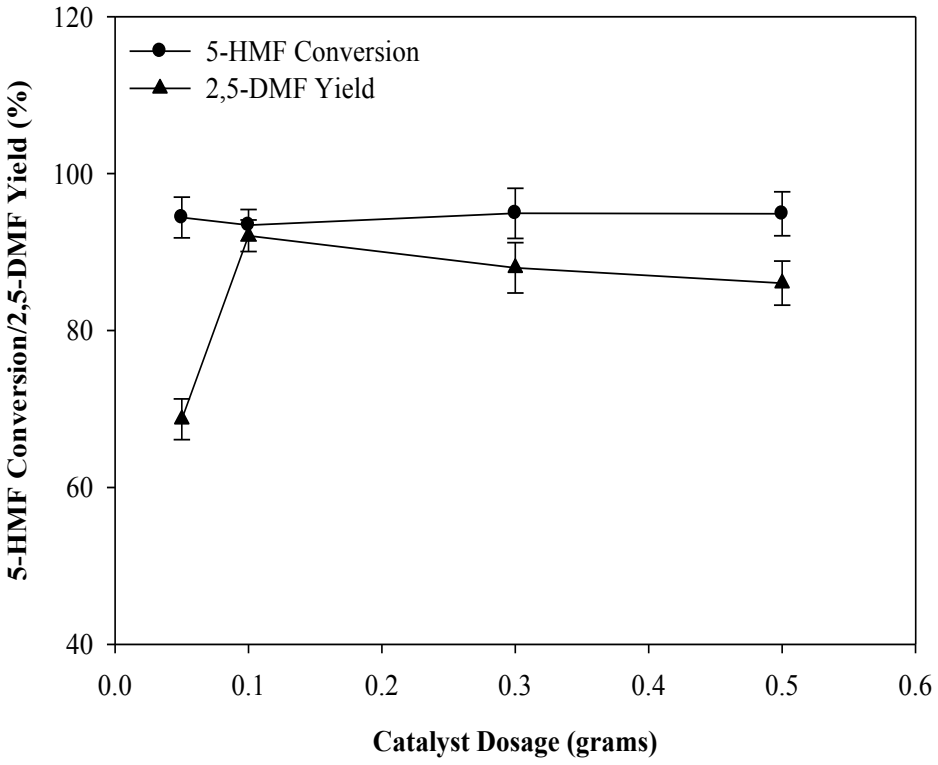

Figure 6.8: Effect of catalyst dosage on 5-HMF conversion and 2,5-DMF yield.

Reaction conditions: 5-HMF =0.3 M; molar ratio = (5:2); HCOOH/Et_3N = 25 ml; agitation speed = 300 rpm; temperature = 210^oC; time = 4 hours. Note: 5-HMF concentration is relative to HCOOH/Et_3N amount. Where error bars are shown, these are calculated as mean ± standard error of the mean from at least three experiments.

6.4.3.6 Effect of Agitation Speed

There is a possibility that the solid-liquid phase between the dissolved 5-HMF in HCOOH/Et_3N mixture and the solid Ru/C catalyst may suffer from severe mass transfer resistance which exert influence on the reaction rate. Thus, the interfacial mass transfer can be decreased by increasing the agitation speed (Devulapelli and Weng, 2009; Peng et al., 2010). The effect of agitation speed was investigated at 100, 300, 500 and 700 rpm respectively. As indicated in Figure 6.9, there was no major difference observed in 5-HMF conversion across the agitation speed range investigated. In contrast to this, a 2,5-DMF yield of 82.1% was obtained at 100 rpm even though we obtained high 5-HMF conversion (94.9%). However, when the agitation speed was further increased to 300 rpm, a 2,5-DMF yield of (92.1%) was obtained with 93.4% 5-HMF conversion. Moreover, when the agitation speed was increased to 500 and 700 rpm, there was no significant difference in 2,5-DMF yield (90.8% and 89.8%) respectively. This suggests that the interfacial mass transfer resistance between the Ru/C catalyst surface and the HCOOH/Et_3N mixture was negligible when the agitation speed was above 300 rpm; thus 300 rpm was the appropriate speed selected in this work.

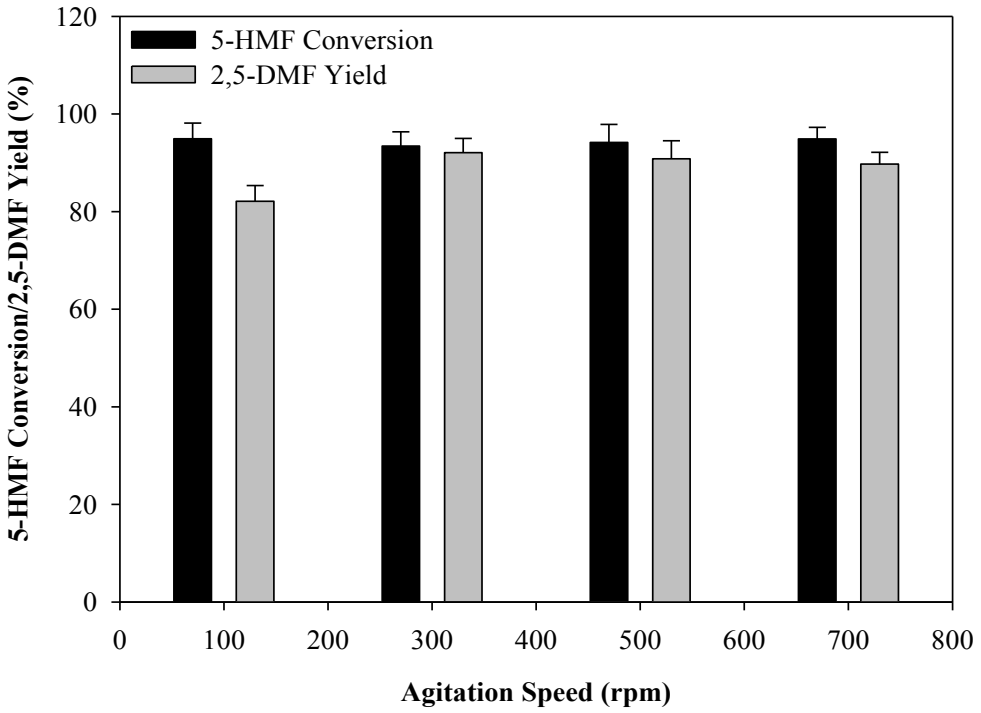

Figure 6.9: Effect of agitation speed on 5-HMF conversion and 2,5-DMF yield.

Reaction conditions: 5-HMF = 0.3 M; 5 wt % Ru/C = 0.1g; HCOOH/Et_3N = 25 ml; molar ratio = (5:2); temperature = 210^oC; time = 4 hours. Note: 5-HMF concentration is relative to HCOOH/Et_3N amount. Where error bars are shown, these are calculated as mean ± standard error of the mean from at least three experiments.

5.4.3.7 Catalyst Recycling

The ability to recycle a solid catalyst after reaction would be important and interesting. However, the spent Ru/C catalyst cannot be recovered after reaction in this study. This is due to the solvent system employed during the hydrogenation of 5-HMF to 2,5-DMF. The reaction is exothermic because more heat is generated from the solvent mixture used during the reaction. As stated earlier in Section 5.2, one of the main disadvantages of using HCOOH/Et_3N in transfer hydrogenation reactions is that some catalysts may either lose their catalytic activity completely or undergo decomposition early in the reaction (Gladiali and Alberico, 2006). It

was observed after the first run of reaction that the Ru/C catalyst decomposed therefore making it difficult to recover after the reaction as shown in the SEM image in Figure 6.10.

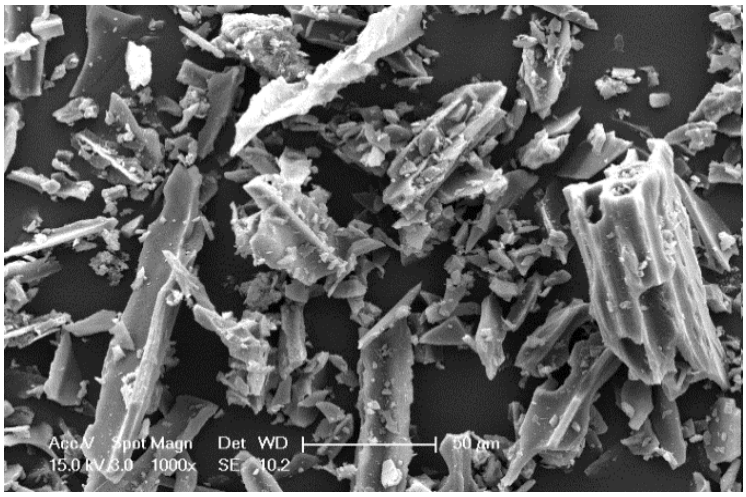

Figure 6.10: SEM Image of the spent Ru/C catalyst (extracted from Figure 4.2c)

6.5 The Use of Bio-supported Metal Catalysts for Transfer Hydrogenation of 5-HMF in HCOOH/Et_3N mixture

This is the first time that bio-catalysts has been tested in 5-HMF hydrogenation to 2,5-DMF and also the first time HCOOH/Et_3N was used as both hydrogen donor and solvent system in 2,5-DMF synthesis. Apart from the commercial catalysts screened, three different bio-supported metal catalysts were also prepared to use for transfer hydrogenation of 5-HMF to 2,5-DMF in HCOOH/Et_3N mixture. (See Section 3.4). It was also possible to exploit the use of bimetallic catalyst on the bio-support for the hydrogenation reaction as it has been reported that bimetallic catalysts performed tremendously well when compared to monometallic catalytic system (Alonso et al., 2012; Corbos et al., 2013; Lee et al., 2014). Therefore, the bio-support metal catalysts employed in this study are 20 wt% Bio-Ru, 5 wt% and 20 wt% Bio-Ru/Pd. It is important to note here that, for the purpose of comparison, all the hydrogenation experiments

with the bio-catalysts were conducted at identical reaction conditions (See Table 6.2). In addition, the use of similar reaction conditions for comparing the performance of all other catalysts is not entirely justified. This is because there is a likelihood that a higher yield of 2,5-DMF could be achieved with all other catalysts tested in this study if optimization of reaction conditions are carried out. However, due to time constraint and insufficient bio-support metal catalysts produced, it was difficult to investigate the optimised reaction conditions for each catalysts studied.

Table 6.2 illustrates how 2,5-DMF yield, 5-HMF conversion and selectivity varied as a function of different bio-supported metal catalyst used in this study. It can be observed that a very high 5-HMF conversion ranging between 93.4 – 97.5% was achieved with all the catalysts investigated. Considering the yield of 2,5-DMF and conversion of 5-HMF obtained, it was observed that the bimetallic 5 wt% Bio-Ru/Pd and 20 wt% Bio-Ru/Pd are more effective when compared to the monometallic 20 wt% Bio-Ru. This is in agreement with the result obtained in chapter 5 and that obtained by (Nishimura et al., 2014; Chai et al., 2013).

Table 6.2: Comparison of bio-supported and commercial catalyst in HCOOH/Et3N.

	5 wt% BioRu/Pd	20 wt% Bio Ru/Pd	20 wt% BioRu	5 wt% Ru/C	5 wt% Pd/C	10 wt% Pd/C
DMF Yield (%)	49.8 ± 0.6	56.7 ± 0.2	52.7 ± 1.2	92.1 ± 0.4	26.5±2	24.4±1.6
5-HMF Conversion (%)	96.8	96.9	96.8	93.4	97.5	97.3
Selectivity (%)	51.5	58.5	54.5	98.6	27.2	25.0

Reaction conditions: Catalyst amount = 0.1 g; HCOOH/Et_3N = 25 ml; molar ratio = (5:2); temperature = 210°C; time = 4 hours; 5-HMF concentration = 0.3 M. Note: 5-HMF concentration is relative to HCOOH/Et_3N amount. Where errors are shown, these are calculated as mean ± standard error of the mean from at least three experiments.

Wei, et al (2012) reported that bimetallic catalysts showed unique properties which make them stand out from monometallic catalysts. One of the unique properties is that, bimetallic catalyst supports more uptake of hydrogen by free radicals to speed up hydrogenation reaction than their monometallic counterpart. The superiority of the bimetallic BioRu/Pd catalyst over the monometallic Bio-Ru is as a result of the synergistic effect of the Ru metal which enhances the catalytic activity. The synergistic effect is prolonged as far the Ru and Pd metal in the bimetallic catalyst remain chemically bound to each other without decomposition. Furthermore, research shows that bimetallic catalysts have a distinct characteristic which is strongly related to their intrinsic geometric/ electronic structures (Alexeev and Gates, 2003). The effects of adding a second metal is an interesting strategy. Some of the effects include stabilizing, bi-functional, synergistic, electronic (or ligand) and geometric (or ensemble) effect. Alonso et al (2012) found out that the stabilizing effects improve the stability of the catalyst, while the bi-functional and synergistic effects generate an improvement in the rates of reaction, but this may result in the creation of new reaction path. The electronic and geometric effects

affect the selectivity and the catalytic activity but it is difficult to experimentally determine which factor is dominant since it is a challenge to isolate the two effects (Childers et al., 2014). The geometric effects arise when reactions require a particular arrangement of atoms to form an active site while the electronic effects are manifested as changes in the strength of surface adsorbate interactions due to changes of the electronic structure when the two metals are alloyed (Childers et al., 2014).

Consequently, Nakagawa and Tomishige, (2010) reported that a RANEY® Ni was less active compared to a bimetallic Ni-Pd for the hydrogenation of 5-HMF and furfural. Also, the selectivity of a reaction can be modified when a bimetallic catalyst is used (Alonso et al., 2012). For example, Sitthisa, et al. (2011) found out that Ni-Fe and Pd-Cu bimetallic catalysts had a lower selectivity toward decarbonylation products but a higher selectivity toward hydrogenation products for conversion of furfural than the monometallic Ni and Pd catalysts. It is noteworthy that in spite of the good catalytic activity of bimetallic catalysts, they have not been widely utilised for biomass conversion into chemical products.

Moreover, the same can be said when the 5 wt% Bio-Ru/Pd was compared to the bimetallic 20 wt% Bio-Ru/Pd. Even though a higher yield of 2,5-DMF (56.68%) was obtained, the difference when compared to that obtained by 5 wt% Bio-Ru/Pd is not that significant. In spite of the higher metal content in 20 wt% Bio-Ru/Pd catalyst, it does not favour the conversion of 5-HMF and intermediates to 2,5-DMF. This suggests that 5 wt% bimetallic Bio-Ru/Pd is a better catalyst than the 20 wt% Bio-Ru/Pd and 20 wt% Bio-Ru catalyst in terms of 2,5-DMF yield obtained and also the cost of the catalyst.

As stated earlier in this Section, for the purpose of comparison, all experiments with different catalysts were performed at identical reaction conditions. Unfortunately, the supplier of the bio-catalyst did not produce the 5 wt% Bio-Ru catalyst so it is difficult to compare the catalytic activity of the bimetallic 5 wt% Bio-Ru/Pd and monometallic 5 wt% Bio-Ru. However, Table 6.2 shows that the bimetallic 20 wt% Bio-Ru/Pd gave a better 2,5-DMF yield than the monometallic 20 wt% Bio-Ru/Pd even though there is no significant difference (4%) in 2,5-DMF yield obtained. Although, Lee, et al. (2014) found out that the catalytic activity of bimetallic catalysts for carbonyl group hydrogenation can be 110 times higher than monometallic catalysts, there was a scenario in their study where monometallic Ru catalyst was more active than the bimetallic catalyst for xylose hydrogenation.

Furthermore, the commercial 5 wt% Ru/C catalyst showed the best catalytic activity amongst all the catalysts tested in this study. A higher yield of 92.1% was achieved after optimization of reaction parameters. However, there is a high possibility that a better 2,5-DMF yield could be obtained with the bimetallic bio-Ru/Pd if all other reaction conditions are optimized. Therefore, comparing all the 5 wt% catalysts used in this study at the same reaction conditions, it can be inferred that the trend in catalytic activity are Ru/C > BioRu/Pd > BioRu > Pd/C.

6.6 Reaction Pathway in HCOOH/Et_3N

To have a better understanding of the reaction mechanism, the possible reaction paths were investigated. Besides the major product (2,5-DMF) obtained, many other by-products such as: 2,5-dihydroxymethylfuran, furfural, 5-methylfurfural, 5-methylfurfuryl alcohol, 2,5-dimethyltetrahydrofuran, 2,5-hexadione, including some unidentifiable products were observed in the hydrogenation of 5-HMF in HCOOH/Et_3N mixture. During the reaction, 5-methylfurfural was believed to be the key intermediate product. This is because it was observed that after 30 minutes of reaction time, 5-methylfurfural and 2,5-dihydroxymethylfuran were the main by-products obtained after analysing the sample. After that, the amount of 5-methylfurfural started decreasing until reaching a negligible level after 4 hours to form the desired product (2,5-DMF). This indicated that 5-methylfurfural is an important intermediate in the hydrogenation of 5-HMF to 2,5-DMF in HCOOH/Et_3N mixture. Based on the compounds identified via GC-MS analysis, a possible reaction path for 5-HMF hydrogenation in HCOOH/Et_3N mixture was proposed (Figure 6.10).

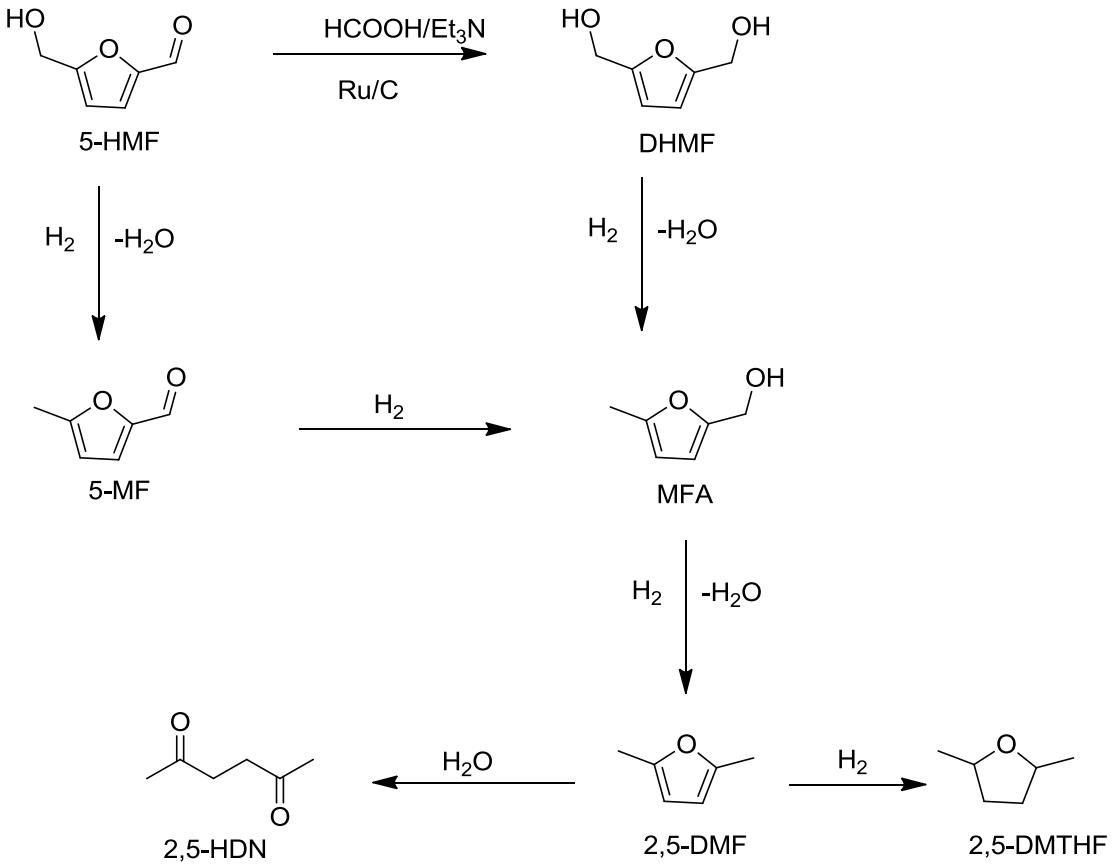

Figure 6.11: Plausible reaction pathway for the hydrogenation of 5-HMF toward 2,5-DMF in HCOOH/Et3N mixture.

6.7 Conclusions

In this chapter, a set of novel catalysts (biomass supported Bio-Ru, Bio-Ru/Pd) including the conventional Ru/C and Pd/C catalysts, were investigated in catalytic transfer hydrogenation of 5-HMF to 2,5-DMF in HCOOH/Et_3N mixture. Catalyst screening showed that Ru/C was a more suitable catalyst for the conversion of 5-HMF to 2,5-DMF using HCOOH/Et_3N as H-donor solvent. An excellent DMF yield of 92.1% was achieved after optimization of the reaction parameters. It has been demonstrated that 5:2 molar ratio of HCOOH/Et_3N mixture is a highly promising medium for facilitating hydrogenation of 5-HMF

to 2,5-DMF over Ru/C catalyst, which is a green and sustainable process. The activity of the Ru/C catalyst plays a major role in the conversion of 5-HMF to 2,5-DMF. A 97.3% conversion of 5-HMF to 2,5-DMF in HCOOH/Et_3N mixture was achieved under relatively mild reaction conditions within the reaction time of 4 hours using Ru/C at 210^oC. The distribution of product depended on different reaction parameters studied such as molar ratio of HCOOH/Et_3N mixture, temperature, time, concentration of 5-HMF, catalyst dosage and agitation speed. Also, varying the reaction conditions offers the ability to achieve either 2,5-DMF, 2,5-DMTHF, 5-methylfurfural (5-MF), 2,5-dihydroxymethylfuran (DHMF), 5-methylfurfuryl alcohol (MFA) and 2,5-hexadione. This study offers the possibility of obtaining a very high yield of 2,5-DMF by the hydrogenation of HMF under mild reaction conditions. In the case of the bio-catalyst, the bimetallic 5 wt% Bio-Ru/Pd gave the highest 2,5-DMF yield when compared to other bio-catalysts used in this chapter. Therefore, based on the comparison conducted in this study, one can conclude that the conventional Ru/C catalyst displayed the best catalytic activity amongst other catalysts investigated.

Chapter 7. **Synthesis of 2,5-DMF in 2-Propanol.**

7.1 Abstract

This chapter investigated the sequential catalytic transfer hydrogenation (CTH) of 5-hydroxymethylfurfural to 2,5-dimethylfuran over both conventional and biomass supported catalysts , with 2-propanol as hydrogen donor. The conventional catalyst studied were 5 wt% Ru/C, 5 wt% Pd/C and 10 wt% Pd/C while the biomass-supported catalysts studied were 5 wt% Bio-Ru/Pd, 5 wt% Bio-Pd, 20 wt% Bio-Ru and 20 wt% Bio-Ru/Pd. It was found that 5-HMF hydrogenation produce 5-methylfurfuryl alcohol, which undergoes hydrogenolysis to form 2,5-dimethylfuran. The yield of 2,5-dimethylfuran was enhanced with increasing reaction temperature and/ or reaction time. Optimum conditions were attained at 260^{o}C after 2 hours of reaction time, where 5-HMF conversion and 2,5-DMF yield reached 94.3% and 70.2% respectively. Optimization of other reaction parameters such as initial 5-HMF concentration, catalyst dosage, agitation speed and nitrogen pressure had significant roles in the selectivity towards 2,5-DMF. The possible reaction mechanism was studied by analysing the reaction intermediates/products obtained by gas chromatography-mass spectroscopy. Of all the catalysts screened, 5 wt% Ru/C catalyst showed the highest catalytic activity in terms of product yield obtained. The novel work in this chapter lies with the use of a bio-support for metal catalysts for use in the CTH of 5-HMF to 2,5-DMF using 2-propanol as hydrogen donor. It was observed that 42.6% yield of 2,5-DMF yield and 94.5% 5-HMF conversion was attained with the 5wt% Bio-Ru/Pd bimetallic catalyst.

7.2 Introduction

An alternative route for the conversion of 5-HMF to 2,5-DMF without using molecular hydrogen could entail catalytic transfer hydrogenation (CTH), which involves the use of a hydrogen donor compound. Among hydrogen donor compounds available, alcohols are usually employed in CTH reactions for a number of reasons. They are non-corrosive, environmentally friendly, cheap, can be produced from biomass (e.g, ethanol) and can serve both as reactants and solvents. Also, the dehydrogenated products of alcohols (aldehydes or ketones) can easily be reused either as chemicals or hydrogenation using base metals (Chai and Dumesic, 2011).

Among all the alcohols used for CTH reactions of biomass-derived compounds, secondary alcohols have been reported as better hydrogen donor solvents than primary alcohols in terms of product yield, selectivity and conversion obtained (Glinski and Ulkowska, 2011). The donor ability of an alcohol decreases with the length of the carbon chain in the alcoholic species and in particular, with the degree of substitution of the alcohol (Scholz et al., 2014). For instance, the CTH of levulinic acid and its esters to ɣ-Valero lactone in butanol over ZrO_2 catalyst was reported by Chai and Dumesic (2011) with a yield of 92% obtained. Also, Kobayashi et al., (2011) investigated the use of 2-propanol as hydrogen donor solvent for the CTH of cellulose to sorbitol and mannitol over Ru/C catalyst obtaining a yield of 45%. In addition, Gandarias et al (2011) described the use of 2-propanol as a donor compound for the hydrogenation of glycerol to 1,2-propanediol over a Ni-Cu/Al_2O_3 catalyst. Similarly, Musolino and co-workers applied unreduced Pd/Fe_2O_3 for the conversion of glycerol to 1,2-propanediol in 2-propanol and reported a 94% yield (Musolino et al., 2009). More recently, Scholz's research group reported the CTH of reductive upgrading of furfural and 5-HMF over in situ

reduced Fe_2O_3 supported Ni, Cu and Pd catalyst, using 2-propanol as hydrogen donor (Scholz et al., 2014). Finally, the liquid phase catalytic transfer hydrogenation of furfural over a Ru/C catalyst using 2-propanol as hydrogen donor was recently reported by Panagiotopoulou and Vlachos (2014). They obtained a furfural conversion of 95% and 61% yield of methyl furan. These findings are in agreement with the literature, which shows that secondary alcohols have a higher ability to release hydrogen than primary alcohols (Scholz et al., 2014).

Clearly, the use of 2-propanol for CTH reactions is of great significance for biomass conversion and it offers advantages over primary alcohols such as methanol and ethanol. Firstly, 2-propanol is not as poisonous as methanol and it is often cheaper to make compared to ethanol. Secondly, it has been reported in the literature that 2-propanol has higher hydrogen donor abilities than primary alcohols (Scholz et al., 2014; Gandarias et al., 2011) hence why 2-propanol was used in this study. Therefore, the CTH of 5-HMF to 2,5-DMF in 2-propanol over both conventional (Ru/C, Pd/C) and biomass-supported (Bio-Ru, Bio-Pd, Bio-Ru/Pd) metal catalysts were studied and reported. The novel aspect of this chapter lies with the use of bio-supported metal catalysts for CTH of 5-HMF in 2-propanol. Thus, the representative procedure for the CTH of 5-HMF to 2,5-DMF is presented in Section 7.3. The catalyst screening, optimization of reaction conditions are presented in Section 7.4, effect of bio-catalysts in Section 7.5, plausible reaction mechanism in Section 7.6 and conclusion of the chapter in Section 7.7.

7.3 Representative Procedure

The catalytic transfer hydrogenation reactions were carried out in a 100 mL stainless steel Parr reactor autoclave with an external temperature and stirring controllers. For a typical reaction, the reactor was charged with 0.17 M 5-HMF, 0.1 g Ru/C catalyst and 25 ml of 2-propanol, sealed, purged of air with 5 bar N_2 and charged with 20 bar N_2. The reactor was heated to 260^{o}C reaction temperature and stirred at a speed of 300 rpm for 2 hours. After completion of the reaction, the reactor was quenched to room temperature in ice-water bath; and the reaction mixture was filtered with 8µm Whatman quantitative filter paper. The liquid products were analysed using GC-FID (Shimadzu GC 2010).

7.4 Results and Discussion

This section describes the result obtained for the catalytic transfer hydrogenation of 5-HMF to 2,5-DMF using 2-propanol as hydrogen donor solvent.

7.4.1 Catalytic Transfer Hydrogenation of 5-HMF to 2,5-DMF in 2-Propanol Over Ru/C Catalyst

2-propanol is converted into acetone and hydrogen during transfer hydrogenation reactions. Thus, the hydrogen generated is been utilised for the conversion of 5-HMF to 2,5-DMF. To determine the amount of H_2 generated from 2-propanol, this was demonstrated by catalysing the conversion of 2-propanol over Ru/C catalyst. It was observed that 2-propanol resulted in the formation of acetone, significant amount of hydrogen, small amount of diisopropyl ether and traces of propane (Figure 7.1). However, as stated in Section (6.4.1), the main concern in CTH is to prevent further hydrogenation of the furan ring structure present in

5-HMF. In addition, the hydroxyl and aldehyde group present in 5-HMF are treated and monitored closely during the reaction. The importance of using a catalyst for the hydrogenation of 5-HMF to 2,5-DMF in 2-propanol cannot be underestimated.

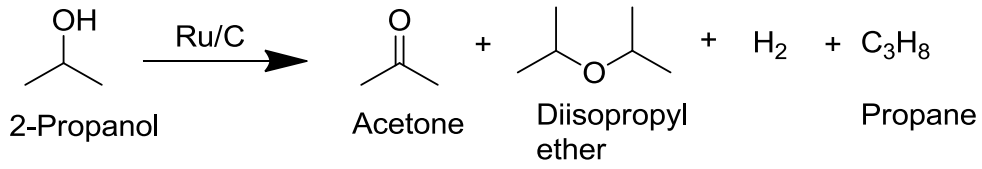

Figure 7.1: Reaction pathway for 2-propanol conversion in Ru/C catalyst.

7.4.2 Catalyst Screening

Similar to Chapters 5 and 6, three different catalysts 5 wt% Ru, 5 wt% and 10 wt% Pd on activated carbon were screened for the CTH of 5-HMF to 2,5-DMF using 2-propanol as hydrogen donor. The results displayed in Table 7.1 were based on identical reaction conditions (as shown in Table 7.1) employed in this study. Although further experiments are needed to determine optimal reaction conditions for all the different catalysts used. A high (94.5%) 5-HMF conversion and 32.6% yield of 2,5-DMF was achieved using the 5 wt% Pd/C catalyst. Other products obtained are 5-methylfurfuryl alcohol, 5-methylfurfural and trace amount of unidentifiable by-products. The same scenario was observed with the 10 wt% Pd/C catalyst. A very high (94.3%) 5-HMF conversion and 32.8% yield of 2,5-DMF was obtained. The main product obtained here was 2,5-dimethyltetrahydrofuran (2,5-DMTHF). This shows that the increase in the Pd loading enhanced further hydrogenation of 5-HMF to 2,5-DMTHF.

Table 7.1: Catalyst screening in 2-propanol

Entry	Catalyst	Conversion (%)	Yield (%)	Selectivity (%)
1	5 wt% Ru/C	94.3	70.2±2.4	74.4
2	5 wt% Pd/C	94.5	32.6±1.8	34.5
3	10 wt% Pd/C	94.3	32.8±1.2	34.8

Reaction conditions: catalyst amount = 0.1 g; 2-propanol = 25 ml; temperature = 260^{o}C; time = 2 hours; 5-HMF concentration = 0.07 M. Note: 5-HMF concentration is relative to 2-propanol amount. Where errors are shown, these are calculated as mean ± standard error of the mean from at least three experiments.

7.4.3 Hydrogenation of 5-HMF to 2,5-DMF Under Different Reaction Parameters

From the results obtained, it was observed that the catalytic activity of the 5 wt% Ru/C catalyst for the hydrogenation of 5-HMF to 2,5-DMF in 2-propanol strongly depends on different reaction parameters such as temperature, time, catalyst amount, 5-HMF concentration, nitrogen pressure and agitation speed. Therefore the reaction conditions listed above were optimized to achieve a maximum yield of 2,5-DMF.

7.4.3.1 Effect of Reaction Temperature

In order to investigate the effect of temperature, the CTH of 5-HMF to 2,5-DMF was performed between 200 and 300^{o}C at 20 degree intervals. Figure 7.2 shows the observed results which indicate that the reaction temperature has an influence on both 5-HMF conversion and 2,5-DMF yield. Being a solvothermal reaction, increasing the temperature naturally enhanced 5-HMF conversion and 2,5-DMF yield. While 5-HMF conversion was already high at 200 ^{o}C (92.2%), 2,5-DMF yield reached only 19.6%. Upon increasing the reaction temperature to 220^{o}C, 5-HMF conversion obtained was 96% and a slight increase in 2,5-DMF yield (24.2%).

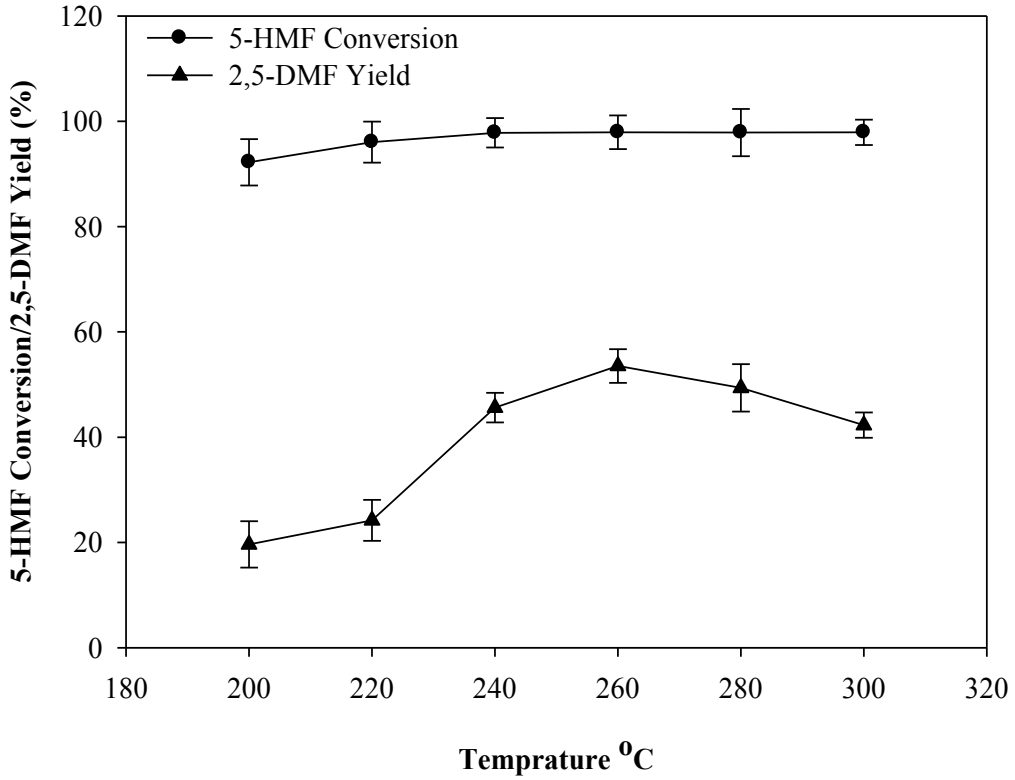

Figure 7.2: Effect of reaction temperature on 5-HMF conversion and 2,5-DMF yield.

Reaction conditions: Agitation speed = 300 rpm; Catalyst amount = 0.1 g; 2-propanol = 25 ml; time = 2 hours; 5-HMF concentration = 0.17 M. Note: 5-HMF concentration is relative to 2-propanol amount. Where error bars are shown, these are calculated as mean ± standard error of the mean from at least three experiments.

From the graph, it can be observed that 5-HMF conversion was almost constant and very high (> 96%) at temperatures between 220 and 300ºC. Below 240ºC, 2,5-DMF yield was extremely low (<24%). However, there was a rapid increase in 2,5-DMF yield between 240 and 260ºC. 2,5-DMF yield increased to 45.6% and 53.5% respectively. Above 260ºC, 2,5-DMF yield started to decrease. From 280 to 300ºC, both 2,5-DMF yield and selectivity decreased to 49.4% and 42.3% respectively. From these observations, it can be concluded that increase in temperature give rise to increase in 2,5-DMF yield and selectivity until a certain temperature when they start to decrease. The decrease in 2,5-DMF yield above 260ºC could be

attributed to the constant increment in reaction temperature giving rise to formation of high yield of 5-methylfurfural which is a reaction intermediate observed via GC-MS analysis. This is in agreement with Zhang et al., (2012). The highest yield of 2,5-DMF (53.5%) and selectivity (54.7%) were observed at 260^{o}C. This is contrary compared to the result reported recently by Jae et al., (2013). Jae and co-workers reported an optimum temperature of 190^{o}C which is similar to that reported by Scholz et al., (2013). An optimum temperature of 180^{o}C was achieved by Scholz's research group.

The rapid increase in 2,5-DMF yield between 220 and 240^{o}C could be attributed to 2-propanol dehydrogenation to acetone and hydrogen. Nielsen et al., (2013) investigated methanol dehydrogenation to hydrogen and formaldehyde at low reaction temperatures (65 - 95^{o}C) using ruthenium complexes as catalyst. The low temperature dehydrogenation reported by Nielsen et al., (2013) was also observed in the conversion of 5-HMF to 2,5-DMF using 2-propanol as hydrogen donor. In addition to this, Jae et al., (2013) observed that at low temperatures, 5-HMF conversion to intermediates is slower than the rate of 2-propanol dehydrogenation hence accumulation of hydrogen was observed in the reactor.

Moreover, as temperature is increased, there is a high possibility that the concentration of intermediates increased as 5-HMF conversion increases. The reaction system can then be linked to Le Chatelier's principle by relating the equilibrium position to the concentration of the reactant (Liu et al., 1996). Le Chatelier's principle states that a behavioural shift to the right occurs when there is an increase in the concentration of the reactant. As a result, more product formation is expected. Therefore, a rapid 2,5-DMF formation was observed when the

concentration of reaction intermediate was increased coupled with the accumulation of hydrogen in the system. Furthermore, it can be observed from the graph that, an increase in temperature is complemented with an increase in 5-HMF conversion, 2,5-DMF yield as well as the rate of the reaction. Thus, a higher temperature suggests a higher average kinetic energy of reactants and more collisions per unit time.

7.4.3.2 Effect of Reaction Time

The effect of reaction time was investigated using a fixed optimum temperature value of 260^{o}C. For this section, the reaction time was noted to start (t = 0) when the set point temperature was attained. From Figure 7.3, it can be observed that by this point, 5-HMF conversion had already reached 97.4% and 2,5-DMF yield was 38%. Upon increasing the reaction time, there was no significant further increase in 5-HMF conversion. A 97.9% 5-HMF conversion was achieved after 2 hours. However, the same cannot be said for 2,5-DMF yield. It increased from 38% at t = 0 to 53.5% after 2 hours. The main by product obtained was 2,5-dihydroxymethylfuran. This implies that 5-HMF undergoes partial hydrogenation to 2,5-DHMF at shorter reaction time. This is in agreement with the result reported by Jae et al., (2013).

Furthermore, prolonging the reaction time above 2 hours did not have a significant effect on 5-HMF conversion. 2,5-DMF yield also reached a maximum of 53.5% at 2 hours reaction time, then slightly decreased to 52.3%, 52%, 50.4% and 50.2% at 4, 6, 8 and 10 hours respectively. The slight decrease in 2,5-DMF yield after 2 hours could be caused by two reasons. The reaction intermediates formed could not convert completely to 2,5-DMF or the

2,5-DMF obtained undergoes further hydrogenation to 2,5-DMTHF at longer reaction times. Therefore, the optimum reaction time was 2 hours which is in agreement with the result reported by Hansen et al., (2012). However, this is contrary to what was reported by Jae et al., (2013) where an optimum reaction time of 6 hours was achieved. This was expected due to the fact that a lower reaction temperature (190^{o}C) was reported by Jae's research group unlike the 260^{o}C reaction temperature which was obtained in our study.

In addition, since 5-HMF conversion was very high at t = 0, it suggests that 5-HMF was converted to intermediates such as 2,5-DHMF, 5-methylfurfuryl alcohol identified via GC-MS analysis. Figure 7.8 illustrates a possible reaction scheme that could occur. It is noteworthy to state here that the plausible reaction scheme was compiled from the result obtained from GC-MS analysis, Hansen et al., (2012), Scholz et al., (2013), and Jae et al., (2013).

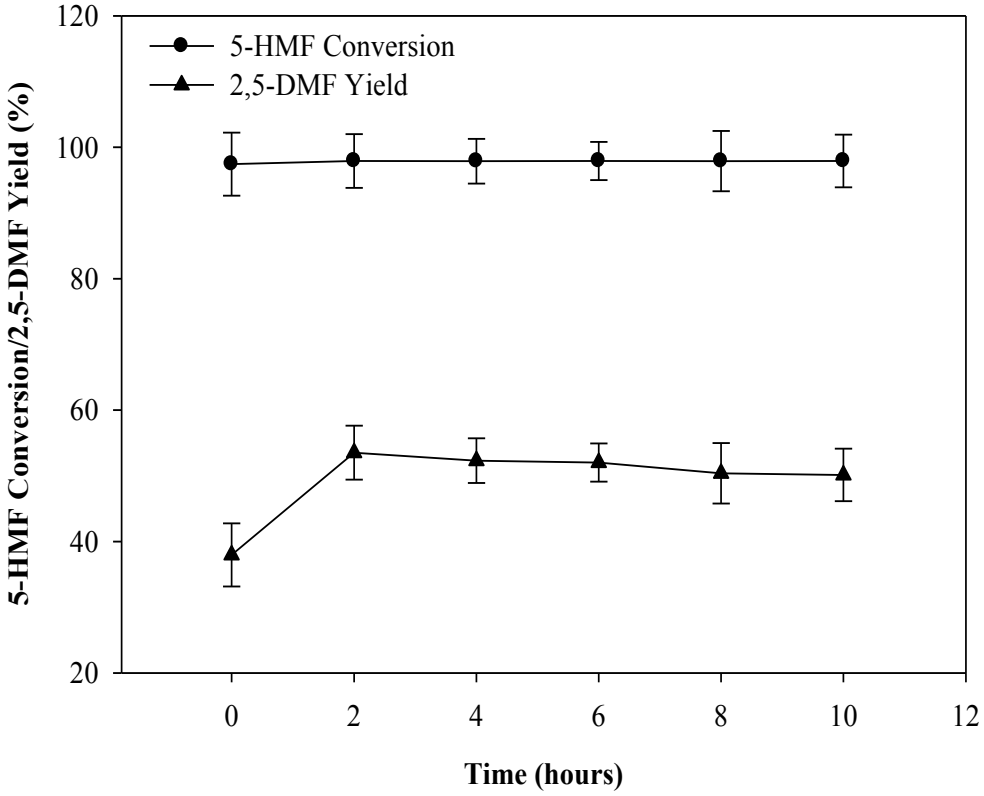

Figure 7.3: Effect of reaction time on 5-HMF conversion and 2,5-DMF yield.

Reaction conditions: Agitation speed = 300 rpm; Catalyst amount = 0.1 g; 2-propanol = 25 ml; temperature = 260°C; 5-HMF concentration = 0.17 M. Note: 5-HMF concentration is relative to 2-propanol amount. Where error bars are shown, these are calculated as mean ± standard error of the mean from at least three experiments.

7.4.3.3 Effect of Initial 5-HMF Concentration

The effect of initial 5-HMF concentration was studied by keeping the optimum reaction temperature and time obtained constant. Figure 7.4 shows the variation of 2,5-DMF yield, 5-HMF conversion and selectivity as a function of initial 5-HMF concentration. As shown in Figure 7.4, at 0.17 M initial 5-HMF concentration, a very high 5-HMF conversion and 53.5% yield of 2,5-DMF was achieved. However, when the initial 5-HMF concentration was reduced to 0.07 M, 5-HMF conversion slightly decreased to 94.3% and 2,5-DMF yield increased

significantly to 70.2%. An explainable reason for this is related to the amount of catalyst used during the reaction. This implies that based on the amount of catalyst used; there were enough active sites for hydrogenation of reaction intermediates to take place. Furthermore, upon increasing the initial 5-HMF concentration to 0.23 M, 5-HMF conversion remained constant at 97.9% and 2,5-DMF yield decrease significantly to 29.4%. In addition, a further increase in initial 5-HMF concentration to 0.3 and 0.33 M was accompanied by a further decrease in 2,5-DMF yield to 15.8% and 13% respectively. The observed decrease was also noticed in 5-HMF conversion (94%, 90.8%) at 0.3 and 0.33 M respectively.

With regards to the catalyst amount, increasing the initial 5-HMF concentration might have resulted in less active sites for hydrogenation of reaction intermediates to take place. Moreover, keeping the amount of 2-propanol constant might cause insufficient hydrogen in the system resulting in higher concentration of reaction intermediates since 2,5-DMF yield is highly dependent on hydrogen. This is in agreement with Hu et al., (2014) where deficiency of hydrogen was reported as the concentration of initial 5-HMF was increased.

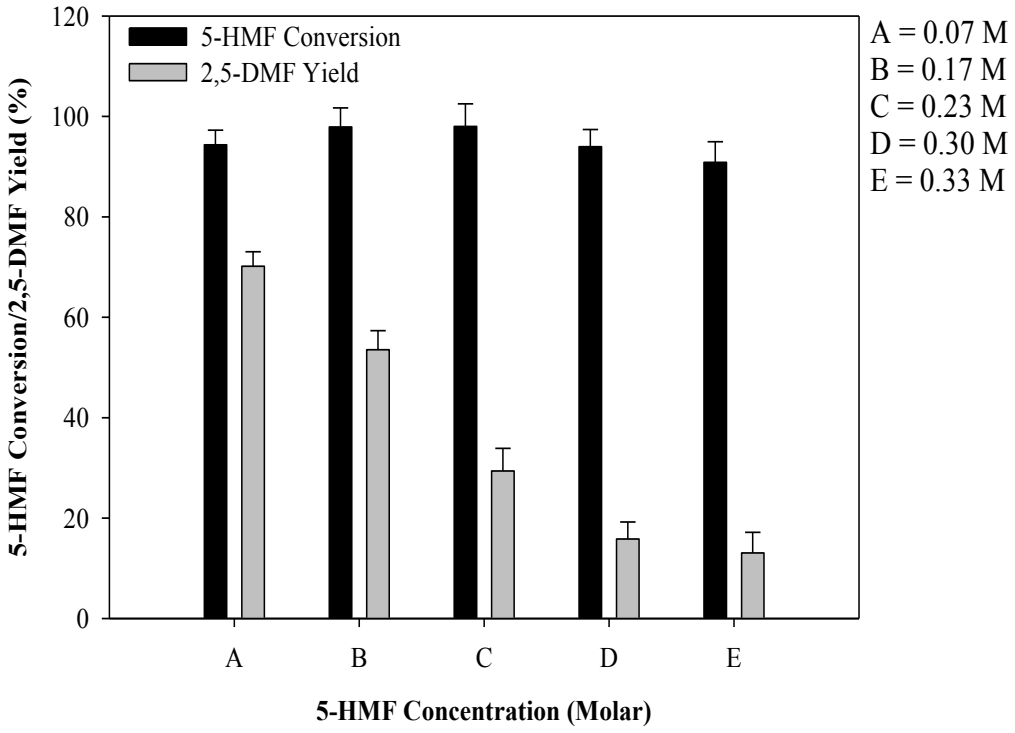

Figure 7.4: Effect of initial 5-HMF concentration on 5-HMF conversion and 2,5-DMF yield.

Reaction conditions: Agitation speed = 300 rpm; Catalyst amount = 0.1 g; 2-propanol = 25 ml; temperature = 260°C; time = 2 hours. Note: 5-HMF concentration is relative to 2-propanol amount. Where error bars are shown, these are calculated as mean ± standard error of the mean from at least three experiments.

7.4.3.4 Effect of Nitrogen Pressure

As stated in (section 7.3), nitrogen was charged before heating up the system to set point temperature. In order to understand the role of N_2 in the reaction medium, the amount of nitrogen charged into the system at different pressures were investigated. Under Le Chatelier's principle, the addition of an inert gas (such as helium) at a constant volume does not cause an equilibrium shift. This is because the partial pressure of other gases in the system does not change upon addition of an inert gas even though the total pressure of the system increases. However, nitrogen is not inert and therefore, known to be reactive at high temperatures. Figure 7.5 illustrates the variation of 2,5-DMF yield and 5-HMF conversion as a function of pressure.

From Figure 7.5, it can be observed that a very high 5-HMF conversion (94.9%) and 38% 2,5-DMF yield was obtained in the absence of N_2 even though it require a longer time for the reaction to heat up to the set point temperature. Upon addition of 10 bar N_2 into the system, 5-HMF conversion remained constant but a slight increase in 2,5-DMF yield (44.8%) was achieved. A further increase in N_2 pressure to 20 bar resulted in a significant increase of 2,5-DMF yield to 70.2% while 5-HMF conversion remained constant at 94%. This is in agreement with the result reported by Jae et al., (2013) where a pressure of 2.04 MPa was employed in their system. Encouraged by this result, we increased the pressure to 30 bar N_2 but a decrease in 2,5-DMF yield (43.3%) was observed while 5-HMF conversion remained constant at 94%. It can be said that pressure does not have a significant effect on 5-HMF conversion and a decrease in 2,5-DMF yield at 30 bar can be attributed to the fact that the reaction heated up quickly to the set point temperature at higher pressure. As a result, 5-HMF was converted to intermediates at a relatively short period of time. Thus, 20 bar N_2 was selected throughout the optimization process.

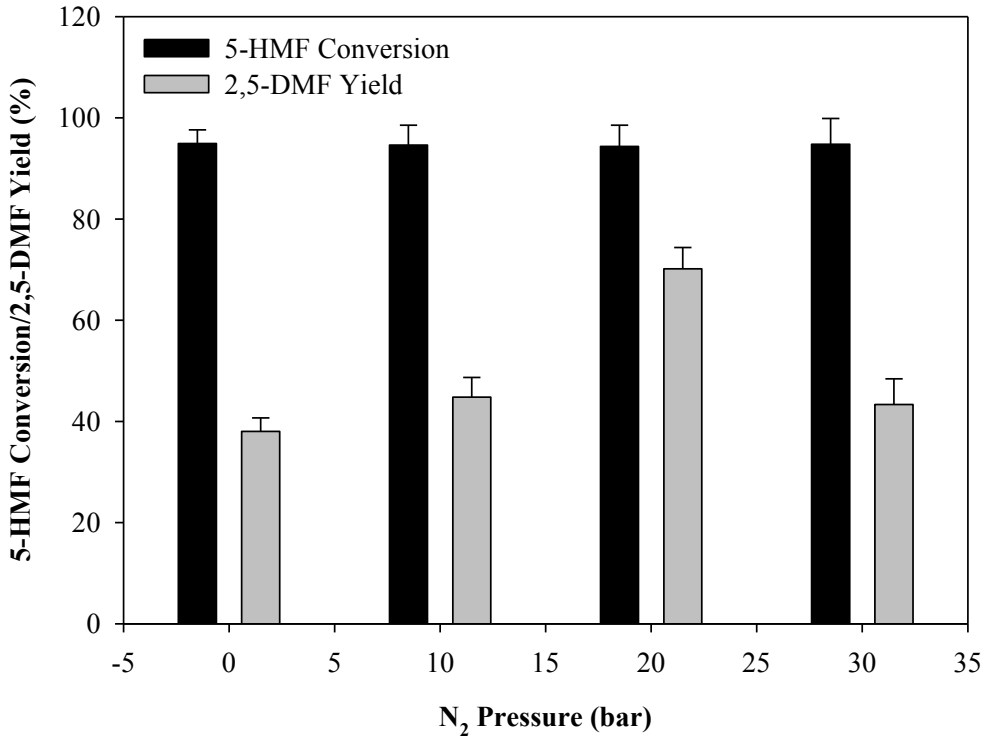

Figure 7.5: Effect of nitrogen pressure on 5-HMF conversion and 2,5-DMF yield.

Reaction conditions: Agitation speed = 300 rpm; Catalyst amount = 0.1 g; 2-propanol = 25 ml; temperature = 260°C; time = 2 hours; 5-HMF concentration = 0.07 M. Note: 5-HMF concentration is relative to 2-propanol amount. Where error bars are shown, these are calculated as mean ± standard error of the mean from at least three experiments.

7.4.3.5 Effect of Catalyst Amount

The effect of catalyst amount was studied utilising the optimum reaction parameters determined previously. The 5 wt% Ru/C catalyst plays a major role in the hydrogenation of 5-HMF and intermediates to 2,5-DMF. The large surface area of the Ru/C catalyst provides more collision sites thus having a significant effect on yield of 2,5-DMF and selectivity. As stated earlier in Section 7.4.1, Ru/C catalyst also catalyses the generation of H_2 from 2-propanol. Figure 7.6 shows how the amount of catalyst affects 5-HMF conversion, 2,5-DMF yield and

selectivity. As illustrated in Figure 7.6, 5-HMF conversion was consistently very high (>94%) for each data point investigated. With regards to 2,5-DMF yield, a similar trend to that in section 7.4.3.4 is observed. When the amount of catalyst was 0.1 g, 70.2% 2,5-DMF yield was attained. However, decreasing the amount of catalyst to 0.05 g resulted in a slight decrease of 2,5-DMF yield to 65.8%. Upon increasing the amount of catalyst from 0.1 g to 0.2, 0.3 and 0.5 g, the amount of 2,5-DMF yield decreased significantly to 55.3%, 40% and 38.6% respectively. Therefore, 0.1 g Ru/C was selected as the optimum catalyst amount.

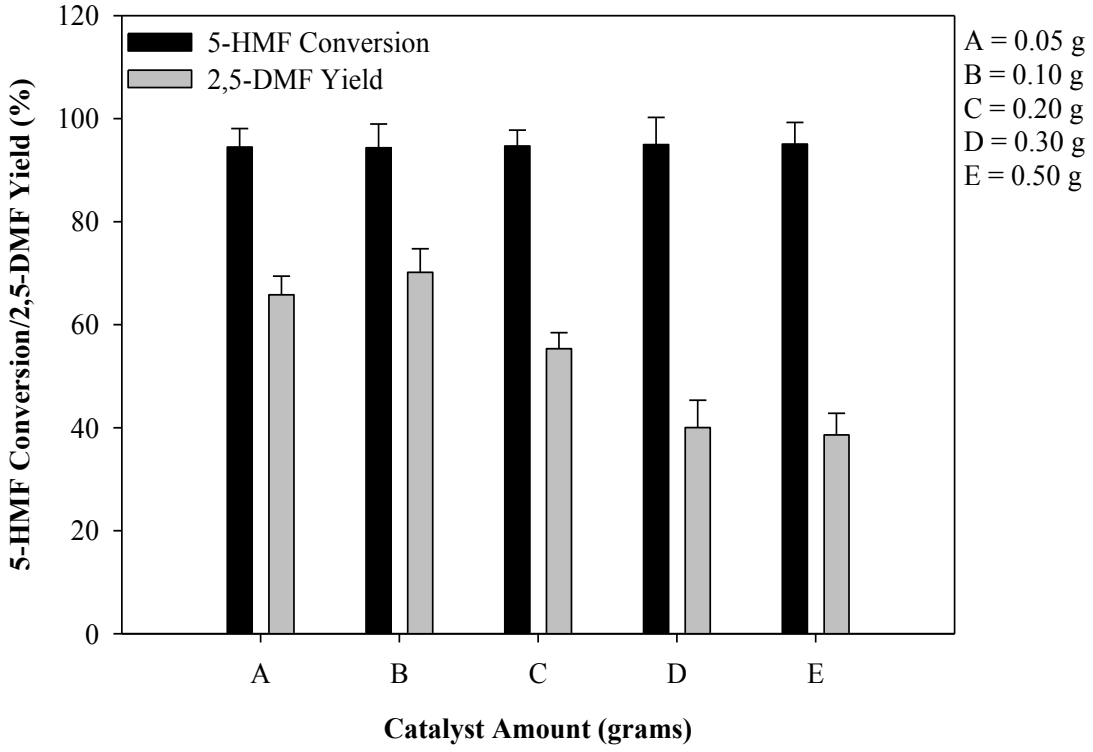

Figure 7.6: Effect of catalyst amount on 5-HMF conversion and 2,5-DMF yield.

Reaction conditions: Agitation speed = 300 rpm; 2-propanol = 25 ml; temperature = 260°C; time = 2 hours; 5-HMF concentration = 0.07 M. Note: 5-HMF concentration is relative to 2-propanol amount. Where error bars are shown, these are calculated as mean ± standard error of the mean from at least three experiments.

The variation in 2,5-DMF yield and selectivity implies that excess Ru/C catalyst does not particularly enhance the formation of 2,5-DMF. It also favours the formation of reaction intermediates which is then converted to by-products. This theory proved to be correct as the GC-MS analysis of reactions conducted at 0.3 and 0.5 g suggested potential intermediates and by-products such as 2-hexanone, 2-butanol, 2(3H)-furanone dihydro-5-propyl and methylisobutylketone (MIBK). It is noteworthy to state here that catalyst amount is relative to initial 5-HMF concentration. At lower catalyst amount, a competition between different reactions occurring is expected resulting in lower 2,5-DMF yield obtained at 0.05 g when compared to 0.1 g catalyst amount. This competition occurred because there is insufficient active sites to expedite the hydrogenation of reaction intermediates to 2,5-DMF.

Moreover, it was observed that the fresh Ru/C catalyst surface is scattered with Ru metal and RuO_2 complexes. The RuO_2 complexes allowed ethers formation and a decrease in 2,5-dihydroxymethylfuran selectivity (Jae et al., 2014). Consequently, increasing the amount of catalyst is expected to cause an increase in the formation of RuO_2 complexes which might generate a low 2,5-DMF yield since a very low amount of 2,5-DHMF is expected to be formed. Thus, one can conclude that a very high 2,5-DMF yield is attained due to the combined effect of the Ru metal and RuO_2 complexes on the catalyst surface.

7.4.3.6 Effect of Agitation Speed

According to Devulapelli and Weng, (2009), "increasing the mixing speed might cause an increase in the area between and relative velocity of two phases, and therefore reduces the interfacial mass transfer resistance." The effect of agitation speed on 5-HMF conversion and

2,5-DMF yield was investigated at no speed, 300, 500, 700 and 1000 rpm. As shown in Figure 7.7, it can be observed that without mixing, a very high 5-HMF conversion (94.5%) was still obtained while 2,5-DMF yield was 41.8%. Increasing the agitation speed to 300 rpm dramatically improved 2,5-DMF yield to 70.2%. The significant increase in 2,5-DMF yield can be explained by an increase in mass transfer between the reaction medium and Ru/C catalyst. However, a further increase in the mixing speed from 300 rpm to 500, 700 and 1000 rpm resulted in a decrease in 2,5-DMF yield to 51.5%, 46.2% and 45.4% respectively while 5-HMF conversion remained constant at 94%. This could be attributed to internal mass transfer effects after 300 rpm was reached. In other words, the intra molecular transfer, adsorption and diffusion are predominant on the catalyst surface. Therefore, 300 rpm was selected as the optimum agitation speed in this study.

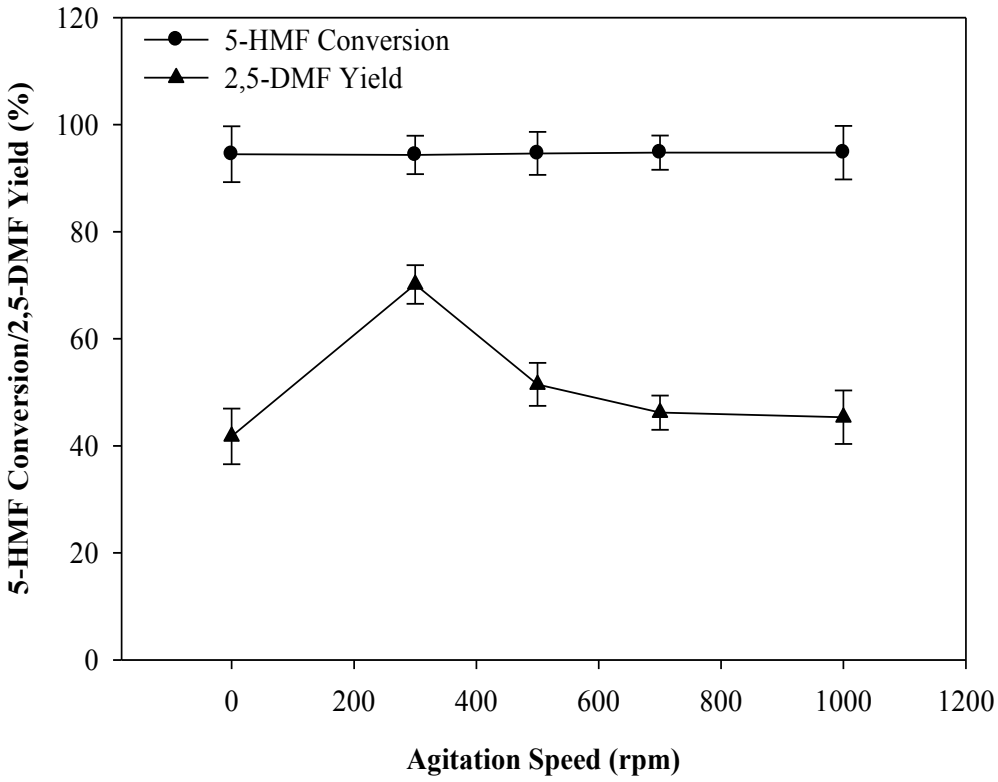

Figure 7.7: Effect of agitation speed on 5-HMF conversion and 2,5-DMF yield.

Reaction conditions: Catalyst amount = 0.1 g; 2-propanol = 25 ml; temperature = 260^{o}C; time = 2 hours; 5-HMF concentration = 0.07 M. Note: 5-HMF concentration is relative to 2-propanol amount. Where error bars are shown, these are calculated as mean ± standard error of the mean from at least three experiments.

7.4.3.7 Catalyst Recycling

Since 5 wt% Ru/C catalyst exhibited the best catalytic activity amongst other solid catalyst employed in this study, it is important to investigate its reusability after the first run of reaction in 2-propanol. Similar to what was observed in Section 5.4.3.7, the right recovery technique was not employed therefore making it difficult to recover the catalyst after the first run. The use of other recovery methods such as centrifugation could be pivotal in recovering the spent catalyst. The optimum catalyst amount obtained was 0.1 g as stated in Section 6.4.3.5.

However, the amount recovered was used for SEM analysis and it was observed that there was no huge difference in the morphology when compared to the fresh Ru/C catalyst as discussed in Section 4.5.2.1 and Figure 4.2 a & d. However, investigation by Jae et al., (2013) showed that the Ru/C catalyst undergoes deactivation after the first run possibly due to the presence of high molecular weight by-products on the ruthenium surfaces. Jae and co-workers went further to determine the ruthenium and carbon content after the first run. They observed that the amount of carbon in the Ru/C catalyst increased from 75% to 81% while the amount of ruthenium decreased from 4.6% to 3.8% after the first run.

7.5 The Use of Bio-Supported Metal Catalysts for Catalytic Transfer Hydrogenation of 5-HMF in 2-Propanol

Similar to Section 5.5 and 6.5, four different biocatalysts were also employed for the CTH of 5-HMF to 2,5-DMF in 2-propanol. The bio-catalysts used are 5 wt% Bio-Pd, 5 wt% and 20 wt% Bio-Ru/Pd and 20 wt% Bio-Ru (See Section 3.4). The effect of bimetallic catalyst on the bio-support was also investigated hence why the 5 and 20 wt% Bio-Ru/Pd was prepared. The properties of bimetallic catalyst have been described previously (See Section 5.5 and 6.5). The use of a second metal as a promoter has been reported to successfully maximize yields to desired products for biomass conversion (Alonso et al., 2012). It is noteworthy to state here that for the purpose of comparison, all the hydrogenation experiments with the bio-catalysts were carried out at identical reaction conditions (as shown in Table 7.2). However, this comparison does not justify the effectiveness and performance of the bio-catalysts for

hydrogenation of 5-HMF. This is due to the fact that different reaction conditions might suite each catalyst investigated.

Table 7.2 illustrates how 5-HMF conversion, 2,5-DMF yield and selectivity varied as a function of different bio-catalyst investigated in this study. It can be seen that 5-HMF conversion remained constant at 94% across all the catalysts investigated. It is clear that regardless of the metal loading in all the bio-catalyst tested, 5-HMF conversion remained constant at 94% throughout. Similar trend was observed with the commercial 5 wt% Ru/C, 5 wt% Pd/C and 10 wt% Pd/C catalysts. Considering the yield of 2,5-DMF obtained using the bio-catalysts, it was observed that the bimetallic 5 wt% Bio-Ru/Pd and 20 wt% Bio-Ru/Pd catalysts shows higher catalytic activity compared to the monometallic counterpart 5 wt% Bio-Pd and 20 wt% Bio-Ru. The same trend was observed in Section 5.5 and 6.5. The catalytic properties of bimetallic catalysts over monometallic catalysts improved significantly since bimetallization increases the properties of the original single metal catalyst and also generate a new catalytic property (Ramsurn and Gupta, 2013). Thus, in most reactions, the introduction of a second metal allows catalyst stability, control of activity and selectivity (Toshima and Yonezawa, 1998).

Table 7.2: Comparison of bio-catalyst and commercial catalyst in 2-propanol.

	5 wt% BioPd	5 wt% Pd/C	5 wt% BioRuPd	20 wt% BioRuPd	20 wt% BioRu	5 wt% Ru/C	10 wt% Pd/C
2,5-DMF Yield (%)	35.8±0.6	32.6±1.8	42.6±1.2	38.6±1.6	37.2±0.7	70.2±2.4	32.8±1.2
5-HMF Conversion (%)	94.1	94.5	94.5	94.3	94.5	94.3	94.3
Selectivity (%)	38.1	34.5	45.1	40.9	39.3	74.4	34.8

Reaction conditions: Catalyst amount = 0.1 g; 2-propanol = 25 ml; temperature = 260°C; time = 2 hours; 5-HMF concentration = 0.07 M. Note: 5-HMF concentration is relative to 2-propanol amount. Where errors are shown, these are calculated as mean ± standard error of the mean from at least three experiments.

Furthermore, comparing the bimetallic bio-supported metal catalyst at different loadings (5 and 20 wt% Bio-Ru/Pd), it is clear that the 5 wt% Bio-Ru/Pd shows higher catalytic activity than the 20 wt% Bio-Ru/Pd. 42.6% 2,5-DMF yield was obtained with the 5 wt% Bio-Ru/Pd while 38.6% was achieved with the 20 wt% loading even though 5-HMF conversion was constant at 94% for both catalyst loading. However, in spite of the higher metal loading (20 wt %), it does not favour the conversion of 5-HMF and intermediates to 2,5-DMF. Instead, the main product obtained was 2,5-DMTHF. This suggests that the higher metal loading undergoes further hydrogenation reaction to 2,5-DMTHF.

As stated earlier in this Section, all experiments with different metal catalysts were conducted at identical reaction conditions. It was difficult to compare the catalytic activity of the bimetallic 5 wt% Bio-Ru/Pd against the monometallic 5 wt% Bio-Ru due to unavailability of the monometallic counterpart. However, Table 7.2 shows the comparison between both commercial and bio-supported metal catalysts tested in this study. The commercial 5 wt% Ru/C

catalyst displayed the best catalytic activity amongst all the catalysts tested. A very high 2,5-DMF yield of 70.2% was achieved after reaction parameters were optimized. One cannot dismiss the fact that a higher 2,5-DMF yield could be attained with other catalyst tested in this study if other reaction parameters are optimized. Thus, based on the comparison in this study, it can be concluded that the trend in the catalytic activity of the catalyst tested for the 5-HMF hydrogenation in 2-propanol are 5 wt% Ru/C > 5 wt% Bio-Ru/Pd > 20 wt% Bio-Ru/Pd > 20 wt% Bio-Ru > 5 wt% Bio-Pd > 10 wt% Pd/C > 5 wt% Pd/C. This result is in agreement with that reported in Section 5.5 and 6.5.

7.6 Reaction Pathway in 2-Propanol

Based on the above findings and reports from Hansen et al., (2012); Scholz et al., (2013); Jae et al., (2013) , the possible reaction pathway for the CTH of 5-HMF to 2,5-DMF in 2-propanol was compiled as shown in Figure 7.8. The reaction intermediates detected via GC-MS analysis are 2,5-dihydroxymethylfuran, 5-methylfurfural, 5-methylfurfuryl alcohol, 2-hexanone, 2-butanol, 2(3H)-furanone dihydro-5-propyl, methylisobutylketone (MIBK) and 2,5-dimethyltetrahydrofuran (2,5-DMTHF). From Figure 7.8, two reaction paths could be proposed. 5-HMF is firstly deoxygenated into 5-methylfurfural (5-MF). After that, it undergoes hydrogenation to 5-methylfurfural alcohol (5-MFA) over Ru/C catalyst. Thereafter, the 5-MFA was quickly converted into 2,5-DMF over Ru/C catalyst. Secondly, 5-HMF is hydrogenated to 2,5-dihydroxymethylfuran (2,5-DHMF) over Ru/C catalyst. The 2,5-DHMF also undergoes deoxygenation to 5-MFA. It can be clearly observed that 5-MFA is an important intermediate in the CTH of 5-HMF to 2,5-DMF. However, because of the current detection methods, further investigation of the reaction pathways is still required as well as the quantification of reaction intermediate.

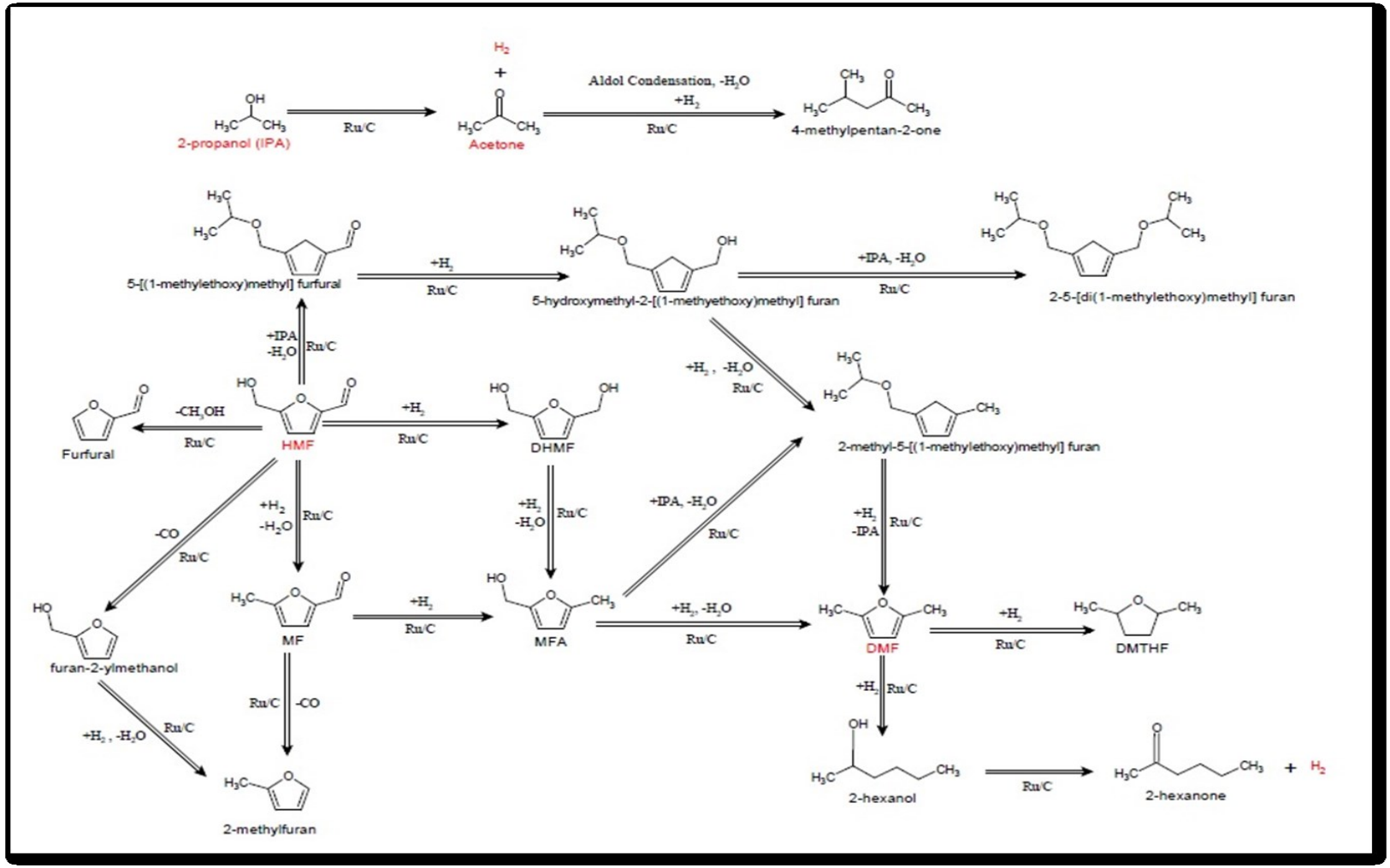

Figure 7.8: Plausible reaction scheme for 5-HMF hydrogenation in 2-propanol. Compiled from GC-MS data, Jae et al., (2013), Scholz et al., (2013) and Hansen et al., (2012).

7.7 Conclusions

In this chapter, a set of catalysts, including the conventional Ru/C, Pd/C and biomass supported catalysts were investigated in the CTH of 5-HMF in 2,5-DMF utilising hydrogen transfer from 2-propanol. Amongst the catalyst screened, Ru/C showed the highest catalytic activity for 5-HMF conversion and 2,5-DMF yield. A 94% 5-HMF conversion and 70.2% 2,5-DMF yield was achieved under reaction conditions of 260^{o}C and 2 hours reaction time, 0.07 M initial 5-HMF concentration, 20 bar N_2, 0.1 g Ru/C and 300 rpm agitation speed. The product distribution is influenced by different reaction conditions listed above. The reaction intermediates identified via GC-MS analysis enables us to predict the possible reaction pathway. The formation of the reaction intermediates is dependent on varying the reaction parameters. Further work is required to explore the reaction mechanism and quantification of reaction intermediates. With regards to the bio-support metal catalysts, 5 wt% Bio-Ru/Pd showed the best catalytic activity with 42.6% 2,5-DMF yield obtained. It is concluded that 5 wt% Ru/C gave the highest yield of 2,5-DMF in the CTH of 5-HMF using 2-propanol as hydrogen donor.

Chapter 8. **Comparison of the three hydrogen-donor solvent systems**

8.1 Introduction

It is generally known that hydrogenation and hydrogenolysis of compounds derived from plant biomass are reactions often conducted in liquid phase, since the highly functionalized biomass molecules cannot be transformed without engaging thermal decomposition. For this reason, a solvent is usually required to serve as a medium in which both solid catalyst and substrate are suspended. However, the contact between the solid catalyst and substrate is still ineffective. As a result, solubilisation of substrate either by solvolysis/thermolysis or by dissolution is required. (Rinaldi, 2015). It is noteworthy to state that an effective transport of hydrogen from gas phase through liquid phase, and onto the catalyst surface is an important technique for catalytic hydrogenations. Therefore, the solubility of hydrogen in the reaction medium is pivotal in order to investigate effect of solvents on catalytic hydrogenations. Logically, the solubility of hydrogen depends on reaction parameters such as pressure and temperature coupled with the composition of the reaction medium (Rinaldi, 2015).

The interaction between reaction rates and solvent properties have been thoroughly studied so as to rationalize solvent effects. For example, Struebing and co-workers recently reported an elegant *in silico* technique to predict the best solvents for use in organic reactions (Struebing et al., 2013; Rinaldi, 2015). Unfortunately, solvent effects in catalytic hydrogenation using heterogeneous catalysts is often neglected and poorly understood. Therefore, solvent properties such as polarity, H-bonding properties, acceptor and donor number are useful to have an idea

of the solvent interactions occurring at the liquid/solid interface, where catalytic reactions take place (Rinaldi, 2015).

One of the main tool to achieve rationalization of solvent effects on heterogeneous catalysts is the interaction of product distributions and reaction rates coupled with solvent polarity or dielectric constant. However, it is not fully understood how solvent properties are able to steer the activity and selectivity of metal catalysts (Rinaldi, 2015). On one hand, it is safe not to assume that the nonspecific (van der Waals) and/or weak specific (H-bonding) interactions involving substrate and solvent would have a significant effect on chemical transformations, which occurs on the catalyst surface by strong interactions between the active sites/support and substrate. On the other hand, the adsorption mechanism of a substrate on the surface of a catalyst may remarkably change based on the solvent properties (Rinaldi, 2015). Moreover, there is a possibility that the solvent itself may compete for the active sites of the catalyst.

Therefore in this chapter, the 3 different H-donor systems employed in Chapters 5,6 and 7 are compared to each other and analysed to show the difference that this research work aim to uncover. This chapter will also focus on the multi-parameter comparison in order to determine and conclude on the advantages and disadvantages of each H-donor system in comparison to the other. Some of the parameters to compare are reaction temperature, time, 5-HMF concentration, catalyst amount, pressure and mixing speed.

8.2 Results and Discussions

This section describes the multi-parameter comparison for each H-donor system employed for catalytic hydrogenation of 5-HMF to produce 2,5-DMF over 5 wt% Ru/C catalyst. The H-donor system employed are molecular H_2, azeotropic mixture of HCOOH/Et_3N and 2-propanol. Table 8.1 shows and compare the optimum reaction parameters obtained for each H-donor system. However, it must be stated here that hydrogen generation from both azeotropic mixture of HCOOH/Et_3N and 2-propanol for use in catalytic reactions is known as Catalytic Transfer Hydrogenation (CTH).

Table 8.1: Comparisons of the Ru/C catalyst optimum conditions obtained for each H-donor system

Parameters/H-donors	**Molecular H_2**	**HCOOH/Et_3N**	**2-Propanol**
Temperature, ^oC	260	210	260
H-Pressure, bar	50	-	-
N-Pressure, bar	-	10	20
Reaction Time, hour	2	4	2
5-HMF Conc, M	0.05	0.3	0.07
Ru/C Amount, grams	0.05	0.1	0.1
Mixing Speed, rpm	700	300	300
HMF Conversion, %	96.4	93.4	94.3
DMF Yield, %	95.1	92.1	70.2

The high conversion of 5-HMF (> 90%) obtained across all hydrogen donors investigated in this research work could be ascribed to the Ru particle size and acidity of the activated carbon support. In addition, the strong metal-support interactions of the Ru/C catalyst could possibly explain the improved product selectivity obtained across the three hydrogen donor systems investigated. Comparing the effect of temperature in the 3 hydrogen sources, it can be observed from Table 8.1 that the optimum reaction temperature across the 3 H-donor system is > 200 ^{o}C. Moreover, it can also be observed that 5-HMF hydrogenation in azeotropic mixture of HCOOH/Et_3N require lesser amount of heat compared to the reactions conducted in both molecular H_2 and 2-propanol. This could be attributed to the fact that the reaction conducted in azeotropic mixture of HCOOH/Et_3N is an exothermic reaction, thereby generating more heat from the solvent mixture.

Furthermore, comparing the effect of time across the H-donors, it can be seen from Table 8.1 that more time is needed (> 2 hours) to achieve high yield of 2,5-DMF in azeotropic mixture of HCOOH/Et_3N. This is expected because the reaction required lesser amount of heat compared to reactions in molecular H_2 and 2-propanol. Therefore, 5-HMF hydrogenation in HCOOH/Et_3N donor system requires more time in order to obtain very high yield of 2,5-DMF. Moreover, comparing the effect of nitrogen pressure across HCOOH/Et_3N and 2-propanol donor system, it can be observed from Table 8.1 that 5-HMF hydrogenation conducted in HCOOH/Et_3N does not require nitrogen pressure during the entire reaction. The 10 bar nitrogen pressure stated was used to purge the system so as to eliminate the air present in the reaction medium. On the other hand, 20 bar nitrogen was required to pressurize the reaction system in 2-propanol. The result obtained is in agreement with that reported by Jae and co-workers where an optimum nitrogen pressure of 2.04 MPa was obtained for hydrogenation of 5-HMF in 2-

propanol. However, when the reaction system in 2-propanol was not charged with nitrogen, It was observed that it took more than 4 hours for the reaction mixture to heat up to the set point temperature.

In addition, comparison of 5-HMF concentration and catalyst amount used across the 3-H donor system is quite challenging. This is because 5-HMF concentration is relative to the amount of catalyst used for each donor system. Therefore, as shown in Table 8.1, it is safe to assume that 5-HMF hydrogenation in molecular H_2 resulted in very high yield of 2,5-DMF (95.1%) compared to that obtained in both HCOOH/Et_3N and 2-propanol (92.1% and 70.2% respectively) when 5-HMF concentration and catalyst amount are put into consideration.

Similarly, it is also difficult to compare the mixing speed across all the 3-H donor systems due to different solvent properties. However, it is necessary to compare the mixing speed across the 3-H donors so as to understand the effect of mass transfer across each H-donor. It must be noted that the use of small Ru/C particles help to efficiently suppress the mass transfer resistance in the catalyst pores. However, based on the comparison in Table 8.1, the 700 rpm observed in molecular H_2 implies that there is enough contact area between the two phases, hence eliminating interfacial mass transfer resistance. This could be another reason why the highest 2,5-DMF yield (95.1%) was obtained in molecular H_2 compared to the reaction carried out in both HCOOH/Et_3N and 2-propanol donor system.

Clearly, the use of molecular H_2 for hydrogenation of 5-HMF to 2,5-DMF still offer advantages over transfer hydrogenating solvents employed in this study considering all the optimized reaction parameters highlighted in Table 8.1. Other factors considered to show that reaction carried out in molecular H_2 possess advantages over 2-propanol and HCOOH/Et_3N includes; H_2 abundance, reproducibility and product separation. Molecular H_2 is relatively available and it is easier to separate the product from the solvent system used. Also, from the SEM analysis, which shows the surface morphology of the spent Ru/C catalyst in molecular H_2, it can be observed that the Ru/C catalyst maintains its morphology. Hence, it can be recycled even though further analyses are required to confirm this.

Using mixture of HCOOH/Et_3N as hydrogen source for hydrogenation of 5-HMF to 2,5-DMF over Ru/C catalyst shows that HCOOH decomposed catalytically into CO_2 and H_2 on the metal particles while the Et_3N forms a complex with Ru to facilitate the generation of the H_2. As a result, the H_2 remains adsorbed forming two metal – hydrogen sites, where the hydrogenation of 5-HMF takes place. However, this reaction is irreversible due to the generation of CO_2 from the azeotropic mixture of formic acid and triethylamine. Therefore, it is reasonable to assume that the mixture of HCOOH/Et_3N for 5-HMF hydrogenation to 2,5-DMF possess advantages over 2 propanol in terms of 2,5-DMF yield obtained and lesser amount of by-products formed. The large amount of by-products formed in 2-propnaol is evident in the reaction pathway shown in Figure 7.8 compared to that formed in HCOOH.Et_3N illustrated in Figure 6.11.

During CTH of 5-HMF in 2-propanol, it is assumed that the nature of the interactions of secondary alcohols with Ru surface should be taken into account. Therefore, the interaction of 2-propanol with Ru (II) surface is believed to cleave the O-H bond and as a result, acetone is released into the gas phase and two H atoms remain adsorbed on the Ru surface. The H atoms are then used in the hydrogenation of 5-HMF to 2,5-DMF. During the CTH of 5-HMF to 2,5-DMF in 2-propanol, there is a possibility that the adsorbed H-atoms formed from decomposition of 2-propanol can have a direct effect on the hydrogenation of 5-HMF adsorbed on Ru instead of being released as H_2 (Jae et al., 2013). However, despite obtaining the lowest yield of 2,5-DMF in 2-propanol, this transfer hydrogenation system still offers advantages over mixture of HCOOH/Et_3N donor system. Some of the advantages includes; easy separation of products from solvent system, cost effective and no catalyst deactivation unlike the HCOOH/Et_3N donor system which could arise due to either the strong adsorption of by-products on the catalyst active sites or the presence of formic acid in the reaction.

8.3 Conclusion

In conclusion, solvents and solvents effects are of high significance for development of catalytic systems for 5-HMF hydrogenation. The solvent system used are not limited only to serve as media for substrate solubilisation but also involved to exert key effects upon heterogeneous catalysts. These effects are associated with solvent reactions on the catalyst surface and competitive adsorption of the solvent. These reactions could generate stable surface species, which may block the catalyst surface. Therefore, screening of solvent for a liquid-phase hydrogenation is of extreme importance when considering a new catalytic system. However, it is therefore safe to state that the effects of solvents on heterogeneous catalysts is still a neglected area in catalysis research and this constitute inadequate understanding of the solvent

interactions at the liquid/solid interfaces (Rinaldi, 2015). Based on the comparison conducted in this study, the use of molecular H_2 for hydrogenation of 5-HMF to 2,5-DMF offers advantages over azeotropic mixture of HCOOH/Et3N and 2-propanol.

Chapter 9. **Preliminary Reaction Kinetics**

9.1 Abstract

In this Chapter, the reaction kinetics for the hydrogenation of 5-HMF in molecular H_2 and 2-propanol is presented and discussed. The reaction kinetics evaluated in molecular hydrogen fitted a second order reaction with respect to 5-HMF as the key reactant with a rate constant of 8.1×10^{-3} mol/L.min and activation energy of 49.5 kJ/mol. Moreover, the kinetic analyses investigated in 2-propanol showed that the experimental data also fitted second order reaction with respect to 5-HMF as the key reactant with an activation energy (Ea) of 229.2 kJ/mol. This implies that doubling 5-HMF concentration will quadruple the reaction rate. However, it must be stated here that, it is challenging to validate the obtained activation energy value due to the lack of reaction kinetics regarding 5-HMF hydrogenation to 2,5-DMF in the literature

Finally, conclusions on the kinetic analyses are drawn in Section 9.5.

9.2 Introduction

To the best of the author's knowledge, there are limited reports regarding the reaction kinetics of 5-HMF to 2,5-DMF found in literature. Ideally, kinetic models such as Langmuir-Hinshelwood or Eley-Rideal are more appropriate since it is a heterogeneous reaction and it would involve adsorption of reactants on the catalyst surface. However due to inability to identify the overall reaction rates of the key components during the course of 5-HMF hydrogenation, time constraint and poor understanding of the kinetic model as at the time of writing this thesis, both models could not be studied. Hence why the kinetic studies of 5-HMF

to 2,5-DMF transformation presented in this chapter was termed preliminary and investigated over the 5 wt% Ru/C catalyst. After recognizing the optimum reaction conditions, further experiments were conducted to study the kinetics of the reaction. The experiments were aimed to determine the rate constant and order of reaction with respect to the reactant as 5-HMF is the starting material. The order of reaction can be determined using two methods; integrated rate law or method of initial rates. Due to time constraints, the integrated rate law method was adopted. The following assumptions were made (Levenspiel, 1999):

- The reaction propagation highly depends on 5-HMF as the key reactant rather than THF and 2-propanol.

- The rate of the reaction is given by the equations below:

$$r = -\frac{d[A]}{dt} \qquad (9.1)$$

$$r = k[A]^n \qquad (9.2)$$

Where [A] represents concentration of reactant (5-HMF) at a given time (t), n is the order of reaction and k is the rate constant. Based on the method of integrated rate law adopted, the equations above were equated and n was substituted for 0, 1 and 2 to generate the three expressions as illustrated in Table 9.1. When n = 0, 1 and 2, the expression represents zero order, first order and second order kinetics respectively. Thereafter, the expressions were integrated and the integrals obtained were rearranged in the format of y = mx + c. This enables for plots of concentration against time and based on the plot characteristic obtained, the rate

constant and order of reaction were determined. Table 9.1 shows the plots of concentration against time used to determine reaction kinetics.

Table 9.1: Plots of concentration against time used to determine reaction kinetics. (Adapted from Silberberg, 2012 and Levenspiel, 1999).

Reaction Order	Integrated rate law (y= mx+c) form	Expected Plot of Concentration vs. time
Zero Order	$r = k[A]^0$ $[A]_t = -kt + [A]_0$	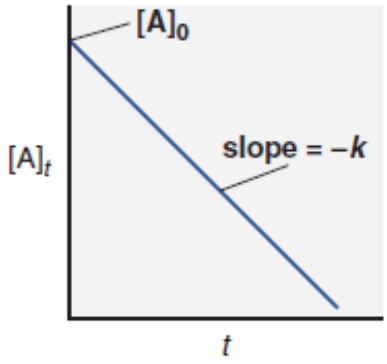
First Order	$r = k[A]$ $\ln[A]_t = -kt + [A]_0$	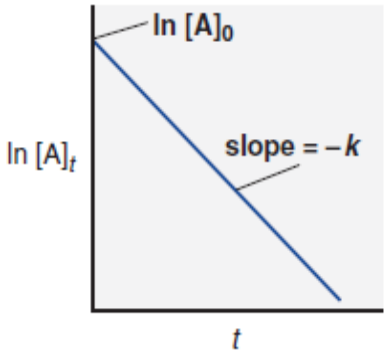
Second Order	$r = k[A]^2$ $\frac{1}{[A]_t} = -kt + [A]_0$	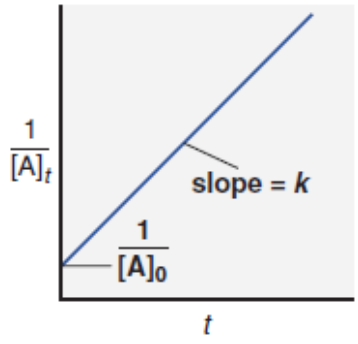

9.3 Reaction Kinetics in Molecular Hydrogen

At the optimum temperature of 260 ^{o}C as obtained in Section 5.4.3.1, three graphs of concentration against time were produced. Among the three plots, a plot of inverse concentration ($1/[HMF]_t$) vs time (Figure 9.1) gave a positive gradient. Therefore, the reaction was considered to be second order with respect to 5-HMF indicating that doubling the concentration of 5-HMF will quadruple the rate of reaction. From Figure 9.1 at 260^{o}C, the rate constant was determined to be 8.1×10^{-3} mol/L.min. It was observed that at lower reaction times, a very high 5-HMF conversion was obtained indicating the rate determining step might involve the reaction of intermediates to 2,5-DMF. Realistically, the reaction rate given by equation (9.2) in a second order reaction would give a more complex equation that would require reactants adsorption on the surface of the catalyst such as Eley-Rideal or Langmuir-Hinshelwood mechanism (Levenspiel, 1999). The other sets of experiments were carried out at the following temperatures, 180, 200 and 240 ^{o}C. The rate constants at the four reaction temperatures are displayed in Table 9.2. However, with the calculated rate constants at the four temperatures, the activation energy (E_a) of the reaction was calculated using the Arrhenius equation given below;

$$k = Ae^{-\frac{E_a}{RT}} \qquad (9.3)$$

$$\ln k = -\frac{E_a}{R}\left(\frac{1}{T}\right) + \ln A \qquad (9.4)$$

Where A is the frequency factor, k is the rate constant at a given temperature (K), R is the universal gas constant ($J.mol^{-1}.K^{-1}$). The frequency factor or Arrhenius constant (A) is determined from the intercept while the activation energy (E_a) is obtained from the slope of the

plot. Equation (9.4) represents the linear form of equation (9.3) in the form of y = mx + c. The plot of ln (k) vs. $\frac{1}{T}$ is presented in Figure 9.1 using the data shown in Table 9.2.

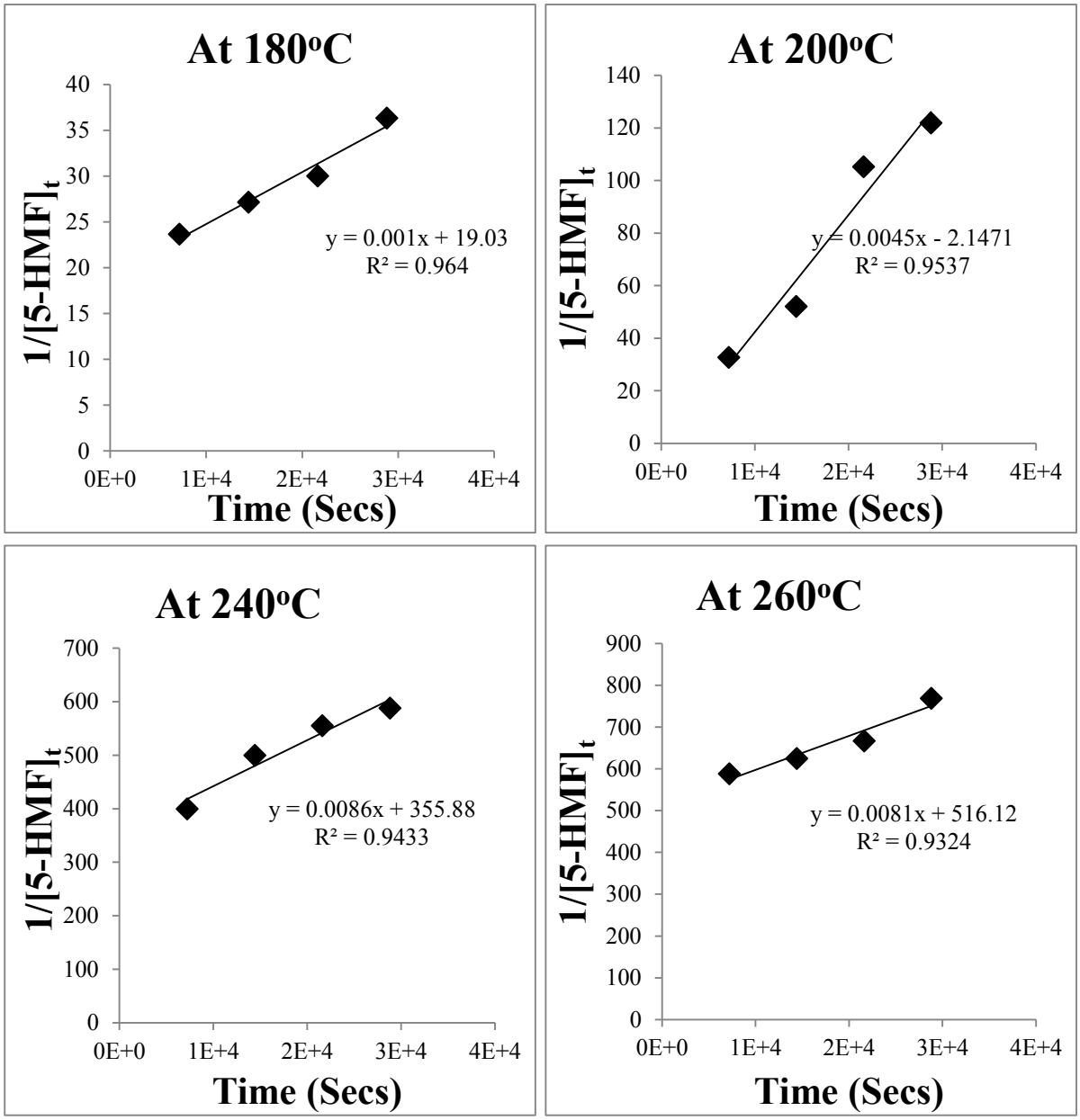

Figure 9.1: Inverse concentration of 5-HMF against time plots for reaction kinetics in molecular hydrogen.

Table 9.2: Reaction rates at different temperatures in molecular hydrogen.

Temperature ^{o}C	k (mol/L.min)
180	1×10^{-3}
200	4.5×10^{-3}
240	8.6×10^{-3}
260	8.1×10^{-3}

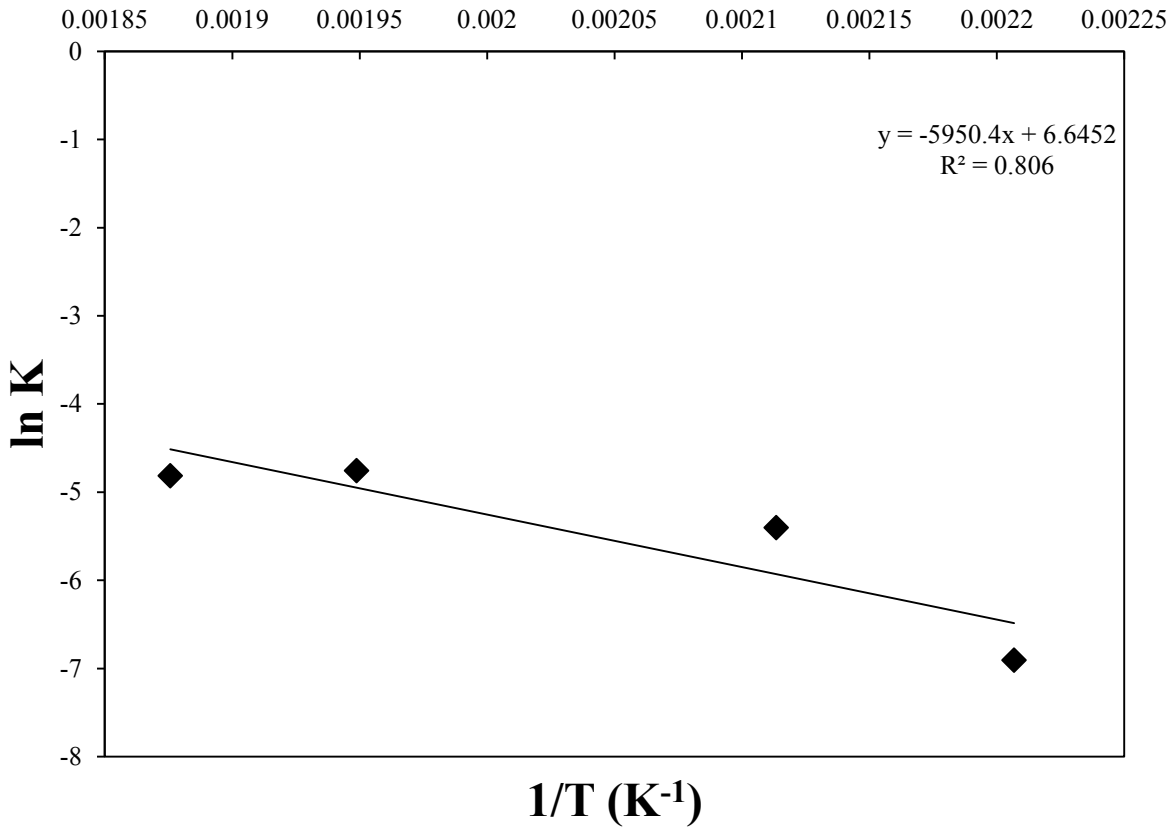

Figure 9.2: Arrhenius plot of data displayed in Table 9.2

The graph shown in Figure 9.2 yielded a negative slope as expected which corresponds to positive activation energy when R is multiplied by value of the slope. However, the poor fit and R^2 value observed in Figure 9.1 and 9.2 could be attributed to the batch system used in this

study. This is because it was difficult to take samples during the experiment without compromising the system. Therefore, all the data points displayed were from different reaction batches and the calculated activation energy (E_a) was 49.5 kJ/mol.

9.4 Reaction Kinetics in 2-Propanol

Similar to Section 9.3, an optimum temperature of 260 ^oC was also obtained (as shown in Section 7.4.3.1) for the CTH of 5-HMF to 2,5-DMF in 2-propanol. Three plots of concentration against time were produced. Of the three plots, a plot of inverse concentration ($1/[HMF]_t$) vs time (Figure 9.3 at 260^oC) gave a positive gradient and was chosen to have the highest coefficient of determination (R^2) in all the plots of concentration against time. Therefore, the reaction fitted the second order with respect to 5-HMF indicating that doubling the concentration of 5-HMF will quadruple the rate of reaction. Similar to Section 9.3, the rate of reaction would not be given by equation (9.2) instead it would be given by a more complex equation such as Eley-Rideal or Langmuir-Hinshelwood mechanism which will require reactants adsorption onto the catalyst surface (Levenspiel, 1999). The other set of experiments were conducted at two other temperatures, 200 and 220 ^oC. The rate constants at these temperatures are displayed in Table 9.3. However, with the calculated rate constants at three temperatures, the activation energy (E_a) of the reaction was calculated using the Arrhenius equation given in equation (9.3) and (9.4). The plot of ln (k) vs. $\frac{1}{T}$ is presented in Figure 9.4 using the data shown in Table 9.3.

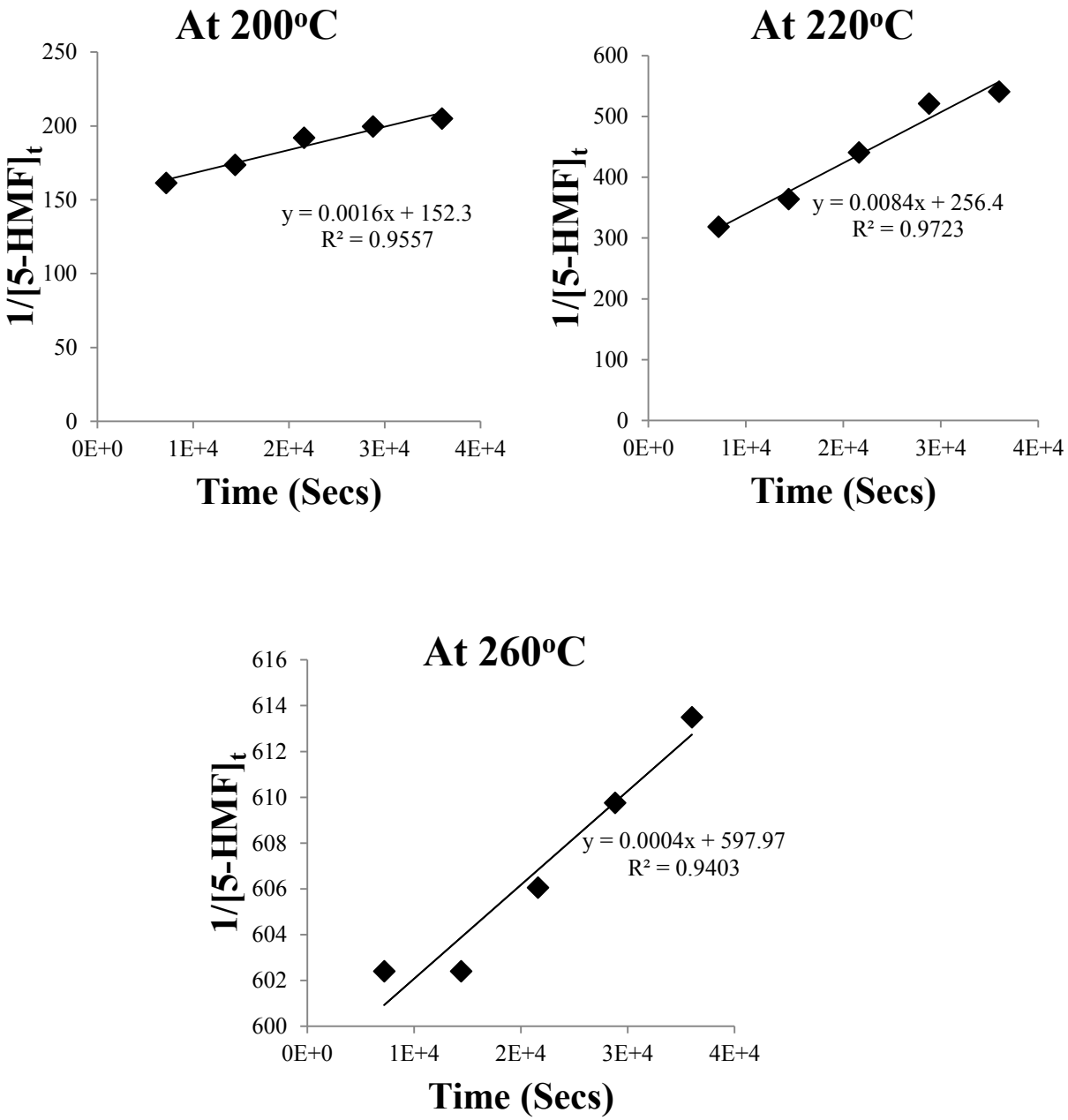

Figure 9.3: Inverse concentration of 5-HMF against time plots for reaction kinetics in 2-propanol.

Table 9.3: Reaction rates at different temperatures in 2-propanol.

Temperature °C	k (mol/L.min)
200	1.6×10^{-3}
220	8.4×10^{-3}
260	4×10^{-4}

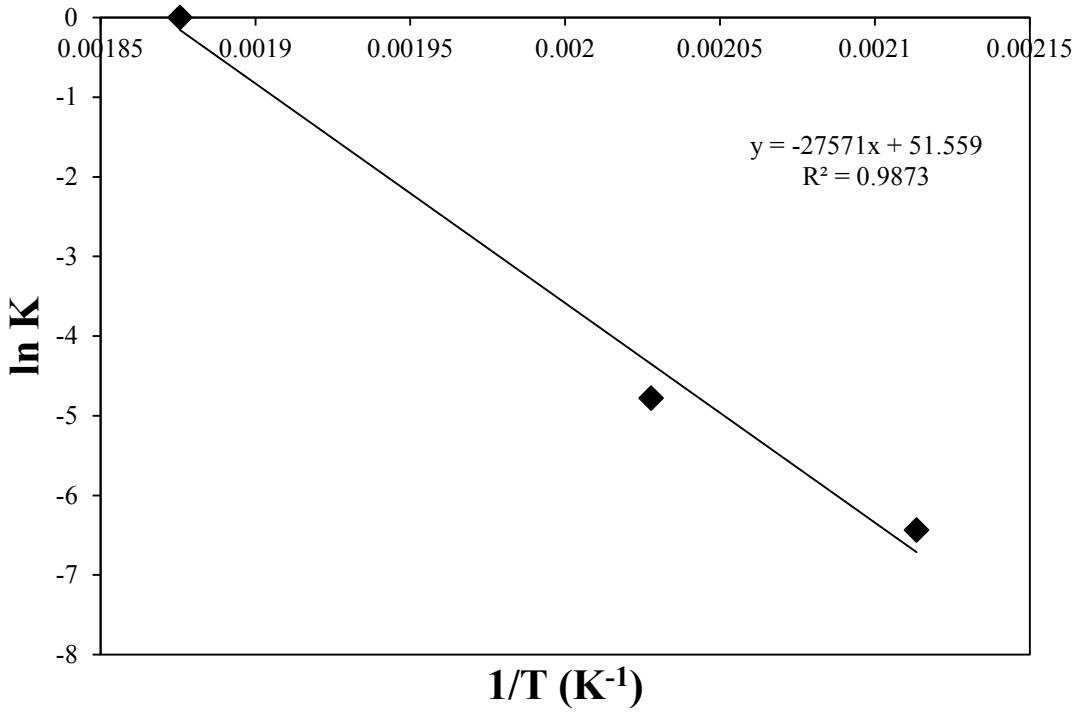

Figure 9.4: Arrhenius plot of data displayed in Table 7.3.

The calculated activation energy (Ea) obtained was 229.2 kJ/mol. Comparing the activation energy obtained in Section 9.3 and Section 9.4, it can be observed that a higher activation energy is needed for 5-HMF hydrogenation in 2-propanol compared to that obtained in molecular hydrogen. This possibly implies that 5-HMF hydrogenation in 2-propanol is a slow reaction and less particles would reach the right conditions at a given time. In addition, the high activation energy obtained using 2-propanol suggests that a strong hydrogen bond is formed between the reactant (5-HMF) and 2-propanol hence, why a large amount of energy is required to initiate the reaction.

9.5 Conclusion

This Chapter presented the preliminary reaction kinetics for 5-HMF hydrogenation to 2,5-DMF in molecular hydrogen and 2-propanol. For 5-HMF hydrogenation to 2,5-DMF in molecular hydrogen, the rate constant was determined to be 8.1×10^{-3} mol/L.min compared to 4×10^{-4} mol/L.min obtained in 2-propanol. In addition, a high activation energy (229.2 kJ/mol) is needed to initiate the hydrogenation of 5-HMF to 2,5-DMF in 2-propanol compared to 49.5 kJ/mol required in molecular H_2. The lower activation energy obtained in molecular H_2 suggests that a greater proportion of the collisions between the 5-HMF and THF results in reaction and proceeds more rapidly. In contrast, 2-propanol as H-donor solvent form a strong H-bonding with 5-HMF hence why higher activation energy is needed to initiate the reaction. As a result of the very strong H-bond, molecules are held together tightly and remain on the surface thus blocking reactive sites and preventing further reaction from taking place. Therefore, this also shows that hydrogenation of 5-HMF in molecular H_2 is a preferred choice of hydrogen source because it require lesser amount of energy for the reaction to occur.

Chapter 10. **Conclusions and Future Work Recommendations**

10.1 Conclusions

In a time of steady decline in petroleum reserves and instability in oil prices, researchers and petroleum industries are actively exploring means of developing cost-effective processes to convert renewable biomass resources into biofuels and other value-added chemicals. 5-HMF, known as one of the most versatile platform chemicals can undergo different reactions to give rise to valuable products. The conversion of 5-HMF through hydrogenation can provide a wide range of value-added chemicals and potential biofuels. In this thesis, the catalytic hydrogenation of 5-HMF into 2,5-DMF via three different hydrogen sources (molecular H_2, mixture of HCOOH/Et_3N and 2-propanol) were explored and compared.

Chapter four described the results obtained for the catalyst characterisation techniques employed in this study. The TEM results showed that the monometallic bio-Pd produced by *D. desulfuricans* were mostly found on the periplasmic surface of the bacterial support while the monometallic bio-Ru produced by *B. benzeovorans* were mostly extracellular with no intracellular deposition of ruthenium particles. However, the bimetallic bio-Pd/Ru synthesised by *B. benzeovorans* were deposited in both extracellular and intracellular compartment with occasional larger agglomerates found within the intracellular region. Since the bimetallic bio-Pd/Ru synthesised by *B. benzeovorans* were mostly found in both extracellular and intracellular region, it could possibly explain why the bimetallic bio-Pd/Ru showed the best catalytic activity amongst other bio-supported metal catalysts investigated in Chapters 5, 6 and 7. The SEM result showed that the experiments conducted with all the catalyst investigated in molecular

hydrogen showed less degradation compared to that in HCOOH/Et_3N and 2-propanol solvent system. These observations can be ascribed to the harsh conditions of the HCOOH/Et_3N solvent system.

In Chapter five, the catalytic hydrogenation of 5-HMF into 2,5-DMF was studied over 5 wt% Ru/C catalyst and novel biocatalysts in molecular H_2 using a batch reactor. It was possible to achieve a very high 5-HMF conversion and 2,5-DMF yield after optimisation of reaction parameters. The 5 wt% Ru/C catalyst showed superior catalytic activity compared to other catalysts investigated in this chapter as shown in Table 10.1. 95% yield of 2,5-DMF was obtained under optimum conditions of 260 ^oC, 2 hours reaction time, 50 bar H_2 pressure, and 700 rpm agitation speed. In addition, a very high (60.3%) yield of 2,5-DMF was attainable with 20 wt% bio-Pd/Ru catalyst at similar reaction conditions to the 5 wt% Ru/C catalyst.

Table 10.1: Result summary of all the catalysts and solvent system used in this study.

Catalysts/H_2 donor system	Molecular H_2 (%)			$HCOOH/Et_3N$ (%)			2-Propanol (%)		
	C	Y	S	C	Y	S	C	Y	S
5 wt% Ru/C	96.4	95.1	98.7	93.4	92.1	98.6	94.3	70.2	74.4
5 wt% Pd/C	96.5	19.9	20.7	97.5	26.5	27.2	94.5	32.6	34.5
10 wt% Pd/C	96.5	18.0	19.4	97.3	24.4	25.0	94.3	32.8	34.8
5 wt% BioPd	88.9	49.5	55.6	-	-	-	94.1	35.8	38.1
5 wt% Bio-Ru/Pd	94.7	55.5	58.5	96.8	49.8	51.5	94.5	42.6	45.1
20 wt% BioRu/Pd	95.3	60.3	63.3	96.9	56.7	58.5	94.3	38.6	40.9
20 wt% Bio-Ru	95.1	47.9	50.4	96.8	52.7	54.5	94.5	37.2	39.3

KEY

C = 5-HMF Conversion (%)

Y = 2,5-DMF Yield (%)

S = Selectivity (%)

In Chapter six, the catalytic transfer hydrogenation (CTH) of 5-HMF into 2,5-DMF was conducted over 5 wt% Ru/C catalyst and novel bio-supported metal catalysts in $HCOOH/Et_3N$ solvent system as shown in Table 10.1. Similar to Chapter 5, the 5 wt% Ru/C catalyst displayed the best catalytic activity amongst other catalyst investigated. 92.1% yield of 2,5-DMF was achieved within the reaction time of 4 hours, 210 ^oC, 5:2 molar ratio of $HCOOH/Et_3N$ and 300 rpm agitation speed. It was also observed that 5-HMF conversion increased as temperature increases. Furthermore, 56.7% yield of 2,5-DMF was obtained with the 20 wt% Bio-Pd/Ru catalyst at the same optimum condition to the 5 wt% Ru/C catalyst. However, due to the

presence of formic acid in the solvent system, it was difficult to recover the spent catalysts after reaction.

In Chapter seven, the CTH of 5-HMF into 2,5-DMF was investigated over 5 wt% Ru/C catalyst and novel bio-supported metal catalysts in 2-propanol. A similar result to chapters five and six was observed. As presented in Table 10.1, 5 wt% Ru/C catalyst showed superior catalytic activity amongst other catalysts studied. Optimum reaction conditions were reached at 260 ^{o}C, 2 hours reaction time, 20 bar N_2 pressure and 300 rpm agitation speed with 70.2% yield of 2,5-DMF and 94.3% 5-HMF conversion obtained. Accordingly, 42.6% yield of 2,5-DMF was obtained with the 5 wt% Bio-Pd/Ru catalyst at similar reaction conditions to the 5 wt% Ru/C catalyst. Chapter eight discussed and compared the different hydrogen donor systems employed. Based on the multi-parameter comparison, product separation from solvents and reproducibility, hydrogenation of 5-HMF in molecular H_2 is still a preferred choice of hydrogen source when compared to both HCOOH/Et_3N and 2-propanol. In chapter nine, the preliminary reaction kinetics was investigated and both molecular H_2 and 2-propanol donor system were assumed to fit a second order reaction. In addition, it was observed that 5-HMF hydrogenation in 2-propnaol is a slower reaction compared to molecular H_2 due to higher activation energy required to initiate the reaction.

In this thesis, the first study on the asymmetric catalytic transfer hydrogenation of 5-HMF into 2,5-DMF in HCOOH/Et_3N over metal supported catalysts was demonstrated. In addition, the first study on the use of bio-supported metal catalysts for hydrogenation of 5-HMF

into 2,5-DMF was investigated and results obtained showed that biocatalysts are also highly selective towards an interesting product with potential to serve as fuel additive or biofuel.

In conclusion, the hydrogenation of 5-HMF to 2,5-DMF in molecular hydrogen gave the highest yield of 2,5-DMF compared to the hydrogen donor compounds investigated. The hydrogen donor compounds studied in this thesis also gave a very high yield of 2,5-DMF. 92.1% yield of 2,5-DMF was obtained in HCOOH/Et_3N azeotropic mixture while 70.2% yield was obtained in 2-propanol. The higher yield of 2,5-DMF obtained in molecular hydrogen could be attributed to lesser amount of reaction intermediates formed during the reaction. However, a higher amount of reaction intermediates were clearly observed in both HCOOH/Et_3N azeotropic mixture and 2-propanol hence why 2,5-DMF yield was lower. This could be due to different other reactions occurring thus competing for catalytic sites on the catalyst surface. In general, the use of HCOOH/Et_3N and 2-propanol as hydrogen donor compounds offers the ability to obtain high yield of 2,5-DMF via transfer hydrogenation instead of using molecular H_2.

10.2 Future Work Recommendations

This study has clearly demonstrated hydrogenation of 5-HMF into 2,5-DMF in both molecular H_2 and hydrogen donor solvents using a batch reactor. However, due to time constraint, equipment and financial challenges, several analysis and experiments could not be conducted in the scope of this research work and hence are recommended as future work. They are:

- After identification of reaction intermediates via GC-MS, quantitative analysis is required to know the amount present in the products and this will also help to have a comprehensive understanding of the reaction mechanisms.

- Since solid catalyst was employed, the ability to investigate its recycling potential is crucial as it will reduce cost and also make full scale technology feasible.

- Separation of 2,5-DMF from the solvent system employed.

- Optimisation of reaction conditions for the Pd/C catalyst and biocatalysts is essential so as to know the maximum yield of 2,5-DMF that is attainable.

- Further work on the biocatalysts will help to improve the catalyst lifetime (mechanical attrition and heating stability), reusability and scaling up production process. If these conditions are met, a cost effective and feasible full scale technology can proceed to an advanced stage.

- Investigation of 5-HMF hydrogenation to 2,5-DMF in a continuous flow reactor in order to improve reactor performance.

- Since catalyst in liquid phase was studied, investigation to show that reaction rates have not been influenced by rates of internal mass transfer is required. A Koros-Nowak or Madon-Boudart test would suffice. The Koros-Nowak test has been developed to detect

mass transfer influence. It is used to yield correct activities and selectivities by comparing rate measurements on catalysts on which the concentration of catalytically active material has been changed. The rate of reaction in the kinetic regime is directly proportional to the concentration of the active component. This technique is made up of mixing catalyst particles with the particles of an inert powder and then making pellets from the mixture. Consequently, Madon and Boudart modified Koros-Nowak test and applied their method in 3 phase reactions and vapour phase reactions. Their method involves changing the concentration of active metal by changing its loading but keeping constant the same or nearly same dispersion (Notheisz et al., 1994). Therefore, absence of mass transfer influences is established by the constancy of turnover frequencies. In other words, the rate of reaction in the kinetic regime is directly proportional to the concentration of exposed metal atoms on the support particle.

- Investigation into the one-pot process to convert fructose or glucose directly to 2,5-DMF via transfer hydrogenating solvents. This would reduce the cost of production as the starting material used in this research work (5-HMF) is expensive than fructose and glucose.

- Application of the catalytic methods employed in this research work to transform furfural to 2-methylfuran.

- Establish a kinetic model such as Langmuir-Hinshelwood or Eley-Rideal mechanism for the hydrogenation of 5-HMF to 2,5-DMF that would involve adsorption of reactants on the catalyst surface.

Appendix A. Calibration Curves

A.1 Calibration Curves

Calibration is an important step in analytical methods which helps to evaluate the results obtained. The calibration curves for 5-HMF are presented in Figure A.0.1 and A.0.2. Two calibration curves were prepared for 5-HMF and 2,5-DMF. This is because after the first calibration curve was prepared and used for the experiments in chapter 5, the GC-FID equipment was faulty and a new calibration curve was needed to be done after it was repaired. Therefore, the 5-HMF calibration curves are presented from Table A.0.1 and A.0.2 below.

Table A.0.1: First calibration table used for 5-HMF calibration curve

Concentration (mg/ml)	Area 1	Area 2	Area 3	Average	S-Deviation	SD %
1	57801	54264	59585	57216.6667	2708.199463	4.733235299
2	119563	108978	109858	112799.667	5873.721847	5.207215607
3	172205	170846	173986	172345.667	1574.719128	0.913698127
4	240377	240314	236364	239018.333	2298.935913	0.961824092
5	300534	300215	308499	303082.667	4693.393264	1.548552187
6	381150	379437	374497	378361.333	3454.474827	0.913009476
7	449013	446830	452960	449601	3107.013518	0.691060188
8	519608	515673	511069	515450	4273.86558	0.82915231
9	538867	566006	576797	560556.667	19543.3531	3.486418816
10	631261	629243	634352	631618.667	2573.2109	0.407399438
20	1205359	1207202	1213795	1208785.33	4435.282667	0.366920622
30	1927218	1958315	1930778	1938770.33	17019.51516	0.877851021
40	2490873	2496134	2522033	2503013.33	16680.23742	0.666406255
50	3079130	3121275	3073465	3091290	26121.79598	0.845012793
60	3667684	3658000	3731366	3685683.33	39857.55248	1.081415544
70	4258005	4303325	4347367	4302899	44682.52307	1.03842835
80	4889219	4948775	4949619	4929204.33	34630.88571	0.702565432
90	5513216	5493127	5492525	5499622.67	11776.01946	0.214124135
100	6898336	7023719	7002968	6975007.67	67205.35211	0.963516534

Note: Calibration Table A.0.1 was used for used in Chapter 5 while calibration Table A.0.2 was used in chapters 4 and 6.

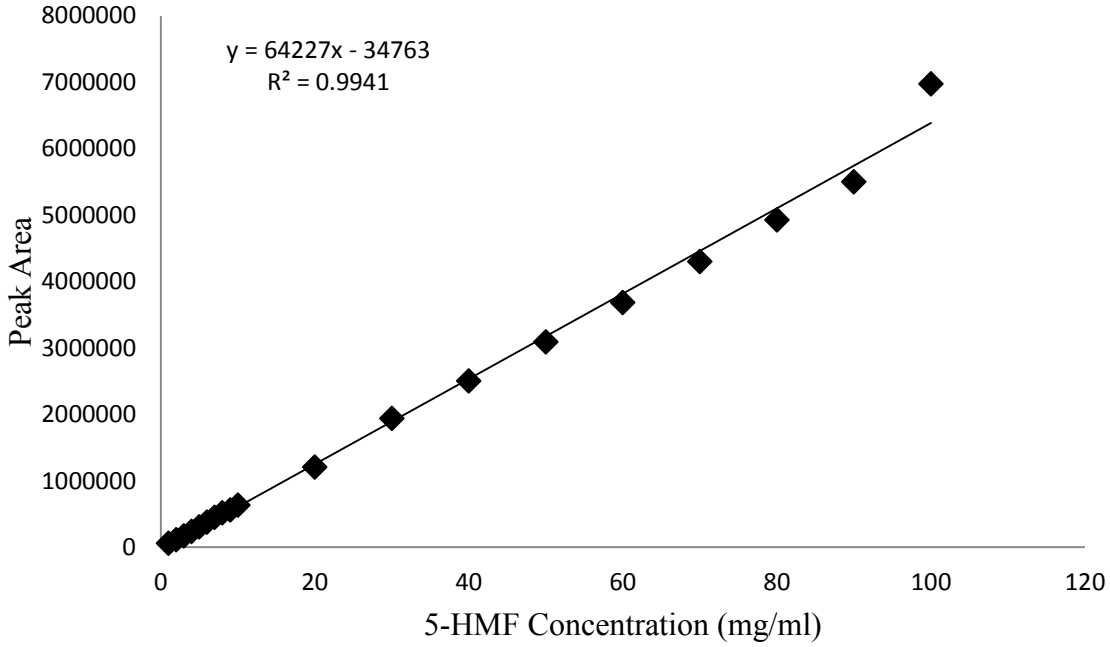

Figure A.0.1: First calibration curve for 5-HMF.

Table A.0.2: Second calibration table used for 5-HMF calibration curve

Concentration (mg/ml)	Area 1	Area 2	Average	S-Deviation	SD %
1	93986	94469	94227.5	341.5325753	0.362455308
2	410589	411413	411001	582.6559877	0.141765102
3	712141	715646	713893.5	2478.409268	0.347167927
4	1033493	1035410	1034451.5	1355.5237	0.131037917
5	1278037	1256404	1267220.5	15296.841	1.207117546
6	1638788	1620868	1629828	12671.35352	0.777465691
7	1972663	1936711	1954687	25421.903	1.300561317
8	2055428	2055373	2055400.5	38.89087297	0.001892131
9	2166207	2176564	2171385.5	7323.504933	0.337273365
10	2499058	2586627	2542842.5	61920.63372	2.435095124
20	5218394	5095518	5156956	86886.45285	1.68483991
30	7505374	7461500	7483437	31023.60292	0.414563561
40	11287553	11484406	11385979.5	139196.0912	1.222521885
50	14002754	14273339	14138046.5	191332.4884	1.353316304
60	15526069	15523429	15524749	1866.761902	0.012024426
70	18690734	18676987	18683860.5	9720.596921	0.052026705
80	21352668	21087188	21219928	187722.7083	0.884652899
90	24443583	24391337	24417460	36943.50089	0.151299525
100	26450867	26644632	26547749.5	137012.5455	0.516098532

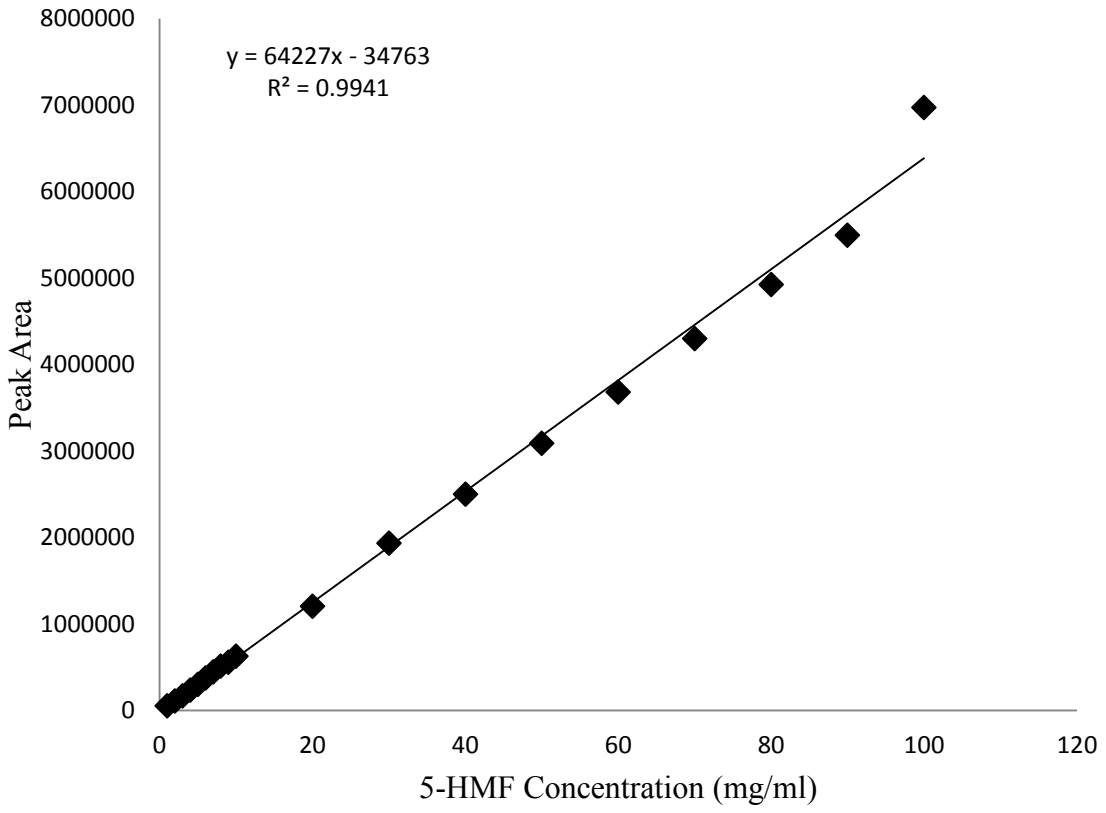

Figure A.0.2: Second calibration curve for 5-HMF.

Similarly, two calibration curves were presented for 2,5-DMF. Calibration Table A.0.3 was used in Chapter 5 while calibration Table A.0.4 was used in Chapters 4 and 6.

Table A.0.3: First calibration table used for 2,5-DMF calibration curve

Concentration (mg/ml)	Area 1	Area 2	Area 3	Avearge	S-Deviation	SD %
1	63592	65027	65165	64594.66667	871.071945	1.348519916
2	142565	142938	141318	142273.6667	848.3845433	0.596304687
3	218423	210832	212369	213874.6667	4013.23988	1.876444715
4	249264	248011	249520	248931.6667	807.5297724	0.32439817
5	374110	371124	377000	374078	2938.130698	0.785432637
6	403324	408528	409300	407050.6667	3250.389105	0.798521995
7	510909	522092	528051	520350.6667	8702.656051	1.672459864
8	595445	604563	593690	597899.3333	5837.237903	0.976291087
9	658691	678033	676971	671231.6667	10873.50915	1.619933876
10	723661	744223	738180	735354.6667	10568.15227	1.437150364
20	1298884	1336521	1260320	1298575	38101.43975	2.934096202
30	1990182	2061557	2063549	2038429.333	41795.28558	2.050367157
40	2927276	2964499	2872843	2921539.333	46096.50304	1.577815589
50	3596245	3613520	3610686	3606817	9264.625033	0.256864294
60	4363819	4314924	4372394	4350379	31002.82931	0.712646629
70	5353406	5412792	5411355	5392517.667	33879.31662	0.628265287
80	5980251	6023432	6015758	6006480.333	23037.05741	0.383536716
90	6729985	6713473	6772435	6738631	30417.00755	0.451382596
100	7149416	7215544	7345253	7236737.667	99623.84891	1.376640325

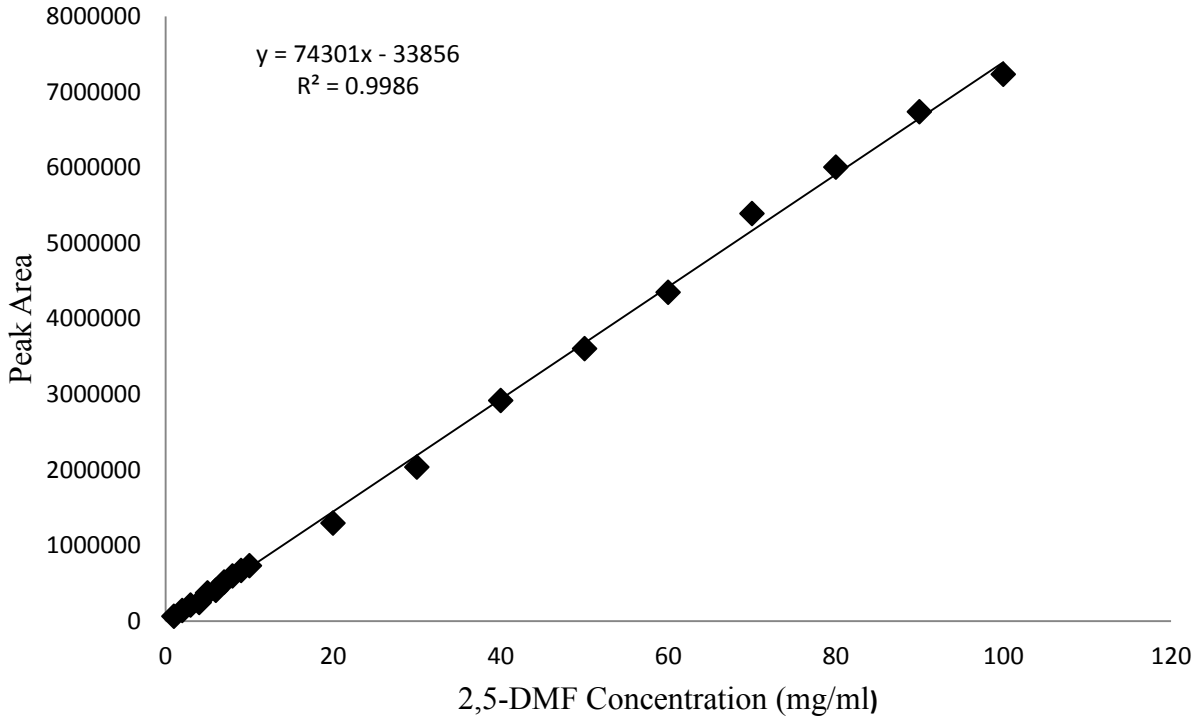

Figure A.0.3: First calibration curve for 2,5-DMF

Table A.0.4: Second calibration table used for 2,5-DMF curve

Concentration (mg/ml)	Area 1	Area 2	Average	S-Deviation	SD %
1	255689	256526	256107.5	591.8483759	0.231093731
2	544487	552141	548314	5412.195303	0.987061301
3	875982	873058	874520	2067.580228	0.236424579
4	1137273	1136749	1137011	370.5239533	0.032587543
5	1392703	1409281	1400992	11722.41622	0.836722566
6	1610598	1604492	1607545	4317.594006	0.268583088
7	1911724	1971908	1941816	42556.51452	2.191583266
8	2207386	2252509	2229947.5	31906.77929	1.430830963
9	2375667	2365004	2370335.5	7539.879608	0.31809335
10	2504490	2466625	2485557.5	26774.59827	1.077206955
20	3810315	3842416	3826365.5	22698.83478	0.593221813
30	7803568	7811028	7807298	5275.016588	0.067565201
40	11920761	11716325	11818543	144558.0819	1.223146389
50	15351007	15241024	15296015.5	77769.72512	0.508431265
60	18545420	18435940	18490680	77414.0504	0.418665243
70	21517324	21338246	21427785	126627.2682	0.590948939
80	24851958	24659515	24755736.5	136077.7503	0.549681688
90	27983715	27679547	27831631	215079.2554	0.772787105
100	29307574	29462194	29384884	109332.8505	0.372071744

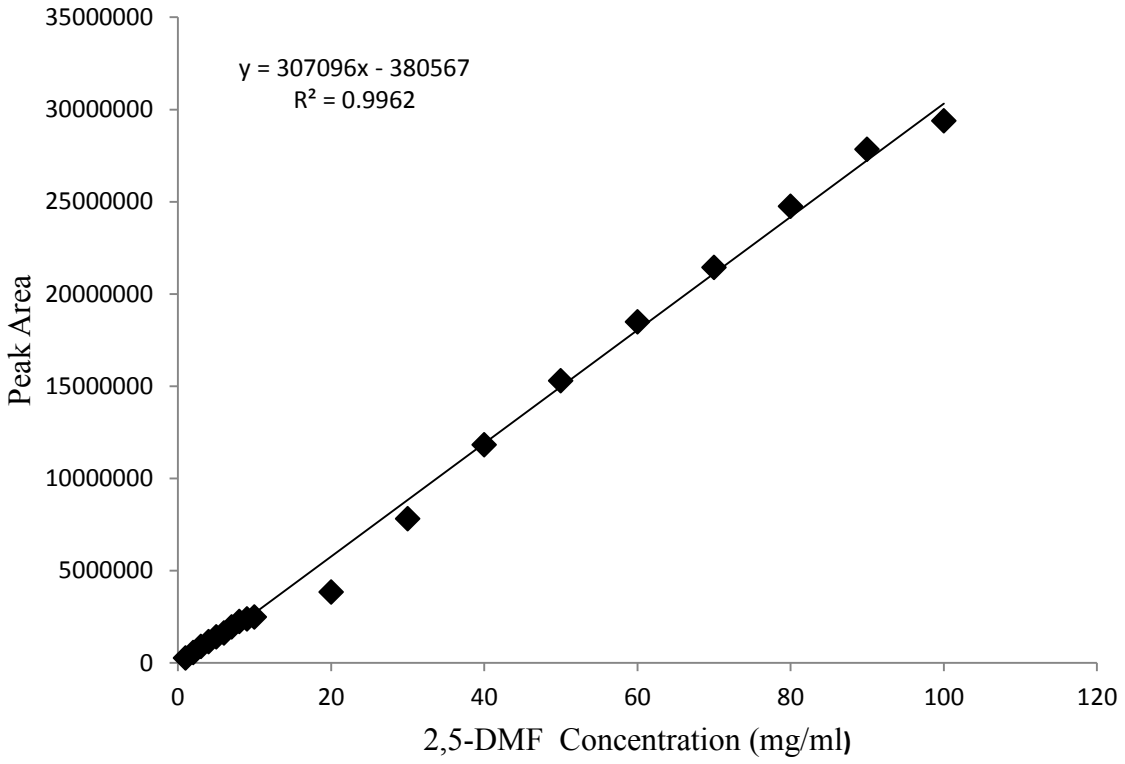

Figure A.0.4: Second calibration curve for 2,5-DMF

Appendix B. EDX spectra of Fresh and Spent Catalysts

B. EDX spectra of fresh and spent catalysts

B.1 EDX spectra of 5 wt% Ru/C

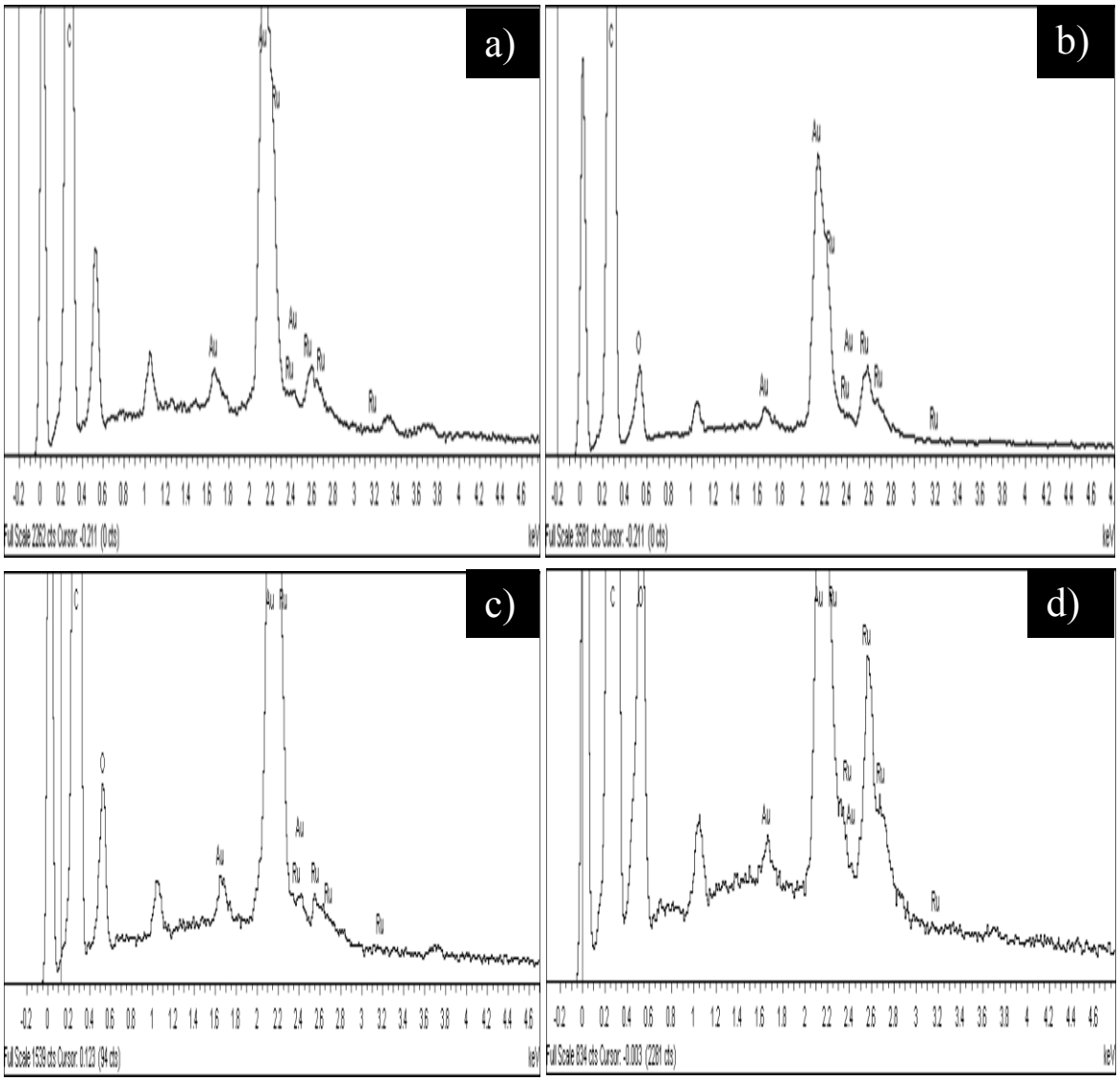

Figure B.0.1: EDX spectra of 5 wt% Ru/C catalyst.
a) EDX spectra of fresh 5wt% Ru/C catalyst; b) EDX spectra of spent Ru/C catalyst in molecular H_2; c) EDX spectra of spent Ru/C catalyst in HCOOH/Et_3N; d) EDX spectra of spent Ru/C catalyst in 2 propanol.

B.2 EDX spectra of 5 wt% Pd/C

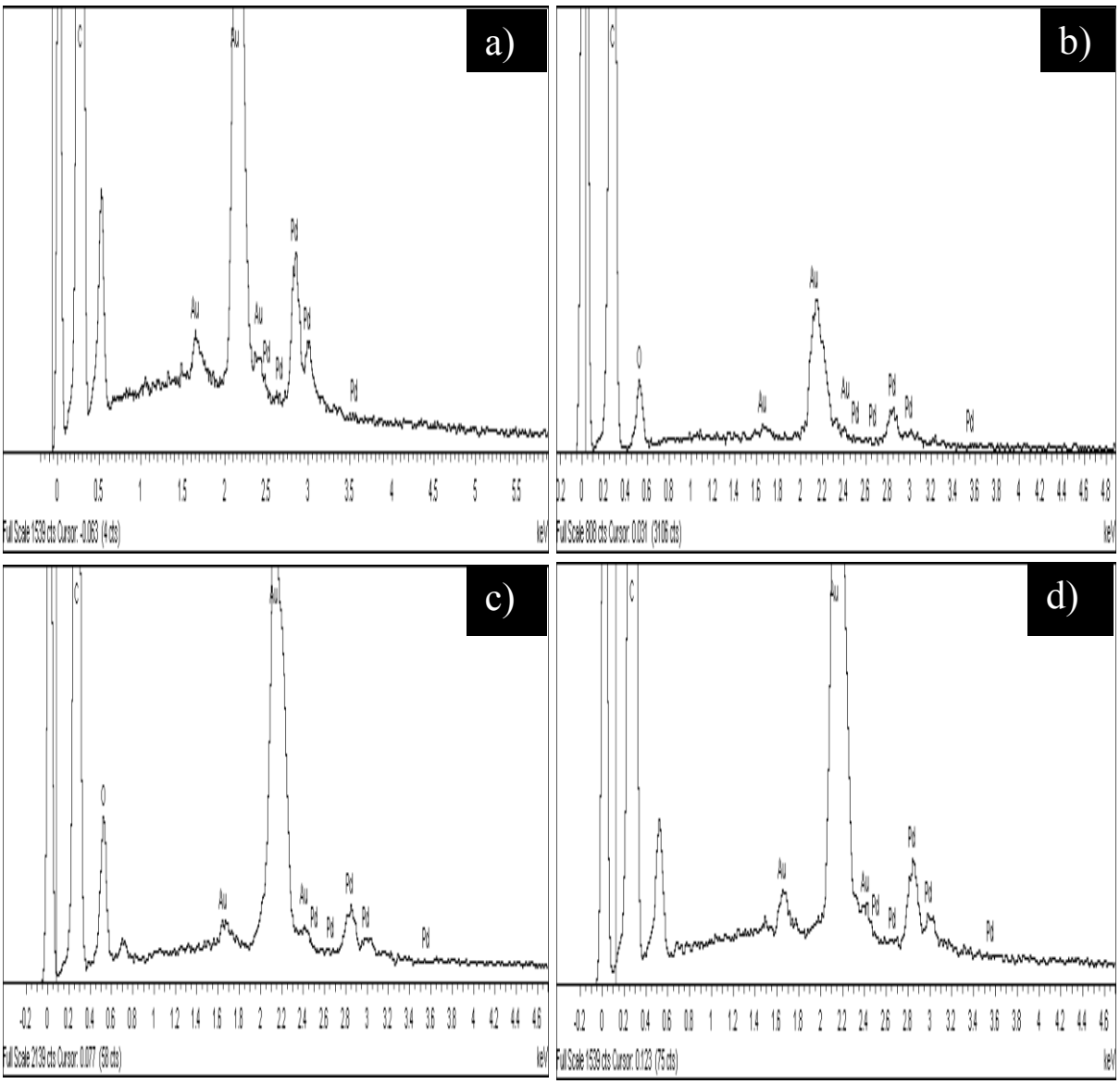

Figure B.0.2: EDX spectra of 5 wt% Pd/C catalyst.

a) EDX spectra of fresh 5wt% Pd/C catalyst; b) EDX spectra of spent 5 wt% Pd/C catalyst in molecular H_2; c) EDX spectra of spent 5 wt% Pd/C catalyst in HCOOH/Et_3N; d) EDX spectra of spent 5 wt% Pd/C catalyst in 2 propanol.

B.3 EDX spectra of 10 wt% Pd/C

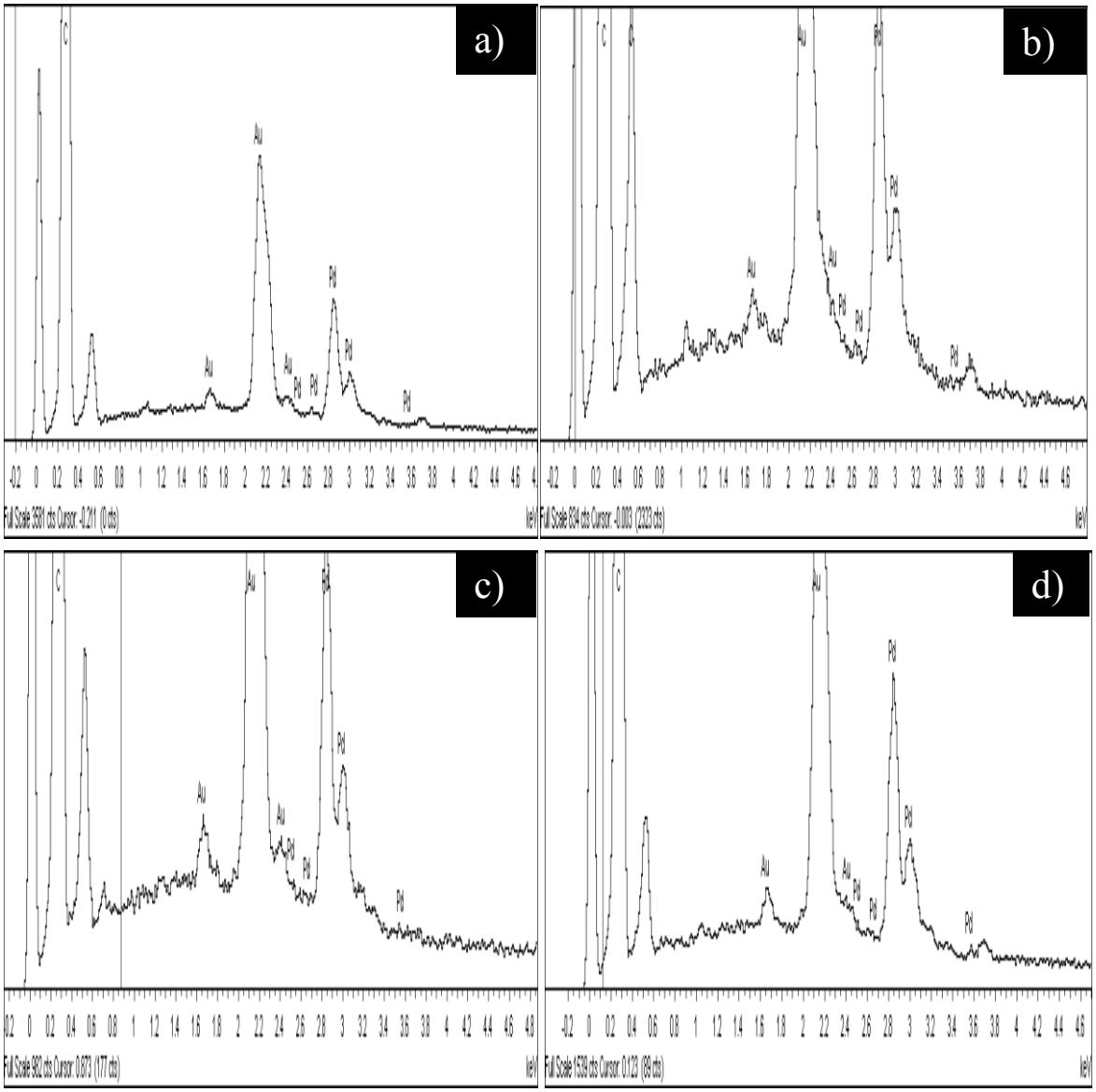

Figure B.0.3: EDX spectra of 10 wt% Pd/C catalyst.

a) EDX spectra of fresh 10 wt% Pd/C catalyst; b) EDX spectra of spent 10 wt% Pd/C catalyst in molecular H_2; c) EDX spectra of spent 10 wt% Pd/C catalyst in HCOOH/Et_3N; d) EDX spectra of spent 10 wt% Pd/C catalyst in 2 propanol.

B.4 EDX spectra of 5 wt% bio-Pd

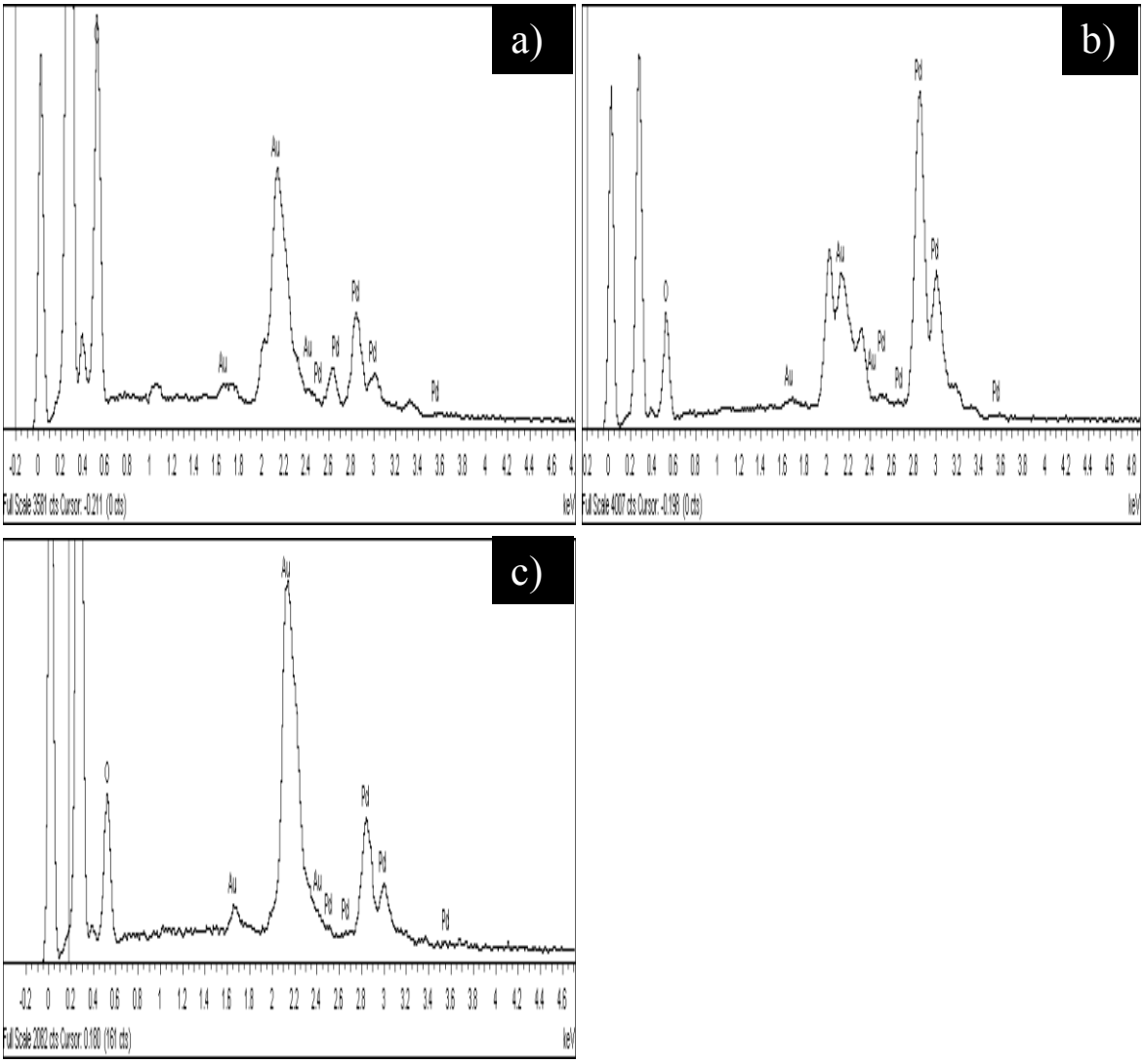

Figure B.0.4: EDX spectra of 5 wt% bio-Pd.

a) EDX spectra of fresh 5 wt% bio-Pd catalyst; b) EDX spectra of spent 5 wt% bio-Pd catalyst in molecular H_2; c) EDX spectra of spent 5 wt% bio-Pd catalyst in 2 propanol.

B.5 EDX spectra of 5 wt% bio-Ru/Pd

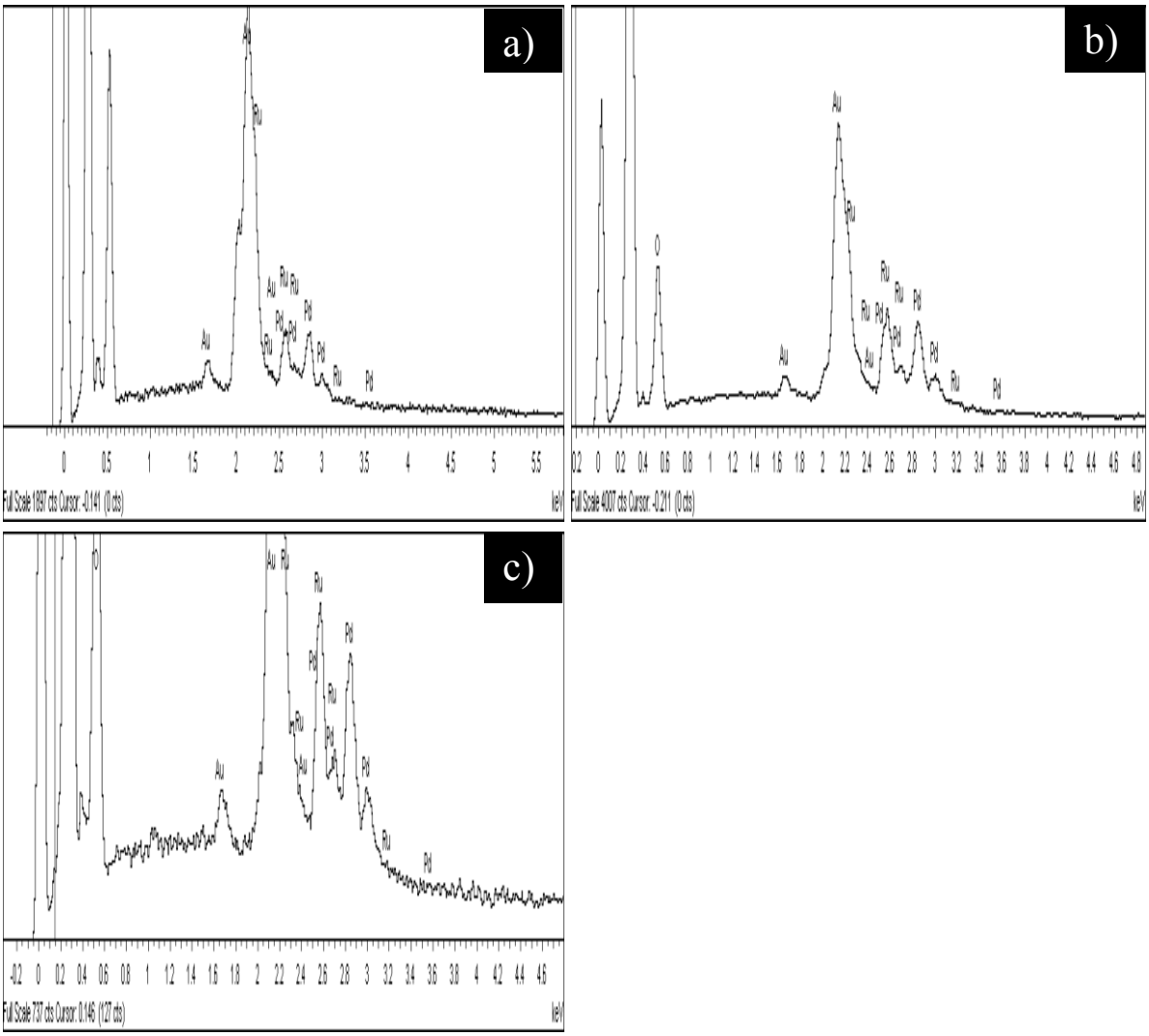

Figure B.0.5: EDX spectra of 5wt% bio-Ru/Pd.

a) EDX spectra of fresh 5 wt% bio-Ru/Pd catalyst; b) EDX spectra of spent 5 wt% bio-Ru/Pd catalyst in molecular H_2; c) EDX spectra of spent 5 wt% bio-Ru/Pd catalyst in 2 propanol.

B.6 EDX spectra of 20 wt% bio-Ru/Pd

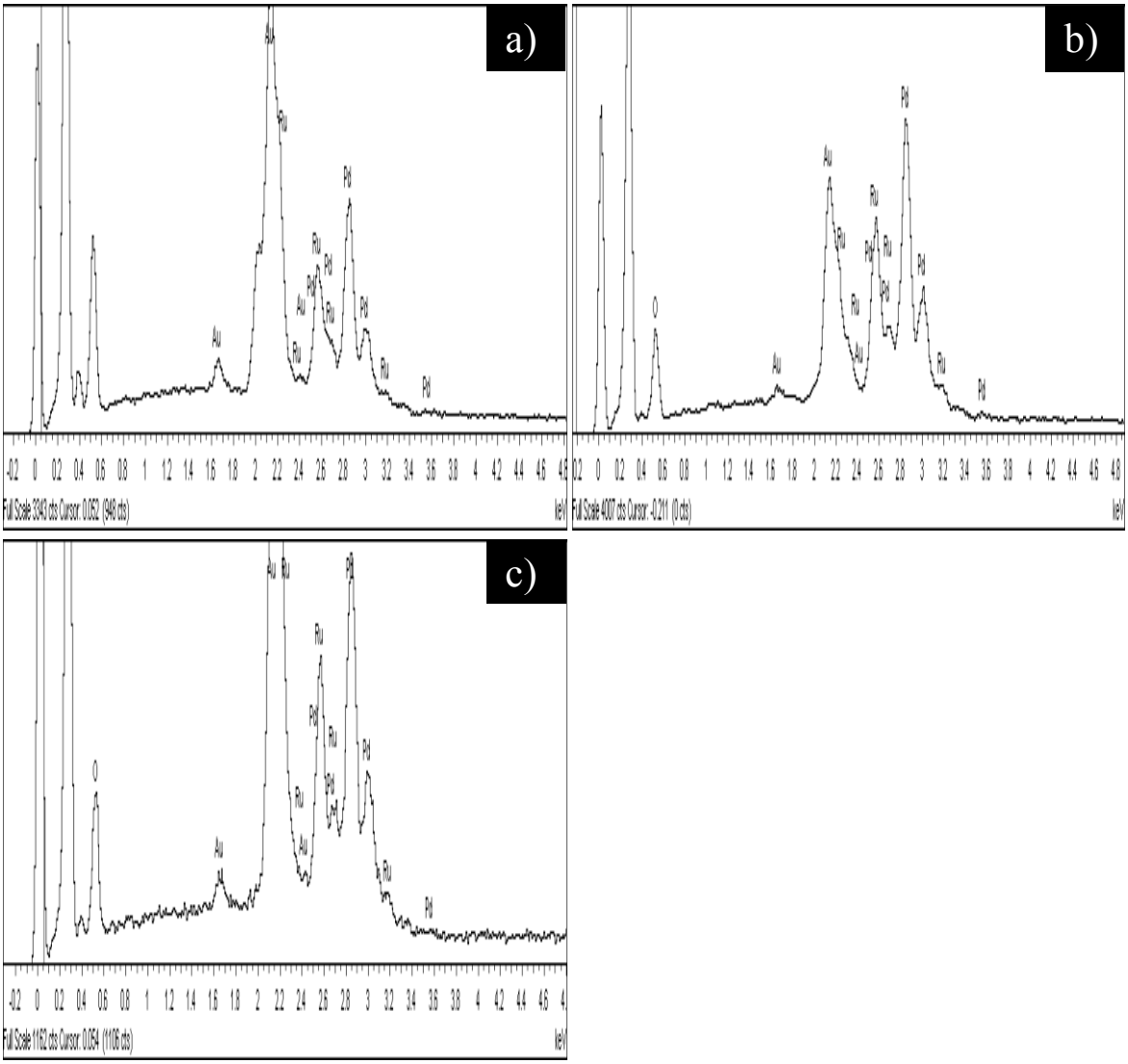

Figure B.0.6: EDX spectra of 20 wt% bio-Ru/Pd.

a) EDX spectra of fresh 20 wt% bio-Ru/Pd catalyst; b) EDX spectra of spent 20 wt% bio-Ru/Pd catalyst in molecular H_2; c) EDX spectra of spent 20 wt% bio-Ru/Pd catalyst in 2 propanol.

B.7 EDX spectra of 20 wt% bio-Ru

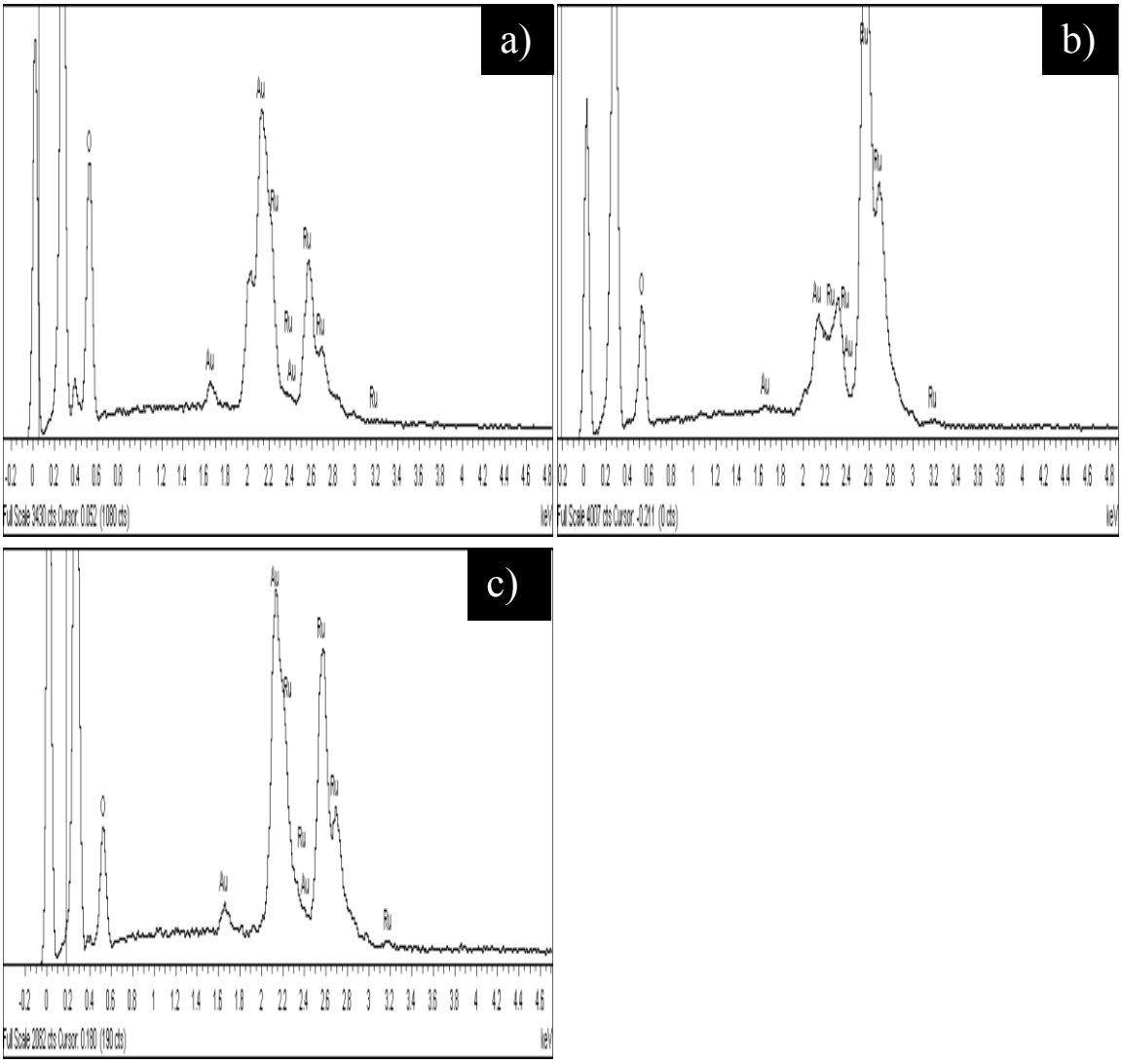

Figure B.0.7: EDX spectra of 20 wt% bio-Ru.

a) EDX spectra of fresh 20 wt% bio-Ru catalyst; b) EDX spectra of spent 20 wt% bio-Ru catalyst in molecular H_2; c) EDX spectra of spent 20 wt% bio-Ru catalyst in 2 propanol.

Appendix C. Plots of [5-HMF] against time

C.1 Plots of [5-HMF] against time in molecular hydrogen.

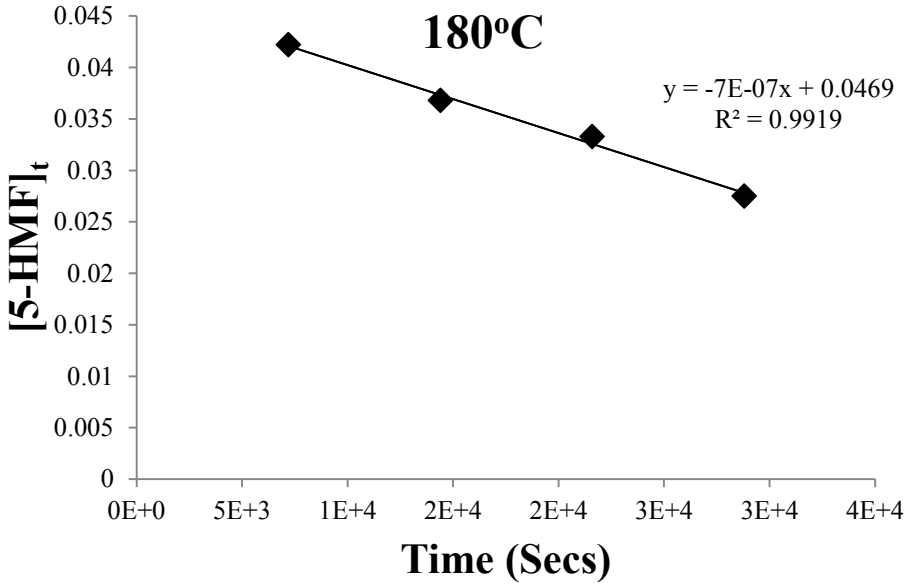

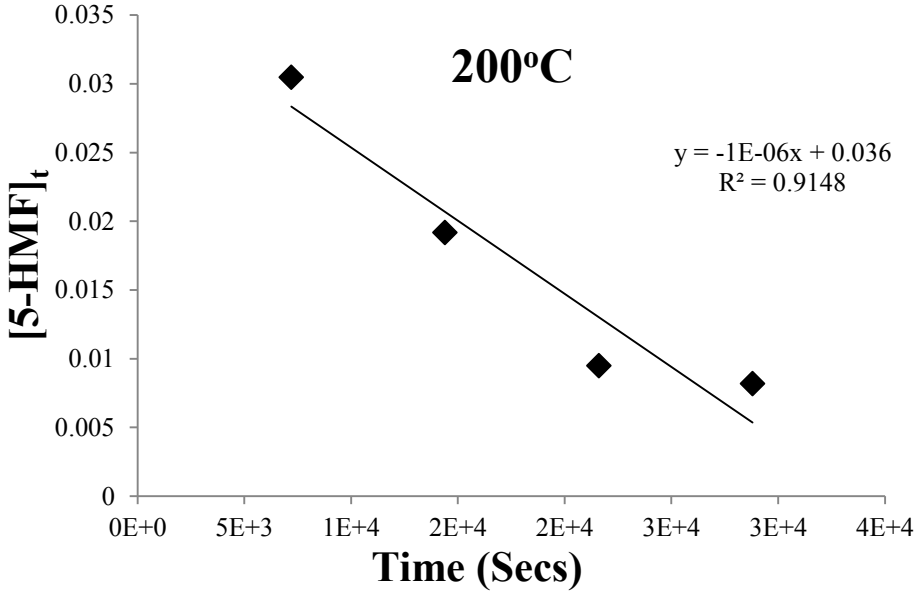

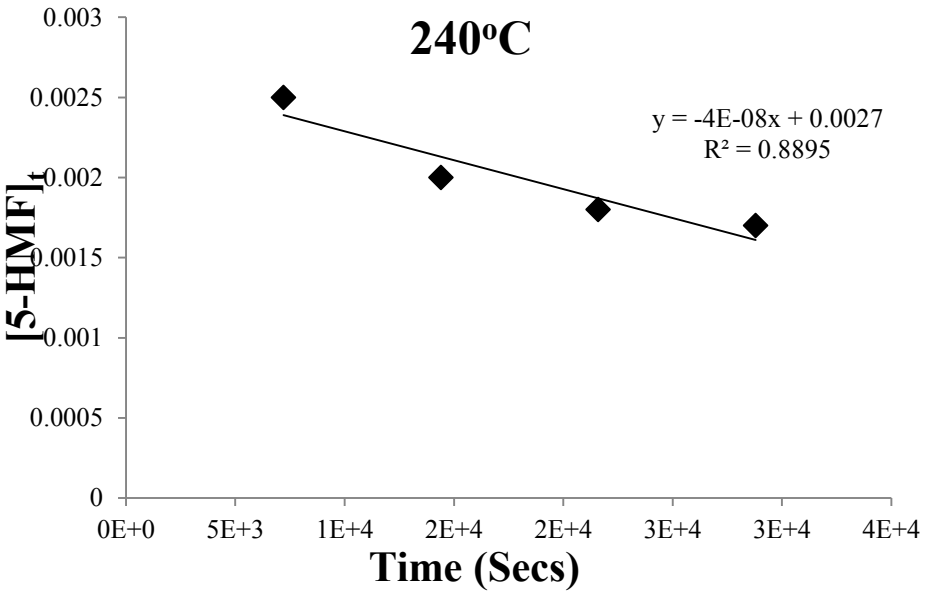
240°C
y = -4E-08x + 0.0027
R² = 0.8895
[5-HMF]t
Time (Secs)
0.003
0.0025
0.002
0.0015
0.001
0.0005
0
0E+0
5E+3
1E+4
2E+4
2E+4
3E+4
3E+4
4E+4

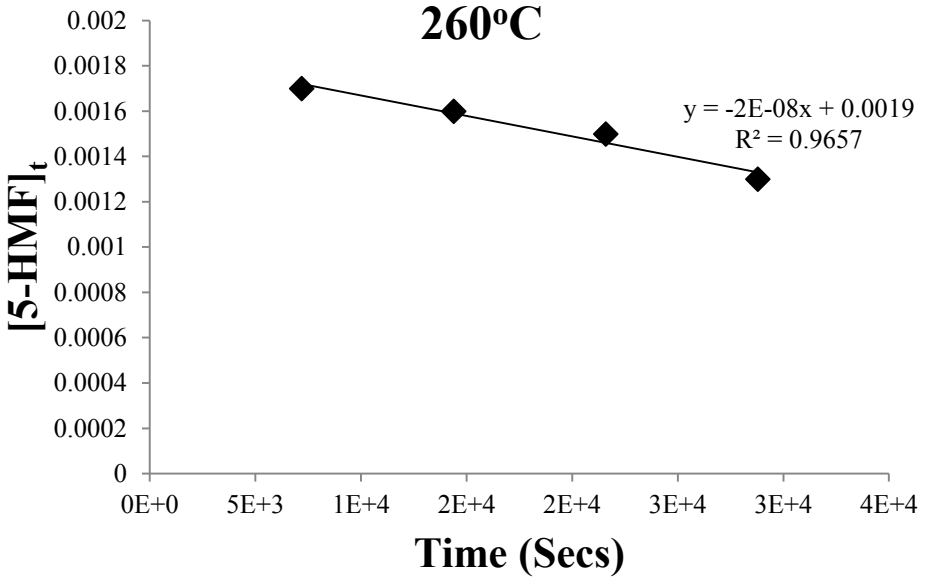
260°C
y = -2E-08x + 0.0019
R² = 0.9657
[5-HMF]t
Time (Secs)
0.002
0.0018
0.0016
0.0014
0.0012
0.001
0.0008
0.0006
0.0004
0.0002
0
0E+0
5E+3
1E+4
2E+4
2E+4
3E+4
3E+4
4E+4

C.2 Plots of ln [5-HMF] against time in molecular hydrogen

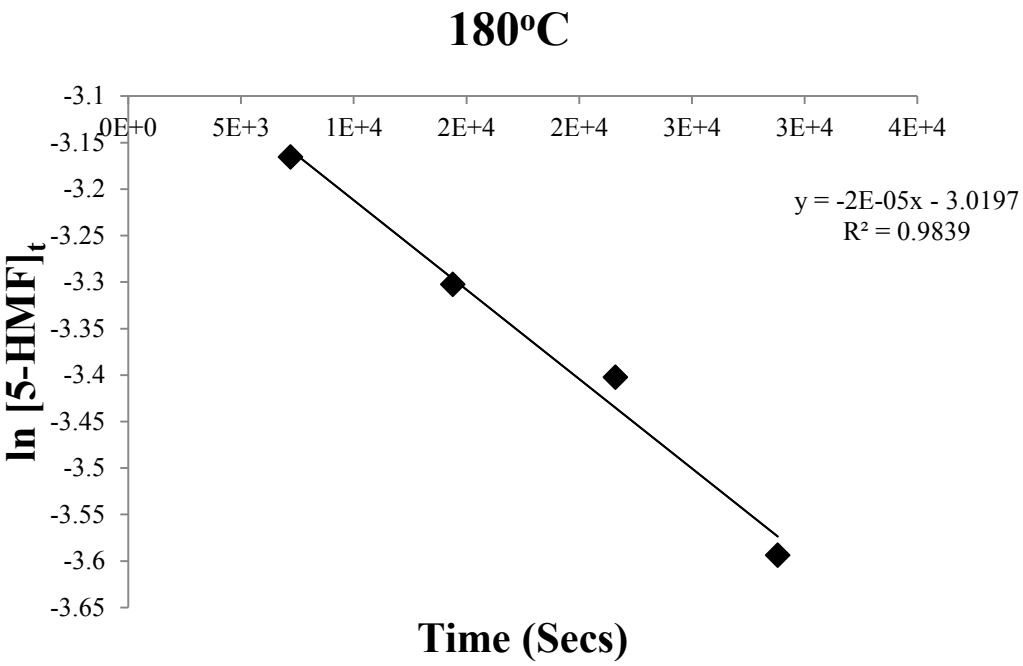

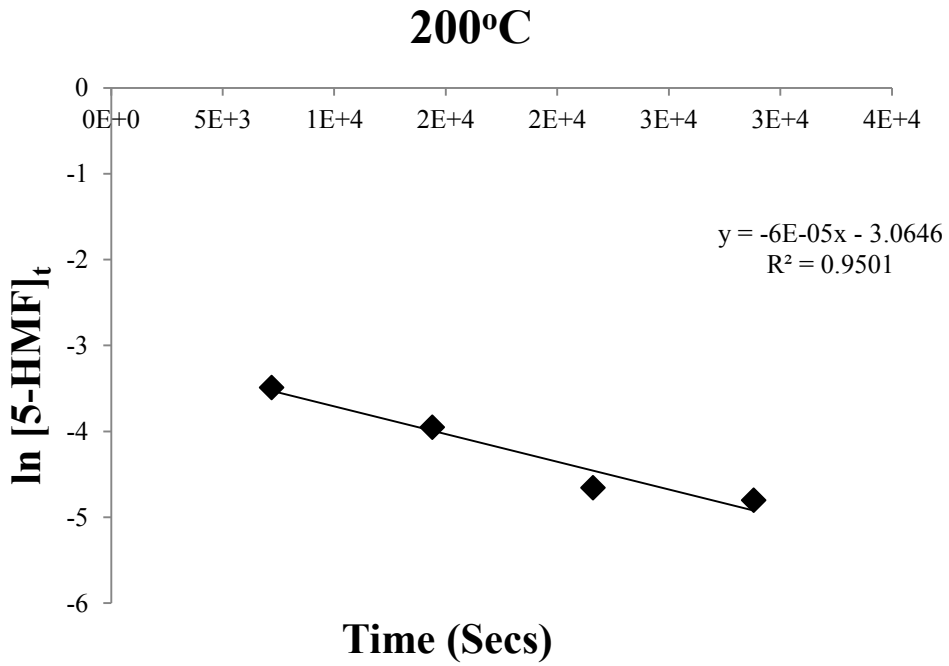

240°C

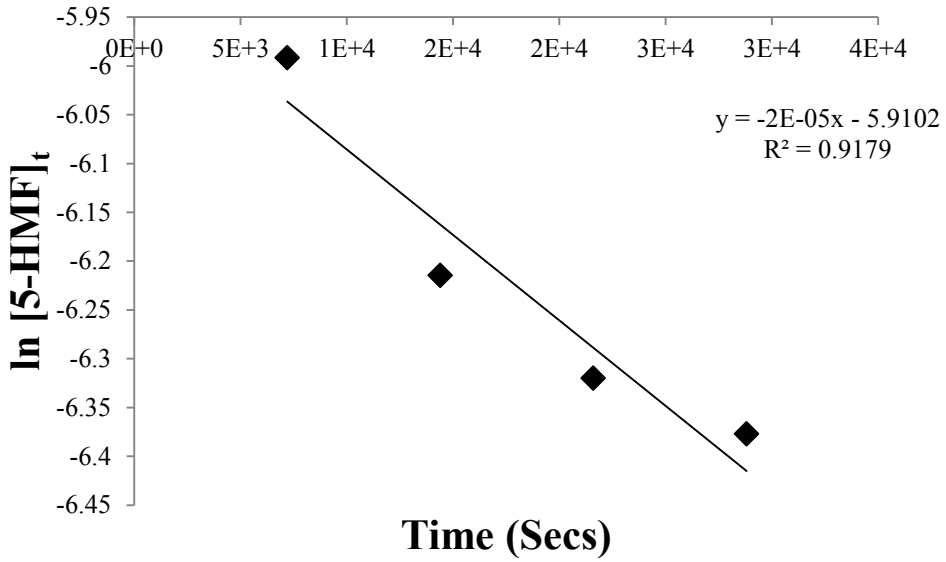
-5.95
-6
-6.05
-6.1
-6.15
-6.2
-6.25
-6.3
-6.35
-6.4
-6.45
0E+0
5E+3
1E+4
2E+4
2E+4
3E+4
3E+4
4E+4
y = -2E-05x - 5.9102
R² = 0.9179
ln [5-HMF]t
Time (Secs)

260°C

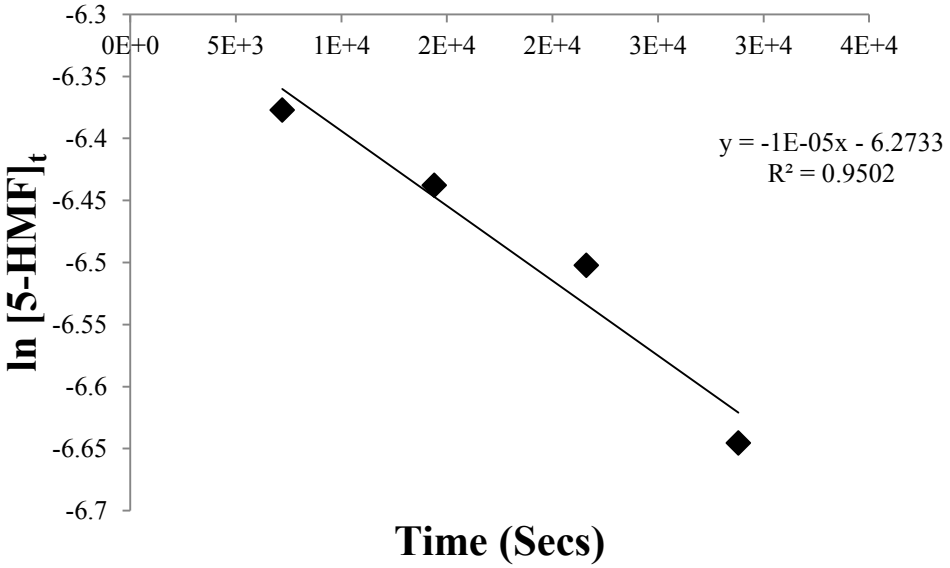
-6.3
-6.35
-6.4
-6.45
-6.5
-6.55
-6.6
-6.65
-6.7
0E+0
5E+3
1E+4
2E+4
2E+4
3E+4
3E+4
4E+4
y = -1E-05x - 6.2733
R² = 0.9502
ln [5-HMF]t
Time (Secs)

C.3 Plots of [5-HMF] against time in 2-propanol

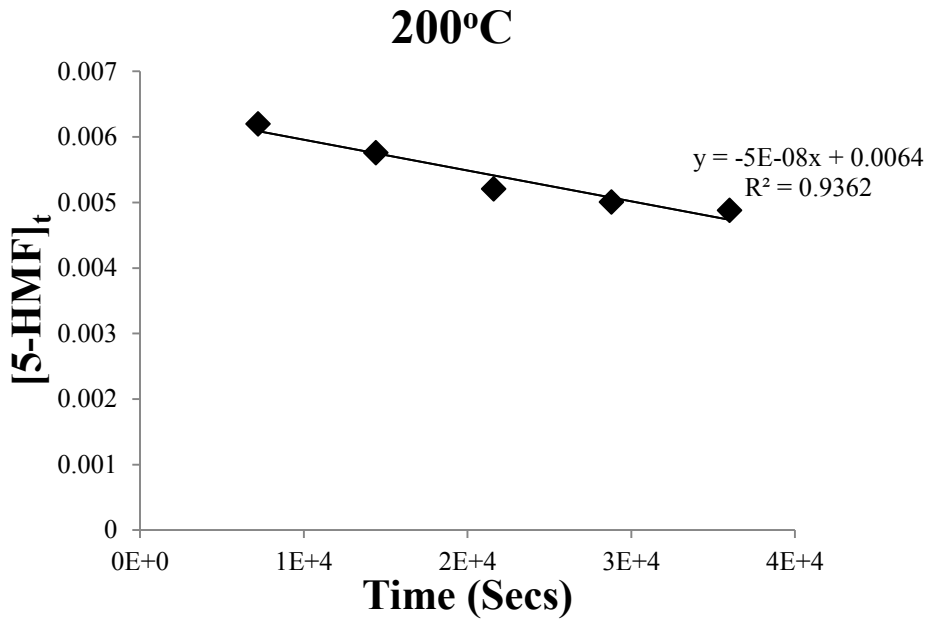

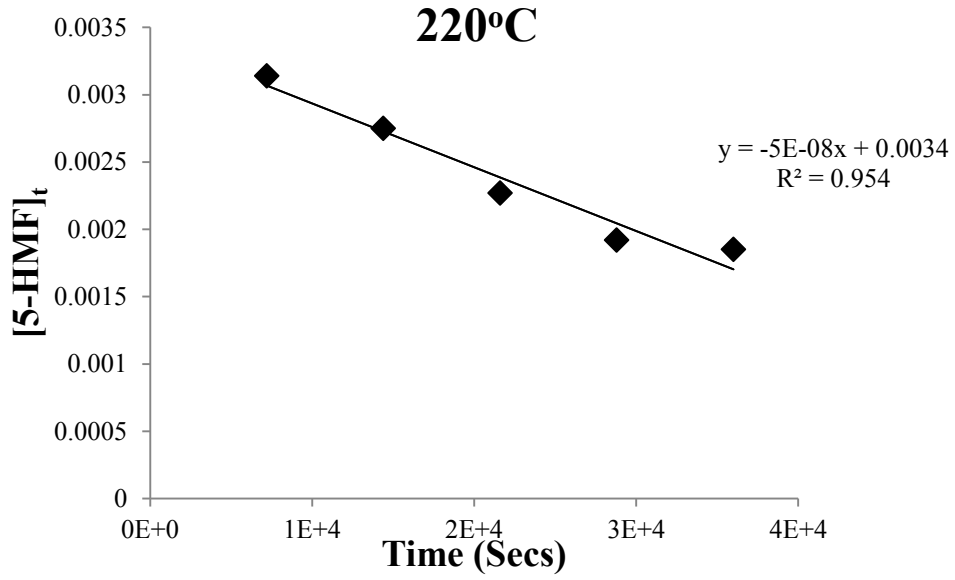

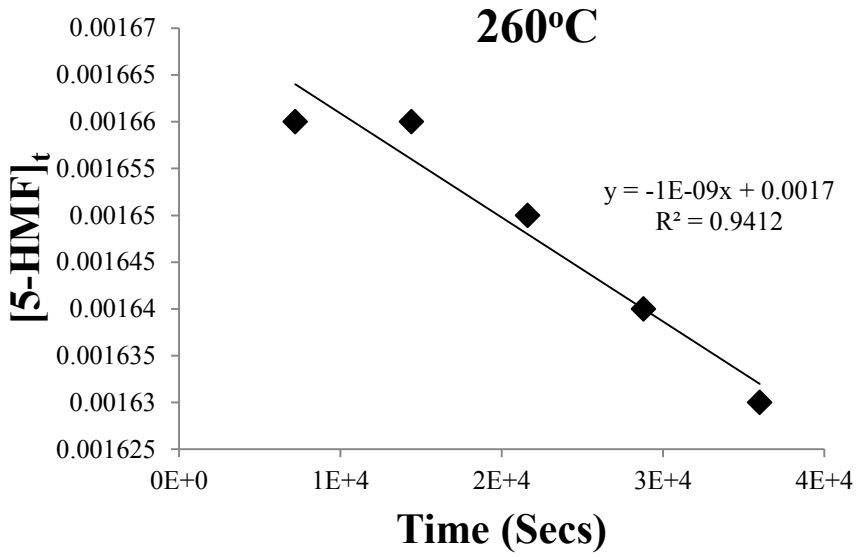

C.4 Plots of ln [5-HMF] against time in 2-propanol

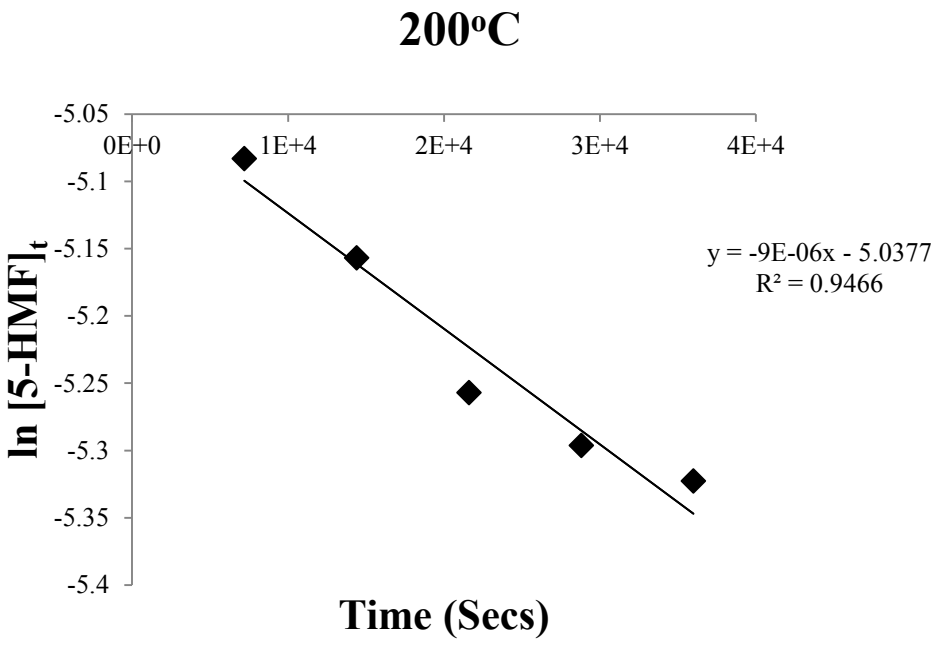

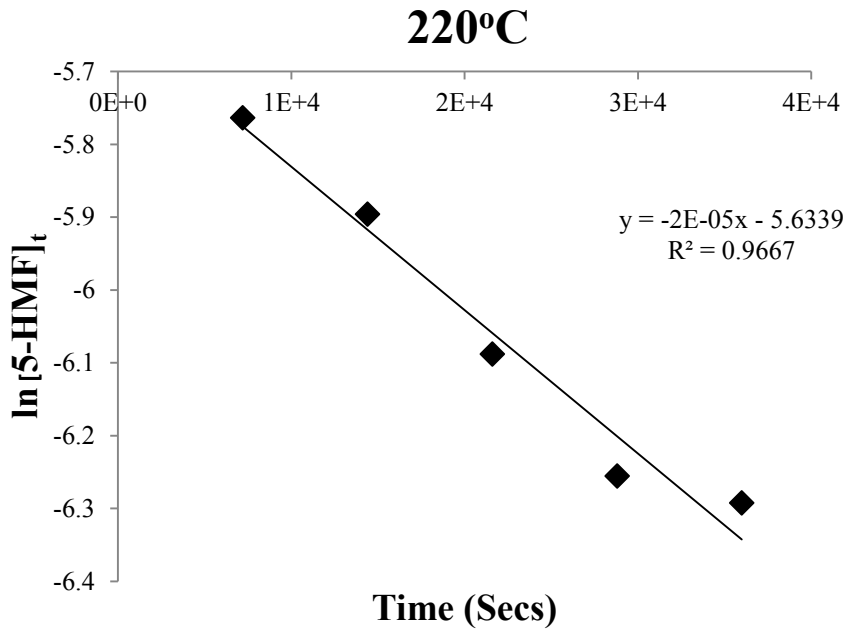
220°C
-5.7
-5.8
-5.9
-6
-6.1
-6.2
-6.3
-6.4
0E+0
1E+4
2E+4
3E+4
4E+4
y = -2E-05x - 5.6339
R² = 0.9667
ln [5-HMF]t
Time (Secs)

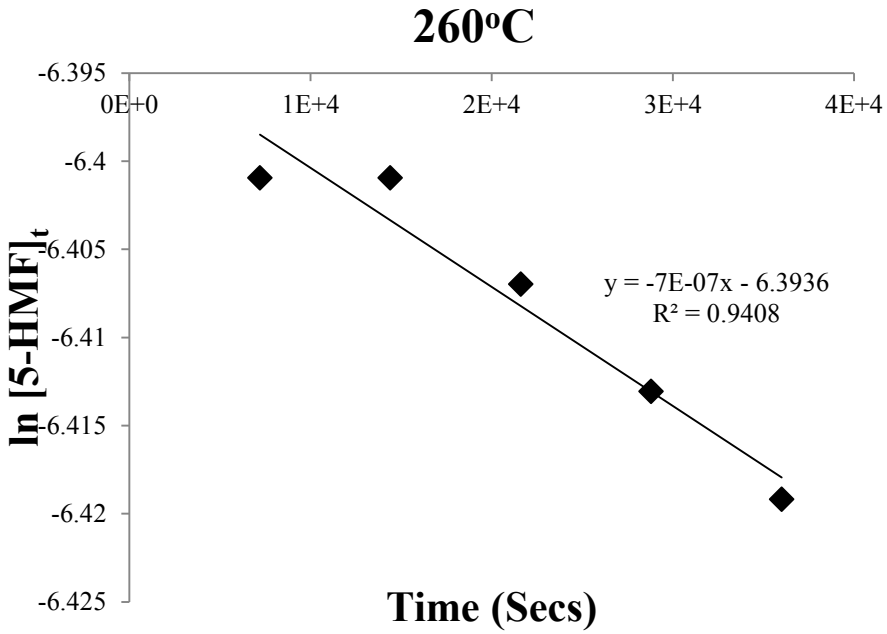
260°C
-6.395
-6.4
-6.405
-6.41
-6.415
-6.42
-6.425
0E+0
1E+4
2E+4
3E+4
4E+4
y = -7E-07x - 6.3936
R² = 0.9408
ln [5-HMF]t
Time (Secs)

Appendix D. Publications and Conferences

D.1 Journal Papers

1. Bayonle Kayode, Jacob Omajali, Mohamed Farah, Joseph Wood, Lynne Macaskie and Bushra Al-Duri, (2015) Catalytic Hydrogenation of 5-Hydroxymethylfurfural to Dimethylfuran over Metal Supported Bio-Catalyst (To be submitted to Journal of Applied Catalysis B: Environmental).

2. Bayonle Kayode, Mohamed Farah, Joseph Wood and Bushra Al-Duri, (2015) Catalytic Transfer Hydrogenation of 5-Hydroxymethylfurfural in Formic acid-Triethylamine to produce Dimethylfuran, (Submitted to Journal of Chemical Engineering Science).

D.2 Conference Papers and Presentations

1. Bayonle Kayode, Jacob Omajali, Mohamed Farah, Joseph Wood, Lynne Macaskie and Bushra Al-Duri, (2015) Novel nanoparticles of Ru and Pd supported on Bacterial Biomass for catalytic hydrogenation of 5-HMF to produce 2,5-DMF. Proceedings of the 2nd International Conference on Past and Present Research Systems of Green Chemistry, Orlando, USA, September 14-16.

2. Bayonle Kayode and Bushra Al-Duri, (2014) Synthesis of Transport Biofuel Components from Biomass-Derived Sugars in Formic acid-Triethylamine Mixture, Proceedings of the 4th International Solvothermal and Hydrothermal Association (ISHA) Conference, Bordeaux, France, October 26-29 (Oral Presentation).

3. Bayonle Kayode, Hongming Xu and Bushra Al-Duri, (2012) Fructose Dehydration into 5-Hydroxymethylfurfural in Aqueous Reaction Solvent, Poster presented at MEGS III Annual Conference; Systems Thinking in Energy, Birmingham, September 18-19.

4. Bayonle Kayode, Hongming Xu, Bushra Al-Duri, (2011) Overview of Biofuel Production: Biodiesel and 2,5-Dimethylfuran, Poster presented at MEGS II Christmas Event and Inaugural Lecture, Loughborough, December 12-13.

References

Abdulmalik, O., Safo, M. K., Chen, Q., Yang, J., Brugnara, C., Ohene-Frempong, K., Abraham, D. J., Asakura, T., (2005). 5-hydroxymethyl-2-furfural modifies intracellular sickle haemoglobin and inhibits sickling of red blood cells. *J. Haematol*, 128, 552- 561.

Abraham, K., Gürtler, R., Berg, K.; Heinemeyer, G., Lampen, A., Appel, K. E., (2011). Toxicology and risk assessment of 5-hydroxymethylfurfural in foods. *Mol. Nutr. Food Res*, 55, 667.

Abura, T., Ogo, S., Watanabe, Y., Fukuzumi, S, (2003), Isolation and Crystal Structure of a Water-Soluble Iridium Hydride: A Robust and Highly Active Catalyst for Acid-Catalyzed Transfer Hydrogenations of Carbonyl Compounds in Acidic Media. *J.Am.Chem.Soc* 125 (14): 4149-4154.

Alexeev, O.S., Gates, B.C, (2003), Supported bimetallic cluster catalysts. *Ind.Eng.Chem.Res*, 42: 1571-1587.

Alonso, D. M., Bond, J. Q., Dumesic, J. A., (2010). Catalytic conversion of biomass to biofuels. *Green Chem, 12*, 1493-1513.

Alonso, D.M., Wettstein, S.G., Dumesic, J.A, (2012), Bimetallic catalysts for upgrading of biomass to fuels and chemicals. Chem.Soc.Rev, 41:8075-8098.

Alonso, M., Godayol, A., Antico, E., Sanchez, J.M., (2010). Assessment of environmental tobacco smoke contamination in public premises: Significance of 2,5-dimethylfuran as an effective marker. *Environ Sci Technol* 44, 8289–8294.

An, H., Wilbert, E., Wilhelm, S., Searcy, W., (2011). Biofuel and petroleum-based fuel supply chain research: A literature review. *Biomass and Bioenergy* 35, 3763 – 3774.

Aramendía, M.A., Borau, V., Jiménez, C., Marinas, J.M., Ruiz, J.R., and Urbano, F., (2003). *Appl. Catal., A*, 249, 1–9.

Armbruster, W.J., Coyle, W.T., Pacific food system outlook 2006-2007: the future role of biofuels. Singapore: Pacific Economic Cooperation Council, http:// www.pecc.org/food/pfso-singapore2006/PECC_Annual_06_07.pdf; 2006.

Asghari, F. S., Yoshida, H., (2006). Dehydration of fructose to 5-hydroxymethylfurfural in sub-critical water over heterogeneous zirconium phosphate catalysts. *Carbohydr. Res*.341, 2379-2387.

Asghari, F. S., Yoshida, H., (2006). Dehydration of fructose to 5-hydroxymethylfurfural in sub-critical water over heterogeneous zirconium phosphate catalysts. *Carbohydr. Res*, 341, 2379-2387.

Asghari, F.S., & Yoshida, H., (2007). Kinetics of the decomposition of fructose catalyzed by hydrochloric acid in subcritical water: Formation of 5-hydroxymethylfurfural, levulinic, and formic acids. *Ind. Eng. Chem. Res*, 46, (23), 7703-7710.

Balcha, T., Strobl, J.R., Fowler, C., Dash, P., Scott, R.W.J., (2011). Selective aerobic oxidation of crotyl alcohol using AuPd core-shell nanoparticles. *ACS Catal*. 1 (5) 425-436.

Bennett, J.A.; Mikheenko, I.P.; Deplanche, K.; Shannon, I.J.; Wood, J.; Macaskie, L.E., (2013). Nanoparticles of Palladium Supported on Bacterial Biomass: New Re-usable Heterogeneous Catalyst with Comparable Activity to Homogeneous Colloidal Pd in the Heck Reaction. *Appl. Catal., B*, *140–141*, 700-707.

Bicker, M., Hirth, J., Vogel, H., (2003). Dehydration of fructose to 5-hydroxymethylfurfural in sub- and supercritical acetone. *Green Chem*, 5, 280-284.

Binder, J. B., Raines, R. T., (2009). (Wisconsin Alumni Research Foundation) Int. Patent WO 2009/155297.

Binder, J. B., Raines, R. T., (2009). Simple chemical transformation of lignocellulosic biomass into furans for fuels and chemicals. *J. Am. Chem. Soc*, 131, 1979−1985.

Blaser, H.U., Schmidt, E., (2007), Asymmetric Catalysis on Industrial Scale: Challenges, Approaches and Solutions, 2nd Edition, Page 209.

Boisen, A., Christensen, T.B., Fu, W., Gorbanev, Y.Y., Hansen, T.S., Jensen, J.S., Klitgaard, S.K., Pedersen, S., Riisager, A., Stahlberg, T., Woodley, J.M., (2009). Process integration for the conversion of glucose to 2,5-furandicarboxylic acid. *Chemical.Eng.Res and Design*, 87, 1318-1327.

Bonner, T.G., Bourne, E.J., Ruszkiewicz, M., (1960). The iodine catalysed conversion of sucrose into 5-hydroxymethylfurfuraldehyde. *J.Chem Soc*. 160, 787-791.

Borgna, A., Anderson, B.G., Saib, A.M., Bluhm, H., Havecker, M., Knop-Gericke, A., Kuiper, A.E.T., Tamminga, Y.de. Niemantsverdriet, J.W (Hans)., (2004). Pt-Co/SiO_2 bimetallic planar model catalysts for selective hydrogenation of crotonaldehyde. *J. Phys. Chem. B* 108 (46), 17905-17914.

Bourne, R.A., Stevens, J.G., Ke, J., and Poliakoff, M., (2007). Maximizing opportunities in supercritical chemistry: the continuous conversion of levulinic acid to ɣ-valerolactone in CO_2. *Chem. Commun*., 4632–4634.

Bui, L., Luo, H., Gunther, W.R., Roman-Leshkov, Y., (2013). Domino reaction catalyzed by zeolites with BrØnsted and Lewis acids sites for the production of ɣ-valerolactone from furfural. *Angew. Chem. Int. Ed*. 52 (31), 7890-8022.

Cao, Q., Guo, X., Yao, S., Guan, J., Wang, X., Mu, X., Zhang, D., (2011). Conversion of hexose into 5-hydroxymethylfurfural in imidazolium ionic liquids with and without a catalyst. *Carbohydr. Res*. 2011, 346, 956-959.

Carlini, C., Giuttari, M., Raspolli Galletti, A. M., Sbrana, G., Armaroli, T., Busca, G., (1999). Selective saccharides dehydration to 5-hydroxymethyl-2-furaldehyde by heterogeneous niobium catalysts. *Appl. Catal*, 183, 295-302.

Carniti, P., Gervasini, A., Biella, S., Auroux, A., (2006). Niobic acid and niobium phosphate highly acidic viable catalysts in aqueous medium: Fructose dehydration reaction. *Catal.Today*, 118, 373-378.

Carniti, P., Gervasini, A., Marzo, M., (2011). Absence of expected side-reactions in the dehydration reaction of fructose to HMF in water over niobic acid catalyst. *Catal. Commun*, 12, 1122-1126.

CDC (Centers for Disease Control and Prevention) (2009). Fourth National Report on Human Exposure to Environmental Chemicals. Available at: http://www.cdc.gov/exposurereport/.

Centi G., Lanzafame P., Perathoner S. (2011). Analysis of the alternative routes in the catalytic transformation of lignocellulosic materials. *Catal. Today,* 167, 14–30.

Chai, M., Dumesic, J.A., (2011). Liquid-phase catalytic transfer hydrogenation and cyclization of levulinic acid and its esters to ɣ-valerolactone over metal oxide catalysts. *ChemCommun*, (47), 12233-12235.

Chai, M., O'Neill, B.J, Alamillo, R., Dietrich, P.J., Ribeiro, F.H., Miller, J.T., Dumesic, J.A, (2013), Bimetallic RhRe/C catalysts for the production of biomass-derived chemicals. *Journal of Catalysis.* 308: 226-236.

Chatt, J., Duncanson, L. A., (1953). Olefin co-ordination compounds. Part III. Infra-red spectra and structure: attempted preparation of acetylene complexes. *J. Chem. Soc,* 2939-2947.

Chatterjee, M., Ishizaka, T., Kawanami, H., (2014). Hydrogenation of 5-hydroxymethylfurfural in supercritical carbon dioxide-water: a tunable approach to dimethylfuran selectivity. *Green Chemistry* 16, 1543−1551.

Chheda, J. N., Dumesic, J. A., (2007). An overview of dehydration, aldol-condensation and hydrogenation processes for production of liquid alkanes from biomass-derived carbohydrates. *Catal. Today*, 123, 59-70.

Chheda, J. N., Román-Leshkov, Y., Dumesic, J. A., (2007). Production of 5-hydroxymethylfurfural and furfural by dehydration of biomass-derived mono- and poly-saccharides. *Green Chem*, 9, 342-350.

Chia, M., Dumesic, J.A, (2011), Liquid-phase catalytic transfer hydrogenation and cyclization of levulinic acids and its esters to valerolactone over metal oxide catalysts. *ChemComm* 47: 12233-12235.

Chidambaram, M., Bell, A. T., (2010). A two-step approach for the catalytic conversion of glucose to 2,5-dimethylfuran in ionic liquids. *Green Chem*.12, 1253−1262.

Childers, D.J., Schweitzer, N.M., Kamal Shahri, S.M., Rioux, R.M., Miller, J.T., Meyer, R.J., (2014), Evidence for geometric effects in neopentane conversion on PdAu catalysts. *Catal. Sci. Technol, 4,* 4366.

Christensen, E., Yanowitz, J., Ratcliff, M., McCormick, R.L., (2011). Renewable oxygenate blending effects on gasoline properties. *Energy Fuels*, 25, 4723 –4733.

Chuntanapum, A., Yong, T. L. K., Miyake, S., Matsumara, Y., (2008). Behaviour of 5-HMF in subcritical and supercritical water. *Ind. Eng. Chem. Res*. 2008, 47, 2956-2962.
Corbos, E.C., Ellis, P.R., Cookson, J., Briois, V., Hyde, T.I., Sankar, G., Bishop, P.T, (2013), Tuning the properties of PdAu bimetallic nanocatalysts for selective hydrogenation reactions. *Catal.Sci.Technol*, 3: 2934-2943.

Corma, A., Iborra, S., Velty, A., (2007). Chemical routes for the transformation of biomass into chemicals. *Chem. Rev,* 107, 2411-2502.

Cossy, J., Eustache, F., Dalko, P.I, (2001), Ruthenium-catalyzed asymmetric reduction of 1,3-diketones using transfer hydrogenation. *Tetrahedron Lett*. 42: 5005–5007.

Daniel, R., Tian, G., Xu, H., Shuai, S., (2012). Ignition timing sensitivities of oxygenated biofuels compared to gasoline in a direct-injection SI engine. *Fuel*, 99, 72–82.

Daniel, R., Wei, L., Xu, H., Wang, C., Wyszynski, M.L., Shuai, S., (2012b). Speciation of hydrocarbon and carbonyl emissions of 2,5-Dimethylfuran combustion. *Energy Fuels*, 26, 6661 –6668.

Davis, M.E., and Davis, R.J., (2003), Chapter 5, Heterogeneous Catalysis, *Fundamentals of Chemical Reaction Engineering*, Pg 133, 1st Edition, ISBN 0-07-245007-X.

De, S., Dutta, S., Saha, B, (2012), One-pot conversions of lignocellulosic and algal biomass into liquid fuels. *ChemSusChem* 5: 826− 1833.

De, S., Dutta, S., Saha, B., (2011). Microwave assisted conversion of carbohydrates and biopolymers to 5-hydroxymethylfurfural with aluminium chloride catalyst in water. *Green Chem*, 13, 2859-2868.

Deplanche K, Merroun M.L, Casadesus M, Tran D.T, Mikheenko I.P, Bennett J.A, Zhu J, Jones I.P, Attard G.A, Wood J, Selenska-Pobell, S, Macaskie, L.E., (2012). Microbial synthesis of core/shell gold/palladium nanoparticles for applications in green chemistry. *Journal of the Royal Society Interface, 9* (72), 1705-1712.

Deplanche, K.; Bennett, J.A.; Mikheenko, I.P.; Omajali, J.; Wells, A.S.; Meadows, R.E.; Wood, J.; Macaskie, L.E., (2014). Catalytic Activity of Biomass-supported Pd Nanoparticles: Influence of the Biological Component in Catalytic Efficacy and Potential Application in 'Green' Synthesis of Fine Chemicals and Pharmaceuticals. *Appl. Catal., B.*, *147*, 651-65.

Deplanche, K.; Caldelari, I.; Mikheenko, I.P.; Sargent, F.; Macaskie, L.E., (2010). Involvement of Hydrogenases in the Formation of Highly Catalytic Pd(0) Nanoparticles by Bioreduction of Pd(II) Using *Escherichia coli* Mutant Strains. *Microbiol-SGM.*, *156*, 2630-2640.

Devulapelli, V.G., Weng, H, (2009), Synthesis of cinnamyl acetate by solid–liquid phase transfer catalysis: Kinetic study with a batch reactor. *Catalysis Communications* 10:1638–1642.

Dorrestijn, E., Laarhoven, L. J. J., Arends, I., Mulder, P., (2000). The occurrence and reactivity of phenoxyl linkages in lignin and low rank coal. *J. Anal. Appl. Pyrolysis* 54, 153-192.

Dragone, G., Fernandes, B., Vicente, A.A., Teixeira, J.A., (2010). Third generation biofuels from microalgae. *Current research, technology and education topics in applied microbiology and microbial technology*. 1355- 1365.

Dry, M. E., (2002). High quality diesel via Fischer-Tropsch process- a review. *J. Chem. Technol. Biotechnol, 77*, 43-50.

Dull, G., (1985). Chem.-Ztg. 19, 216.

Dutta, S., De, S., Patra, A. K., Sasidharan, M., Bhaumik, A., Saha, B., (2011). Microwave assisted rapid conversion of carbohydrates into 5-hydroxymethlfurfural catalysed by mesoporous TiO2 nanoparticles. *Appl. Catal., A*, 409−410, 133-139.

Earle, M.J., & Seddon, K.R., (2000). Ionic liquids: Green solvents for the future. *Pure Appl.Chem.*, 72, (7), 1391-1398.

Eberle, U., Felderhoff, M., Schuth, F, (2009), Physical and chemical solutions for the storage of hydrogen. *Angew Chem* 121: 6732-6757.

Edwards, J.K., Ntainjua, E., Carley, A.F., Herzing, A.A., Kiely, C.J., Hutchings G.J., (2009). Direct synthesis of H_2O_2 from H_2 and O_2 over Gold, Palladium and Gold-Palladium catalysts supported on acid pre-treated TiO_2. *Angew. Chem. Int. Ed.* (48) 8512. (b).

Edwards, J.K., Solsona, B., Ntainjua, E., Carley, A.F., Herzing, A.A., Kiely, C.J., Hutchings, G.J., (2009). Switching off hydrogen peroxide hydrogenation in direct synthesis process. *Science* 323 (5917) 1037 – 1041. (a).

Enache, D.I., Edwards, J.K., Landon, P., Solsona-Espriu, B., Herzing, A.A., Watanabe, M., Kiely, C.J., Knight, D.W., Hutchings, G.J., (2006). Solvent free oxidation of primary alcohols to aldehydes using Au-Pd/TiO_2 catalysts. *Science* 311 (5759) 362-365.

Enslow, K.R., and Bell, A.T., (2012), The Kinetics of Bronsted acid-catalysed hydrolysis of hemicellulose dissolved in 1-ethyl-3-methylimidazolium chloride. *RSC Advances, 2*, 10028 – 10036.

Escobar, J.C., Lora, E.S., Venturini, O.J., Yanez, E.E., Castillo, E.F., Almazan, O., (2009). Biofuels: environment, technology and food security. *Renew Sustain Energy Rev*, 13, 1275-1287.

Fahmy, K.; Merroun, M.; Pollmann, K.; Raff, J.; Savchuk, O.; Hennig, C.; Selenska-Pobell, S., (2006). Secondary Structure and Pd-(II) Coordination in S-Layer Proteins from *Bacillus sphaericus* Studied by Infrared and X-ray Absorption Spectroscopy. *Biophys. J.*, *91*, 996-1007.

Fan, C., Guan, H., Zhang, H., Wang, J., Wang, S., Wang, X., (2011). Conversion of fructose and glucose into 5-hydroxymethylfurfural catalysed by a solid heteropolyacid salt. *Biomass Bioenergy*, 35, 2659-2665.

Fellay, C., Dyson, PJ., Laurenczy, G, (2008), A Viable Hydrogen-Storage System Based On Selective Formic Acid Decomposition with a Ruthenium Catalyst. *Angew Chem* 120: 4030-4032.

Feller, D., Simmie, J.M., (2012). High-level ab initio enthalpies of formation of 2,5-Dimethylfuran, 2-methylfuran and furan. *J. Phys. Chem. A*, 116, 11768– 11775.

Fengel, D., Wegener, G., (1984). Wood: Chemistry, Ultrastructure, Reactions, Berlin. 1984.

Fenton, H.J.H., Gostling, M (1899). Bromomethylfurfuraldehyde. *J.Chem.Soc.Trans*, 75, 423-433.

Fenton, H.J.H., Robinson, F., (1909). Homologues of furfuraldehyde. *J.Chem.Soc.Trans*, 95, 1334-1340.

Florian, S., Bauer-Marinovic, M., Taugner, F.; Dobbernack, G., Monien, B. H., Meinl, W., Glatt, H., (2012). Study of 5-hydroxymethylfurfural and its metabolite 5-sulfooxymethylfurfural on induction of colonic aberrant crypt foci in wild-type mice and transgenic mice expressing human sulfotransferases 1A1 and 1A2. *Mol. Nutr. Food Res*, 56, 593.

Frey, D. D. and Jugulum, R. (2006), The mechanisms by which adaptive one-factor-at-a-time experimentation leads to improvement. *Journal of Mechanical Design*, 128 (5): 1050 -1060.

Frey, D. D., Engelhardt, F., and Greitzer, E. M., (2003), A Role for One Factor at a Time Experimentation in Parameter Design, *Research in Engineering Design* 14, pp. 65-74.

Friedman, M., and Savage, L.J., (1947), "Planning experiments seeking maxima" *in Techniques of Statistical Analysis*, McGraw-Hill, New York, pp 365 – 372.

Fromowitz, M., Shuga, J., Wlassowsky, A.Y., Zhang, L., Smith, M.T., (2012). Studies on the genotoxicity of 2,5-dimethylfuran, a potential biofuel. *Environ Mol Mutagen* 53.

Fu, Z.Q., Wang, M.Y., Cai, B.C., (2008). Discussion of 5-hydroxymethylfurfural (5-HMF) in Chinese native medicine research present situation.

Fukuzumi, S., Kobayashi, T., Suenobu, T, (2008), Efficient Catalytic Decomposition of Formic Acid for the Selective Generation of H_2 and H/D Exchange with a Water-Soluble Rhodium Complex in Aqueous Solution. *ChemSusChem* 1: 827-834.

Furimsky, E., (2000). Catalytic hydrodeoxygenation. *Appl. Catal., A, 199*, 147-190.

Gandarias, I., Arias, P.L., Requies, J., El Doukkali, M., Guemez, M.B, (2011), Liquid-phase glycerol hydrogenolysis to 1,2-propanediol under nitrogen pressure using 2-propanol as hydrogen source. *J.Catal*. 282: 237-247.

Gandarias, I., Arias, P.L., Requies, J., El Doukkali, M., Guemez, M.B., (2011). Liquid-phase glycerol hydrogenolysis of 1,2-propanediol under nitrogen pressure using 2-propanol as hydrogen source. *J. Catalysis*, 282, (1), 237-247.

Gaset, A., Rigal, L., Paillassa, G., J.-P., S., Flèche, G. (Roquette Freres), (1986). U.S. Patent 4,590,283.

Geboers, J.A., De Vyver, S.V., Ooms, R., de Beeck, B.O., Jacobs, P.A., Sels, B.F., (2011). *Catal. Sci. Technol* 1,714 –726.

Gladiali, S., Alberico, E, (2006), Asymmetric transfer hydrogenation: chiral ligands and applications. *Chem.Soc.Rev*. 35: 226–236.

Glatt, H., Schneider, H., Murkovic, M., Monien, B. H., Meinl, W., (2012). Hydroxymethyl-substituted furans: mutagenicity in Salmonella typhimurium strains engineered for expression of various human and rodent sulphotransferases. *Mutagenesis*, 27, 41.

Glinski, M. and Ulkowska, U. (2011), Reactivity of alcohols in chemoselective transfer hydrogenation of acrolein over magnesium oxide as the catalyst. *Catalysis letters*, 141 (2): 293-299.

Goswami, D. Y., (1986). Alternative Energy in Agriculture. *CRC Press*.

Grela, M.A., Amorebieta, V.T., Colussi, A.J., (1985). Very low pressure pyrolysis of furan, 2-methylfuran and 2,5-dimethylfuran. The stability of the furan ring. *J. Phys. Chem*, 89, 38–41.

Haack, J., Hashiguchi, S., Fujii, A., Ikariya, T., Noyori, R, (1997), The Catalyst Precursor, Catalyst, and Intermediate in the Ru^{II}-Promoted Asymmetric Hydrogen Transfer between Alcohols and Ketones. *Angew Chem.* Int. Ed. 36: 288–290.

Hansen, T. S., Barta, K. and Anastas, P.T, (2012), One-pot reduction of 5-hydroxymethylfurfural via hydrogen transfer from supercritical methanol. *Green Chemistry,* 14 (9): 2457-2461.

Hansen, T. S., Mielby, J., Riisager, A., (2011). Synergy of boric acid and added salts in the catalytic dehydration of hexoses to 5-hydroxymethylfurfural in water. *Green Chem*, 13, 109-114.

Heeres, H., Handana, R., Chunai, D., Rasrendra, C.B., Girisuta, B., Heeres, H.J, (2009), Combined dehydration/(transfer)-hydrogenation of C6-sugars (D-glucose and D-fructose) to ɣ-valerolactone using ruthenium catalysts. *Green Chem*.11: 1247 – 1255.

Himeda, Y., Miyazawa, S., Hirose, T, (2011), Interconversion between Formic Acid and H_2/CO_2 using Rhodium and Ruthenium Catalysts for CO_2 Fixation and H_2 Storage. ChemSusChem 4: 487-493.

Holladay, J.E., Bozell, J.J., White, J.F., and Johnson, D., (2007). Top Value Added Chemicals from Biomass. Volume II – Results of Screening for Potential Candidates from Biorefinery Lignin, Pacific Northwest National Laboratory, Richland, WA, PNNL-16983, (file: http://www.pnl.gov/main/ publications/external/technical reports/PNNL-16983.pdf).

Horiuti, I., Polanyi, M., (1934). Exchange reactions of hydrogen on metallic catalysts. *Trans. Faraday Soc. 30*, 1164-1172.

Hu, E., Hu, X., Wang, X., Xu, Y., Dearn, K.D., Xu, H., (2012). On the fundamental lubricity of 2,5-Dimethylfuran as a synthetic engine fuel. *Tribol.Int*, 55, 119–125.

Hu, L., Tang, X., Xu, J., Wu, Z., Lin, L., Liu, S, (2014), Selective transformation of 5-hydroxymethylfurfural into the liquid fuel 2,5-dimethylfuran over carbon-supported ruthenium. *IECR 2014*. Dx.doi.org/10.1021/ie404441a.

Hu, S., Zhang, Z., Song, J., Zhou, Y., Han, B., (2009). Efficient conversion of glucose into 5-hydroxymethylfurfural catalyzed by a common Lewis acid SnCl4 in an ionic liquid. *Green Chem*, 11, 1746-1749.

Hu, S., Zhang, Z., Zhou, Y., Han, B., Fan, H., Li, W., Song, J., Xie, Y., (2008). Conversion of fructose to 5-hydroxymethylfurfural using ionic liquids prepared from renewable materials. *Green Chem*, 10, 1280-1283.

Huang, Y., Chen, M., Yan, L., Guo, Q., Fu, Y, (2014). Nickel-Tungsten carbide catalysts for the production of 2,5-dimethylfuran from biomass-derived molecules. ChemSusChem, 7: 1068-1070.

Huber, G. W., Iborra, S., Corma, A., (2006). Synthesis of transportation fuels from biomass: chemistry, catalysts and engineering *Chem. Rev, 106*, 4044-4098.

INFORSE, (2015). Biomass energy, Available at: www.inforse.org/europe/dieret/Biomass/biomass.html. Accessed 5/02/2015.

Jae, J., Zheng, W. and Karim, A. (2014), The Role of Ru and RuO_2 in the Catalytic Transfer Hydrogenation of 5-Hydroxymethylfurfural for the Production of 2,5-Dimethylfuran. *ChemCatChem,* 6(3): 848-856.

Jae, J., Zheng, W., Lobo, R. F. and Vlachos, D. G. (2013), Production of Dimethylfuran from Hydroxymethylfurfural through Catalytic Transfer Hydrogenation with Ruthenium Supported on Carbon. *ChemSusChem,* 6 (7): 1158-1162.

James, O.O., Maity, S., Usman, L.A., Ajanaku, K.O and Ajani, O.O., (2010). Towards the conversion of carbohydrate biomass feedstocks to biofuels via hydroxymethylfurfural. *Energy Environ. Sci*, 3, 1833–1850.

James, R. B., (1973). Homogeneous Hydrogenation. *John Wiley & Sons, Inc*.

Jan van Putten, R., van der Waal, Jan C., Jong, Ed de., Rasrendra, C.B., Heeres, H.J., Vries, G.de., (2013). Hydroxymethylfurfural, A versatile platform chemical made from renewable resources. *Chem.Rev*, 113, 1499-1597.

Janzowski, C., Glaab, V., Samimi, E., Schlatter, J., Eisenbrand, G., (2000). 5-Hydroxymethylfurfural: assessment of mutagenicity, DNA-damaging potential and reactivity towards cellular glutathione. *Food Chem. Toxicol*, 38, 801-809.

Jing, Q., Lü, X., (2008). Kinetics of non-catalysed decomposition of glucose in high-temperature liquid water. *Chin. J. Chem. Eng*, 16, 890-894.

Kamm, B., Gruber, P. R., Kamm, M., (2006). Biorefineries. Industrial Process and Products, *Ullmann's Encyclopaedia of Industrial Chemistry*.

Kawasaki, I., Tsunoda, K., Tsuji, T., Yamaguchi, T., Shibuta, H., Uchida, N., Yamashita, M., Ohta, S, (2005), A recyclable catalyst for asymmetric transfer hydrogenation with a formic acid-triethylamine mixture in ionic liquid. *ChemCommun*, 2134-2136.

Kazi, F. K., Patel, A. D., Serrano-Ruiz, J. C., Dumesic, J. A., Anex, R. P., (2011). Techno-economic analysis of dimethylfuran (DMF) and hydroxymethylfurfural (HMF) production from pure fructose in catalytic processes. *Chem. Eng. J*, 169, 329-338.

Kiermayer, J., (1985). Chem.-Ztg. 19, 1003.

Klaewkla, R., Arend, M., Hoelderich, W.F., (2011), A Review of Mass Transfer Controlling the Reaction Rate in Heterogeneous Catalytic Systems, Mass Transfer – *Advanced Aspects,* Dr. Hironori Nakajima (Ed.), ISBN: 978-953-307-636-2.

Kobayashi, H., Komanoya, T., Guha, S.K., Hara, K., Fukuoka, A., (2011). Conversion of cellulose into renewable chemicals by supported metal catalysis. *J. Applied Catalysis A*, 409-410, 13-20.

Kobayashi, H., Matsuhashi, H., Komanoya, T., Hara, K., Fukuoka, A, (2011), Transfer hydrogenation of cellulose to sugar alcohols over supported ruthenium catalysts. *ChemComm* 47: 2366-2368.

Koita, R., (1994), "Strategies for Sequential Design of Experiments," SM thesis, Massachusetts Institute of Technology, Massachusetts.

Kragl, U., Eckstein, M., Kaftzik, N., (2002). Enzyme catalysis in ionic liquids. *Current Opinion in Biotechnology* 13, (6), 565-571.

Kroh, L. W., (1994). Caramelization in food and beverages. *Food Chem*, 51, 373.

Kus, S., Gogus, F., Eren, S., (2005). Hydroxymethylfurfural content of concentrated food products. *Int. J. Food Prop*, 8, (2), 367-375.

Kuster, B. F. M., van der Baan, H. S., (1977). The influence of the initial and catalyst concentrations on the dehydration of D-fructose. *Carbohydrate. Res*, 54, 165-176.

Kwon, Y., de Jong, E., Raoufmoghaddam, S., Koper, M.T.M., (2013). Electrocatalytic hydrogenation of 5-hydroxymethylfurfural in the absence and presence of glucose. *Chem.Sus.Chem*. 6, 1659-1667.

Lange, J.-P., (2007). Lignocellulose conversion: an introduction to chemistry, process and economics. *Biofuels, Bioprod. Biorefin, 1*, 39-48.

Lange, J.P., van der Heide, E., van Buijtenen, J., Price, R., (2012). Furfural- a promising platform for lignocellulosic biofuels. *ChemSusChem* 5 (1), 150-166.

Lansalot-Matras, C., Moreau, C., (2003). Dehydration of fructose into 5-hydroxymethylfurfural in the presence of ionic liquids. *Catal. Commun*, 4, 517-520.

Larson, E.D., (2008). Biofuel production technologies: status, prospects and implications for trade and development. Report No. UNCTAD/DITC/TED/2007/10. United Nations Conference on Trade and Development, New York and Geneva.

Lee, J., Kim, Y.T., Huber, G.W, (2014), Aqueous-phase hydrogenation and hydrodeoxygenation of biomass-derived oxygenates with bimetallic catalysts. *Green Chem*, 16: 708-718.

Li, C., Zhang, Z., Zhao, Z. K., (2009). Direct conversion of glucose and cellulose to 5-hydroxymethylfurfural in ionic liquid under microwave irradiation. *Tetrahedron Lett*, 50, 5403-5405.

Li, Y., Lu, X., Yuan, L., Liu, X., (2009). Fructose decomposition kinetics in organic acids-enriched high temperature liquid water. *Biomass Bioenergy*, 33, 1182-1187.

Licht, F.O., (2008). World ethanol & biofuels report. Kent, UK: Agra Informa Ltd., http:// www.agra-net.com/portal/puboptions.jsp?Option¼menu&pubId¼ag072.

Lifshitz, A., Tamburu, C., Shashua, R., (1998). Thermal decomposition of 2,5-Dimethylfuran. Experimental results and computer modelling. *J. Phys. Chem. A*, 102, 10655 –10670.

Lima, S., Antunes, M. M., Fernandes, A., Pillinger, M., Ribeiro, M. F., Valente, A. A., (2010). Acid-catalysed conversion of saccharides into furanic aldehydes in the presence of three-dimensional mesoporous AI-TUD-1. *Molecules*, 15, 3863-3877.

Lima, S., Neves, P., Antunes, M.M., Pillinger, M., Ignatyev, N., Valente, A.A., (2009). Appl. Catal., A, 363, 93–99.

Liu, Z., Agren, J. and Hillert, M. (1996). Application of the Le Chatelier's principle on gas reactions. *Fluid phase Equilibria*, 121(1): 167-177.

Loges, B., Albert, B., Felix, G, (2010), Catalytic generation of hydrogen from formic acid and its derivatives: Useful hydrogen storage materials. *Top Catal*, 53: 902-914.

Lourvanij, K., Rorrer, G. L., (1993). Reactions of aqueous glucose solutions over solid-acid Y-zeolite catalyst at 110-160 degree C. *Ind. Eng. Chem. Res*, 32, 11-19.

Luo, J., Arroyo-Ramirez, L., Gorte, R.J., (2014). Hydrodeoxygenation of HMF over Pt/C in a continuous flow reactor. *AIChE Journal*, Vol.00, No. 00. DOI 10.1002/aic.14660.

Luque, R., Herrero-Davila, L., Campelo, J.M., Clark, J.H., Hidalgo, J.M., Luna, D., Marinas, J.M., Romero, A.A., (2008). Biofuels: A technological perspective. *Energy Environ Sci* 1,542–564.

Makowski, P., Thomas, A., Kuhn, P., Goettmann, F, (2009), Organic materials for hydrogen storage applications: from physisorption on organic solids to chemisorption in organic molecules. *Energy Environ Sci* 2: 480-490.

Martins, S. I. F. S., Van Boekel, M. A. J. S., (2005). Kinetics of the glucose/glycerine Maillard pathways: Influence of pH and reactant initial concentrations. *Food Chem*, 92, 437.

Matharu, D., Morris, D.J., Clarkson, G.J., Wills, M, (2006), An outstanding catalyst for asymmetric transfer hydrogenation in aqueous solution and formic acid/triethylamine. *ChemCommun*, 3232-3234.

Matkovskiy, P.E., Sedov, I.V., (2011). Technologies for producing liquid motor fuels from wastes of renewable vegetable resources. *Polymer Science*, Series D, 4 (3), 252-258.

Matsumoto, J., (2011). Kinetics of the reactions of ozone with 2,5-Dimethylfuran and its atmospheric implications. *Chem. Lett*, 40, 582 –583.

Maxted, E. B., Moon, K. L., Overgage, E., (1950). The relationship between sensitivity to poisoning and catalytic surface. *Discuss. Faraday Soc, 8*, 135-140.

McDaniel, W.R., and Ankenman, B.E., (2000), Comparing Experimental Design Strategies for Quality Improvement with Minimal Changes to Factor Levels, *Qual. Reliab. Eng Int*, 16, pp 355 – 362.

McKone, T., Nazaroff, W., Berck, P., Auffhammer, M., Lipman, T., Torn, M., Masanet, E., Lobscheid, A., Santero, N., Mishra, U., (2011). Grand challenges for life-cycle assessment of biofuels. *Environ Sci Technol* 45, 1751–1756.

McNeff, C. V., Nowlan, D. T., McNeff, L. C., Yan, B., Fedie, R. L., (2010). Continuous production of 5-hydroxymethylfurfural from simple and complex carbohydrates. *Appl. Catal., A*, 384, 65-69.

Mikheenko, I.P.; Rousset, M.; Dementin, S.; Macaskie, L.E., (2008). Bioaccumulation of Palladium by *Desulfovibrio fructosovorans* Wild-Type and Hydrogenase-Deficient Strains. *Appl. Environ. Microbiol*., *74*, 6144-6146.

Moreau, C., Durand, R., Razigade, S., Duhamet, J., Faugeras, P., Rivalier, P., Ros, P., Avignon, G., (1996). Dehydration of fructose to 5-hydroxymethylfurfural over H-mordenites *Appl. Catal., A*, 145, 211-224.

Musau, R. M., Munavu, R. M., (1987). The preparation of 5-hydroxymethyl-2-furaldehyde (HMF) from d-fructose in the presence of DMSO. *Biomass*, 13, 67-74.

Musau, R. M., Munavu, R. M., (1987). The preparation of 5-hydroxymethyl-2-furaldehyde (HMF) from D-fructose in the presence of DMSO. *Biomass*, 13, 67-74.

Musolino, M., Scarpino, L., Mauriello, F., Pietropaolo, R, (2009), Selective transfer hydrogenolysis of glycerol promoted by palladium catalysts in absence of hydrogen. *Green Chem*. 11: 1511-1513.

Nakagawa, Y., Tomishige, K, (2010), Total hydrogenation of furan derivatives over silica supported Ni-Pd catalyst. *Catal.Commun*, 12: 154-156.

Nakamura, Y., & Morikawa, S., (1980). The dehydration of D-fructose to 5-hydroxymethy-2-furaldehyde. *Bulletin of the chemical society of Japan*, 53, (12), 3705-3706.

Navalikhina, M. D., Krylov, O. V. (1998). Heterogeneous catalysts of hydrogenation. *Russ. Chem. Rev*, 67, 587-616.

Newton, M. A. & Van Beek, W., (2010). Combining synchrotron-based X-ray techniques with vibrational spectroscopies for the in situ study of heterogeneous catalysts: a view from a bridge. *Chem. Soc. Rev.* 39, 4845-4863.

Nielsen, M., Alberico, E. and Baumann, W. (2013), Low-temperature aqueous-phase methanol dehydrogenation to hydrogen and carbon dioxide**.** *Nature*, 495: 85-89.

Nigam, P.S., Singh, A., (2011). "Production of liquid biofuels from renewable resources". *Progress in Energy and Combustion Science* 37, 52-68.

Nikbin, N., Caratzoulas, S., Vlachos, D.G., (2013). On the BrØnsted acid-catalyzed homogeneous hydrolysis of furans. *ChemSusChem*, 6(11), 2066-2068.

Nikolau, A., Remrova, M., Jeliazkov, I., (2003). Biomass availability in Europe, December.

Nilges, P., Schröder, U., (2013). Electrochemistry for biofuel generation: Production of furans by electrocatalytic hydrogenation of furfurals. *Energy Environ. Sci*. (6), 2925−2931.

Nishimura, S., Ikeda, N., Ebitani, K, (2014), Selective hydrogenation of biomass-derived 5-hydroxymethylfurfural (HMF) to 2,5-dimethylfuran (DMF) under atmospheric hydrogen pressure over carbon supported PdAu bimetallic catalyst. *Catalysis Today*. 232: 89-98.

Notheisz, F., Zsigmond, A., Bartok, M., Szegletes, Z., Smith, G.V., (1994), Mass Transfer Test and Maximum Rate Determination during Liquid-Phase Hydrogenations. *Applied Catalysis A:* General 120, 105 – 114.

Noyori, R., Hashiguchi, S, (1997), Asymmetric Transfer Hydrogenation Catalyzed by Chiral Ruthenium Complexes. *Acc Chem Res* 30: 97-102.

Ohara, M., Takagaki, A., Nishimura, S., Ebitani, K., (2010). Synthesis of 5-hydroxymethylfurfural and levoglucosan by selective dehydration of glucose using solid acid and base catalysts. *Appl. Catal., A*, 383, 1-2, 149-155.

Okuhara, T., (2002). Water-tolerant solid acid catalysts. *Chem.Rev*, 102, 3641-3666.

Omajali, J.B., Mikheenkho, I.P., Merroun, L.M., Wood, J., Macaskie, L.E., (2015). Characterization of intracellular palladium nanoparticles synthesized by *Desulfovibrio desulfuricans* and *Bacillus benzeovorans*. *J Nanopart Res* 17, 264, 1 -17.

Palkovits, R., (2011). Cellulose and heterogeneous catalysis- A combination of the future. *Chem. Ing. Tech. 83*, (4), 411-419.

Panagiotopoulou, P., Vlachos, D.G, (2014), Liquid phase catalytic transfer hydrogenation of furfural over Ru/C catalyst. *Applied Catalysis A.* 480: 17-24.

Parr Instrument Company (n.d) **Series 4590 Micro Stirred Reactors, 25-100 mL** [online]. Available from: http://www.parrinst.com/products/stirred-reactors/series-4590-micro-stirred-reactors/specifications/ [Accessed: 12/11/2014].

Peng, L. C., Lin, L., Zhang, J. H., Zhuang, J. P., Zhang, B. X., Gong, Y, (2010), Catalytic Conversion of Cellulose to Levulinic Acid by Metal Chlorides. *Molecules* 15: 5258−5272.

Perbellini, L., Princivalle, A., Cerpellon, M., Pasini, F., Brugnone, F., (2003). Comparison of breath, blood and urine concentrations in the biomonitoring of environmental exposure to 1, 3-butadiene, 2, 5-dimethylfuran, and benzene. *Int Arch Occup Environ Health* 76,461–466.

Peterson, A. A., Vogel, F., Lachance, R. P., Froling, M., Antal, M. J., Tester, J. W., (2008). Thermochemical biofuel production in hydrothermal media: A review of sub- and supercritical water technologies. *Energy Environ. Sci* 1, 32-65.

Phuong, J., Kim, S., Thomas, R., Zhang, L., (2012). Predicted toxicity of the Biofuel candidate 2,5-Dimethylfuran in environmental and Biological systems. *Environmental and Molecular Mutagenesis*, 53, 478-487.

Polato, C.M.S., Henriques, C.A., Rodrigues, A.C.C., and Monteiro, J.L.F., (2008). *Catal. Today*, 133–135, 534–540.

Pollmann, K.; Raff, J.; Schnorpfeil, M.; Radeva, G.; Selenska-Pobell, S., (2005). Novel Surface Layer Protein Genes in *Bacillus sphaericus* Associated with Unusual Insertion Elements. *Microbiol-SGM.*, *151*, 2961-2973.

Postgate, J.R, (1979). The sulphate-reducing bacteria. Cambridge University Press, Cambridge U.K. 26 p

Prem Kumar Seelam, (2015). Lecture Notes on Heterogeneous Catalysis. Catalysts, Mechanism, Kinetics, Mass Transfer (Film and Pore Diffusion) Non-ideal reactors.

Pupovac, K., (2013). PhD thesis on solid acid-catalyzed dehydration of sugars to 5-hydroxymethylfurfural, subsequent aldol condensation and hydrogenation over bifunctional spinel oxides. RWTH Aachen University, Germany.

Qi, X., Watanabe, M., Aida, T. M., Smith, R. L., (2009). Efficient process for conversion of fructose to 5-hydroxymethylfurfural with ionic liquids. *Green Chem*, 11, 1327-1331.

Qi, X., Watanabe, M., Aida, T. M., Smith, R. L., (2009). Sulfated zirconia as a solid acid catalyst for the dehydration of fructose to 5-hydroxymethylfurfural. *Jr. Catal. Commun*, 10, (13), 1771-1775.

Qi, X., Watanabe, M., Aida, T. M., Smith, R. L., Jr., (2009). Efficient catalytic conversion of fructose into 5-hydroxymethylfurfural in ionic liquids at room temperature. ChemSusChem, 2, 944-946.

Qi, X., Watanabe, M., Aida, T. M., Smith, R. L., Jr., (2010). Efficient one-pot production of 5-hydroxymethylfurfural from inulin in ionic liquids. *Green Chem*, 12, 1855-1860.

Qi, X., Watanbe, M., Aida, T.M., Smith, R.L., (2012). Synergistic conversion of glucose into 5-hydroxymethylfurfural in ionic liquid-water mixtures. *J.Bioresource. Technology*, 109, 224-228.

Qu, Y., Huang, C., Zhang, J., Chen, B., (2012). Efficient dehydration of fructose to 5-hydroxymethylfurfural catalyzed by a recyclable sulfonated organic heteropolyacid salt. *Bioresour. Technol*, 106, 170-172.

Ramsurn, H., Gupta, R.B., (2013). Hydrogenation by nanoparticle catalysts. Chapter 15, catalysis by nanoparticles, Department of Chemical Engineering, Auburn University, Auburn, AL 36849, USA. http://dx.doi.org/10.1016/B978-0-444-53874-1.00016-0.

Rao, R.S., Baker, R.T.K., Vannice, M.A., (1999). Furfural hydrogenation over carbon-supported copper. *Catal Lett*, 60, 51-57.

Ravindranath, N.H., SitaLakshmi, C., Manuvie, R., Balachandra, P., (2011). Biofuel production and implications for land use, food production and environment in India. *Energy Policy* 39, 5737–5745.

Ren, H., Chen, Y., Huang, Y., Deng, W., Vlachos, D.G., Chen, J.G., (2014). Tungsten carbides as selective deoxygenation catalysts: experimental and computational studies of converting C_3 oxygenates to propene. *Green Chem*., 16, 761-769.

Reutemann, W., Kieczka, H., (2005). Formic Acid in Ullmann's Encyclopaedia of Industrial Chemistry, Wiley-VCH, Weinheim.

Richard, B., (2012). PhD thesis on Catalytic systems for carbohydrate conversions, University of Wisconsin-Madison.

Rigal, L., Gorrichon, J. P., Gaset, A., Heughebaert, J.-C., (1985). *Biomass*,7, 27.

Rinaldi, R., (2015), Chapter 4, Solvents and Solvent Effects in Biomass Conversion. *Catalytic Hydrogenation for Biomass Valorisation*, Edited by Roberto Rinaldi (2015). ISBN 978-1-884973-801-9.

Román-Leshkov, Y., Barrett, C. J., Liu, Z. Y., Dumesic, J. A, (2007), Production of Dimethylfuran for liquid fuels from biomass-derived carbohydrates. *Nature* 447: 982−986.

Román-Leshkov, Y., Chheda, J. N., Dumesic, J. A., (2006). Phase modifiers promote efficient production of 5-hydroxymethylfurfural from fructose. *Science*, 312, (5782), 1933-1937.

Román-Leshkov, Y., Dumesic, J. A., (2009). Solvent effects on fructose dehydration to 5-hydroxymethylfurfural in biphasic systems saturated with inorganic salts. *Top. Catal*, 52, 297-303.

Rosatella, A.A., Simeonov, S.P., Frade, R.F.M., Afonso, C.A.M., (2011). 5-Hydroxymethylfurfural (HMF) as a building block platform: Biological properties, synthesis and synthetic applications. *ChemSusChem*, 4, 451–458.

Rothamer, D.A., Jennings, J.H., (2012). Study of the knocking propensity of 2,5-Dimethylfuran-gasoline and ethanol-gasoline blends. *Fuel*, 98, 203–212.

Schmidt, L.D., and Dauenhauer, P.J., (2007). Chemical engineering: Hybrid routes to biofuels. *Nature*, 447, 914-915.

Scholz, D., Aellig, C., Hermans, I, (2014), Catalytic Transfer hydrogenation/hydrogenolysis of reductive upgrading of furfural and 5-hydroxymethylfurfural. *ChemSusChem*, 7 (1): 268-275.

Seddon, K.R., (1997). Ionic liquids for clean technology. *J. Chemical Technology and Biotechnology,* 68 (4), 351-356.

Seri, K., Inoue, Y., Ishida, H., (2000). Highly efficient catalytic activity of lanthanide (III) ions for conversion of saccharides to 5-hydroxymethylfurfural in organic solvents. *Chem. Lett*. 29, 1, 22-23.

Seri, K., Inoue, Y., Ishida, H., (2001). Catalytic activity of Lanthanide (III) ions for the dehydration of hexose to 5-hydroxymethyl-2-furaldehyde in water. *Bull. Chem. Soc. Japan*. 74, 1145-1150.

Severin, I., Dumont, C., Jondeau-Cabaton, A., Graillot, V., Chagnon, M.-C., (2010). Genotoxic activities of the food contaminant 5-hydroxymethylfurfural using different in vitro bioassays. *Toxicol. Lett*, 192, (2), 189-194.

Shimizu, K. I., Uozumi, R., Satsuma, A., (2009). Enhanced production of hydroxymethylfurfural from fructose with solid acid catalysts by simple water removal methods. *Catal. Commun*, 10, 14, 1849-1853.

Sidhpuria, K. B., Daniel-da-Silva, A. L., Trindade, T., Coutinho, J. A. P., (2011). Supported ionic liquid silica nanoparticles (SILnPs) as an efficient and recyclable heterogeneous catalyst for the dehydration of fructose to 5-hydroxymethylfurfural. *Green Chem*, 13, 340-349.

Simkovic, I., Leesonboon, T., Mok, W., Antal Jr, M.J., (1987). Dehydration of carbohydrates in supercritical water. *American.Chem.Soc*, 32, (2), 129-132.

Simmie, J.M., and Curran, H.J., (2009). Energy Barriers for the Addition of H, $\dot{C}H_3$, and $\dot{C}_2H_5$ to $CH_2{=}CHX$ [X = H, CH_3, OH] and for H-Atom Addition to $RCH{=}O$ [R = H, CH_3, $\dot{C}_2H_5$, *n*-C_3H_7]: Implications for the Gas-Phase Chemistry of Enols. *J.Phys.Chem. A,* 113(27), 7834-7845.

Simmie, J.M., and Würmel, J., (2013). Harmonising production, properties and environmental consequences of liquid transport fuels from biomass- 2,5-Dimethylfuran as a case study. ChemSusChem, 6, 36-41.

Sims, R., Mabee, W., Saddler, J.N., Taylor, M., (2010). An overview of second generation biofuel technologies. *Bioresource Technology* 101, 1570–1580.

Sims, R., Taylor, M., Saddler, J., Mabee, W., (2008). From 1st to 2nd Generation Biofuel Technologies: An Overview of Current Industry and RD&D Activities — extended Executive Summary. OECD/IEA, Paris, France.

Sing, K.S.W., Everett, D.H., Moscou, L., Haul, R.A.W., Pierotti, R.A., Rouquerol, J., Siemieniewska, T., (1985). Reporting physisorption data for gas/solid systems with special reference to the determination of surface area and porosity. *International union of pure and applied chemistry*, 57, 4, 603-619.

Singh, A., Pant D., Korres N. E., Nizami A. S., Prasad, S., Murphy J. D., (2010). Key issues in 46 life cycle assessment of ethanol production from lignocellulosic biomass: 47 Challenges and perspectives. *Bioresource Technol*, 101, 13, 5003-5012.

Sitthisa, S., An, W., Resasco, D.E, (2011), Selective conversion of furfural to 2-methylfuran over supported silica Ni-Fe bimetallic catalyst. *J.Catal*, 284: 90-101.

Sitthisa, S., and Resasco, D.E., (2011). Hydrodeoxygenation of furfural over supported metal catalysts: A comparative study of Cu, Pd and Ni. *Catal Lett*, 141, 784-791.

Sitthisa, S., Pham, T., Prasomsri, T., Sooknoi, T., Mallinson, R.G, Resasco, D.E, (2011), Conversion of furfural and 2-methylpentanal on Pd/SiO_2 and $Pd-Cu/SiO_2$ catalysts. *J.Catal*, 280: 17-27.

Stahlberg, T., Rodriguez-Rodriguez, S., Fristrup, P., Riisager, A., (2011). Metal-free dehydration of glucose to 5-(hydroxymethyl) furfural in ionic liquids with boric acid as a promoter. *Chem. Eur. J*, 17, 1456.

Stevens, J.G., Bourne, R.A., Twigg, M.V., and Poliakoff, M., (2010). Real time product switching using a twin catalytic system for the hydrogenation of furfural in supercritical CO_2. *Angew. Chem., Int. Ed*., 2010, 49, (47) 8856–8859.

Stuebing, H., Ganase, Z., Karamertzanis, P.G., Siougkrou, E., Haycock, P., Piccione, P.M., Armstrong, A., Galindo, A., Adjiman, C.S., (2013), *Nature, Chem, 5*, 952 – 957.

Surh, Y. J., Liem, A., Miller, J. A., Tannenbaum, S. R., (1994). 5-Sulfooxymethylfurfural as a possible ultimate mutagenic and carcinogenic metabolite of the Maillard reaction product, 5-hydroxymethylfurfural. *Carcinogenesis*, 15, 2375.

Szmant, H. H., Chundury, D. D. J., (1981). The preparation of 5-chloromethylfurfuraldehyde from high fructose corn syrup and other carbohydrates. *Chem. Tech. Biotechnol*, 31, 135.

Tao, F., (2012). Synthesis, catalysis, surface chemistry and structure of bimetallic nanocatalysts. *Chem. Soc. Rev*. 41, 7977-7979.

Thananatthanachon, T and Rauchfuss, B.T. (2010), Efficient Production of the Liquid Fuel 2, 5-Dimethylfuran from Fructose Using Formic Acid as a Reagent. *Angewandte Chemie International Edition,* 49(37): 6616-6618.

Tian, G., Daniel, R., Xu, H., (2011). Chapter 19, A New Biofuel Candidate, Biofuel Production-Recent Developments and Prospects, Edited by Marco Aurelio dos Santos Bernardes, ISBN 978-953-307-478-8, Published by; InTech.

Tong, X., Ma, Y., Li, Y., (2010). Biomass into chemicals: Conversion of sugars to furan derivatives by catalytic processes. *J.Applied.Catalysis A*, 385, 1-13.

Torres, A. I., Tsapatsis, M., Daoutidis, P., (2012). Biomass to chemicals: Design of an extractive-reaction process for the production of 5-hydroxymethylfurfural. *Comput. Chem. Eng*, 42, 130-137.

Toshima, N., Yonezawa, T, (1998), Bimetallic nanoparticles- novel materials for chemical and physical applications. *New J. Chem*, Pages 1179-1201.

Tsang, S. C., Cailuo, N., Oduro, W., Kong, A.T.S., Clifon, L., Yu, K.M.K., Thiebaut, B., Cookson, J., Bishop, P., (2008). Engineering preformed cobalt-doped platinum nanocatalysts for ultraselective hydrogenation. *ACS Nano* 2 (12), 2547-2553.

Tumurlu, J.S., Wright, C.T., Boardman, R.D., Yancey, N.A. A Review on Biomass Classification and composition, Co-firing Issues and Pretreatment Methods, August, (2011). Proceedings of the ASABE Annual International Meeting, Louisville, Kentucky.

Uematsu, N., Fujii, A., Hashiguchi, S., Ikariya, T., Noyori, R, (1996), Asymmetric Transfer Hydrogenation of Imines. *J.Am.Chem.Soc*. 118: 4916–4917.

Van Dam, H. E., Kieboom, A. P. G., Van Bekkum, H., (1986). The conversion of fructose and glucose in acidic media: Formation of Hydroxymethylfurfural. Starch/Staerke, 38, (3), 95-101.

Van de Vyver, S., Geboers, J., Jacobs, P.A., Sels, B.F., (2011). Recent advances in the catalytic conversion of cellulose. *ChemCatChem*, 3, 82 –94.

Van Enenstein, W.A., and Blanksma, J.J., (1909). Weeklad, 6, 717.

Verevkin, S.P., Welle, F.M., (1998). Thermochemical studies for ethers. *Structural Chem*, 9(3), 215 –221.

Wang, A., Zhang, T., (2013). One-Pot conversion of cellulose to ethylene glycol with multifunctional tungsten based catalyst. *Acc.Chem. Res*. 46 (7), 1377-1386.

Wang, F., Shi, A.-W., Qin, X.-X., Liu, C.-L., Dong, W.-S., (2011). Dehydration of fructose to 5-hydromethylfurfural by rare earth metal trifluoromethanesulfonates in organic solvents. *Carbohydr. Res*, 346, 982-985.

Wang, G.H., Hilgert, J., Richter, F.H., Wang, F., Bongard, H.J., Spliethoff, B., Weidenthaler, C., Schuth, F., (2014). Platinum-cobalt bimetallic nanoparticles in hollow carbon nanospheres for hydrogenolysis of 5-hydroxymethylfurfural. *Nature Materials*, Vol 13. DOI 10.1038nmat3872.

Wasserscheid, P., and Keim, W., (2000). Ionic liquids: new solutions for transition metal catalysis. *Angew. Chem,* 147.231.204.152.

Watanabe, M., Aizawa, Y., Iida, T., Nishimura, R., Inomata, H., (2005b). Catalytic glucose and fructose conversions with TiO_2 and ZrO_2 in water at 473 K: Relationship between reactivity and acid–base property determined by TPD measurement *Appl. Catal*., A, 295, 150.

Watanabe, M.; Aizawa, Y.; Iida, T.; Aida, T. M.; Levy, C.; Sue, K.; Inomata, H., (2005a). Glucose reactions with acids and base catalysts in hot compressed water at 473 K. *Carbohydrate Research*, 340, 1925-1930.

Wei, Z., Li, Y., Thushara, D., Liu, Y., Ren, Q. J., (2011). *Taiwan Inst. Chem. Eng*, 42, 363.

Wei, Z., Sun, J., Li, Y., Datye, A.K., Wang, Y, (2012), Bimetallic catalysts for hydrogen generation. *Chem.Soc.Rev*, 41: 7994-8008.

Wu, B. H., Huang, H. Q., Yang, J., Zheng, N. F. & Fu, G., (2012). Selective hydrogenation of alpha, beta-unsaturated aldehydes catalyzed by amine-capped platinum-cobalt nanocrystals. *Angew. Chem. Int. Ed*. 51, 3440-3443.

Wu, S.X., Fan, H.I., Xie, Y., Cheng, Y., Wang, Q., Zhang, Z.F., and Han, B.X., (2010). Effect of CO_2 on the conversion of inulin to 5-hydroxymethylfurfural and propylene oxide to 1,2-propanediol in water. Green Chem., 12, 1215–1219.

Wu, X., Wang, C., Xiao, J, (2010), Asymmetric transfer hydrogenation in water with platinum group metal catalysts. *Platinum Metals Rev*. 54,(1),3 – 19.

www.biofuel.org.uk. Accessed 20-03-2015.

Xiong, W., Li, X., Xiang, J., Wu, O., (2008). High-density fermentation of microalga Chlorella protothecoides in bioreactor for microbiodiesel production. *Appl Microb Biotechnol*, 78, 29-36.

Yan, H., Yang, Y., Tong, D., Xiang, X., Hu, C., (2009). Catalytic conversion of glucose to 5-hydroxymethylfurfural over $SO_4^{2-/}ZrO_2$ and $SO_4^{2-/}ZrO_2$-Al_2O_3 solid acid catalysts. *Catal. Commun*, 10, 1558-1563.

Yang, F., Liu, Q., Bai, X., Du, Y., (2011). Conversion of biomass into 5-hydroxymethylfurfural using solid acid catalyst. *Bioresource. Technology*, 102, (3), 3424-3429.

Yuan, X., Sun, G., Asakura, H., Tanaka, T., Chen, X., Yuan, Y., Laurenczy, G., Kou, Y., Dyson, P.J., Yan, N., (2013). Development of palladium surfaced-enriched heteronuclear Au-Pd nanoparticle dehalogenation catalysts in an ionic liquid. *Chem. Eur. J.* (19) 1227-1234.

Zeiger, E., Anderson, B., Haworth, S., Lawlor, T., Mortelmans, K., (1992). Salmonella mutagenicity tests. V. Results from the testing of 311 chemicals. *Environ Mol Mutagen* 19, 2–141.

Zhang, J., Lin, L. and Liu, S. (2012), Efficient Production of Furan Derivatives from a Sugar Mixture by Catalytic Process. *Energy & Fuels*, 26(7): 4560–4567.

Zhang, Y., Pidko, E. A., Hensen, E. J. M., (2011). Molecular aspects of glucose dehydration by chromium chlorides in ionic liquids. *Chem. Eur. J*, 17, 5281-5288.

Zhang, Z., Wang, Q., Xie, H., Liu, W., Zhao, Z., (2011). Catalytic conversion of carbohydrates into 5-hydroxymethylfurfural by germanium (IV) chloride in ionic liquids. *ChemSusChem*, 4, 131-138.

Zhao, Q., Wang, L., Zhao, S., Wang, X., Wang, S., (2011). High selective production of 5-hydroxymethylfurfural from fructose by a solid heteropolyacid catalyst. *Fuel*, 90, 2289-2293.

Zheng, H.Y., Zhu, Y.L., Teng, B.T., Bai, Z.Q., Zhang, C.H., Xiang, H.W., Li, Y.W., (2006). Towards understanding the reaction pathway in vapour phase hydrogenation of furfural to 2-methylfuran. *J. Mol. Catal. A: Chem*. 246, 18-23.

Zhong, S., Daniel, R., Xu, H., Zhang, J., Turner, D., Wyszynski, M.L., Richards, P., (2010). Combustion and emissions of 2,5-dimethylfuran in a direct injection spark-ignition engine. *Energy Fuels* 24, 2891–2899.

Zhou, X., Wu, X., Yang, B., Xaio, J, (2012), Varying the ratio of formic acid to triethylamine impacts on asymmetric transfer hydrogenation of ketones. *Journal of Molecular Catalysis A: Chemical* 357: 133-140.

Zhu, Ju., (2014). PhD Thesis titled Synthesis of precious metal nanoparticles supported on bacterial biomass for catalytic applications in chemical transformations. Submitted to University of Birmingham, UK.

Zu, Y.H., Yang, P.P., Wang, J.J., Liu, X.H., Ren, J.W., Lu, G.Z., Wang, Y.Q., (2014). Efficient production of the liquid fuel 2,5-dimethylfuran from 5-hydroxymethylfurfural over Ru/Co_3O_4 catalyst. *Appl. Catal*., B, 146, 244-248.